THE UNIVERSITY OF ARIZONA
University Libraries

UA CAMPUS
REPOSITORY

The Context of Megadrought: Multiproxy Paleoenvironmental Perspectives from the South San Juan Mountains, Colorado

Item Type	text; Electronic Dissertation
Authors	Routson, Cody Craig
Publisher	The University of Arizona.
Rights	Copyright © is held by the author. Digital access to this material is made possible by the University Libraries, University of Arizona. Further transmission, reproduction or presentation (such as public display or performance) of protected items is prohibited except with permission of the author.
Download date	13/05/2019 14:11:23
Link to Item	http://hdl.handle.net/10150/320004

THE CONTEXT OF MEGADROUGHT: MULTIPROXY PALEOENVIRONMENTAL PERSPECTIVES FROM THE SOUTH SAN JUAN MOUNTAINS, COLORADO

By

Cody Craig Routson

A Dissertation Submitted to the Faculty of the
DEPARTMENT OF GEOSCIENCES
In Partial Fulfillment of the Requirements
For the Degree of
DOCTOR OF PHILOSOPHY
In the Graduate College
THE UNIVERSITY OF ARIZONA

2014

THE UNIVERSITY OF ARIZONA
GRADUATE COLLEGE

As members of the Dissertation Committee, we certify that we have read the dissertation prepared by Cody Routson entitled: The Context of Megadrought: Multiproxy Paleoenvironmental Perspectives from the South San Juan Mountains, Colorado and recommend that it be accepted as fulfilling the dissertation requirement for the Degree of Doctor of Philosophy

____Date: 11/25/13
Jonathan T. Overpeck

____Date: 11/25/13
Connie A. Woodhouse

____Date: 11/25/13
Andrew Cohen

____Date: 11/25/13
David Meko

____Date: 11/25/13
Julio Betancourt

Final approval and acceptance of this dissertation is contingent upon the candidate's submission of the final copies of the dissertation to the Graduate College.

I hereby certify that I have read this dissertation prepared under my direction and recommend that it be accepted as fulfilling the dissertation requirement.

____ Date: 11/25/13
Dissertation Director: Jonathan T. Overpeck

____ Date: 11/25/13
Dissertation Co-Director: Connie A. Woodhouse

STATEMENT BY AUTHOR

This dissertation has been submitted in partial fulfillment of requirements for an advanced degree at the University of Arizona and is deposited in the University Library to be made available to borrowers under rules of the Library.

Brief quotations from this dissertation are allowable without special permission, provided that accurate acknowledgment of source is made. Requests for permission for extended quotation from or reproduction of this manuscript in whole or in part may be granted by the head of the major department or the Dean of the Graduate College when in his or her judgment the proposed use of the material is in the interests of scholarship. In all other instances, however, permission must be obtained from the author.

SIGNED: Cody Routson

ACKNOWLEDGEMENTS

I thank my advisors Jonathan Overpeck and Connie Woodhouse, and my committee members Andrew Cohen, David Meko, and Julio Betancourt for their time, insights, and discussions, all of which greatly improved this research. I thank Kanin Routson, Dick Yetman, Jock Favor and Clare Stielstra for their extensive help in the field. I thank Jesse Martinez and Chelsea Powers for laboratory assistance. I also thank the Geoscience staff with special thanks to Anne Chase for her support. Conversations and feedback from colleagues, and current and former graduate students including Nick McKay, Jessica Conroy, Toby Ault, Sarah Truebe, Sarah Leroy, Jason Addison, Sarah Hayes, Dan Griffin, Brewster Malevitch, Kyle Miller, Greg Pederson, Jeremy Weise, Scott St. George, and Diane Thompson also substantially improved this research. I also thank my family for their ongoing support.

The NOAA climate program office, a National Science Foundation Graduate Research Fellowship, an Arizona Science Foundation Graduate Fellowship, the Colorado Scientific Society Memorial Research Fund, the Climate Assessment for the Southwest, the Bert S. Buttler Scholarship Fund, the Wilson Thompson Scholarship Fund, the Keith Katzer Scholarship Fund, the Global Change Dissertation Improvement Grant, the Bristlecone Award, the Galileo Circle Scholar Award, and the Department of Geoscience have all supported this research.

TABLE OF CONTENTS

LIST OF FIGURES 6
LIST OF TABLES 8
ABSTRACT 9
INTRODUCTION 11
PRESENT STUDY 17
REFERENCES 22
APPENDIX A 29
SECOND CENTURY MEGADROUGHT IN THE RIO GRANDE HEADWATERS, COLORADO: HOW UNUSUAL WAS MEDIEVAL DROUGHT? 29
A.1 Abstract 29
A.2 Introduction 30
A.3 Tree-Ring and Climate Analysis 32
A.4 Second Century Droughts 34
A.5 Conclusions and Implications 39
A.6 References 41
A.7 Tables and Figures 45
A.8 Supporting Information 49
A.9 Supporting References 53
A.10 Summitville Chronology 54
APPENDIX B 71
1100 YEARS OF OCEANIC FINGERPRINTS ON WESTERN NORTH AMERICAN DROUGHTS AND PLUVIALS 71
B.1 Abstract 71
B.2 Introduction 72
B.3 Methods 75
B.4 Results 78
B.5 Discussion 82
B.6 Conclusion 87
B.7 References 88
B.8 Figures 93
B.9 Supplemental Figures 102
B.10 Supplemental Circulation Reconstruction Analysis 105
B.11 Supplemental Circulation References: 106
B.12 Supplemental Circulation Figure 107
B.13 Supplemental Tables 108
APPENDIX C 111
THREE MILLENNIA OF SOUTHWEST NORTH AMERICAN DUSTINESS AND FUTURE IMPLICATIONS 111
C.1 Abstract 111
C.2 Introduction 112
C.3 Reconstructing Dustiness 113

C.4 Conclusion ... 118
C.5 Methods ... 119
C.6 References ... 124
C.7 Figures ... 131
C.8 Supplemental Figures ... 134
C.9 Supplemental Tables ... 142
APPENDIX D ... 144
THE MEGADROUGHT ENVIRONMENT ... 144
D.1 Abstract: ... 144
D.2 Body ... 144
D.3 Methods ... 152
D.4 References ... 155
D.5 Figures ... 160
D.6 Supplemental Text ... 164
D.7 Supplemental Figures ... 166
D.8 Supplemental Tables ... 176
D.9 Supplemental Comparison of Calibrations ... 185
APPENDIX E: PERMISSIONS ... 187

LIST OF FIGURES

Figure A.1 ... 45
Figure A.2 ... 46
Figure A.3 ... 47
Figure A.S1 ... 51
Figure A.S2 ... 52
Figure B.1 ... 93
Figure B.2 ... 94
Figure B.3 ... 95
Figure B.4 ... 96
Figure B.5 ... 97
Figure B.6 ... 98
Figure B.7 ... 99
Figure B.8 ... 100
Figure B.S1 ... 102
Figure B.S2 ... 103
Figure B.S3 ... 104
Figure B.S4 ... 107
Figure C.1 ... 131
Figure C.2 ... 132
Figure C.3 ... 133
Figure C.S1 ... 134
Figure C.S2 ... 135
Figure C.S3 ... 136
Figure C.S4 ... 137
Figure C.S5 ... 138
Figure C.S6 ... 139

Figure C.S7 140
Figure C.S8 141
Figure D.1 160
Figure D.2 161
Figure D.3 162
Figure D.4 163
Figure D.S1 166
Figure D.S2 167
Figure D.S3 168
Figure D.S4 169
Figure D.S5 170
Figure D.S6 171
Figure D.S7 172
Figure D.S8 173
Figure D.S9 174
Figure D.S10 175
Figure D.S11 186

LIST OF TABLES

Table A.1 48
Table B.1 101
Table B.S1 108
Table B.S2 109
Table B.S3 110
Table C.S1 142
Table C.S2 143
Table D.S1 176
Table D.S2 177
Table D.S3 178
Table D.S4 179
Table D.S5 180
Table D.S6 181

ABSTRACT

The context of megadrought, drought more severe than any we have experienced over the past 100 years, is assessed in this dissertation. A set of new climate reconstructions including drought, dustiness, and temperature from the south San Juan Mountains in southern Colorado is presented here and provides unforeseen insights into these unusual events. The global context of megadroughts is also analyzed using a network of reconstructions. The new drought record is from bristlecone tree-rings, spans the last 2000 years, and shows two periods with anomalous aridity and drought in the south San Juan Mountains. The later period corresponds with well-characterized medieval climate anomaly (MCA; 900-1400 AD) aridity in southwestern North America (henceforth the Southwest). The earlier interval coincides with the Roman Period (1-400 AD). A severe drought with, almost 50 consecutive years of below average tree-growth, occurs in the middle of the Roman Period during the 2nd century AD. Assessment of Roman and MCA droughts in the context of global climate reconstructions reveals that similar hemisphere scale circulation patterns during both intervals might have contributed to severe aridity in the Southwest. Next relationships between droughts and pluvials in western North America (henceforth the West) and global sea surface temperature (SST) patterns over the last 1100 years are examined. Several methods are used including teleconnection patterns imbedded in tree-ring reconstructed drought maps, and a global network of SST reconstructions. Teleconnection patterns during droughts and pluvials suggest that megadroughts and pluvials were likely forced in part by

sequences of anomalous years in the Pacific and Atlantic Ocean, but the analyses also reveals contradictory results that may require new ways of understanding the relationship between SSTs and drought on long timescales. Next, returning to the south San Juan Mountains, we developed a new dust reconstruction from a lake sediment core. The reconstruction illustrates that dustiness has been an important component of Southwestern climate over the past 2941 years. The record shows high dust deposition in the past especially around 900 BC and during the MCA. High dust deposition before recent land use changes suggests that megadroughts or associated periods of aridity were widespread and severe enough to mobilize dust, perhaps resulting in further reductions to mountain snowpack and stream flow. Finally, a new biomarker based temperature reconstruction is presented. The reconstruction spans the last 2000 years and shows that the warmest temperatures during that interval occurred during the Roman Period and the MCA. The record suggests these periods were warmer than today, indicating the San Juan Mountains are a sensitive region to temperature change. Both past warm periods coincide with anomalous drought and dustiness, suggesting that temperature and dust may have acted as megadrought enhancing feedbacks. In summary, this dissertation helps characterize the timing and causes of southwest North American Megadroughts over the past 2000 years; separately addressing changes in moisture balance, dustiness, temperature, hemispheric circulation, and sea surface temperature forcing patterns during these unusual events.

INTRODUCTION

Droughts have widespread impacts on environmental and natural resources. Since the 1980's, droughts and heat waves have caused over 200 billion dollars worth of damage, and rank second only to tropical cyclones as the most costly natural disasters in the United States (Smith and Katz 2013). In summer of 2011, record-breaking drought exacerbated by unusually warm temperatures had devastating impacts on rangeland and agriculture across much of northern Mexico, the Southwest, and Texas (Seager et al., 2013; Weiss et al., 2012). In 2012, North America experienced the most extensive drought since the 1930's; over half of the continental United States was in moderate to severe drought (Cook et al., 2013a; Hoerling et al., 2013), and estimated economic impacts reached 30 billion dollars (NCDC 2013). Recent drought-induced bark beetle and spruce budworm attacks have caused widespread forest mortality across the West (Breshears et al., 2008; Van Mantgem et al., 2009), and warming temperatures and droughts are linked with increased occurrence and severity of wildfires (Westerling et al., 2006). Over 9.2 million acres and hundreds of homes burned in 2012 alone (NCDC 2013). Droughts, warming, and forest mortality in mountain regions have been linked to reduced snowpack, faster ablation, and shorter snow covered seasons, all of which result in reduced runoff and stream flow in the mountain headwaters of major river systems like the Colorado River and the Rio Grande (Barnett et al., 2005; Harpold et al., 2012a; 2012b; Biederman et al., 2012). In the Southwest over 33 million people depend on the Colorado River for drinking water (CRWUA 2013), and over-allocation of Colorado River water highlights this key vulnerability to drought (Woodhouse et al., 2005).

With current climate models predicting even warmer and drier conditions in the future, these feedbacks foreshadow a grim outlook for Southwestern climate (Overpeck and Udall 2010; Seager et al., 2007, 2012).

Whereas recent droughts have had devastating impacts, they pale in comparison to droughts that occurred in past 2000 years (Woodhouse and Overpeck 1998). Natural archives including tree-rings and sediments indicate the Southwest has been prone to a wide range of hydroclimatic variability, and multidecadal length droughts unprecedented in the last 100 years (Megadroughts) have occurred several times over the past two millennia (Cook et al., 2007; 2010; Meko et al., 2007; Routson et al., 2011; Stine 1994; Woodhouse and Overpeck 1998; Woodhouse 2004). The medieval climate anomaly (MCA; ~900-1400 AD) is noted for several megadroughts in the West (Cook et al., 2007; 2010; Meko et al., 2007). MCA droughts are recorded by tree-growth, lake sediments, loess deposition, and dune mobilization (Cook et al., 2007, 2010; Halfen and Johnson 2013; Laird et al., 1996; Miao et al., 2007; Routson et al., 2011; Woodhouse and Overpeck 1998; Woodhouse 2004), and are associated with dramatic decreases in Colorado River flows (Meko et al., 2007), and the reorganization and eventual collapse of the Ancient Pueblo culture on the Colorado Plateau (Douglas 1929).

The causes of droughts are diverse. Climate variability and droughts in the West are closely linked with sea surface temperature (SST) patterns. The El Niño Southern Oscillation (ENSO) in the tropical Pacific has a strong influence on temperature and precipitation in the West (e.g., Cayan et al. 1999; Dettenger et al., 1998; Redmond and Koch 1991; Schubert et al. 2009). La Niña events are an intensification of easterly trade winds that cause increased upwelling water off the South American coastline and cool eastern tropical pacific SST (Horel and Wallace 1981). La Niña is associated with a general northward displacement of storm tracks over the West and warm, dry conditions in the Southwest. El Niño events are roughly the opposite of La Niña, whereby weakening of the easterly trade winds causes reduced upwelling and anomalously warm SSTs in the eastern equatorial Pacific (Cayan et al. 1999; Dettenger et al., 1998; Redmond and Koch 1991). El Niño is associated with more southward-displaced storm tracks in the West and cooler and wetter than average conditions in the Southwest.

SSTs in the North Pacific and North Atlantic Oceans have also been linked with Western climate and drought. The leading mode of SST in north Pacific is known as the Pacific Decadal Oscillation (PDO; Mantua et al. 1997). The PDO has a similar teleconnection pattern to ENSO (Cook et al., 2013b), and it is unclear if the PDO is a unique oscillation, or a lower frequency resonance of ENSO (Newman et al., 2003). Nonetheless, the PDO tends to modulate Western climate on decadal timescales (McCabe et al 2004). North Atlantic SST, when detrended and smoothed, varies on multidecadal length timescales and is known as the Atlantic Multidecadal Oscillation (AMO; Enfield 2001). The AMO has a broad teleconnection pattern whereby the positive phase (warm SST) is correlated with drier than average conditions across the United States (Cook et al., 2013b), and is related to the timing and extent of droughts (McCabe et al., 2004).

Many studies have linked megadroughts to SSTs. A common notion is that persistent “La Niña-like” conditions forced MCA aridity and megadroughts in the

West (e.g., Conroy et al. 2009b; Graham et al. 2007; Herweijer et al. 2007; Seager et al. 2007; Stahle et al. 2000). Long records from the tropical Pacific are scarce, but SST reconstructions generally support the La Niña Like MCA hypothesis (Cobb et al., 2003; Conroy et al., 2009; Kennett and Kennett 2000; Oppo et al., 2009). Precipitation-based reconstructions of ENSO, however, suggest the opposite and indicate the MCA was El Niño-like (Conroy et al., 2008; Oppo et al., 2009; Tierney et al., 2010a; Yan et al., 2011). Together the records suggest a tropical Pacific with no modern analogue whereby SSTs are decoupled from local precipitation (e.g., Tierney et al., 2010a), or stronger El Niño events were imposed on a La Niña like background (Conroy et al., 2009a; Routson et al., 2011).

Warm North Atlantic SSTs have also been linked to past Western megadroughts (Conroy et al., 2009b; Feng et al. 2008, 2011; Gray et al., 2004; Hidalgo 2004; McCabe et al., 2008; Oglesby et al. 2012). Warm intervals in a tree-ring reconstruction of the AMO (Gray et al., 2004) have been associated with periods of drought in the West (Conroy et al., 2009b; Nowak et al., 2012; McCabe et al., 2008). Low-resolution SST reconstructions also indicate there may be a long-term relationship between warm North Atlantic SST and increased Western aridity (Conroy et al., 2009b; Feng et al. 2008, 2011; Oglesby et al. 2012).

Windblown dust is a more regional scale drought feedback than SSTs. Much of the Southwest is characterized by arid landscapes, and dust is entrained by spring winds and southwesterly storm systems (Painter et al., 2007). Large quantities of dust are often deposited on Rocky Mountain snowpack (Lawrence et al 2010; Painter et al., 2007, 2012; Skyles et al., 2012). Dust darkens the snow surface, reducing albedo and causing the snow to absorb more heat. Warmer snow increases ablation rates, shortens the snow-covered season, and reduces runoff (Painter et al., 2007, 2010, 2012; Skyles et al., 2012). Dust clouds can also reduce rainfall by shading the earth's surface and reducing convective storm formation (Miller and Tegan 1998). Persistent dust clouds during the 1930's Dust Bowl likely enhanced the drought severity and shifted the drought epicenter from the Southwest into the Great Plains (Cook et al., 2008).

Land use has caused substantial increases in Southwestern dustiness (Neff et al., 2008), but dustiness is also enhanced by drought (Munson et al., 2011). Aeolian sediment deposits from the mid-Holocene suggest intervals of widespread loess deposits and dune migration (Halfen and Johnson 2013; Miao et al., 2007). Dune activation has also occurred in many regions of the Southwest (Forman et al., 2006; Reheis et al., 2005; Stokes and Breed 1994; Wells et al., 1990). Recent work suggests windblown dust clouds enhanced the length of megadroughts in the Great Plains by increasing atmospheric stratification and inhibiting convective storm formation, (Cook et al., 2013b); however, much uncertainty still remains regarding the influence of dust on exacerbating megadroughts.

Warm temperatures also enhance severe droughts. In the intermountain West, recent warming has been linked to declines in the ratio of snowfall to rainfall, faster snowpack ablation, and a reduced snow-covered season, leading to less available water for runoff and stream flow (Barnett et al., 2005; Bales et al., 2006; Harpold et al., 2012). Warming also exacerbates drought severity by enhancing evaporation and transpiration rates (Breshears et al., 2005; Weiss et al., 2009; Williams et al., 2012).

The influence of warm temperature on droughts is clearly illustrated by differences between the 1950's and 2000's droughts in the Southwest (Weiss et al., 2009). The two droughts had similar precipitation deficits, but the warmer 2000's drought caused widespread forest mortality. On the Colorado Plateau recent work shows warm temperatures are related to increased moisture stress, increased vegetation mortality (Munson et al., 2011a), and increased dustiness (Munson et al., 2011b).

The temperature history of the West is less well characterized than moisture over the past two millennia. Limited evidence suggests some iconic megadroughts may have occurred under elevated regional temperatures (Woodhouse et al., 2010). The MCA is characterized by warmer than average Northern Hemisphere temperatures (e.g., Ljungqvist 2010; Mann et al., 2008, 2009). North American temperatures, as constrained by three pollen records, were warm during the MCA (Trouet et al., 2013). Western grid points from a temperature field reconstruction also indicate the MCA was warm (Mann et al., 2009). A new temperature reconstruction from the Great Basin using bristlecone pine ring width and changes in the position of treeline shows a long-term cooling trend over the past five millennia (Salzer et al., 2013). The record, however, doesn't show pronounced anomalies coincident with changes in aridity and drought. A bristlecone pine ring-width temperature reconstruction from the San Francisco Peaks in Northern Arizona shows some megadroughts coincide with warm temperatures, but has little centennial scale change (Salzer and Kipfmueller 2005). Together these reconstructions highlight the need for more regional temperature reconstructions in the Southwest to assess links between temperature and past droughts.

Much uncertainty still surrounds the ultimate causes of megadroughts. The combined research suggests multiple factors likely worked in concert to sustain multidecadal length droughts in the Southwest. Limited numbers of records are available with which to assess the environmental context of megadroughts, and many have poor age control and sample resolution. Numerous key questions surrounding megadroughts persist. Did anomalous SSTs force megadroughts? Were megadroughts severe enough to mobilize dust? Could dust have acted as a megadrought feedback? Did anomalous temperatures exacerbate megadroughts? This study helps address these and other questions by contributing a new set of climate records including drought, dustiness, and temperature, in addition to providing new perspectives and analyses of existing regional and global records.

PRESENT STUDY

Given the potential impacts if a megadrought were to occur in the Southwest today, it is important we understand the local and global conditions that lead to droughts that persist for decades. This research dissertation assesses the environmental context of megadroughts using a series of climate reconstructions from the south San Juan Mountains in southern Colorado. The south San Juan Mountains are a narrow mountain chain forming the northeastern boundary of the high desert Colorado Plateau. Centrally located in the southwest, the south San Juan Mountains host the headwaters to the San Juan and Rio Grande Rivers and were at the epicenter of several Megadroughts (Cook et al., 2008). During summer field seasons of 2008, 2009, 2010, and 2011 sediment cores and surface sediments were collected from a series of alpine and subalpine lakes and tree cores were collected from several five bristlecone pine stands. Using a subset of these samples, a set of high-resolution climate records were developed including moisture balance, dustiness, and temperature. By analyzing these new records along with proxy climate records from around the globe this research provides new insights into the nature of megadroughts. We base our assessments in the context of modern climate relationships, and analyze the evidence linking local, regional, and global scale climate forces to the most extreme droughts in the Southwest over the past two millennia.

This dissertation is divided into four chapters, each of which contributes to characterizing different aspects of Megadroughts. Each chapter is published or intended for publication as an independent, peer-reviewed journal article. In this dissertation, each of these articles is included in an appendix (Appendices A, B, C, and D). The region characterized in this study in Appendices A, C, and D includes the San Juan Mountains and the greater Southwest. In Appendix B we expand our geographic window to assess megadroughts across western North America.

In Appendix A, drought in the south San Juan Mountains is characterized using a bristlecone pine chronology. The chronology was developed from small stand growing near the abandoned mining town of Summitville. Living and remnant wood were combined to create a record over 2000 years long. A series of analyses were conducted to understand the record. Seasonal correlations (using the program seascorr: Meko et al., 2011) between the bristlecone record and instrumental gridded PRISM data (Daly et al., 2002) show the bristlecone growth at this site is most strongly limited by spring moisture balance. Moving correlations between the chronology and tree-ring reconstructed PDSI (Cook et al., 2008) shows the moisture signal is consistent through time. The new record highlights two periods of anomalous aridity and drought. The first period corresponds with well-characterized medieval aridity in the Southwest. Earlier in time the bristlecone show a second interval corresponding with the Roman period, which contains the most severe drought in our record. This drought occurs during the second century AD when our record shows almost 50 consecutive years of below average tree-growth, interrupted only once by a slightly above average year. Furthermore, this drought occurs within a much broader interval of unusual aridity. Other regional tree-ring records from Utah (Knight et al., 2010), New Mexico (Grissino-Mayor 1998), and tree-ring reconstructed PDSI (Cook et al., 2008) corroborate the occurrence of severe drought during the 2nd century. Assessing global climate records during these two intervals, similar hemispheric scale patterns occur during the Roman and medieval periods in the Southwest. These patterns include increased solar irradiance (Steinhilber et al., 2009), warm Northern Hemisphere temperature (Ljungqvist et al., 2010), a warm North Atlantic (Sicre et al., 2010), and an unusual pattern in the tropical Pacific, which we infer to reflect increased El Niño frequency or intensity imposed on a strong La Niña like temperature gradient (Conroy et al., 2008; Oppo et al., 2009). This chapter was published in Geophysical Research Letters in the fall of 2011.

In appendix B relationships between global SST patterns and Western megadroughts and pluvials are assessed. In this chapter we focus on the last 1100 years, helping to characterized changes during the MCA that resulted in frequent droughts in the Southwest. The analysis encompasses both the driest most persistent megadroughts and the wettest most persistent pluvials. Two primary methods are used: first teleconnection patterns of instrumental circulation indexes including ENSO, PDO, and AMO imbedded in tree-ring reconstructed PDSI (Cook et al., 2008) are assessed, and second a network of SST reconstructions is assessed. We find little change in tropical Pacific teleconnection patterns between the MCA and post MCA, whereas SST reconstructions show a pronounced shift toward a La Niña like background state during the MCA. Precipitation-based reconstructions of ENSO however, indicate that the MCA was El Niño like, in direct contrast to the SST reconstructions. There are increases in the strength of a widespread teleconnection pattern we link to the AMO during the MCA. Teleconnection patterns indicate that many severe droughts and pluvials were forced by multiple consecutive or nearly consecutive La Niña and El Niño events, respectively. Poor resolution of SST reconstructions limits our ability to assess relatively short drought and pluvial time scales, but droughts tend to have a La Niña like pattern in the Pacific and a warm North Atlantic, consistent with the inferences drawn from teleconnection pattern maps. This manuscript is intended for publication in Journal of Climate.

In appendix C a new 2941-year-long dust reconstruction from Fish Lake in the south San Juan Mountains is presented. Two methods are used to reconstruct dust deposition: grain size analysis and µXray-fluorescence (µXRF). The grain size distribution of dust deposited on local San Juan Mountains snowpack was used to characterize changes in the fraction of dust in the sediment through time. µXRF was also used to characterize the geochemistry of dust on snow, local, bedrock and sediment. Dust was reconstructed using a geochemical end-member mixing model. Elemental abundance ratios of dust off snow and local bedrock represent the two end-members of which the sediment is a mixture. Applying the mixing model to µXRF measurements taken down the core calculates the fraction of dust deposited in the lake through time. The grain size and geochemical records were combined to reduce method dependent variance and to reconstruct total dust deposition in our lake for the past 2941 years. The dust record shows an anomalously dusty period before 900 BC, after which dustiness declines slowly. The record shows a small increase in dustiness associated with Roman Period aridity, and persistent high dustiness during the MCA. Finally the record also shows a large increase in dustiness associated with the introduction of livestock and increased human land use starting in the mid to late 1800's. The dust record shows that dust is an important component of southwestern climate and that medieval and earlier droughts were severe enough to mobilize dust, which may have subsequently altered snowmelt and reduced runoff and stream flow during periods of extreme aridity in the past.

In appendix D 2000 years of temperature variability from Blue Lake in the south San Juan Mountains is reconstructed. A new biomarker proxy is used, which links the relative abundance of gycerol dialkyl glycerol tetraether (GDGT) membrane lipids to mean annual temperature (e.g., Loomis et al., 2012; Tierney et al., 2010b). The reconstructed temperature record closely matches local snow telemetry station temperatures, capturing recent rapid warming in the region. The GDGT record shows that temperatures in the San Juan Mountains were warmer in the past than today and that anomalously warm temperatures coincided with periods of extreme drought and aridity and in the Southwest. The warmest period in the record coincides with Roman Period aridity identified in the Summitville tree-rings. The medieval period was also anomalously warm. Together the temperature and dust records suggest that temperature and dust may have been important feedbacks during the most severe droughts in the Southwest. The rate of recent warming in the San Juan Mountains, combined with rapid rates of change in the GDGT record, indicate that the San Juan Mountains are highly sensitive to temperature change, and will likely respond in kind to future warming.

REFERENCES

Ault, T. R., et al., 2013: The continuum of hydroclimate variability in western North America during the last millennium. *Journal of Climate*,

Bales, R. C., N. P. Molotch, T. H. Painter, M. D. Dettinger, R. Rice, and J Dozier, 2006: Mountain hydrology of the western United States. *Water Resources Research*, *42*(8).

Barnett, T. P., J. C. Adam, and D. P. Lettenmaier, 2005: Potential impacts of a warming climate on water availability in snow-dominated regions. *nature*, *438*(17), 303-309, doi:10.1038/nature04141

Breshears, D. D., et al. 2005: Regional vegetation die- off in response to global- change- type drought, *Proc. Natl. Acad. Sci. U. S. A.*, 102(42), 15,144–148, doi:10.1073/pnas.0505734102.

Breshears, D. D., et al., 2008: Tree die-off in response to global change-type drought: mortality insights from a decade of plant water potential measurements. *Frontiers in Ecology and the Environment*, *7*(4), 185-189.

Cayan, D. R., K. T. Redmond, and L. G. Riddle, 1999: ENSO and Hydrologic Extremes in the Western United States. *Journal of Climate*, 12 (9), 2881-2893. doi: http://dx.doi.org/10.1175/1520-0442(1999)012<2881:EAHEIT>2.0.CO;2

Cobb, K. M., C. D. Charles, H. Cheng, and R. L. Edwards, 2003: El Niño/Southern

Oscillation and tropical Pacific climate during the last millennium. *Nature,* 424 (6946), 271–276, doi:doi:10.1038/nature01779.

Conroy, J. L., J. T. Overpeck, J. E. Cole, T. M. Shanahan, and M. Steinitz- Kannan, 2008: Holocene changes in eastern tropical Pacific climate inferred from a Galápagos lake sediment record, *Quaternary Science Reviews,* 27, 1166–1180, doi:10.1016/j.quascirev.2008.02.015.

Conroy, J. L., A. Restrepo, J. T. Overpeck, M. Steinitz-Kannan, J. E. Cole, M. B. Bush, and P. A. Colinvaux, 2009a; Unprecedented recent warming of surface temperatures in the eastern tropical Pacific Ocean. *Nature Geoscience,* 2, 46–50, doi:10.1038/ngeo390.

Conroy, J. L., J. T. Overpeck, J. E. Cole, and M. Steinitz-Kannan, 2009b: Variable oceanic influences on western North American drought over the last 1200 years. *Geophysical Research Letters*, 36 (17), doi:10.1029/2009GL039558.

Conroy, J. L., J. T. Overpeck, and J. E. Cole, 2010: El Niño/Southern Oscillation and changes in the zonal gradient of tropical Pacific sea surface temperature over the last 1.2 ka. *PAGES news*, 18 (1), 32-34.

Cook, B. I., J. E. Smerdon, R. Seager, and E. R. Cook, 2013a: Pan-continental droughts in North America over the last millennium. *Journal of Climate*

Cook, B. I., R. Seager, R. L. Miller, and J. A. Mason, 2013b: Intensification of North American megadroughts through surface and dust aerosol forcing. *Journal of Climate*

Cook, E. R., C. A. Woodhouse, C. M. Eakin, D. M. Meko, and D. W. Stahle, 2004: Long- Term Aridity Changes in the Western United States. *Science,* 306 (5698), 1015–1018, doi:10.1126/science.1102586.

Cook, E. R., R. Seager, M. A. Cane, and D. W. Stahle, 2007: North American drought: Reconstructions, causes, and consequences. *Earth Science Reviews*, 81 (1-2), 93–134, doi: http://dx.doi.org/10.1016/j.earscirev.2006.12.002.

Cook, E. R., R. Seager, R. R. Heim Jr, R. S. Vose, C. Herweijer, and C. Woodhouse, 2010: Megadroughts in North America: placing IPCC projections of hydroclimatic change in a long-term palaeoclimate context. *Journal of Quaternary Science*, 25 (1), 48–61, doi: 10.1002/jqs.1303.

Cook, E.R., et al. 2008: North American summer PDSI reconstructions, version 2a, IGBP PAGES World Data Cent. Paleoclimatology Data Contributions Service 2008-046, Paleoclimatology Program, NGDC, NOAA, Boulder, Colorado.

CRWUA 2013: Colorado River Water Users Association: http://www.crwua.org

Daly, C., W. P. Gibson, G. H. Taylor, G. L. Johnson, and P. Pasteris, 2002: A knowledge- based approach to the statistical mapping of climate, *Clim. Res.*, 22, 99–113, doi:10.3354/cr022099.

Dettinger, M. D., D. R. Cayan, H. F. Diaz, and D. M. Meko, 1998: North-south precipitation patterns in western North America on interannual-to-decadal timescales. *Journal of Climate*, *11*(12), 3095-3111.

Douglass, A. E., 1929: The Secret of the Southwest Solved With Talkative Tree Rings, pp. 736–770, Judd and Detweiler, Washington, D. C.

Feng, S., R. J. Oglesby, C. M. Rowe, D. B. Loope, and Q. Hu, 2008: Atlantic and Pacific SST influences on Medieval drought in North America simulated by the Community Atmospheric Model. *Journal of Geophysical Research: Atmospheres,* 113 (D11), doi: 10.1029/2007JD009347.

Feng, S., Q. Hu, and R. J. Oglesby, 2011: Influence of Atlantic sea surface temperatures on persistent drought in North America. *Climate dynamics*, 37 (3-4), 569-586 doi:10.1007/s00382-010-0835-x.

Forman, S. L., M. Spaeth, L. Marín, J. Pierson, J. Gómez, F. Bunch, and A. Valdez, 2006: Episodic Late Holocene dune movements on the sand-sheet area, Great Sand Dunes National Park and Preserve, San Luis Valley, Colorado, USA. *Quaternary Research*, 66 (1), 97-108.

Graham, N. E., et al., 2007: Tropical Pacific-mid-latitude teleconnections in medieval times, *Climatic Change*, 83, 241–285, doi:10.1007/s10584- 007-9239-2.

Graham, N. E., C. M. Ammann, D. Fleitmann, K. M. Cobb, and J. Luterbacher, 2011: Support for global climate reorganization during the "Medieval Climate Anomaly". *Climate Dynamics*, 37, 1217–1245, doi:http://dx.doi.org/10.1007/s00382-010-0914-z.

Gray, S. T., L. J. Graumlich, J. L. Betancourt, and G. T. Pederson, 2004: A tree-ring based reconstruction of the Atlantic Multidecadal Oscillation since 1567 A.D. *Geophysical Research Letters*, 31 (12), doi:10.1029/2004GL019932.

Grissino- Mayor, H. 1996: A 2129- year reconstruction of precipitation for northwestern New Mexico, USA, in Tree Rings, Environment, and Humanity, edited by J. S. Dean, D. M. Meko, and T. W. Swetnam, pp. 191–204, Radiocarbon, Tucson, Ariz.

Halfen, A. F., and W. C. Johnson, 2013: A review of Great Plains dune field chronologies. *Aeolian Research*.

Harpold, A. A., P. Brooks, S. Rajagopal, J. Heidbuchel, A. Jardine, and C. Stielstra, 2012a: Changes in snowpack accumulation and ablation in the intermountain west. *Water Resources Research*, *48*(11).

Harpold, A. A., et al., 2013: Changes in snow accumulation and ablation following the Las Conchas Forest Fire, New Mexico, USA. *Ecohydrology*.

Herweijer, C., R. Seager, E. R. Cook, and J. Emile-Geay, 2007: North American Droughts of the Last Millennium from a Gridded Network of Tree-Ring Data. *Journal of Climate,* 20(7), 1353–1376, doi:http://dx.doi.org/10.1175/JCLI4042.1.

Hidalgo, H. G., 2004: Climate precursors of multidecadal drought variability in the western United States. *Water Resources Research,* 40(12), W12504 doi:10.1029/2004WR003350.

Hoerling, et al., 2013: Causes and Predictability of the 2012 Great Plains Drought. *Bulletin of the American Meteorological Society*.

Horel, J. D., and J. M. Wallace, 1981: Planetary-scale atmospheric phenomena associated with the Southern Oscillation. *Monthly Weather Review*, *109*(4), 813-829.

Kennett, D. J., and J. P. Kennett, 2000: Competitive and cooperative responses to climatic instability in coastal southern California. *American Antiquity,* 379-395.

Knight, T. A., D. M. Meko, and C. H. Baisan, 2010: A bimillennial-length tree-ring reconstruction of precipitation for the Tavaputs Plateau, north-eastern Utah, *Quat. Res.,* 73, 107–117, doi:10.1016/j.yqres.2009.08.002.

Ljungqvist, F. C. 2010: A new reconstruction of temperature variability in the extra-tropical Northern Hemisphere during the last two millennia, *Geogr. Ann.,* 92, 339–351, doi:10.1111/j.1468-0459.2010.00399.x.

Loomis, S. E., J. M. Russell, B. Ladd, F. A. Street-Perrott, and J. S. Sinninghe Damsté, 2012: Calibration and application of the branched GDGT temperature proxy on East African lake sediments. *Earth and Planetary Science Letters*, *357*, 277-288.

Mann, M. E., et al., 2009: Global signatures and dynamical origins of the Little Ice Age and Medieval Climate Anomaly. *Science,* 326 (5957), 1256–1260, doi:10.1126/science. 1177303.

Mantua, N. J., S. R. Hare, Y. Zhang, J. M. Wallace, and R. C. Francis, 1997: A Pacific Interdecadal Climate Oscillation with Impacts on Salmon Production.

Bulletin of the *American Meteorological Society*, 78 (6), 1069–1079, doi:http://dx.doi.org/10.1175/ 1520-0477(1997)078⟨1069:APICOW⟩2.0.CO;2.

McCabe, G. J., M. A. Palecki, and J. L. Betancourt, 2004: Pacific and Atlantic Ocean influences on multidecadal drought frequency in the United States. *Proceedings of the National Academy of Sciences*, 101 (12), 4136–4141, doi:10.1073/pnas.0306738101.

Meko, D. M., C. A. Woodhouse, C. A. Baisan, T. Knight, J. J. Lukas, M. K. Hughes, and M. W. Salzer, 2007: Medieval drought in the upper Colorado River Basin. *Geophysical Research Letters*, 34 (10), 10 705–10 709, doi:10.1029/2007GL029988.

Meko, D. M., R. Touchan, and K. J. Anchukaitis, 2011: Seascorr: A MATLAB program for identifying the seasonal climate signal in an annual tree- ring time series, *Comput. Geosci.*, 37, 1234–1241, doi:10.1016/j.cageo.2011.01.013.

Munson, S. M., J. Belnap, and G. S. Okin, 2011: Responses of wind erosion to climate-induced vegetation changes on the Colorado Plateau. *Proceedings of the National Academy of Sciences*, *108*(10), 3854-3859.

NCDC 2013: Billion-Dollar Weather/Climate Events. Available online: http://www.ncdc.noaa.gov/billions

Newman, M., G. P. Compo, and M. A. Alexander, 2003: ENSO-Forced Variability of the Pacific Decadal Oscillation. *Journal of Climate*, 16 (23), 3853–3857, doi:10.1175/ 1520-0442(2003)016⟨3853:EVOTPD⟩2.0.CO;2.

Nowak, K., M. Hoerling, B. Rajagopalan, and E. Zagona, 2012: Colorado River Basin Hydroclimatic Variability. *Journal of Climate* 25(12), 4389-4403 doi: http://dx.doi.org/10.1175/JCLI-D-11-00406.1.

Oglesby, R., S. Feng, Q. Hu, and C. Rowe, 2012: The role of the Atlantic Multidecadal Oscillation on medieval drought in North America: Synthesizing results from proxy data and climate models. *Global and Planetary Change*, 84 - 85 (0), 56 – 65, doi:10.1016/j. gloplacha.2011.07.005.

Oppo, D. W., Y. Rosenthal, and B. K. Linsley, 2009: 2,000-year-long temperature and hydrology reconstructions from the Indo-Pacific warm pool, *Nature*, 460, 1113–1116, doi:10.1038/nature08233.

Painter, T. H., et al., 2007: Impact of disturbed desert soils on duration of mountain snow cover. *Geophysical Research Letters*, *34*(12), L12502.

Painter, T. H., J. S. Deems, J. Belnap, A. F. Hamlet, C. C. Landry, and B. Udall, 2010: Response of Colorado River runoff to dust radiative forcing in snow. *Proceedings of the National Academy of Sciences*, *107*(40), 17125-17130.

Painter, T. H., S. M. Skiles, J. S. Deems, A. C. Bryant, and C. C. Landry, 2012: Dust radiative forcing in snow of the Upper Colorado River Basin: 1. A 6-year record of energy balance, radiation, and dust concentrations. *Water Resources Research*, *48*(7).

Redmond, K. T., and R. W. Koch, 1991: Surface climate and streamflow variability in the western United States and their relationship to large-scale circulation indices. *Water Resources Research*, 27 (9), 2381-2399.

Routson, C. C., C. A. Woodhouse, and J. T. Overpeck, 2011: Second century megadrought in the Rio Grande headwaters, Colorado: How unusual was medieval drought? *Geophysical Research Letters,* 38 (22), L22 703, doi:10.1029/2011GL050015.

Salzer, M. W., and K. F. Kipfmueller 2005: Reconstructed temperature and precipitation on a millennial timescale from tree- rings in the southern Colorado Plateau, *Clim. Change*, 70, 465–487, doi:10.1007/s10584-005-5922-3.

Salzer, M. W., A. G. Bunn, N. E. Graham, and M. K. Hughes, 2013: Five millennia of paleotemperature from tree-rings in the Great Basin, USA. *Climate Dynamics*, 1-10.

Schubert, S., et al., 2009: A US CLIVAR Project to Assess and Compare the Responses of Global Climate Models to Drought-Related SST Forcing Patterns: Overview and Results. *Journal of Climate,* 22 (19), 5251–5272, doi:http://dx.doi.org/10.1175/2009JCLI3060.1.

Seager, R., R. Burgman, Y. Kushnir, A. Clement, E. Cook, N. Naik, and J. Miller, 2008: Tropical Pacific forcing of North American Medieval Megadroughts: Testing the Concept with an Atmosphere Model Forced by Coral-Reconstructed SSTs. *Journal of Climate,* 21 (23), 6175–6190, doi:http://dx.doi.org/10.1175/2008JCLI2170.1.

Seager, R., N. Graham, C. Herweijer, A. L. Gordon, Y. Kushnir, and E. Cook, 2007: Blueprints for Medieval hydroclimate. *Quaternary Science Reviews,* 26 (19-21), 2322– 2336, doi:http://dx.doi.org/10.1016/j.quascirev.2007.04.020.

Seager, R., M. Ting, C. Li, N. Naik, B. Cook, J. Nakamura, and H. Liu, 2012: Projections of declining surface-water availability for the southwestern United States. *Nature Climate Change*.

Seager, R., L. Goddard, J. Nakamura, N. Henderson, and D. E. Lee, 2013: Dynamical causes of the 2010/11 Texas-northern-Mexico drought. *Journal of Hydrometeorology*, (2013).

Stine, S., 1994: Extreme and persistent drought in California and Patagonia during mediaeval time. *Nature*, 369 (6481), 546–549, URL http://dx.doi.org/10.1038/369546a0.

Steinhilber, F., J. Beer, and C. Fröhlich 2009: Total solar irradiance during the Holocene, *Geophys. Res. Lett.*, 36, L19704, doi:10.1029/ 2009GL040142.

Tierney, J. E., D. W. Oppo, Y. Rosenthal, J. M. Russell, and B. K. Linsley, 2010a: Coordinated hydrological regimes in the Indo-Pacific region during the past two millennia. *Paleoceanography*, 25(1), doi:10.1029/2009PA001871.

Tierney, J. E., J. M. Russell, H. Eggermont, E. C., Hopmans, D. Verschuren, and J. S. Sinninghe Damsté, 2010b: Environmental controls on branched tetraether lipid distributions in tropical East African lake sediments. *Geochimica et Cosmochimica Acta*, *74*(17), 4902-4918.

Van Mantgem, et al., 2009: Widespread increase of tree mortality rates in the western United States. *Science*, *323*(5913), 521-524.

Weiss, J. L., C. L. Castro, and J. T. Overpeck, 2009: Distinguishing pronounced droughts in the southwestern United States: Seasonality and effects of warmer temperatures, *Journal of Climate*, 22, 5918–5932, doi:10.1175/ 2009JCLI2905.1.

Weiss, J. L., J. T. Overpeck, J. E. Cole, 2012: Warmer Led to Drier: Dissecting the 2011 Drought in the Southern U.S. *Southwest Climate Outlook*, http://climas.arizona.edu/feature-articles

Williams, et al., 2012: Temperature as a potent driver of regional forest drought stress and tree mortality. *Nature Climate Change*

Woodhouse, C. A. and J. T. Overpeck, 1998: 2000 Years of Drought Variability in the Central United States. *Bulletin of the American Meteorological Society*, 79 (12), 2693– 2714, doi:http://dx.doi.org/10.1175/1520-0477(1998)079⟨2693:YODVIT⟩2.0.CO;2.

Yan, H., L. Sun, Y. Wang, W. Huang, S. Qiu, and C. Yang, 2011: A record of the Southern Oscillation Index for the past 2,000 years from precipitation proxies. *Nature Geoscience*, 4(9), 611-614.

APPENDIX A

SECOND CENTURY MEGADROUGHT IN THE RIO GRANDE HEADWATERS, COLORADO: HOW UNUSUAL WAS MEDIEVAL DROUGHT?

Cody C. Routson,[1] Connie A. Woodhouse,[2] and Jonathan T. Overpeck [1,3,4]

[1]Department of Geosciences, University of Arizona, Tucson, Arizona, USA

[2]School of Geography and Development, University of Arizona, Tucson, Arizona, USA

[3]Institute of the Environment, University of Arizona, Tucson, Arizona, USA

[4]Department of Atmospheric Sciences, University of Arizona, Tucson, Arizona, USA

This appendix has been published in Geophysical Research Letters, and reproduced with written permission from John Wiley and Sons. See APPENDIX E.

CITATION: Routson, C. C., C. A. Woodhouse, and J. T. Overpeck, 2011: Second century megadrought in the Rio Grande headwaters, Colorado: How unusual was medieval drought? Geophysical Research Letters, 38 (22), L22 703, doi:10.1029/2011GL050015.

A.1 Abstract

[1] A new tree-ring record from living and remnant bristlecone pine (Pinus aristata) wood from the headwaters region of the Rio Grande River, Colorado is used in conjunction with other regional records to evaluate periods of unusually severe drought over the past two millennia (B.C. 268 to A.D. 2009). Our new record contains a multi-century period of unusual dryness between 1 and 400 A.D., including an extreme drought during the 2nd century. Characterized by almost five

decades of drought (below average ring width), we hypothesize this megadrought is equally, if not more severe than medieval period megadroughts in this region. Published paleoclimate time series help define the spatial extent, severity, and potential causes of the 2nd century megadrought. Furthermore, this early period of unusual dryness has intriguing similarities to later medieval period aridity. Our findings suggest we should anticipate similar severe drought conditions in an even warmer and drier future.

A.2 Introduction

[2] A better understanding of the range of long-term moisture variability is critical for anticipation of, and adaptation to, projected increases in aridity and drought frequency in the southwestern US (henceforth referred to as the Southwest) [Overpeck and Udall, 2010]. Many Southwestern high-resolution proxy records show numerous droughts over the past millennium, including droughts far more severe than we have experienced during the historical period [e.g., Woodhouse and Overpeck, 1998; Cook et al., 2004, 2010; Meko et al., 2007]. The medieval interval (ca. A.D. 900 to 1400), a period with relatively warm Northern Hemisphere temperatures [e.g., Mann et al., 2008], has been highlighted as a period in western North America with increased drought severity, duration, and extent [e.g., Stine, 1994; Cook et al., 2004, 2010; Meko et al., 2007; Woodhouse et al., 2010]. Iconic decades-long "megadroughts," including Mono Lake low-stands [Stine, 1994], the mid-12th century drought associated with dramatic decreases in Colorado River flow [Meko et al., 2007], and the "Great Drought" associated with the abandonment of Ancient

Pueblo civilization in the Colorado Plateau region [Douglass, 1929], all occur during the medieval period.

[3] Were medieval drought magnitude, severity, frequency, and extent unique? New longer paleoclimate records indicate that medieval droughts were not entirely matchless in prior centuries [i.e., Knight et al., 2010]. Medieval drought was likely influenced by numerous factors including warmer Northern Hemisphere temperatures, warmer regional temperatures, cold eastern equatorial Pacific sea surface temperatures (SSTs), and warm North Atlantic SSTs [Seager et al., 2007; Conroy et al., 2009a; Graham et al., 2010; Cook et al., 2010]. Did these same factors influence extreme drought before medieval time? In this paper we compare a new 2200 year long moisture sensitive bristlecone (Pinus aristata) tree-ring chronology from the southern San Juan Mountains, Colorado, with existing records in the broader Four-Corners region (Colorado, Utah, Arizona, and New Mexico). We selected this region because it serves as a key headwaters region for the Southwest (e.g., Colorado and Rio Grande Rivers) and because it was located in the epicenter of known medieval megadroughts [Cook et al., 2008]. We find evidence that indicates centuries-long periods of aridity and Southwestern megadrought were not just a medieval phenomenon. Comparing the possible drivers of medieval drought with potential drivers during the 2nd century suggests that similar factors could have influenced drought during the two periods, helping us understand fundamental causes of severe and persistent drought.

A.3 Tree-Ring and Climate Analysis

[4] Our new chronology was developed from living and remnant samples of moisture sensitive Rocky Mountain bristlecone pine (Pinus aristata) growing near Summitville in the southern San Juan Mountains, Colorado (Figure A.1). Increment cores were taken from living trees and cross-sections were obtained from dead remnant wood within the stand. Cores and cross-sections were dated to the calendar year using skeleton plots and crossdating [Stokes and Smiley, 1968]. Individual growth rings were measured to the nearest 0.01 mm, and crossdating accuracy was checked statistically [Holmes, 1983]. Negative exponential detrending was employed to preserve the most low frequency variance while removing biological growth trends and generating standardized tree-ring indices [Cook, 1985]. To further preserve low frequency climate related variability, only tree-ring series longer than 470 years were included in the final chronology [Cook et al., 1995]. The final composite chronology (Figure A.2) includes 28 trees and extends from B.C. 268 to A.D. 2009. Sample depth drops steadily before A.D. 700 to one tree prior to B.C. 200. Six trees span the 2nd century drought. Subsample signal, a measure of common variance between trees, is 0.85 or greater after 10 B.C. (0.85 is a general threshold used to indicate good signal strength [Wigley et al., 1984]).

[5] Bristlecone pine grows on high elevation mountain slopes and growth has a notoriously complex relationship between temperature and moisture [e.g., Fritts, 1969; LaMarche and Stockton, 1974]. Here, we have used a set of methods designed to define the tree growth/climate response of this site and its consistency over time

(details in the auxiliary material). Correlation analysis with instrumental gridded PRISM data (monthly precipitation and temperature) [Daly et al., 2002] spanning A.D. 1895-2009 from the Rio Grande headwaters hydrologic unit (WestMap, 2010, accessed 31 August 2010, available at http://www.cefa. dri.edu/Westmap/) was used to evaluate the climate sensitivity of our new bristlecone chronology during the period covered by instrumental records. The Rio Grande headwaters hydrologic unit (Figure A.1) was used because it encompasses Summitville and the San Luis Valley, through which the Rio Grande flows. Seasonal correlation analysis and partial correlation analysis [Meko et al., 2011] with the PRISM data show tree growth has a significant positive relationship with March through July precipitation ($r = 0.47$, $p < 0.01$) and has a statistically independent significant negative relationship, based on partial correlations, with March through July temperature ($r = -0.37$, $p < 0.01$). A positive relationship with late winter through early summer precipitation suggests snowpack influences on soil moisture at the beginning of the growing season, as well as early growing season precipitation both promote tree growth. A negative relationship with March through July temperature suggests that warm spring and early summer months hasten the timing of snowmelt in addition to driving increased evaporation contributing to moisture stress in the trees. The inset in Figure A.2 shows the relationship of March through July precipitation and ring-width from 1895 to the present. We also evaluated potential relationships between growth and late summer temperatures, which are sometimes important to high elevation tree growth, using PRISM data. We found that tree growth responded positively to warm August temperature during years with wet spring months, but August temperatures had no influence on spring moisture sensitivity (see auxiliary material). Moving correlation analysis between our bristlecone chronology and regional PDSI and temperature reconstructions [Salzer and Kipfmueller, 2005; Cook et al., 2008] indicates our chronology has a consistent moisture balance signal over the past 2000 years (see auxiliary material). Although the climate signal is not as strong as that found in lower elevation species, bristlecone pine allows us to develop a much longer record than possible using lower elevation species.

A.4 Second Century Droughts

[6] Our new record smoothed with a 25-year running mean shows how moisture balance in the southern San Juan Mountains has varied on decadal time scales over the past 2200 years (Figure A.2). The smoothed chronology reveals two periods of enhanced drought frequency and severity relative to the rest of the record. The later period, A.D. ~1050–1350, corresponds with medieval aridity well documented in other records [Woodhouse and Overpeck, 1998; Cook et al., 2004; Meko et al., 2007]. The earlier period is more persistent (A.D.~1–400), and includes the most pronounced event in the Summitville chronology: a multidecadal-length drought during the 2nd century. This drought includes the unsmoothed record's driest 25-year interval (A.D. 148 to A.D. 173) as well as a longer 51-year period, A.D. 122–172, that has only two years with ring width slightly above the long-term mean. The smoothed chronology shows the periods A.D. 77–282 and A.D. 301–400 are the longest (206 and 100 years, respectively, below the long-term average) droughts of

the entire 2276-yr record.

[7] Because the climate response of bristlecone pine is not as robust as lower elevation species, and because the new Summitville chronology only includes six trees during the 2nd century drought interval, we assessed the reliability of our record using other moisture-sensitive reconstructions from the region. Comparing the Summitville chronology with reconstructed Colorado Plateau PDSI [Cook et al., 2008], annual precipitation from El Malpais, New Mexico (included in PDSI, so not strictly an independent record) [Grissino-Mayor, 1996] and Tavaputs, Utah [Knight et al., 2010] (Figure A.3, top) highlights the regional significance of the 2nd century drought. Consistent severity of the 2nd century drought among the records, across elevation (1630 m – 3500 m), space (Figure A.1), and tree species (Pinus aristata, Pseudotsuga menziesii) gives us more confidence in the timing and severity of this drought. Medieval megadroughts, including the 1150's and late 1200's droughts are not as pronounced in the high-elevation Summitville chronology. The 2nd century drought, however, appears to have been equal to, or more extreme, than the iconic medieval mega- droughts in these other proxy records. Sample size and climate response of the Summitville chronology limits the conclusions we can make. However, with limitations in mind and the support of the other records, we hypothesize the 2nd century drought may be one of the most severe and persistent droughts the Colorado Plateau region has experienced during the last 2000 years (Table A.1). Assessing the spatial extent of the drought with composite maps of gridded PDSI reconstructions for the years A.D. 148–173 (Figure A.S1 in the auxiliary material) [Cook et al., 2008] indicates that the 2nd century drought impacted

a region that extends from southern New Mexico north and west into Idaho. The drought was less severe in Nevada and California, and no PDSI data are available for the 2nd century in the central and eastern United States. The spatial pattern of the 2nd century mega- drought appears similar to the mid-12th century megadrought highlighted in PDSI and Colorado River flow reconstructions [Meko et al., 2007; Cook et al., 2008].

[8] We investigated potential broad-scale climatic influences on Four Corners hydroclimate by comparing our new drought record with published records from regions hypothesized to have influenced Southwestern drought. Due to a limited number of available records during the 2nd century which all contain uncertainties, the following analyses should be viewed as exploratory.

[9] Warm regional temperatures exacerbated recent drought severity [e.g., Breshears et al., 2005; Weiss et al., 2009; Woodhouse et al., 2010], and a Colorado Plateau temperature reconstruction [Salzer and Kipfmueller, 2005] indicates that medieval period droughts during the mid 12th and late 13th centuries were potentially influenced by warmer than average temperatures as well. A small positive temperature anomaly on the Colorado Plateau also occurs during the 2nd century, indicating that local temperature anomalies may be a common influence on megadrought in the region. Warm global or hemispheric temperatures can also influence Southwest drought through changes in circulation [Cook et al., 2010]. Few hemispheric temperature reconstructions extend back to the 2nd century, making a comparison between medieval and 2nd century temperature difficult. A multiproxy Northern Hemisphere temperature reconstruction [Moberg et al., 2005] shows no

anomalous warming during the 2nd century (Figure A.3). A more recent multiproxy Northern Hemisphere temperature reconstruction however, shows a “Roman Warm Period” spanning 1–300 A.D. [Ljungqvist, 2010] that could be analogous to warmth associated with Southwestern megadroughts during medieval times. Both Moberg et al. [2005] and Ljungqvist [2010] show warm Northern Hemisphere temperatures during the medieval period. In addition, both megadrought periods may have occurred under somewhat elevated levels of solar irradiance that were above the past 2200 year average (Figure A.3).

[10] Although elevated temperatures may have accompanied this drought, other factors were likely important as well. Sea surface temperature (SST) can have a significant impact on Southwestern hydroclimate through changes in oceanic and atmospheric circulation. Tropical Pacific SST, modulated by the El Niño/Southern Oscillation (ENSO), has an important influence on Southwestern precipitation. The tropical Pacific warm phase (El Niño) is typically associated with increased regional precipitation, whereas the cool phase (La Niña) is typically associated with decreased regional precipitation and drought [e.g., Hoerling and Kumar, 2003; Seager et al., 2005]. Atlantic SST’s have a less well understood, but important correspondence with Southwestern hydroclimate, whereby warm North Atlantic SST’s are thought to influence the rainfall and drought severity, most strongly in summer [Hoerling and Kumar, 2003; McCabe et al., 2004; Kushnir et al., 2010]. Medieval megadroughts were likely associated with persistent “La Niña like” conditions, and warm North Atlantic SST [Seager et al., 2007; Conroy et al., 2009a; Graham et al., 2010].

[11] Again limited records are available to evaluate potential SST influences

on 2nd century megadrought. An ocean sediment record reflecting western equatorial Pacific SST shows positive anomalies during both the medieval period and the 2nd century [Oppo et al., 2009], suggesting that persistent or stronger La Niña-like conditions may have forced both 2nd century and medieval drought. The 2nd century and late medieval period aridity also coincide with intervals of increased El Niño frequency in the eastern tropical Pacific inferred from changes in grain size in sediment cores from Lake El Junco in the Galapagos Islands [Conroy et al., 2008]. Changes in El Junco grain size are a function of precipitation, which is closely connected in the Galapagos with some types of strong El Niño events, suggesting that strong El Niño events may have punctuated the persistent La Niña-like conditions. An SST record also from Lake El Junco shows La Niña-like background conditions spanning the medieval period, supporting our interpretation [Conroy et al., 2009b]. The coincidence of heightened El Niño frequency within a La Niña-like background state corresponds closely to one mode of ENSO variance characterized by Fedorov and Philander [2000]. On the other hand, the extended period of increased El Niño frequency, as inferred from El Junco, contains two abrupt decreases that correspond fairly well to the two droughts in the early part of the Summitville record (Figure A.3) supportive of strong La Niña conditions. Dating uncertainty and limited other records make these assessments less than robust, and it is clear that more work is needed to understand the equatorial Pacific conditions that may promote megadrought. The influence of North Atlantic SST on the 2nd century is even more uncertain due to the scarcity of high-resolution paleodata available. Northern Iceland SSTs [Sicre et al., 2008] have a positive anomaly during the medieval period, but are equivocal with respect to the 2nd century period, although modest warmth spans most of the period characterized by drought. The equatorial North Atlantic appears however to be more important for influencing Southwestern drought, at least during the instrumental period [Kushnir et al., 2010], and unfortunately, no proxy records that could resolve this period of drought are currently available.

A.5 Conclusions and Implications

[12] A new millennial-length moisture-sensitive bristlecone pine chronology from the San Juan River (a major tributary of the Colorado River) and Rio Grande headwaters region of southern Colorado provides insight on droughts and changes in aridity over the past two millennia in the Southwest. Our new record extends back 2200 years and shows a broader range of drought variability, including a drought that persisted from A.D. 122 to A.D. 172. Based on our findings, we hypothesize that megadroughts are not unique to the medieval period. Available regional moisture records indicate the 2nd century drought likely extended from southern New Mexico to Idaho, possibly comparable in extent to the mid 12th century drought. More high-resolution moisture records are needed to evaluate both the severity and full extent of the 2nd century drought. Additional bristlecone pine chronologies in the southern Colorado region would allow a calibrated reconstruction of moisture variability.

[13] Attributing potential causes of megadrought is challenging due to scarcity of millennial-length records. Reconstructed Colorado Plateau temperature suggests warmer than average temperature could have influenced both 2nd century and

medieval drought severity. Available data also suggest that the Northern Hemisphere may have been warm during both intervals. Tropical Pacific SST and El Niño frequency reconstructions indicate similar conditions could have prevailed during the medieval and 2nd century periods, potentially contributing to drought severity and duration. Warm North Atlantic SST likely prevailed during the medieval period, but possible connections with the Atlantic remain ambiguous with respect to the 2nd century.

[14] Given the effects of recent drought on water resources and ecosystems in the Southwest [Breshears et al., 2005; Overpeck and Udall, 2010], it will be important to test our hypothesis that 2nd century drought severity rivaled medieval megadroughts and more closely examine potential relationships with hemispheric climate patterns. Testing our hypothesis will require a better network of millennial length moisture proxy records that retain both short and long time-scale climate variability in addition to more high-resolution reconstructions of global climate patterns. Until the climate dynamics of megadrought are thoroughly understood, managers of water and natural resources in the Four Corners, Rio Grande, and Colorado regions should take note that megadroughts as long, or longer, than 50 years could reoccur with the caveat that future droughts will likely be even warmer than those in the past [Karl et al., 2009; Weiss et al., 2009; Overpeck and Udall, 2010].

[15] Acknowledgments. We thank the NOAA Climate Program Office-funded Climate Assessment for the Southwest Project and NSF Graduate Research Fellowship program, and the SFAZ Graduate Research Fellowship for support of this project. We also thank David Meko, Julio Betancourt, Troy Knight, Jessica Conroy

and Nick McKay for data, discussion and insights. We value the reviews from David Stahle and Richard Seager, which helped us strengthen the paper.

[16] The Editor thanks David Stahle and Richard Seager for their assistance in evaluating this paper.

A.6 References

Breshears, D. D., et al. (2005), Regional vegetation die-off in response to global change type drought, Proc. Natl. Acad. Sci. U. S. A., 102(42), 15,144–15,148, doi:10.1073/pnas.0505734102.

Conroy, J. L., J. T. Overpeck, J. E. Cole, T. M. Shanahan, and M. Steinitz-Kannan (2008), Holocene changes in eastern tropical Pacific climate inferred from a Galápagos lake sediment record, Quat. Sci. Rev., 27, 1166–1180, doi:10.1016/j.quascirev.2008.02.015.

Conroy, J. L., J. T. Overpeck, J. E. Cole, and M. Steinitz-Kannan (2009a), Variable oceanic influences on western North American drought over the last 1200 years, Geophys. Res. Lett., 36, L17703, doi:10.1029/ 2009GL039558.

Conroy, J. L., et al. (2009b), Unprecedented recent warming of surface temperatures in the eastern tropical Pacific Ocean, Nat. Geosci., 2, 46– 50, doi:10.1038/ngeo390.

Cook, E. R. (1985) A time series analysis approach to tree-ring standardization, Ph.D. dissertation, Univ. of Ariz., Tucson.

Cook, E. R., K. R. Briffa, D. M. Meko, D. A. Graybill, and G. Funkhouser (1995), The “segment length curse” in long tree-ring chronology development for palaeolclimatic studies, Holocene, 5(2), 229–237, doi:10.1177/ 095968369500500211.

Cook, E. R., C. A. Woodhouse, C. M. Eakin, D. M. Meko, and D. W. Stahle (2004), Long-term aridity changes in the western United States, Science, 306(5698), 1015–1018, doi:10.1126/science.1102586.

Cook, E. R., et al. (2008), North American summer PDSI reconstructions, version 2a, IGBP PAGES World Data Cent. Paleoclimatol. Data Contrib. Ser. 2008-046, Paleoclimatol. Program, NGDC, NOAA, Boulder, Colo.

Cook, E. R., et al. (2010), Megadroughts in North America: Placing IPCC projections of hydroclimatic change in a long-term palaeoclimate context, J. Quat. Sci., 25, 48–61, doi:10.1002/jqs.1303.

Daly, C., W. P. Gibson, G. H. Taylor, G. L. Johnson, and P. Pasteris (2002), A knowledge-based approach to the statistical mapping of climate, Clim. Res., 22, 99–113, doi:10.3354/cr022099.

Douglass, A. E. (1929), The Secret of the Southwest Solved With Talkative Tree Rings, pp. 736–770, Judd and Detweiler, Washington, D. C.

Fedorov, A. V., and S. G. Philander (2000), Is El Niño changing?, Science, 288, 1997–2002, doi:10.1126/science.288.5473.1997.

Fritts, H. C. (1969), Bristlecone pine in the White Mountains of California. Growth and ring-width characteristics, Pap. Lab. Tree Ring Res., 4, 1–44.

Graham, N. E., C. M. Ammann, D. Fleitmann, K. M. Cobb, and J. Luterbacher (2010), Support for global climate reorganization during the Medieval Climate Anomaly, Clim. Dyn., doi:10.1007/s00382-010-0914-z.

Grissino-Mayor, H. (1996), A 2129-year reconstruction of precipitation for northwestern New Mexico, USA, in Tree Rings, Environment, and Humanity, edited by J. S. Dean, D. M. Meko, and T. W. Swetnam, pp. 191–204, Radiocarbon, Tucson, Ariz.

Hoerling, M., and A. Kumar (2003), The perfect ocean for drought, Science, 299, 691–694, doi:10.1126/science.1079053.

Holmes, R. L. (1983), Computer-assisted quality control in tree-ring dating and measurement, Tree Ring Bull., 43, 69–78.

Karl, T. R., J. M. Melillo, and T. C. Peterson (Eds.) (2009), Global Climate Change Impacts in the United States, Cambridge Univ. Press, Cambridge, U. K.

Knight, T. A., D. M. Meko, and C. H. Baisan (2010), A bimillennial-length tree-ring reconstruction of precipitation for the Tavaputs Plateau, north-eastern Utah, Quat. Res., 73, 107–117, doi:10.1016/j.yqres.2009.08.002.

Kushnir, Y., et al. (2010), Mechanisms of tropical Atlantic SST influence on North American hydroclimate variability, J. Clim., 23, 5610–5628,doi:10.1175/2010JCLI3172.1.

LaMarche, V. C., and C. W. Stockton (1974), Chronologies from temperature-sensitive bristlecone pines at upper treeline in western United States, Tree Ring Bull., 34, 21–45.

Ljungqvist, F. C. (2010), A new reconstruction of temperature variability in the extra-tropical Northern Hemisphere during the last two millennia, Geogr. Ann., 92, 339–351, doi:10.1111/j.1468-0459.2010.00399.x.

Mann, M. E., Z. Zhang, M. K. Hughes, R. S. Bradley, S. K. Miller, S. Ruthford, and F. Ni (2008), Proxy-based reconstructions of hemispheric and global surface temperature variations over the past two millennia, Proc. Natl. Acad. Sci. U. S. A., 105(36), 13,252–13,257, doi:10.1073/pnas.0805721105.

McCabe, G. J., M. A. Palecki, and J. L. Betancourt (2004), Pacific and Atlantic Ocean influences on multidecadal drought frequency in the United States, Proc. Natl. Acad. Sci. U. S. A., 101(12), 4136–4141, doi:10.1073/pnas.0306738101.

Meko, D. M., C. A. Woodhouse, C. H. Baisan, T. Knight, J. J. Lukas, M. K. Hughes, and W. Salzer (2007), Medieval drought in the Upper Colorado River Basin, Geophys. Res. Lett., 34, L10705, doi:10.1029/ 2007GL029988.

Meko, D. M., R. Touchan, and K. J. Anchukaitis (2011), Seascorr: A MATLAB program for identifying the seasonal climate signal in an annual tree-ring time series, Comput. Geosci., 37, 1234–1241, doi:10.1016/j.cageo. 2011.01.013.

Moberg, A., et al. (2005), Highly variable Northern Hemisphere temperatures reconstructed from low-and high-resolution proxy data, Nature, 433, 613–617, doi:10.1038/nature03265.

Oppo, D. W., Y. Rosenthal, and B. K. Linsley (2009), 2,000-year-long temperature and hydrology reconstructions from the Indo-Pacific warm pool, Nature, 460, 1113–1116, doi:10.1038/nature08233.

Overpeck, J. T., and B. Udall (2010), Dry times ahead, Science, 328, 1642–1643, doi:10.1126/science.1186591.

Salzer, M. W., and K. F. Kipfmueller (2005), Reconstructed temperature and precipitation on a millennial timescale from tree-rings in the southern Colorado Plateau, Clim. Change, 70, 465–487, doi:10.1007/s10584-005-5922-3.

Seager, R., Y. Kushnir, C. Herweijer, N. Naik, and J. Velez (2005), Modeling of tropical forcing of persistent droughts and pluvials over western North America: 1856–2000, J. Clim., 18(19), 4065–4088, doi:10.1175/ JCLI3522.1.

Seager, R., et al. (2007), Blueprints for Medieval hydroclimate, Quat. Sci. Rev., 26, 2322–2336, doi:10.1016/j.quascirev.2007.04.020.

Sicre, M. A., et al. (2008), Decadal variability of sea surface temperatures off North Iceland over the last 2000 yrs, Earth Planet. Sci. Lett., 268, 137–142, doi:10.1016/j.epsl.2008.01.011.

Steinhilber, F., J. Beer, and C. Fröhlich (2009), Total solar irradiance during the Holocene, Geophys. Res. Lett., 36, L19704, doi:10.1029/ 2009GL040142.

Stine, S. (1994), Extreme and persistent drought in California and Patagonia during medieval time, Nature, 369(6481), 546–549, doi:10.1038/ 369546a0.

Stokes, M. A., and T. L. Smiley (1968), An Introduction to Tree-Ring Dating, 73 pp., Univ. of Chicago Press, Chicago, Ill.

Weiss, J. L., C. L. Castro, and J. T. Overpeck (2009), Distinguishing pronounced droughts in the southwestern United States: Seasonality and effects of warmer temperatures, J. Clim., 22, 5918–5932, doi:10.1175/ 2009JCLI2905.1.

Wigley, T. M. L., K. R. Briffa, and P. D. Jones (1984), On the average value of correlated time series, with applications in dendroclimatology and hydrometeorology, J. Clim. Appl. Meteorol., 23, 201–213, doi:10.1175/1520-0450(1984)023<0201:OTAVOC>2.0.CO;2.

Woodhouse, C. A., and J. T. Overpeck (1998), 2000 years of drought variability in the central United States, Bull. Am. Meteorol. Soc., 79, 2693–2714, doi:10.1175/1520-0477(1998)079<2693:YODVIT>2.0. CO;2.

Woodhouse, C. A., D. M. Meko, G. M. MacDonald, D. W. Stahle, and E. R. Cook (2010), A 1,200-year perspective of 21st century drought in the southwestern North America, Proc. Natl. Acad. Sci. U. S. A., 107(50), 21,283–21,288, doi:10.1073/pnas.0911197107.

A.7 Tables and Figures

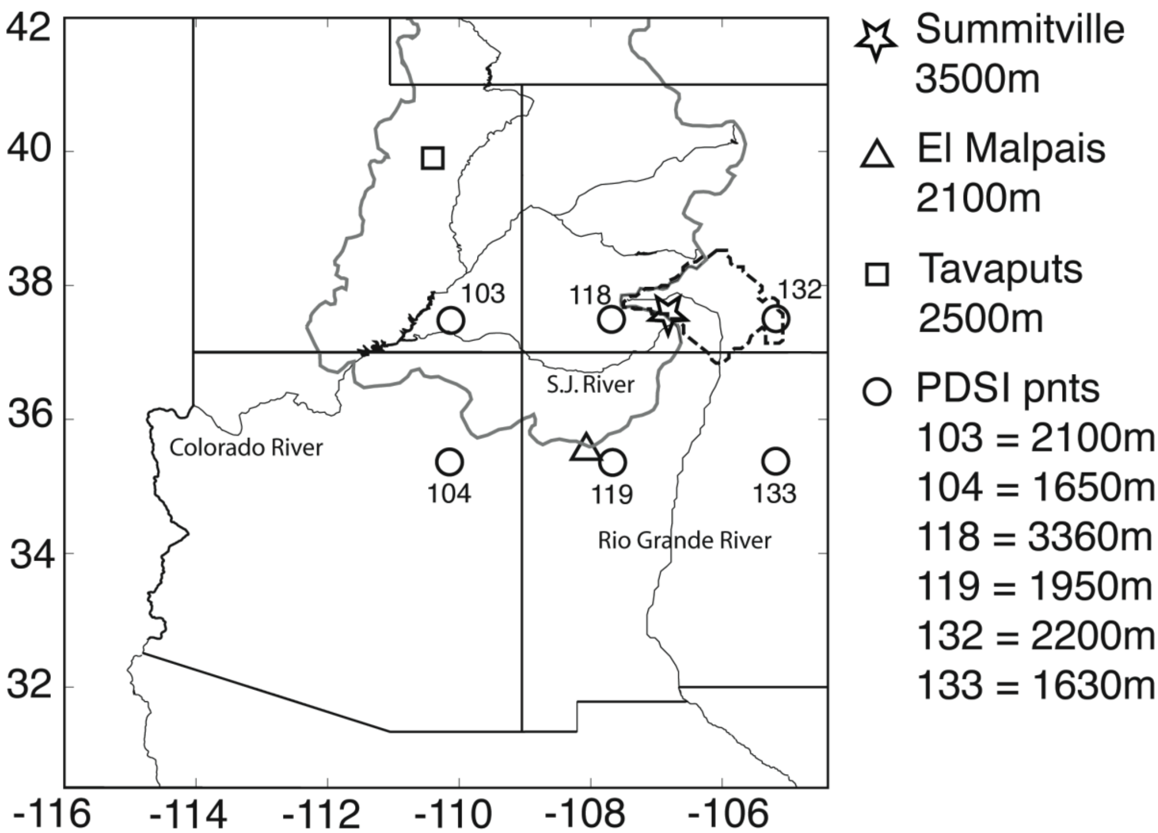

Figure A.1: Regional map showing locations and elevations of moisture records employed. PDSI points 132 and 133 only extend back to A.D. 210 and do not cover the 2nd century drought. The upper Colorado River basin is outlined in grey. The Rio Grande headwaters hydrologic unit is outlined in dashed black.

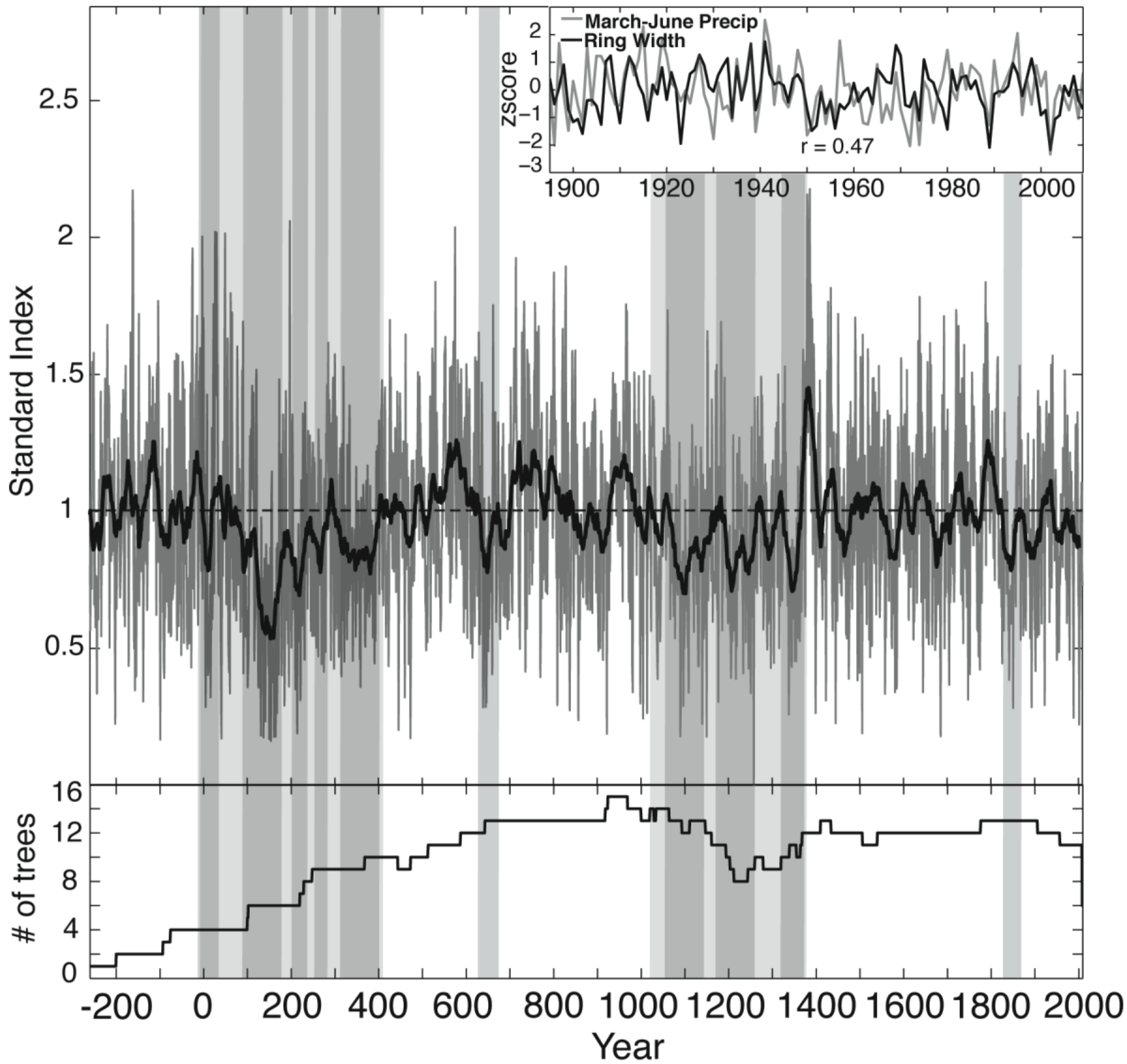

Figure A.2: Summitville bristlecone chronology standard index (grey) smoothed with a 25-yr moving average (black) and number of trees (bottom). Narrow shaded bars are the 10 driest 25-yr periods defined by the Summitville chronology. Wide shaded bars highlight multicentury periods of increased aridity and drought frequency. Upper right inset: ring width (black) with March-July PRISM precipitation data from Rio Grande headwaters hydrologic unit (grey)

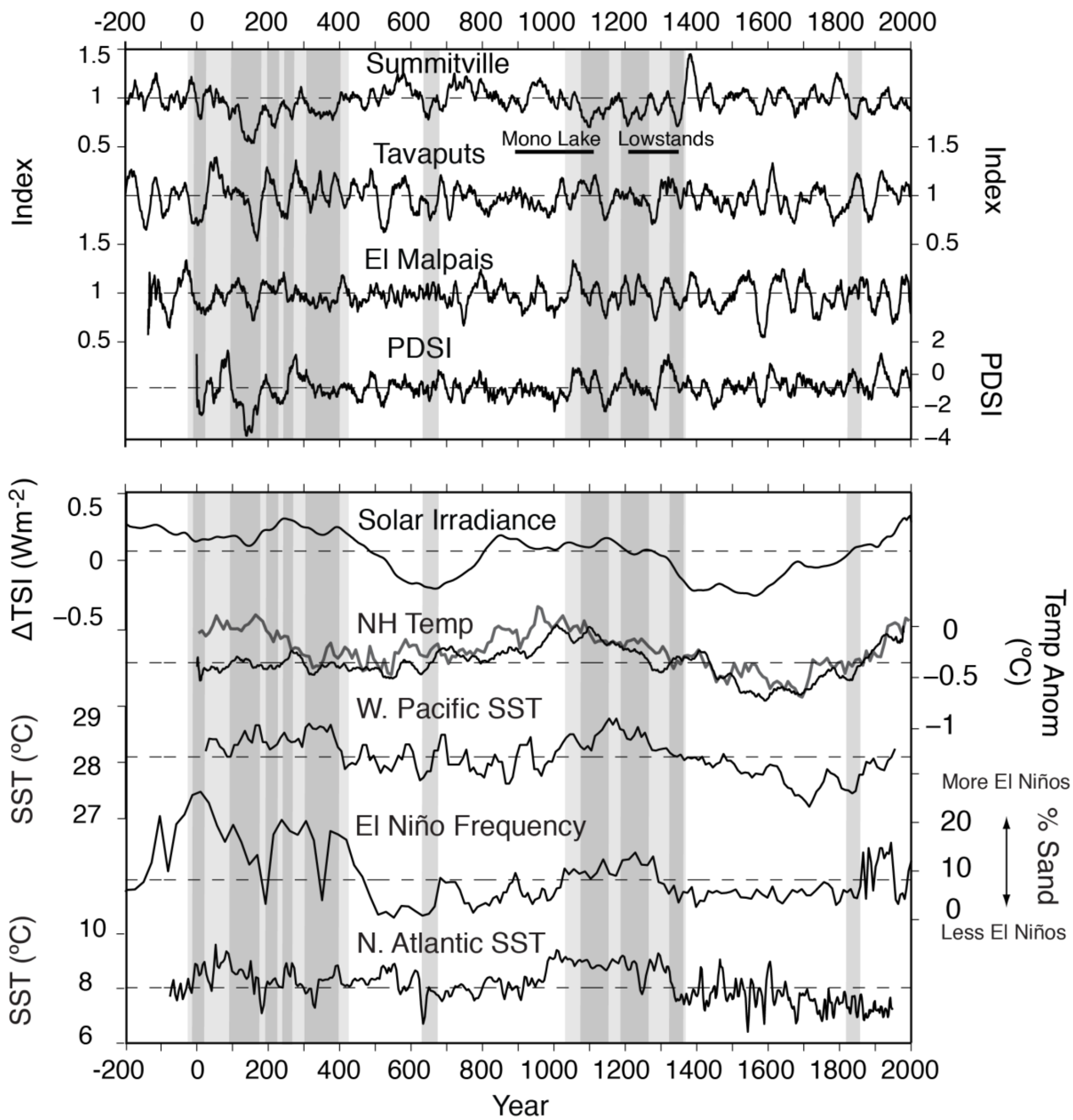

Figure A.3: (top) Colorado Plateau region moisture records including Summitville CO, Tavaputs UT [Knight et al., 2010], El Malpais NM [Grissino-Mayor, 1996], PDSI [Cook et al., 2008] showing the timing and severity of the 2nd century megadrought. (bottom) Records of variables that may influence drought in the Four Corners region: inferred total solar irradiance (smoothed with a 50 yr MA) [Steinhilber et al., 2009], Northern Hemisphere temperature (smoothed with a 50 yr MA) [Moberg et al., 2005] (black) and [Ljunqvist, 2010] (grey), west Pacific warm-pool sea surface temperature [Oppo et al., 2009], El Niño frequency [Conroy et al., 2008], and Northern Iceland SST [Sicre et al., 2008]. Shaded bars are the same as in Figure 2.

Table A.1: Drought persistence (years A.D.) assessed using a 25-yr running mean[a]

Summitville	PDSI[b]	El Malpais	Tavaputs
119-229	97-181	979-1039	938-1006
297-399	426-481	1441-1500	1762-1830
1072-1160	347-399	-8-46	782-842
1193-1264	979-1017	349-395	132-184
62-109	222-257	895-936	¯23-27
1876-1914	1438-1473	443-483	633-676
632-672	1130-1163	¯99-¯60	1254-1297
1327-1364	505-537	1335-1373	¯243-¯202
1662-1696	1261-1292	1567-1604	507-545
1561-1591	1568-1596	138-174	1130-1168

[a]Drought initiation and termination are defined as when the smoothed series drops below or rises above the long-term mean. The ten most persistent droughts in each record are shown from top to bottom. The 2nd century megadrought is highlighted in grey.

[b]PDSI points 103, 104, 118, 119, 132, 133 are averaged to represent four corners region

A.8 Supporting Information

We applied 30 year moving correlations between the Summitville chronology and tree-ring reconstructed PDSI [i.e., *Woodhouse et al.,* 2011] to evaluate the consistency of the moisture sensitivity back in time before the instrumental record and account for potential changes in climate sensitivity caused by changes in the position of tree-line [e.g., *Salzer et al.*, 2009]. We averaged PDSI grid points 103, 104, 118, 119, 132 and 133 [*Cook et al.*, 2008] to roughly represent the Colorado Plateau region. PDSI points 132 and 133 only extend back to A.D. 210, so the PDSI is an average of the four other points before AD 210. Moving correlations from A.D. 1-2009 indicate a relatively consistent moisture balance signal through the length of the PDSI record. Correlations decrease toward the earlier part of the records (pre ~A.D. 300) possibly caused by decreases in sample depth. Moving correlations were also conducted between the Summitville chronology and Colorado Plateau maximum annual temperature reconstruction [*Salzer and Kipfmueller,* 2005], revealing no clear or consistent relationship, in support of our analysis of instrumental data.

Because some high elevation bristlecone pine stands are limited in growth by summer temperatures [e.g., *Salzer and Kipfmueller,* 2005], we investigated possible intermittent relationships between Summitville ring-width and growing season temperature, particularly in extreme temperature years. Instrumental August temperature and ring-width series were both ranked by year, according to dry to wet spring (March-June) precipitation, and then the series were correlated, using a 20 year moving window. Bootstrap significance testing shows that ring width has no significant relationship with late summer temperature during years with dry to normal spring conditions [*Biondi and Waikul,* 2004]. During years with the wettest springs however, August temperature has a significant positive relationship with ring width (Figure A.S2). This relationship between tree growth and August temperature suggests that wet spring conditions prime growth to take advantage of growing season temperatures. To evaluate if high growing season temperature influences the moisture sensitivity, ring-width and spring precipitation were ranked by August temperature and correlated, again using a 20-year moving window. Correlations show no consistent change in the moisture sensitivity during years with warm or cool August temperatures. This shows that periods with warm late summer temperatures do not change the moisture sensitivity of tree growth. The relationship between ring width and late summer temperature only occurs during years with the wettest spring months. These results give us confidence that ring width is primarily a function of spring moisture balance. During the wettest years or periods, ring width can be influenced by temperature causing us to have more confidence in the ability of this chronology to track changes in drought rather than wet extremes (pluvials).

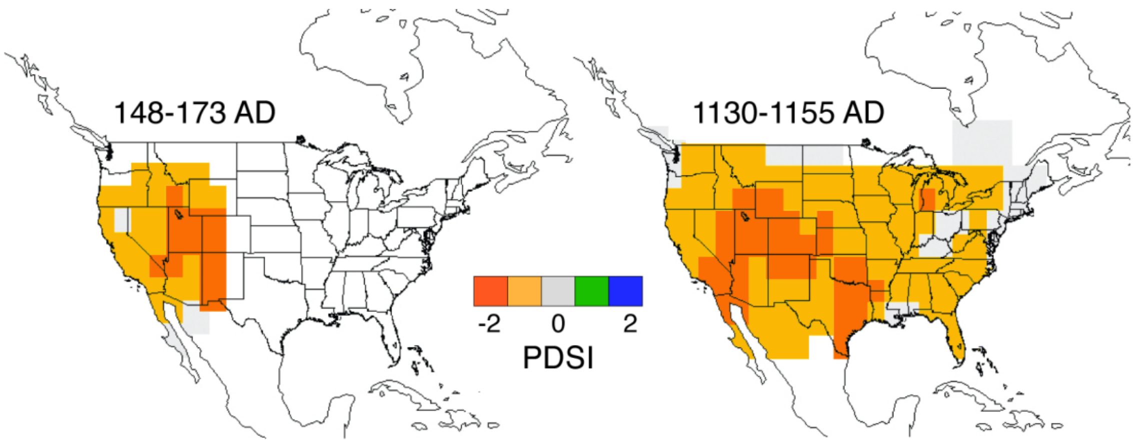

Figure A.S1: Drought area plots using reconstructed PDSI of the 2nd century drought (left) and mid 1100's drought (right). Sparse data coverage for the 2nd century drought makes difficult to assess the drought's full extent.

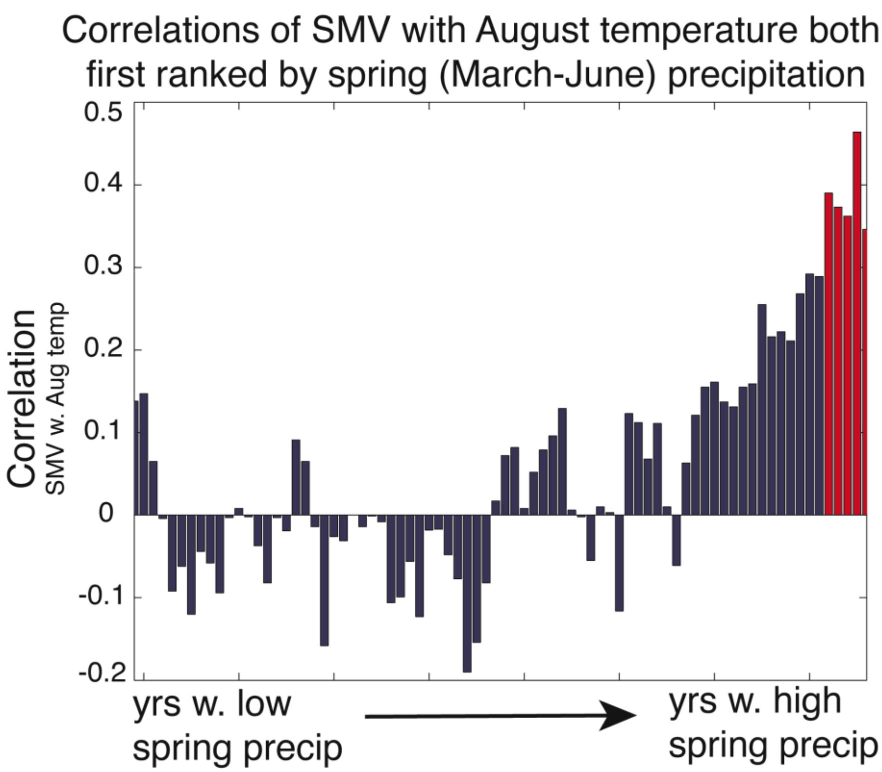

Figure A.S2: Ranked Summitville ring width correlated with August temperature. Data were ranked by years with the wettest to driest spring months (March-June). Ring width was then correlated with August temperature using a 25 yr moving window. Bootstrap correlation significance testing was applied; correlations significant at the 95% level are plotted in red.

A.9 Supporting References

Biondi, F. and K. Waikul (2004) DENDROCLIM2002: A C++ program for statistical calibration of climate signals in tree-ring chronologies. *Computers and Geosciences*, 30, 3, 303-311.

Salzer, M. W., and K. F. Kipfmueller (2005), Reconstructed temperature and precipitation on a millennial timescale from tree-rings in the southern Colorado Plateau. *Climate Change*, 70, 465-487

Salzer, M. W., M. K. Hughes, A. G. Bunn, K. F. Kipfmueller (2009) Recent unprecedented tree-ring growth in bristlecone pine at the highest elevations and possible causes. *P. Natl. Acad. Sci.* 106, 48, 20348-20353 doi:10.1073/pnas.0903029106

Woodhouse, C. A., G. Pederson, S. Gray (2011) Using Bristlcone Pine to Investigate Long-Term Hydroclimatic Variability of the Arkansas River. *Quaternary Research*

Cook, E. R. et al. (2008) North American Summer PDSI Reconstructions, Version 2a. IGBP PAGES/World Data Center for Paleoclimatology, Data Contribution Series # 2008-046. NOAA/NGDC Paleoclimatology Program, Boulder CO, USA.

A.10 Summitville Chronology

```
SMV.rwl -- no data title --                    1st itrdb line missing  raw
SMV.rwl -- no data title --                    2nd itrdb line missing  raw
SMV.rwl -- no data title --                    3rd itrdb line missing  raw
SMV.rw-2689990  09990  01395  2 899  2 872  2 941  2 997  2 854  2 266  2 552  2  raw
SMV.rw-260 741  2 518  2 787  2 979  2 653  21405  21128  21259  21190  21412  2  raw
SMV.rw-250 591  2 847  2 590  2 513  2 655  2 674  2 295  2 635  2 614  2 527  2  raw
SMV.rw-240 680  2 971  2 952  2 811  2 866  21243  2 471  2 722  21065  2 905  2  raw
SMV.rw-230 684  2 774  2 734  2 732  21086  21235  2 928  2 816  2 856  21186  2  raw
SMV.rw-2201383  21042  21170  21194  21155  2 411  21000  2 887  2 663  2 762  2  raw
SMV.rw-210 676  2 932  2 940  2 712  2 675  2 856  2 991  2 529  2 177  2 683  2  raw
SMV.rw-200 773  3 404  3 602  3 699  3 815  31013  3 560  3 575  3 512  3 431  3  raw
SMV.rw-190 547  3 619  3 642  31061  3 865  3 787  3 981  31043  3 444  3 686  3  raw
SMV.rw-180 447  3 804  3 886  3 761  3 698  3 674  3 525  3 521  3 489  3 279  3  raw
SMV.rw-170 522  3 636  3 608  3 733  3 899  3 653  3 723  3 934  31476  31485  3  raw
SMV.rw-160 601  3 337  3 859  3 233  3 417  3 285  3 288  3 527  3 477  3 430  3  raw
SMV.rw-150 627  3 898  31168  3 465  3 766  3 821  3 795  3 798  3 477  3 715  3  raw
SMV.rw-140 712  3 825  3 174  3 452  3 566  3 497  3 846  3 726  3 621  3 455  3  raw
SMV.rw-130 649  3 259  3 430  3 614  3 346  3 566  3 949  3 933  3 677  3 754  3  raw
SMV.rw-120 808  3 674  3 667  3 766  3 977  3 797  3 630  3 792  3 852  3 748  3  raw
SMV.rw-110 900  3 540  3 372  3 950  3 903  3 454  31126  3 893  3 524  3 409  3  raw
SMV.rw-100 392  3  61  3 444  3 584  3 419  3 454  3 712  3 367  4 461  4 248  4  raw
SMV.rw -90 233  4 360  4 334  4 469  4 486  4 354  4 655  4 558  4 612  4 573  4  raw
SMV.rw -80 340  4 750  4 618  4 697  4 453  5 223  5 296  5 596  5 405  5 237  5  raw
SMV.rw -70 185  5 349  5 519  5 332  5 687  5 558  5 409  5 434  5 768  5 238  5  raw
SMV.rw -60 408  5 659  5 619  5 301  5 367  5 259  5 343  5 480  5 400  5 222  5  raw
SMV.rw -50 475  5 418  5 600  5 566  5 430  5 288  5 512  5 483  5 354  5 354  5  raw
SMV.rw -40 450  5 359  5 216  5 218  5 357  5 191  5 304  5 242  5 529  5 373  5  raw
SMV.rw -30 551  5 335  5 229  5 482  5 590  5 513  5 331  5 240  5 455  5 217  5  raw
SMV.rw -20 426  5 553  5 712  5 723  5 363  5 582  5 463  5 283  5 388  5 453  5  raw
SMV.rw -10 712  5 680  5 786  5 278  5 366  5 321  5 320  5 963  5 252  5 526  5  raw
SMV.rw   0 585  5 459  5 382  5 548  5 199  5 118  5 286  5 488  5 637  5 228  5  raw
SMV.rw  10 160  5 150  5 211  5 255  5 295  5 347  5 145  5 263  5 260  5 595  5  raw
SMV.rw  20 282  5 269  5 664  5 636  5 301  5 504  5 656  5 633  5 632  5 635  5  raw
SMV.rw  30 865  5 578  5 609  5 317  5 260  5 292  5 319  5 256  5 381  5 231  5  raw
SMV.rw  40  95  5  78  5 305  5 362  5 303  5 456  5 335  5 352  5 489  5 652  5  raw
SMV.rw  50 334  5 337  5 269  5 482  5 380  5 491  5 282  5 158  5 175  5 191  5  raw
SMV.rw  60 120  5 529  5 579  5 268  5 480  5 591  5 257  5 439  5 227  5 237  5  raw
SMV.rw  70 254  5 341  5 375  5 386  5 319  5 193  5 458  5 524  5 503  5 443  5  raw
SMV.rw  80 307  5 287  5 268  5 360  5 236  5 197  5 362  5 241  5 624  5 463  5  raw
SMV.rw  90 620  5 146  5 319  5 260  5 296  5 174  5 237  5 309  5 213  5 256  5  raw
SMV.rw 100 229  6 113  6 167  7 164  7 264  7 263  7 367  7 292  7 385  7 392  7  raw
SMV.rw 110 409  7 458  7 342  7 384  7 447  7 282  7 148  7 179  7 193  7 199  7  raw
SMV.rw 120 480  7 484  7 274  7 241  7 229  7 122  7 125  7 250  7 200  7 193  7  raw
SMV.rw 130 167  7  58  7 301  7 153  7 171  7 217  7 207  7  58  7 159  7 242  7  raw
SMV.rw 140 180  7  80  7 132  7 285  7 168  7 258  7 237  7 195  7 138  7 251  7  raw
SMV.rw 150  51  7 126  7  96  7 192  7  55  7 328  7 299  7 182  7 117  7 112  7  raw
SMV.rw 160 158  7  57  7 152  7 221  7  56  7  36  7 161  7 234  7  74  7 274  7  raw
SMV.rw 170 273  7 161  7 131  7 453  7 262  7 340  7 304  7 364  7 213  7 128  7  raw
SMV.rw 180 326  7 250  7 387  7 258  7 179  7  82  7 141  7 315  7 291  7 223  7  raw
SMV.rw 190 188  7 261  7 249  7 153  7 240  7 111  7 241  7 493  7 257  7 234  7  raw
SMV.rw 200 247  7 140  7 313  7 370  7 293  7 193  7 252  7 233  7 191  7 155  7  raw
SMV.rw 210 111  7 203  7 261  7 273  7  57  7 240  7 192  7 312  7 256  7 155  7  raw
SMV.rw 220 261  8 115  8  99  8 396  8 382  8 206  8 279  8 468  8 205  8 275  9  raw
```

```
SMV.rw 230 217  9 191  9 556  9 463  9 328  9 290  9 362  9 466  9 269  9 533  9  raw
SMV.rw 240 397  9 336  9 411  9 562  9 506  9 225  9 317  9 428  9 223 10 427 10  raw
SMV.rw 250 483 10 412 10 461 10 169 10 440 10 325 10 383 10 269 10 206 10 309 10  raw
SMV.rw 260 373 10 202 10  80 10 434 10 389 10 194 10 202 10 274 10 367 10 296 10  raw
SMV.rw 270 154 10 301 10 163 10 231 10 151 10 146 10 370 10 344 10 201 10 168 10  raw
SMV.rw 280 411 10 403 10 498 10 413 10 391 10 493 10 313 10 297 10 460 10 375 10  raw
SMV.rw 290 322 10 155 10 440 10 225 10 238 10 430 10 427 10 208 10 117 10 351 10  raw
SMV.rw 300 468 10 402 10 187 10 360 10 409 10 291 10 207 10 190 10 324 10 143 10  raw
SMV.rw 310 374 10 360 10 390 10 149 10 374 10 127 10 402 10 399 10 204 10 270 10  raw
SMV.rw 320 460 10 179 10 130 10 293 10 273 10 217 10 204 10 200 10 147 10 369 10  raw
SMV.rw 330 273 10 176 10 230 10 415 10 422 10 231 10 273 10 233 10 282 10 245 10  raw
SMV.rw 340 272 10 153 10 187 10 247 10 245 10 238 10 327 10 271 10 157 10 375 10  raw
SMV.rw 350 230 10 228 10 249 10 265 10 281 10 247 10 282 10 163 10 261 10 101 10  raw
SMV.rw 360 289 10 318 10 307 10 222 10 237 10 304 10 293 10 388 10 313 11 126 11  raw
SMV.rw 370 121 11 311 11 348 11 185 11 250 11 362 11 286 10 198 10 241 10 184 10  raw
SMV.rw 380 222 10 353 10 224 10 293 10 292 10 250 10 269 10 145 10 190 10 252 10  raw
SMV.rw 390 165 10 128 10 200 10 159 10 287 10 412 10 299 10 328 10 403 10 295 10  raw
SMV.rw 400 294 10 456 10 207 10 317 10 341 10 356 10 468 10 443 10 488 10 243 10  raw
SMV.rw 410 400 10 215 10 387 10 446 10 438 10 517 10 272 10 173 10 224 10 221 10  raw
SMV.rw 420 232 10 273 10 304 10 122 10 202 10 399 10 562 10 328 10 508 10 274 10  raw
SMV.rw 430 392 10 288 10 244 10 376 10 271 10 263 10 387 10 314 10 406 10 348 10  raw
SMV.rw 440 173 10 355 10 267 10 450 10 298  9 247  9  72  9 239  9 369  9 422  9  raw
SMV.rw 450 418  9 356  9 356  9 373  9 314  9 268  9 269  9 396  9 366  9 276  9  raw
SMV.rw 460 114  9 299  9 509  9 251  9 303  9 404  9 254  9 315  9 355  9 134  9  raw
SMV.rw 470 231  9 228  9 254  9  63 10 165 10 341 10 390 10 324 10 243 10 292 10  raw
SMV.rw 480 389 10 247 10 264 10 330 10 316 10 345 10 330 10 401 10 359 10 397 10  raw
SMV.rw 490 499 10 423 10 396 10 281 10 511 10 444 10 433 10 325 10 389 10 325 10  raw
SMV.rw 500 304 10 280 10 424 10 310 10 400 10 361 10 357 10 249 10 223 10 157 10  raw
SMV.rw 510 219 10 272 10 181 10 305 11 368 11 396 11 319 11 375 11 493 11 175 11  raw
SMV.rw 520 343 11 286 11 392 11 531 11 481 11 444 11 270 11 516 11 414 11 465 11  raw
SMV.rw 530 633 11 227 11 378 11 467 11 421 11 247 11 279 11 343 11 313 11 248 11  raw
SMV.rw 540 281 11 278 11 192 11 207 11 314 11 288 11 377 11 319 11 363 11 449 11  raw
SMV.rw 550 429 11 516 11 511 11 501 11 330 11 305 11 384 11 408 11 319 11 429 11  raw
SMV.rw 560 323 11 275 11 399 11 516 11 247 11 271 11 422 11 505 11 292 11 470 11  raw
SMV.rw 570 351 11 558 11 534 11 510 11 486 11 677 11 379 11 312 11 257 11 407 11  raw
SMV.rw 580 343 11 522 11 432 11 374 11 297 11 371 11 415 11 448 12 278 12 493 12  raw
SMV.rw 590 418 12 266 12 405 12 372 12 306 12 192 12 414 12 435 12 359 12 205 12  raw
SMV.rw 600 421 12 492 12 433 12 166 12 331 12 327 12 375 12 434 12 455 12 378 12  raw
SMV.rw 610 240 12 160 12 222 12 305 12 311 12 146 12 305 12 313 12 400 12 314 12  raw
SMV.rw 620 184 12 497 12 405 12 379 12 440 12 232 12 190 12 326 12 420 12 526 12  raw
SMV.rw 630 166 12 272 12 171 12 370 12 339 12 326 12 440 12 397 12 262 12  89 12  raw
SMV.rw 640 139 12 293 12 332 12 223 13 213 13  85 13 273 13 100 13 237 13 288 13  raw
SMV.rw 650 293 13 166 13 361 13 216 13 338 13 351 13 328 13 328 13 239 13 278 13  raw
SMV.rw 660 146 13 394 13 548 13 282 13 390 13 400 13 378 13 420 13 356 13 203 13  raw
SMV.rw 670 243 13 306 13 331 13 302 13 438 13 297 13 277 13 188 13 177 13 316 13  raw
SMV.rw 680 286 13 220 13 359 13 407 13 360 13 439 13 189 13 267 13 328 13 377 13  raw
SMV.rw 690 213 13 218 13 220 13 239 13 307 13 191 13 320 13 334 13 196 13 388 13  raw
SMV.rw 700 270 13 244 13 456 13 417 13 278 13 213 13 204 13 294 13 398 13 420 13  raw
SMV.rw 710 524 13 525 13 424 13 453 13 583 13 419 13 361 13 305 13 325 13 335 13  raw
SMV.rw 720 278 13 189 13 237 13 151 13 259 13 365 13 316 13 330 13 544 13 337 13  raw
SMV.rw 730 446 13 391 13 522 13 522 13 469 13 227 13 144 13 364 13 217 13 194 13  raw
SMV.rw 740 530 13 514 13 315 13 406 13 505 13 240 13 450 13 289 13 398 13 291 13  raw
SMV.rw 750 334 13 239 13 437 13 291 13 298 13 363 13 504 13 496 13 583 13 414 13  raw
SMV.rw 760 348 13 273 13 517 13 438 13 450 13 448 13 547 13 357 13 393 13 434 13  raw
SMV.rw 770 134 13 196 13 347 13 459 13 226 13 337 13 353 13 252 13 334 13 247 13  raw
SMV.rw 780 333 13 374 13 235 13 224 13 347 13 468 13 218 13 342 13 391 13 385 13  raw
```

```
SMV.rw 790 342 13 328 13 397 13 370 13 458 13 447 13 447 13 376 13 313 13 302 13  raw
SMV.rw 800 525 13 599 13 505 13 414 13 412 13 440 13 309 13 253 13 370 13  98 13  raw
SMV.rw 810 340 13 325 13 258 13 355 13 423 13 377 13 190 13 337 13 245 13 159 13  raw
SMV.rw 820 456 13 529 13 413 13 283 13 264 13 205 13 365 13 562 13 630 13 370 13  raw
SMV.rw 830 155 13 353 13 337 13 424 13 364 13 270 13 218 13  86 13 214 13 198 13  raw
SMV.rw 840 227 13 348 13 465 13 542 13 427 13 393 13 185 13 237 13 372 13 492 13  raw
SMV.rw 850 554 13 287 13 368 13 322 13 406 13 392 13 279 13  67 13 248 13 191 13  raw
SMV.rw 860 177 13 245 13 235 13 347 13 311 13 241 13 250 13 266 13 216 13 295 13  raw
SMV.rw 870 432 13 440 13 331 13 317 13 254 13 198 13 419 13 418 13 229 13 291 13  raw
SMV.rw 880 397 13 366 13 244 13 273 13 176 13 217 13 392 13 318 13 406 13 191 13  raw
SMV.rw 890 466 13 402 13 293 13 372 13 471 13 452 13 462 13 222 13 275 13 315 13  raw
SMV.rw 900 251 13 233 13 203 13 169 13 347 13 354 13 207 13 182 13 383 13 437 13  raw
SMV.rw 910 369 13 389 13 411 13 157 13 249 13 190 13 323 13 378 13 424 14 369 14  raw
SMV.rw 920 307 14 309 14  72 14 397 14 240 15 266 15 415 15 243 15 333 15 303 15  raw
SMV.rw 930 413 15 436 15 387 15 543 15 372 15 491 15 603 15 441 15 520 15 566 15  raw
SMV.rw 940 531 15 606 15 455 15 552 15 366 15 429 15 492 15 358 15 357 15 369 15  raw
SMV.rw 950 439 15 522 15 334 15 448 15 312 15 357 15 452 15 385 15 255 15 431 15  raw
SMV.rw 960 550 15 416 15 395 15 420 15 469 15 510 15 648 15 656 15 666 15 394 14  raw
SMV.rw 970 507 14 403 14 236 14 573 14 527 14 185 14 283 14 369 14 372 14 412 14  raw
SMV.rw 980 170 14 114 14 331 14 345 14 399 14 560 14 497 14 517 14 421 14 475 14  raw
SMV.rw 990 280 14 475 14 382 14 431 14 428 14 560 14 347 14 506 14 165 14 103 14  raw
SMV.rw1000 323 13 190 13 273 13 207 13 305 13  90 13 361 13 515 13 397 13 445 13  raw
SMV.rw1010 398 13 362 13 348 13 322 13 105 13 249 13 333 13 279 13 357 13 401 13  raw
SMV.rw1020 512 14 309 14 360 14 205 14 435 14 440 14 399 14 486 14 434 14 510 13  raw
SMV.rw1030 453 13 282 13 406 13 449 13 355 14 261 14 198 14 170 14 140 14 260 14  raw
SMV.rw1040 283 14 275 14 271 14 276 14 180 14 240 14 311 14 407 14 410 14 306 14  raw
SMV.rw1050 300 14 387 14 492 14 422 14 364 14 428 14 444 14 262 14 311 14 371 14  raw
SMV.rw1060 469 14 612 14 393 14 312 14 336 13 453 13 429 13 248 13 325 13 290 13  raw
SMV.rw1070 399 13 285 13 339 13 318 13 300 13 224 13 351 13 305 13 185 13 392 13  raw
SMV.rw1080 326 13 389 13 368 13 258 13 243 13 270 13 290 13 269 13 426 13 333 13  raw
SMV.rw1090  60 13 106 13 280 13 263 12 281 12 291 12 310 12 102 12 187 12 172 12  raw
SMV.rw1100 230 12 385 12 310 12 303 12 267 12 190 12 270 12 175 12 215 12 119 12  raw
SMV.rw1110 296 12 266 13 354 13 293 13 311 13 318 13 364 13 420 13 353 13 236 13  raw
SMV.rw1120 291 13 170 13 363 13 258 13 282 13 414 13 308 13 218 13 292 13 376 13  raw
SMV.rw1130 234 13 122 13 123 13 232 13 253 13 311 13 315 13 400 13 358 13 289 13  raw
SMV.rw1140  74 13 323 13 371 13 171 13 165 13 303 13 220 13 360 12 177 12 229 12  raw
SMV.rw1150  57 12 313 12 511 12 464 12 215 12 279 12 276 12 357 12 270 12 297 12  raw
SMV.rw1160 300 12 227 11 424 11 405 11 176 11 220 11 241 11 235 11 221 11 223 11  raw
SMV.rw1170 307 11 452 11 458 11 451 11 206 11 196 11 294 11  88 11 354 11 332 11  raw
SMV.rw1180 356 11 282 11 303 11 450 11 487 11 342 11 181 11 297 11 214 11 283 11  raw
SMV.rw1190 293 11 440 11 327 11 276 11 292 10 272 10 190 10 261 10 213 10 170 10  raw
SMV.rw1200 198 10 265 10 234 10 263  9 112  9 164  9 113  9 163  9 206  9 155  9  raw
SMV.rw1210 158  9 364  9 211  8 159  8 171  8 292  8 214  8 130  8 220  8 131  8  raw
SMV.rw1220 351  8 208  8 329  8 266  8 275  8 345  8 250  8 274  8 306  8 231  8  raw
SMV.rw1230 259  8 329  8 210  8 174  8 122  8 260  8 240  8 236  8 313  8 241  8  raw
SMV.rw1240 165  8 314  8 314  8 251  8 226  9 192  9 122  9 201  9 144  9 277  9  raw
SMV.rw1250 152  9  75  9 170  9 365  9 177  9 296  9 240  9 302  9   0  9 238  9  raw
SMV.rw1260 384 10 299 10 184 10 281 10 295 10 188 10 198 10 332 10 308 10 327 10  raw
SMV.rw1270 279 10 355 10 361 10 228 10 204 10 434 10 314 10 401 10 316 10 321  9  raw
SMV.rw1280 196  9 230  9 354  9 324  9 362  9 241  9 351  9 337  9 177  9 141  9  raw
SMV.rw1290 266  9 111  9 274  9 239  9 171  9 245  9 244  9 129  9 298  9 336  9  raw
SMV.rw1300 219  9 379  9 351  9 228  9 129  9 240  9 262  9 257  9 265  9 322  9  raw
SMV.rw1310 365  9 364  9 204  9 329  9 402  9 341  9 152  9 227  9 207  9 280  9  raw
SMV.rw1320 362 10 317 10 365 10 208 10 283 10 396 10 345 10 333 10 327 10 476 10  raw
SMV.rw1330 298 10 347 10 311 10 243 10 308 10 241 10 220 10 243 10  79 10 167 11  raw
SMV.rw1340 259 11 196 11 227 11 300 11 131 11 136 11 251 11 241 11 262 11 175 11  raw
```

```
SMV.rw1350 260 11 310 11 141 11 278 11 240 11 127 10 299 10 210 10 218 10 342 10  raw
SMV.rw1360 154 10 228 10 379 10 158 10 183 11 339 11 381 11 211 11 321 12 254 12  raw
SMV.rw1370 505 12 554 12 520 12 452 12 486 12 208 12 207 12 478 12 389 12 530 12  raw
SMV.rw1380 657 12 512 12 391 12 445 12 458 12 612 12 617 12 385 12 560 12 537 12  raw
SMV.rw1390 314 12 465 12 533 12 272 12 321 12 531 12 515 12 364 12 358 12  83 12  raw
SMV.rw1400 178 12 241 12 315 12 294 12 333 12 376 12 432 12 248 12 268 12 468 12  raw
SMV.rw1410 364 13 366 13 295 13 259 13 238 13 192 13 251 13 240 13 304 13 254 13  raw
SMV.rw1420 235 13 249 13 272 13  96 13 238 13 328 13 457 13 470 13 562 13 284 13  raw
SMV.rw1430 454 13 447 13 364 13 408 13 532 12 413 12 413 12 229 12 180 12 309 12  raw
SMV.rw1440 326 12 378 12 203 12 311 12 306 12  61 12 305 12 374 12 316 12 179 12  raw
SMV.rw1450 307 12 516 12 330 12 280 12 335 12 219 12 221 12 203 12 197 12 189 12  raw
SMV.rw1460 333 12 246 12 240 12 290 12 318 12 267 12 230 12 234 12 228 12 163 12  raw
SMV.rw1470 259 12 134 12 327 12 388 12 275 12 105 12 157 12 203 12 335 12 399 12  raw
SMV.rw1480 245 12 365 12 250 12 181 12 269 12 354 12 363 12 253 12 223 12 325 12  raw
SMV.rw1490 472 12 439 12 281 12 233 12 328 12 111 12 196 12 303 12 329 12 220 12  raw
SMV.rw1500 121 12 279 12 448 12 311 12 401 12 267 12  51 11 453 11 375 11 261 11  raw
SMV.rw1510 278 11 300 11 339 11 210 11 288 11 303 11 163 11 251 11 257 11 442 11  raw
SMV.rw1520 298 11 426 11 143 11 347 11 129 11 353 11 342 11 278 11 144 11 372 11  raw
SMV.rw1530 412 11 319 11 399 11 252 11 223 11 341 11 399 11 301 11 170 11 316 11  raw
SMV.rw1540 393 12 353 12 303 12 318 12 455 12 215 12 167 12 207 12 300 12 315 12  raw
SMV.rw1550 362 12 223 12 234 12 296 12 344 12 366 12 400 12 259 12  94 12 218 12  raw
SMV.rw1560 158 12 232 12 250 12 352 12 386 12 256 12 308 12 190 12 296 12 389 12  raw
SMV.rw1570 270 12 284 12 268 12 143 12 146 12 257 12 265 12 246 12 218 12 172 12  raw
SMV.rw1580 184 12  93 12 328 12 244 12  94 12 141 12 222 12 270 12 377 12 322 12  raw
SMV.rw1590 242 12 239 12 294 12 281 12 284 12 449 12 316 12 391 12 265 12 360 12  raw
SMV.rw1600 363 12 230 12 268 12 403 12 388 12 257 12 190 12 250 12 381 12 223 12  raw
SMV.rw1610 303 12 344 12 137 12 347 12 299 12 213 12 200 12 257 12 242 12 280 12  raw
SMV.rw1620 251 12 319 12 200 12 142 12 172 12 166 12 220 12 291 12 248 12 328 12  raw
SMV.rw1630 351 12 188 12 285 12 264 12 450 12 244 12 341 12 487 12 407 12 420 12  raw
SMV.rw1640 442 12 242 12 385 12 351 12 248 12  94 12 292 12 337 12 314 12 186 12  raw
SMV.rw1650 198 12 342 12 249 12 150 12 238 12 430 12 324 12 314 12 146 12 244 12  raw
SMV.rw1660 315 12 447 12 357 12 408 12 294 12 348 12 142 12 227 12 218 12 273 12  raw
SMV.rw1670 302 12 360 12 190 12 135 12 213 12 152 12 226 12 183 12 288 12 186 12  raw
SMV.rw1680 217 12 210 12 234 12 229 12 180 12  51 12 166 12 232 12 274 12 392 12  raw
SMV.rw1690 320 12 331 12 398 12 483 12 135 12 222 12 190 12 311 12 333 12 330 12  raw
SMV.rw1700 293 12 368 12 193 12 235 12 157 12 101 12 291 12 183 12 204 12 284 12  raw
SMV.rw1710 319 12 258 12 233 12 300 12 218 12 241 12 184 12 214 12 327 12 357 12  raw
SMV.rw1720 369 12 478 12 412 12 282 12 302 12 271 12 462 12 278 12 317 12 253 12  raw
SMV.rw1730 308 12 401 12 219 12 268 12 417 12 182 12 269 12 138 12 361 12 448 12  raw
SMV.rw1740 244 12 257 12 221 12 326 12 262 12 166 12 287 12 328 12  90 12 267 12  raw
SMV.rw1750 299 12 246 12 109 12 253 12 351 12 248 12 332 12 424 12 364 12 309 12  raw
SMV.rw1760 248 12 364 12 334 12 300 12 314 12 319 12 271 12 281 12 222 12 176 12  raw
SMV.rw1770 154 12 254 12 126 12 194 12 250 12 120 12 205 13 312 13 232 13 189 13  raw
SMV.rw1780 237 13 293 13 335 13 415 13 457 13 280 13 321 13 408 13 541 13 253 13  raw
SMV.rw1790 445 13 408 13 466 13 349 13 308 13 452 13 342 13 336 13 257 13 297 13  raw
SMV.rw1800 340 13 252 13 330 13 403 13 338 13 304 13 215 13 290 13 261 13 214 13  raw
SMV.rw1810 318 13 365 13 334 13 293 13 434 13 412 13 406 13 320 13 185 13 186 13  raw
SMV.rw1820 228 13 201 13 221 13 265 13 179 13 198 13 113 13 358 13 309 13 223 13  raw
SMV.rw1830 159 13 398 13 315 13 320 13 263 13 267 13 208 13 269 13 280 13 216 13  raw
SMV.rw1840 150 13 170 13 106 13 203 13 203 13 182 13 207 13 191 13 188 13 199 13  raw
SMV.rw1850 275 13  71 13 255 13 231 13 259 13 222 13 201 13 177 13 293 13 317 13  raw
SMV.rw1860 350 13 263 13 320 13 391 13 324 13 328 13 461 13 354 13 130 13 286 13  raw
SMV.rw1870 348 13 209 13 266 13 217 13 137 13 196 13 265 13 259 13 338 13 156 13  raw
SMV.rw1880 161 13 228 13 308 13 265 13 265 13 350 13 231 13 305 13 230 13 242 13  raw
SMV.rw1890 151 13 245 13 250 13  69 13 171 13 324 13 209 13 260 13 349 13 194 13  raw
SMV.rw1900 139 13 148 13 101 13 228 13 217 13 186 13 135 12 400 12 395 12 203 12  raw
```

```
SMV.rw1910 113 12 269 12 329 12 315 12 270 12 214 12 146 12 300 12 238 12 365 12  raw
SMV.rw1920 232 12 288 12 262 12  75 12 208 12 292 12 282 12 350 12 293 12 229 12  raw
SMV.rw1930 202 12 293 12 371 12 358 12 138 12 294 12 185 12 252 12 403 12 165 12  raw
SMV.rw1940 215 12 446 12 285 12 260 12 254 12 230 12 189 12 257 12 259 12 266 12  raw
SMV.rw1950 182 12 105 12 125 12 229 12 164 12 194 12 117 12 199 11 173 11 203 11  raw
SMV.rw1960 284 11 197 11 264 11 249 11 147 11 278 11 273 11 285 11 284 11 381 11  raw
SMV.rw1970 362 11 187 11 168 11 272 11 161 11 396 11 322 11 261 11 260 11 234 11  raw
SMV.rw1980 102 11 343 11 244 11 314 11 306 11 277 11 291 11 176 11 197 11  64 11  raw
SMV.rw1990 236 11 226 11 211 11 220 11 342 11 310 11 237 11 271 11 385 11 305 11  raw
SMV.rw2000 161 11 182 11  51 11 161 11 182 11 265 11 217 11 256 11 176  6 162  6  raw
SMV.rw20109990  09990  09990  09990  09990  09990  09990  09990  09990  09990  0  raw
SMV.rwl -- no data title --                    1st itrdb line missing  std
SMV.rwl -- no data title --                    2nd itrdb line missing  std
SMV.rwl -- no data title --                    3rd itrdb line missing  std
SMV.rw-2689990  09990  01479  2 959  2 932  21008  21075  2 923  2 286  2 599  2  std
SMV.rw-260 803  2 567  2 862  21074  2 718  21545  21250  21400  21330  21579  2  std
SMV.rw-250 660  2 950  2 666  2 577  2 741  2 763  2 335  2 727  2 699  2 606  2  std
SMV.rw-240 779  21115  21093  2 933  2 995  21437  2 544  2 839  21247  21068  2  std
SMV.rw-230 806  2 917  2 873  2 871  21300  21485  21114  2 985  21041  21441  2  std
SMV.rw-2201681  21273  21427  21458  21411  2 503  21230  21095  2 819  2 946  2  std
SMV.rw-210 840  21168  21182  2 897  2 855  21088  21263  2 677  2 225  2 875  2  std
SMV.rw-200 989  3 644  3 872  3 938  31132  31268  31053  3 999  3 840  3 686  3  std
SMV.rw-190 748  3 855  3 897  31356  31108  31105  31443  31346  3 621  3 890  3  std
SMV.rw-180 581  31372  31531  3 997  31332  31155  3 982  3 967  3 914  3 436  3  std
SMV.rw-170 996  31152  31028  31653  31310  3 954  31250  31371  32172  32038  3  std
SMV.rw-160 822  3 500  31181  3 347  3 576  3 395  3 400  3 734  3 913  3 673  3  std
SMV.rw-150 879  31306  31721  3 657  31085  31166  31181  31139  3 782  31025  3  std
SMV.rw-1401206  31189  3 306  3 655  3 929  3 821  31259  31147  3 918  3 809  3  std
SMV.rw-1301325  3 640  3 822  31316  3 893  31099  31531  31508  31097  31383  3  std
SMV.rw-1201325  31145  31283  31256  31490  31219  3 966  31326  31312  31155  3  std
SMV.rw-1101393  3 929  3 622  31481  31541  3 816  31768  31510  31073  31116  3  std
SMV.rw-100 622  3 167  3 759  31163  3 785  3 884  31302  3 633  4 910  4 459  4  std
SMV.rw -90 392  4 609  4 612  4 960  4 950  4 671  41231  41183  41182  41190  4  std
SMV.rw -80 559  41430  41119  41422  41044  5 544  5 550  51074  5 915  5 679  5  std
SMV.rw -70 700  5 731  51008  5 735  51549  51388  51053  51099  51576  5 530  5  std
SMV.rw -60 963  51345  51570  5 582  5 903  5 665  5 745  51403  51085  5 476  5  std
SMV.rw -501085  5 977  51546  51505  5 874  5 520  51445  51066  5 809  5 870  5  std
SMV.rw -401151  5 847  5 537  5 499  5 755  5 644  5 657  5 518  51183  5 909  5  std
SMV.rw -301467  5 741  5 430  51490  51893  51960  5 719  5 720  51096  5 646  5  std
SMV.rw -201247  51431  51442  51575  51058  51714  51013  5 586  5 763  51038  5  std
SMV.rw -101475  51379  51597  5 882  5 932  5 783  5 979  52003  5 682  51081  5  std
SMV.rw   01705  5 947  5 789  51134  5 448  5 286  5 667  51097  51426  5 620  5  std
SMV.rw  10 403  5 434  5 434  5 536  5 621  5 732  5 321  5 586  5 569  51305  5  std
SMV.rw  20 607  5 710  51465  51757  5 701  51125  52021  51497  51429  51763  5  std
SMV.rw  302018  51420  51534  5 975  5 700  5 834  5 692  5 789  5 968  5 553  5  std
SMV.rw  40 246  5 171  5 757  51118  5 765  51255  51000  5 893  51513  52015  5  std
SMV.rw  501237  51141  5 661  51286  51262  51631  5 793  5 490  5 413  5 605  5  std
SMV.rw  60 336  51322  51797  5 832  51490  51726  5 755  5 998  5 705  5 640  5  std
SMV.rw  70 666  51060  5 912  5 907  5 749  5 602  51201  51602  51456  51103  5  std
SMV.rw  80 732  5 748  51155  5 984  5 648  5 561  51063  5 616  51513  51125  5  std
SMV.rw  901693  5 409  5 834  5 643  5 924  5 543  5 630  5 764  5 597  5 637  5  std
SMV.rw 100 507  6 358  6 434  7 488  7 867  7 868  71275  7 949  71292  71303  7  std
SMV.rw 1101160  71459  71081  71193  71433  7 897  7 456  7 547  7 602  7 624  7  std
SMV.rw 1201481  71517  7 882  7 759  7 648  7 366  7 357  7 756  7 626  7 550  7  std
SMV.rw 130 480  7 182  7 978  7 478  7 510  7 753  7 755  7 175  7 532  7 828  7  std
SMV.rw 140 601  7 234  7 465  7 879  7 597  7 806  7 707  7 590  7 438  7 802  7  std
```

SMV.rw 150 169 7 406 7 465 7 867 7 162 71037 71146 7 624 7 377 7 392 7 std
SMV.rw 160 502 7 177 7 470 7 705 7 204 7 178 7 532 7 865 7 264 7 883 7 std
SMV.rw 170 838 7 552 7 405 71482 7 922 71107 71029 71208 7 682 7 402 7 std
SMV.rw 1801050 7 899 71354 7 891 7 769 7 291 7 508 71062 71439 7 853 7 std
SMV.rw 190 604 7 901 7 763 7 518 7 773 7 361 71108 72060 71186 71072 7 std
SMV.rw 200 828 7 503 7 983 71354 71082 7 643 7 805 7 801 7 675 7 597 7 std
SMV.rw 210 351 7 630 7 783 7 826 7 190 7 723 7 535 7 954 7 789 7 525 7 std
SMV.rw 220 680 8 311 8 330 81113 81075 8 584 8 707 81357 8 793 8 938 9 std
SMV.rw 230 617 9 459 91398 91199 9 866 9 774 9 949 91136 9 645 91294 9 std
SMV.rw 240 897 9 834 91002 91277 91182 9 564 9 736 91043 9 545 101149 10 std
SMV.rw 2501251 101074 101196 10 546 101177 10 870 10 822 10 575 10 503 10 925 10 std
SMV.rw 2601029 10 673 10 471 101299 101119 10 732 10 777 10 980 101188 10 854 10 std
SMV.rw 270 442 10 897 10 558 10 738 10 479 10 414 101119 10 932 10 573 10 487 10 std
SMV.rw 2801284 101180 101462 101218 101182 101616 10 947 101009 101406 101132 10 std
SMV.rw 2901013 10 458 101321 10 774 10 794 101318 101488 10 729 10 426 101227 10 std
SMV.rw 3001574 101261 10 569 101163 101346 10 929 10 718 10 574 10 999 10 470 10 std
SMV.rw 3101134 101101 101231 10 491 101149 10 398 101247 10 995 10 603 10 854 10 std
SMV.rw 3201528 10 606 10 452 101022 10 789 10 743 10 705 10 749 10 533 101243 10 std
SMV.rw 330 901 10 640 10 775 101255 101387 10 712 10 855 10 736 10 869 10 905 10 std
SMV.rw 340 940 10 455 10 645 10 815 10 818 10 867 10 935 10 781 10 543 101163 10 std
SMV.rw 350 694 10 665 10 811 10 963 101038 10 886 10 939 10 461 10 817 10 359 10 std
SMV.rw 3601050 101021 101032 10 723 10 807 101097 101038 10 968 10 894 11 517 11 std
SMV.rw 370 506 11 959 111111 11 630 11 782 111168 11 906 10 671 10 803 10 617 10 std
SMV.rw 380 721 101093 10 699 10 928 10 966 10 853 10 949 10 540 10 682 10 883 10 std
SMV.rw 390 634 10 445 10 727 10 528 10 959 101219 101016 101084 101239 10 888 10 std
SMV.rw 400 929 101331 10 699 10 986 101010 101083 101357 101387 101479 10 717 10 std
SMV.rw 4101086 10 657 101149 101225 101411 101453 10 860 10 542 10 714 10 696 10 std
SMV.rw 420 727 10 882 10 951 10 435 10 660 101232 101699 101049 101489 10 921 10 std
SMV.rw 4301223 10 929 10 792 101212 10 881 10 781 101093 10 971 101304 101205 10 std
SMV.rw 440 706 101177 10 868 101437 10 998 9 850 9 202 9 767 91225 91431 9 std
SMV.rw 4501319 91123 91144 91212 9 919 9 832 9 843 91256 91164 9 882 9 std
SMV.rw 460 321 9 945 91646 9 789 9 962 91246 9 805 91002 91124 9 442 9 std
SMV.rw 470 738 9 728 9 794 9 172 10 543 101079 101185 10 978 10 729 10 914 10 std
SMV.rw 4801186 10 747 10 815 101037 10 979 101033 10 944 101222 101114 101194 10 std
SMV.rw 4901508 101303 101233 10 895 101492 101209 101321 10 968 101198 10 964 10 std
SMV.rw 500 900 10 832 101159 10 944 101157 101075 10 913 10 675 10 643 10 493 10 std
SMV.rw 510 631 10 801 10 523 10 907 111071 111136 11 957 111104 111420 11 540 11 std
SMV.rw 5201038 11 862 111138 111595 111440 111271 11 811 111541 111220 111411 11 std
SMV.rw 5301838 11 689 111099 111361 111243 11 775 11 845 111018 11 910 11 690 11 std
SMV.rw 540 825 11 805 11 564 11 625 11 863 11 876 111153 11 953 111088 111394 11 std
SMV.rw 5501309 111579 111595 111637 11 994 11 909 111147 111225 11 976 111247 11 std
SMV.rw 560 959 11 844 111101 111524 11 668 11 801 111288 111529 11 772 111251 11 std
SMV.rw 570 907 111619 111479 111539 111514 112037 111104 11 944 11 757 111200 11 std
SMV.rw 5801001 111552 111347 111161 11 903 111052 111465 111392 12 862 121519 12 std
SMV.rw 5901306 12 807 121265 121225 12 945 12 559 121249 121342 121132 12 646 12 std
SMV.rw 6001310 121537 121410 12 538 121063 121030 121192 121395 121446 121160 12 std
SMV.rw 610 776 12 518 12 710 12 967 12 982 12 466 12 955 121003 121286 121019 12 std
SMV.rw 620 582 121563 121375 121268 121547 12 810 12 692 121043 121327 121653 12 std
SMV.rw 630 515 12 867 12 551 121165 121092 121036 121470 121303 12 827 12 285 12 std
SMV.rw 640 423 12 898 121047 12 716 13 684 13 286 13 867 13 302 13 734 13 897 13 std
SMV.rw 650 908 13 490 131052 13 572 131027 13 977 13 980 13 987 13 707 13 864 13 std
SMV.rw 660 406 131208 131753 13 877 131250 131247 131246 131362 131097 13 597 13 std
SMV.rw 670 732 13 947 131004 13 944 131325 13 901 13 865 13 616 13 534 13 947 13 std
SMV.rw 680 868 13 666 131084 131236 131074 131320 13 620 13 795 131037 131134 13 std
SMV.rw 690 614 13 687 13 708 13 704 13 893 13 571 13 969 131039 13 604 131244 13 std
SMV.rw 700 844 13 776 131453 131306 13 868 13 666 13 630 13 953 131222 131272 13 std

SMV.rw 7101595 131574 131325 131406 131925 131412 131251 131020 131195 131157 13 std
SMV.rw 720 926 13 617 13 834 13 498 13 900 131169 131088 131061 131653 131104 13 std
SMV.rw 7301467 131255 131661 131766 131459 13 696 13 415 131103 13 716 13 572 13 std
SMV.rw 7401590 131533 13 928 131173 131537 13 699 131426 13 858 131302 13 860 13 std
SMV.rw 7501000 13 733 131294 13 812 131075 131102 131514 131492 131761 131286 13 std
SMV.rw 7601099 13 942 131654 131383 131312 131470 131676 131086 131111 131297 13 std
SMV.rw 770 395 13 582 131065 131360 13 683 131019 131064 13 752 131003 13 777 13 std
SMV.rw 7801042 131148 13 709 13 707 131000 131397 13 699 131045 131133 131186 13 std
SMV.rw 7901065 131006 131262 131208 131307 131420 131372 131214 13 904 13 987 13 std
SMV.rw 8001662 131872 131574 131272 131243 131331 13 942 13 757 131108 13 293 13 std
SMV.rw 810 998 13 952 13 759 13 967 131138 131105 13 487 13 994 13 809 13 569 13 std
SMV.rw 8201444 131666 131351 13 867 13 759 13 629 131135 131698 131894 131074 13 std
SMV.rw 830 488 131051 131136 131322 131151 13 843 13 635 13 274 13 617 13 582 13 std
SMV.rw 840 706 131082 131361 131586 131247 131187 13 614 13 808 131167 131551 13 std
SMV.rw 8501588 13 846 131181 131035 131245 131084 13 756 13 238 13 837 13 623 13 std
SMV.rw 860 532 13 744 13 739 13 988 13 889 13 751 13 816 13 847 13 687 13 941 13 std
SMV.rw 8701320 131324 131054 131060 13 867 13 662 131229 131184 13 642 13 766 13 std
SMV.rw 8801233 131104 13 711 13 864 13 640 13 707 131250 131095 131329 13 629 13 std
SMV.rw 8901363 131156 13 883 131135 131410 131346 131368 13 704 13 836 13 946 13 std
SMV.rw 900 760 13 707 13 625 13 491 131019 131040 13 601 13 501 131123 131293 13 std
SMV.rw 9101116 131154 131245 13 458 13 753 13 566 13 956 131028 131144 141019 14 std
SMV.rw 920 893 14 870 14 188 141106 14 694 15 740 151098 15 640 15 992 15 783 15 std
SMV.rw 9301008 151186 15 980 151369 15 953 151263 151506 151069 151309 151351 15 std
SMV.rw 9401397 151465 151164 151429 15 984 151127 151269 15 891 15 932 15 960 15 std
SMV.rw 9501142 151326 15 873 151167 15 877 15 920 151213 151005 15 672 151159 15 std
SMV.rw 9601476 151117 151082 151247 151266 151379 151756 151697 151731 151045 14 std
SMV.rw 9701322 141041 14 671 141471 141466 14 608 14 716 14 987 141072 141130 14 std
SMV.rw 980 437 14 340 14 964 14 922 141032 141507 141305 141306 141129 141317 14 std
SMV.rw 990 768 141275 141070 141156 141180 141494 14 954 141293 14 398 14 299 14 std
SMV.rw1000 930 13 548 13 793 13 609 13 917 13 244 131047 131512 131086 131207 13 std
SMV.rw10101141 131054 131015 13 918 13 264 13 744 13 910 13 855 131001 131180 13 std
SMV.rw10201496 14 917 141056 14 564 141246 141310 141237 141419 141261 141406 13 std
SMV.rw10301316 13 729 131128 131196 13 971 14 784 14 583 14 470 14 388 14 760 14 std
SMV.rw1040 752 14 836 14 792 14 792 14 526 14 681 14 862 141151 141220 14 884 14 std
SMV.rw1050 837 141013 141304 141171 141056 141243 141239 14 824 14 883 141050 14 std
SMV.rw10601319 141734 141074 14 907 14 978 131277 131175 13 607 13 877 13 813 13 std
SMV.rw10701064 13 740 13 847 13 839 13 785 13 618 13 940 13 854 13 537 131000 13 std
SMV.rw1080 881 131096 13 981 13 718 13 696 13 780 13 859 13 831 131251 13 940 13 std
SMV.rw1090 179 13 295 13 815 13 756 12 815 12 808 12 854 12 290 12 609 12 500 12 std
SMV.rw1100 588 121042 12 879 12 848 12 738 12 638 12 770 12 505 12 617 12 339 12 std
SMV.rw1110 891 12 790 131165 13 859 13 916 13 989 131088 131315 131098 13 709 13 std
SMV.rw1120 893 13 560 131090 13 797 13 834 131237 13 926 13 662 13 891 131118 13 std
SMV.rw1130 649 13 435 13 435 13 739 13 882 13 998 13 971 131234 131130 13 914 13 std
SMV.rw1140 225 13 946 131134 13 535 13 569 13 949 13 697 131078 12 591 12 712 12 std
SMV.rw1150 178 12 943 121658 121530 12 676 121005 12 838 121157 12 867 12 919 12 std
SMV.rw1160 932 12 747 111409 111243 11 597 11 749 11 760 11 779 11 763 11 703 11 std
SMV.rw1170 931 111514 111383 111535 11 683 11 640 11 942 11 305 111163 111094 11 std
SMV.rw11801126 11 973 11 972 111692 111598 111068 11 566 111004 11 715 11 869 11 std
SMV.rw1190 961 111488 111105 11 951 11 999 10 913 10 689 10 866 10 812 10 592 10 std
SMV.rw1200 669 10 927 10 810 10 948 9 570 9 539 9 393 9 570 9 771 9 526 9 std
SMV.rw1210 638 91278 9 741 8 566 8 594 8 932 8 759 8 389 8 747 8 507 8 std
SMV.rw12201210 8 712 81082 8 962 81010 81270 8 937 8 968 81065 8 832 8 std
SMV.rw1230 895 81133 8 744 8 621 8 409 8 938 8 849 8 861 81105 8 798 8 std
SMV.rw1240 523 81037 81097 8 849 8 825 9 709 9 426 9 778 9 548 91018 9 std
SMV.rw1250 608 9 337 9 614 91307 9 617 91082 9 862 91122 9 0 9 919 9 std
SMV.rw12601415 101085 10 722 101087 101103 10 712 10 702 101418 101188 101198 10 std

SMV.rw12701019 101272 101155 10 863 10 729 101492 101104 101423 101133 10 988 9 std
SMV.rw1280 569 9 665 91095 9 986 91172 9 708 91105 91034 9 562 9 496 9 std
SMV.rw1290 943 9 591 9 955 9 662 9 605 9 904 9 748 9 428 91022 91129 9 std
SMV.rw1300 725 91172 91186 9 737 9 447 9 850 9 936 9 941 91303 91138 9 std
SMV.rw13101324 91273 9 724 91179 91500 91165 9 501 9 884 9 654 9 951 9 std
SMV.rw13201128 101006 101171 10 675 10 876 101393 101065 101066 101138 101529 10 std
SMV.rw1330 939 101216 10 981 10 829 10 967 10 656 10 721 10 853 10 259 10 541 11 std
SMV.rw1340 865 11 647 11 720 11 870 11 438 11 432 11 897 11 750 11 849 11 609 11 std
SMV.rw1350 868 11 837 11 454 11 822 11 819 11 453 10 975 10 717 10 699 101163 10 std
SMV.rw1360 537 10 857 101147 10 526 10 643 111088 111271 11 635 111041 12 788 12 std
SMV.rw13701480 121591 121507 121414 121532 12 677 12 617 121547 121231 121628 12 std
SMV.rw13802157 121690 121289 121398 121516 122083 122177 121206 121829 121699 12 std
SMV.rw1390 996 121363 121702 12 844 12 976 121610 121510 121156 121164 12 264 12 std
SMV.rw1400 557 12 710 12 958 12 906 121127 121311 121359 12 798 12 834 121478 12 std
SMV.rw14101139 131114 13 915 13 785 13 764 13 606 13 786 13 778 13 918 13 822 13 std
SMV.rw1420 752 13 778 13 868 13 310 13 769 131052 131512 131517 131765 13 996 13 std
SMV.rw14301554 131474 131237 131340 131816 121397 121352 12 716 12 565 121022 12 std
SMV.rw14401086 121289 12 674 121061 12 932 12 227 121077 121282 121086 12 601 12 std
SMV.rw14501029 121721 121091 12 936 121160 12 740 12 787 12 769 12 703 12 693 12 std
SMV.rw14601053 12 872 12 818 12 969 121155 12 825 12 792 12 755 12 781 12 550 12 std
SMV.rw14701022 12 536 121123 121329 12 937 12 389 12 526 12 725 121178 121400 12 std
SMV.rw1480 890 121274 12 893 12 644 121017 121304 121231 12 902 12 806 121186 12 std
SMV.rw14901708 121527 12 978 12 858 121180 12 383 12 674 121133 121193 12 833 12 std
SMV.rw1500 411 12 993 121564 121130 121402 121150 12 190 111645 111214 11 949 11 std
SMV.rw1510 817 111148 111203 11 732 11 999 111093 11 589 11 908 11 904 111592 11 std
SMV.rw15201091 111313 11 531 111226 11 468 111237 111201 11 962 11 509 111310 11 std
SMV.rw15301486 111101 111487 11 917 11 811 111228 111434 111062 11 624 111200 11 std
SMV.rw15401361 121206 121131 121080 121531 12 780 12 614 12 713 121108 121103 12 std
SMV.rw15501234 12 787 12 829 121036 121193 121256 121334 12 928 12 334 12 741 12 std
SMV.rw1560 540 12 817 12 844 121256 121368 12 891 12 985 12 674 121038 121350 12 std
SMV.rw1570 923 12 983 12 953 12 521 12 501 12 918 12 933 12 863 12 781 12 627 12 std
SMV.rw1580 667 12 340 121112 12 867 12 353 12 361 12 749 12 967 121307 121199 12 std
SMV.rw1590 893 12 799 121080 121054 12 966 121559 121099 121238 12 937 121277 12 std
SMV.rw16001310 12 846 12 973 121355 121353 12 930 12 785 12 945 121516 12 810 12 std
SMV.rw16101108 121217 12 604 121237 121108 12 764 12 724 12 943 12 860 121018 12 std
SMV.rw1620 914 121213 12 751 12 532 12 664 12 599 12 887 121060 12 853 121200 12 std
SMV.rw16301279 12 666 121040 12 971 121622 12 919 121240 121783 121472 121507 12 std
SMV.rw16401575 12 670 121361 121275 12 851 12 340 121042 121192 121113 12 685 12 std
SMV.rw1650 755 121208 12 872 12 539 12 919 121545 121152 121135 12 515 12 844 12 std
SMV.rw16601104 121615 121374 121534 121013 121286 12 515 12 852 12 759 12 981 12 std
SMV.rw16701071 121307 12 677 12 494 12 781 12 542 12 834 12 669 121030 12 661 12 std
SMV.rw1680 795 12 672 12 824 12 839 12 655 12 179 12 654 12 843 121011 121424 12 std
SMV.rw16901155 121183 121416 121713 12 500 12 794 12 689 121148 121293 121194 12 std
SMV.rw17001105 121372 12 704 12 885 12 549 12 367 121027 12 667 12 731 121004 12 std
SMV.rw17101063 12 902 12 798 121053 12 773 12 856 12 671 12 791 121177 121261 12 std
SMV.rw17201367 121735 121588 121007 121240 12 953 121677 121032 121139 12 922 12 std
SMV.rw17301113 121429 12 698 12 840 121486 12 674 12 953 12 519 121304 121608 12 std
SMV.rw1740 887 12 940 12 792 121312 12 956 12 651 121025 121179 12 313 12 972 12 std
SMV.rw17501070 12 917 12 406 12 900 121249 12 957 121210 121507 121313 121140 12 std
SMV.rw1760 876 121383 121269 121115 121053 121103 12 977 121009 12 828 12 572 12 std
SMV.rw1770 563 12 954 12 470 12 722 12 880 12 422 12 802 131164 13 844 13 666 13 std
SMV.rw1780 852 131038 131146 131411 131537 13 968 131196 131464 131837 13 804 13 std
SMV.rw17901651 131509 131687 131304 131113 131428 131218 131050 13 922 131069 13 std
SMV.rw18001226 13 998 131218 131366 131214 131055 13 830 131097 13 972 13 749 13 std
SMV.rw18101169 131374 131258 131063 131436 131549 131564 131229 13 741 13 721 13 std
SMV.rw1820 882 13 782 13 836 13 935 13 651 13 782 13 445 131194 131193 13 824 13 std

SMV.rw1830 565 131360 131187 131228 131079 131059 13 700 131072 13 944 13 798 13 std
SMV.rw1840 566 13 653 13 385 13 703 13 710 13 623 13 728 13 591 13 684 13 781 13 std
SMV.rw1850 951 13 282 13 964 13 899 131009 13 908 13 805 13 653 131086 131184 13 std
SMV.rw18601158 13 973 131161 131417 131195 131098 131532 131222 13 531 131164 13 std
SMV.rw18701260 13 793 13 930 13 753 13 547 13 679 13 974 131008 131168 13 593 13 std
SMV.rw1880 566 13 852 131045 131023 131024 131284 13 922 131061 13 763 13 911 13 std
SMV.rw1890 537 13 914 13 935 13 285 13 714 131114 13 795 131004 131262 13 724 13 std
SMV.rw1900 571 13 606 13 417 13 838 13 844 13 773 13 541 121327 121440 12 891 12 std
SMV.rw1910 550 121092 121382 121256 121032 12 912 12 591 121037 12 921 121246 12 std
SMV.rw1920 850 121216 12 975 12 293 12 880 121189 121219 121402 121279 121006 12 std
SMV.rw1930 945 121153 121268 121356 12 596 121265 12 845 121080 121535 12 722 12 std
SMV.rw1940 963 121569 121173 121038 121055 121017 12 821 121092 121152 121049 12 std
SMV.rw1950 721 12 458 12 512 12 940 12 668 12 834 12 487 12 793 11 733 11 817 11 std
SMV.rw19601063 11 850 11 947 11 993 11 797 111232 111156 111075 111058 111515 11 std
SMV.rw19701383 11 784 11 751 11 945 11 593 111350 111108 111034 11 865 11 719 11 std
SMV.rw1980 459 111215 11 948 111090 111145 11 966 111034 11 858 11 744 11 247 11 std
SMV.rw1990 917 11 950 11 943 111017 111317 111173 11 895 111121 111362 111070 11 std
SMV.rw2000 656 11 711 11 222 11 604 11 647 11 997 11 886 111105 11 836 6 729 6 std
SMV.rw20109990 09990 09990 09990 09990 09990 09990 09990 09990 09990 0 std
SMV.rwl -- no data title -- 1st itrdb line missing res
SMV.rwl -- no data title -- 2nd itrdb line missing res
SMV.rwl -- no data title -- 3rd itrdb line missing res
SMV.rw-2689990 09990 01379 2 778 2 955 2 952 21039 2 887 2 315 2 825 2 res
SMV.rw-260 881 2 676 21075 21152 2 763 21711 21065 21416 21177 21469 2 res
SMV.rw-250 418 21055 2 550 2 677 2 838 2 854 2 451 2 999 2 797 2 787 2 res
SMV.rw-240 971 21236 21116 2 982 21055 21436 2 403 21043 21212 2 997 2 res
SMV.rw-230 829 2 982 2 873 2 923 21348 21395 21002 2 972 21004 21388 2 res
SMV.rw-2201508 21063 21343 21238 21216 2 312 21347 2 869 2 813 2 984 2 res
SMV.rw-210 829 21222 21124 2 878 2 899 21113 21223 2 610 2 360 21083 2 res
SMV.rw-200 981 3 615 31019 3 971 31183 31324 3 969 3 930 3 777 3 714 3 res
SMV.rw-190 909 3 958 3 958 31413 31033 31133 31420 31210 3 435 31014 3 res
SMV.rw-180 649 31718 31584 31090 31398 31017 3 788 3 894 3 773 3 416 3 res
SMV.rw-1701127 31095 31176 31525 31459 3 771 31355 31202 32057 31517 3 res
SMV.rw-160 520 3 483 31108 3 242 3 784 3 473 3 693 3 958 31037 3 854 3 res
SMV.rw-1501139 31400 31709 3 607 31301 31026 31330 31111 3 649 31137 3 res
SMV.rw-1401212 31211 3 267 3 947 3 982 3 900 31416 31103 3 881 3 810 3 res
SMV.rw-1301363 3 509 3 939 31308 3 811 31137 31600 31356 3 957 31364 3 res
SMV.rw-1201141 3 975 31151 31083 31359 3 995 3 882 31284 31170 31042 3 res
SMV.rw-1101338 3 774 3 603 31530 31180 3 751 31839 31152 3 900 31019 3 res
SMV.rw-100 409 3 293 31053 31145 3 772 31030 31414 3 608 41097 4 485 4 res
SMV.rw -90 652 4 825 4 791 41094 41047 4 735 41398 4 907 41189 4 981 4 res
SMV.rw -80 554 41558 4 927 41374 4 860 5 535 5 742 51147 5 812 5 729 5 res
SMV.rw -70 807 5 894 51187 5 762 51601 51221 5 975 5 981 51556 5 242 5 res
SMV.rw -60 803 51520 51217 5 711 51241 5 691 5 981 51484 51010 5 791 5 res
SMV.rw -501234 5 925 51533 51352 5 973 5 279 51392 5 946 5 770 5 810 5 res
SMV.rw -401062 5 777 5 648 5 692 5 941 5 628 5 893 5 732 51363 51165 5 res
SMV.rw -301688 5 687 5 666 51234 51302 51382 5 548 5 707 51125 5 507 5 res
SMV.rw -201324 51420 51515 51324 5 765 51315 5 874 5 477 5 955 51014 5 res
SMV.rw -101388 51231 51605 5 675 5 984 5 549 5 915 51780 5 280 51377 5 res
SMV.rw 01283 5 817 5 378 51062 5 410 5 436 5 926 51231 51525 5 609 5 res
SMV.rw 10 612 5 518 5 742 5 685 5 893 5 896 5 623 5 900 5 789 51557 5 res
SMV.rw 20 648 5 839 51553 51482 5 572 51261 51749 51286 51312 51423 5 res
SMV.rw 301576 5 858 51042 5 495 5 518 5 869 5 700 5 664 51193 5 689 5 res
SMV.rw 40 462 5 575 5 980 51352 5 916 51499 5 864 51037 51330 51774 5 res
SMV.rw 50 811 51035 5 577 51286 5 980 51542 5 554 5 556 5 357 5 743 5 res
SMV.rw 60 562 51649 51633 5 623 51497 51471 5 426 51078 5 565 5 672 5 res

SMV.rw 70 693 51216 51175 51105 5 793 5 783 51411 51450 51311 51072 5 res
SMV.rw 80 624 5 779 51116 5 981 5 712 5 709 51221 5 497 51723 5 950 5 res
SMV.rw 901625 5 195 5 996 5 794 51084 5 558 51023 5 975 5 789 5 951 5 res
SMV.rw 100 753 6 579 6 800 7 748 71156 71060 71353 7 989 71407 71249 7 res
SMV.rw 1101269 71284 7 866 71078 71216 7 766 7 425 7 660 7 700 7 798 7 res
SMV.rw 1201702 71402 7 815 7 809 7 766 7 420 7 658 71006 7 861 7 822 7 res
SMV.rw 130 877 7 453 71360 7 585 7 883 7 977 7 903 7 407 7 916 71074 7 res
SMV.rw 140 840 7 535 7 836 71134 7 777 71101 7 857 7 821 7 717 71071 7 res
SMV.rw 150 394 7 812 7 758 71195 7 361 71532 71239 7 740 7 560 7 560 7 res
SMV.rw 160 727 7 431 7 868 71033 7 411 7 644 7 934 71198 7 474 71320 7 res
SMV.rw 1701026 7 731 7 697 71762 7 807 71255 7 985 71160 7 621 7 503 7 res
SMV.rw 1801273 7 845 71444 7 855 7 889 7 409 7 722 71287 71496 7 833 7 res
SMV.rw 190 817 71049 7 866 7 608 7 991 7 596 71383 72085 7 960 71140 7 res
SMV.rw 200 724 7 529 71186 71254 7 926 7 671 7 946 7 854 7 739 7 765 7 res
SMV.rw 210 563 7 945 71016 7 953 7 538 71100 7 773 71047 7 925 7 858 7 res
SMV.rw 220 876 8 570 8 732 81305 81143 8 611 8 960 81525 8 708 81115 9 res
SMV.rw 230 828 9 613 91554 91214 9 780 9 817 91009 91133 9 618 91458 9 res
SMV.rw 240 965 9 860 91089 91252 91140 9 457 9 869 91091 9 569 101446 10 res
SMV.rw 2501190 101017 101153 10 553 101313 10 789 101057 10 748 10 700 101109 10 res
SMV.rw 2601008 10 710 10 616 101514 101011 10 771 10 970 101030 101233 10 817 10 res
SMV.rw 270 457 101088 10 574 10 976 10 632 10 703 101386 101065 10 672 10 717 10 res
SMV.rw 2801505 101131 101503 101107 101139 101513 10 654 10 980 101299 10 921 10 res
SMV.rw 290 927 10 435 101495 10 605 10 905 101401 101355 10 597 10 576 101367 10 res
SMV.rw 3001422 101078 10 483 101222 101168 10 849 10 789 10 660 101184 10 461 10 res
SMV.rw 3101407 101150 101227 10 453 101390 10 195 101451 10 987 10 563 10 976 10 res
SMV.rw 3201544 10 426 10 653 101199 10 815 10 865 10 828 10 901 10 681 101483 10 res
SMV.rw 330 779 10 797 101029 101223 101274 10 627 101030 10 715 101044 10 928 10 res
SMV.rw 3401015 10 531 10 903 101010 10 954 10 999 101133 10 888 10 674 101379 10 res
SMV.rw 350 777 10 874 101002 101007 101077 10 895 101009 10 568 101084 10 401 10 res
SMV.rw 3601357 101091 101096 10 817 10 869 101163 101022 101242 10 952 11 558 11 res
SMV.rw 370 662 111164 111221 11 592 111014 111262 11 976 10 826 101031 10 726 10 res
SMV.rw 380 894 101256 10 736 101101 10 976 10 898 101032 10 610 10 893 101019 10 res
SMV.rw 390 755 10 666 10 974 10 716 101266 101325 10 948 101148 101234 10 846 10 res
SMV.rw 400 961 101379 10 491 101136 101062 101120 101393 101155 101364 10 457 10 res
SMV.rw 4101289 10 500 101275 101170 101285 101320 10 573 10 583 10 796 10 752 10 res
SMV.rw 420 886 101052 101071 10 544 10 936 101406 101606 10 897 101513 10 623 10 res
SMV.rw 4301167 10 755 10 787 101228 10 762 10 838 101259 10 878 101291 101115 10 res
SMV.rw 440 640 101264 10 860 101402 10 805 9 851 9 246 91057 91318 91406 9 res
SMV.rw 4501198 91090 91103 91132 9 801 9 746 9 833 91233 91047 9 875 9 res
SMV.rw 460 291 91050 91626 9 533 91080 91140 9 716 91097 91129 9 418 9 res
SMV.rw 470 959 9 822 9 957 9 334 10 948 101327 101306 101018 10 804 10 993 10 res
SMV.rw 4801210 10 712 10 949 101084 10 976 101081 101010 101232 101005 101157 10 res
SMV.rw 4901426 101049 101042 10 719 101498 101012 101194 10 879 101112 10 821 10 res
SMV.rw 500 909 10 763 101306 10 866 101209 101039 10 948 10 728 10 800 10 595 10 res
SMV.rw 510 823 10 957 10 709 101165 111199 111175 11 936 111146 111309 11 395 11 res
SMV.rw 5201206 11 809 111200 111516 111211 111009 11 601 111529 11 901 111235 11 res
SMV.rw 5301548 11 234 111141 111175 111065 11 673 11 823 111052 11 880 11 711 11 res
SMV.rw 540 958 11 894 11 692 11 850 111142 11 951 111268 11 959 111115 111397 11 res
SMV.rw 5501147 111427 111274 111293 11 547 11 797 111053 111060 11 849 111258 11 res
SMV.rw 560 844 11 785 111115 111413 11 530 11 890 111260 111418 11 706 111314 11 res
SMV.rw 570 841 111557 111232 111192 111121 111708 11 577 11 770 11 580 111093 11 res
SMV.rw 580 825 111480 111043 11 951 11 766 111052 111194 111242 12 631 121558 12 res
SMV.rw 5901050 12 660 121292 121058 12 872 12 608 121348 121203 12 967 12 609 12 res
SMV.rw 6001418 121358 121191 12 391 121189 12 918 121152 121347 121255 12 983 12 res
SMV.rw 610 644 12 523 12 794 121042 121000 12 569 121188 121044 121310 12 953 12 res
SMV.rw 620 606 121680 121086 121066 121296 12 619 12 685 121006 121233 121362 12 res

SMV.rw 630 286 121015 12 508 121288 12 993 121042 121476 121109 12 691 12 349 12 res
SMV.rw 640 649 121103 121106 12 787 13 838 13 469 131199 13 442 131105 131077 13 res
SMV.rw 6501080 13 662 131302 13 711 131119 131063 131013 13 987 13 725 13 947 13 res
SMV.rw 660 498 131447 131667 13 622 131338 131195 131062 131221 13 854 13 482 13 res
SMV.rw 670 824 131006 131052 13 958 131378 13 777 13 876 13 624 13 680 131118 13 res
SMV.rw 680 936 13 787 131292 131242 131038 131316 13 501 13 910 131097 131120 13 res
SMV.rw 690 592 13 821 13 832 13 881 131067 13 647 131191 131104 13 650 131436 13 res
SMV.rw 700 765 13 879 131545 131106 13 750 13 683 13 703 131028 131237 131244 13 res
SMV.rw 7101508 131330 131070 131199 131594 13 904 131005 13 784 131021 13 972 13 res
SMV.rw 720 825 13 594 13 935 13 546 131216 131185 131062 13 998 131547 13 835 13 res
SMV.rw 7301358 131014 131431 131409 131097 13 416 13 410 131260 13 632 13 716 13 res
SMV.rw 7401777 131342 13 775 131261 131420 13 488 131484 13 627 131323 13 683 13 res
SMV.rw 7501049 13 698 131389 13 749 131129 131075 131453 131258 131549 13 861 13 res
SMV.rw 760 916 13 691 131577 131052 131211 131302 131409 13 747 131047 131082 13 res
SMV.rw 770 177 13 769 131169 131371 13 615 131147 131056 13 731 131114 13 783 13 res
SMV.rw 7801088 131165 13 678 13 850 131088 131378 13 548 131189 131080 131154 13 res
SMV.rw 790 989 13 990 131240 131077 131264 131302 131261 13 982 13 779 13 880 13 res
SMV.rw 8001562 131554 131212 13 997 131005 131098 13 693 13 705 131123 13 185 13 res
SMV.rw 8101263 13 964 13 856 131162 131131 131076 13 482 131127 13 720 13 736 13 res
SMV.rw 8201642 131466 131172 13 701 13 832 13 600 131214 131610 131619 13 777 13 res
SMV.rw 830 417 131139 13 920 131092 131034 13 736 13 653 13 348 13 930 13 745 13 res
SMV.rw 840 953 131302 131445 131504 131072 131053 13 458 13 863 131179 131495 13 res
SMV.rw 8501351 13 608 131174 13 909 131211 13 862 13 730 13 294 131104 13 751 13 res
SMV.rw 860 758 131012 13 869 131148 13 948 13 850 13 938 13 931 13 792 131112 13 res
SMV.rw 8701370 131226 13 991 131004 13 749 13 636 131387 131103 13 684 13 986 13 res
SMV.rw 8801235 13 942 13 711 131012 13 668 13 855 131402 13 979 131295 13 529 13 res
SMV.rw 8901496 13 964 13 820 131158 131298 131134 131204 13 485 13 883 13 958 13 res
SMV.rw 900 741 13 797 13 754 13 681 131238 131092 13 689 13 734 131366 131298 13 res
SMV.rw 9101049 131140 131180 13 371 13 950 13 634 131147 131190 131170 14 986 14 res
SMV.rw 920 907 14 929 14 236 141371 14 673 15 947 151225 15 664 151207 15 847 15 res
SMV.rw 9301129 151215 15 973 151392 15 836 151272 151372 15 889 151269 151187 15 res
SMV.rw 9401193 151305 15 869 151261 15 692 151005 151158 15 753 15 913 15 940 15 res
SMV.rw 9501155 151311 15 716 151220 15 753 15 956 151218 15 938 15 685 151292 15 res
SMV.rw 9601431 15 894 151042 151191 151102 151244 151563 151408 151335 15 771 14 res
SMV.rw 9701090 14 786 14 515 141447 141185 14 433 14 872 141062 141080 141131 14 res
SMV.rw 980 396 14 540 141213 14 977 141140 141556 141204 141235 14 967 141238 14 res
SMV.rw 990 575 141289 14 849 141078 141061 141399 14 714 141298 14 252 14 476 14 res
SMV.rw10001175 13 601 131042 13 744 131117 13 358 131436 131558 13 974 131240 13 res
SMV.rw10101039 13 958 13 948 13 879 13 319 131005 131055 13 931 131103 131291 13 res
SMV.rw10201481 14 781 141090 14 596 141373 141191 141148 141308 141076 141262 13 res
SMV.rw10301126 13 520 131204 131140 13 917 14 756 14 620 14 644 14 612 141071 14 res
SMV.rw1040 947 14 982 14 982 14 956 14 674 14 957 141051 141298 141247 14 862 14 res
SMV.rw1050 918 141100 141340 141089 14 972 141197 141112 14 643 14 952 141073 14 res
SMV.rw10601321 141623 14 914 14 787 14 825 131188 131082 13 557 13 991 13 831 13 res
SMV.rw10701196 13 766 131048 13 951 13 937 13 709 131075 13 934 13 725 131308 13 res
SMV.rw1080 959 131152 13 998 13 783 13 828 13 911 13 990 13 947 131381 13 900 13 res
SMV.rw1090 283 13 596 131064 13 902 121029 121032 121076 12 418 12 867 12 707 12 res
SMV.rw1100 889 121335 12 970 121017 12 882 12 847 12 953 12 644 12 888 12 561 12 res
SMV.rw11101217 12 906 131350 13 837 131048 131058 131116 131305 131009 13 663 13 res
SMV.rw1120 973 13 580 131294 13 752 13 952 131341 13 880 13 769 131024 131164 13 res
SMV.rw1130 656 13 611 13 678 13 997 131048 131132 131102 131297 131063 13 873 13 res
SMV.rw1140 285 131241 131185 13 551 13 794 131134 13 725 131257 12 627 12 929 12 res
SMV.rw1150 374 121298 121669 121362 12 623 121128 12 775 121209 12 828 12 960 12 res
SMV.rw1160 942 12 768 111549 111174 11 508 11 894 11 902 11 862 11 853 11 838 11 res
SMV.rw11701081 111458 111280 111325 11 500 11 680 111005 11 292 111419 111039 11 res
SMV.rw11801153 11 898 111007 111689 111387 11 964 11 408 111021 11 600 11 959 11 res

SMV.rw11901008 111503 11 904 11 897 11 995 10 904 10 695 10 958 10 859 10 727 10 res
SMV.rw1200 866 101184 10 922 101099 9 652 9 746 9 603 9 831 9 961 9 715 9 res
SMV.rw1210 938 91491 9 701 8 762 8 819 81173 8 817 8 634 8 993 8 657 8 res
SMV.rw12201446 8 711 81334 8 939 81006 81280 8 844 81074 81035 8 817 8 res
SMV.rw1230 991 81222 8 648 8 734 8 547 81165 8 946 8 994 81240 8 851 8 res
SMV.rw1240 718 81305 81154 8 918 8 920 9 758 9 582 91001 9 658 91254 9 res
SMV.rw1250 682 9 576 9 907 91578 9 619 91337 9 872 91214 9 79 91311 9 res
SMV.rw12601382 10 989 10 740 101184 101041 10 644 10 839 101477 101015 101090 10 res
SMV.rw1270 901 101238 101174 10 695 10 746 101628 10 807 101349 10 880 10 949 9 res
SMV.rw1280 632 9 855 91168 91002 91197 9 739 91193 91056 9 574 9 672 9 res
SMV.rw12901050 9 655 91146 9 872 9 690 91047 9 913 9 543 91309 91192 9 res
SMV.rw1300 780 91384 91158 9 665 9 493 9 949 9 961 91028 91394 91000 9 res
SMV.rw13101288 91153 9 571 91214 91354 91009 9 410 9 996 9 661 91065 9 res
SMV.rw13201058 10 977 101195 10 622 101001 101433 10 948 101023 101058 101454 10 res
SMV.rw1330 764 101233 10 864 10 851 10 949 10 773 10 819 10 948 10 428 10 815 11 res
SMV.rw13401086 11 758 11 980 111159 11 567 11 755 111138 111048 11 982 11 700 11 res
SMV.rw13501071 111105 11 547 111206 11 841 11 630 101240 10 756 10 936 101342 10 res
SMV.rw1360 533 101080 101302 10 506 10 823 111321 111266 11 601 111188 12 748 12 res
SMV.rw13701602 121486 121416 121159 121314 12 379 12 629 121498 12 944 121565 12 res
SMV.rw13801855 121187 12 884 121172 121149 121732 121644 12 644 121543 121106 12 res
SMV.rw1390 556 121228 121381 12 455 12 929 121502 121181 12 868 12 942 12 198 12 res
SMV.rw1400 742 12 816 121103 12 974 121180 121235 121300 12 715 12 896 121485 12 res
SMV.rw1410 960 131075 13 865 13 778 13 804 13 656 13 923 13 905 131058 13 880 13 res
SMV.rw1420 867 13 866 13 962 13 401 131050 131161 131639 131455 131654 13 757 13 res
SMV.rw14301508 131204 131005 131157 131535 121104 121180 12 447 12 528 121022 12 res
SMV.rw14401018 121265 12 598 121145 12 881 12 352 121288 121287 121055 12 630 12 res
SMV.rw14501181 121687 12 903 12 926 121109 12 629 12 818 12 799 12 727 12 807 12 res
SMV.rw14601215 12 880 12 943 121083 121149 12 921 12 832 12 893 12 852 12 660 12 res
SMV.rw14701106 12 648 121375 121330 12 934 12 453 12 731 12 862 121318 121459 12 res
SMV.rw1480 770 121357 12 767 12 714 121066 121288 121205 12 875 12 768 121213 12 res
SMV.rw14901635 121325 12 678 12 740 121118 12 255 12 868 121237 121204 12 820 12 res
SMV.rw1500 610 121157 121675 12 926 121444 121057 12 172 111777 11 983 11 846 11 res
SMV.rw1510 936 111005 111121 11 646 111080 111060 11 595 111079 11 953 111655 11 res
SMV.rw1520 963 111486 11 285 111309 11 357 111364 111099 11 908 11 538 111452 11 res
SMV.rw15301348 111019 111434 11 720 11 729 111214 111308 11 946 11 601 111288 11 res
SMV.rw15401229 121097 121050 12 988 121449 12 553 12 628 12 748 121150 121088 12 res
SMV.rw15501269 12 779 12 890 121074 121196 121226 121259 12 832 12 332 12 921 12 res
SMV.rw1560 620 121014 12 989 121398 121375 12 867 121134 12 626 121157 121317 12 res
SMV.rw1570 877 121048 12 930 12 460 12 636 121062 12 999 121033 12 902 12 753 12 res
SMV.rw1580 864 12 527 121426 12 909 12 496 12 777 12 991 121117 121307 121247 12 res
SMV.rw1590 857 12 881 121092 12 994 121049 121560 12 911 121347 12 780 121238 12 res
SMV.rw16001095 12 653 121002 121318 121209 12 904 12 775 12 880 121352 12 720 12 res
SMV.rw16101179 121173 12 523 121383 121030 12 786 12 835 121046 12 854 121103 12 res
SMV.rw1620 948 121294 12 731 12 663 12 825 12 749 121108 121192 12 964 121313 12 res
SMV.rw16301260 12 630 121169 12 871 121646 12 736 121326 121635 121194 121315 12 res
SMV.rw16401301 12 602 121262 121060 12 706 12 333 121160 121128 121096 12 713 12 res
SMV.rw1650 876 121290 12 832 12 628 121088 121598 121057 121198 12 476 12 947 12 res
SMV.rw16601120 121589 121141 121360 12 801 121173 12 285 12 947 12 759 12 983 12 res
SMV.rw16701092 121309 12 620 12 614 12 945 12 619 121077 12 797 121249 12 751 12 res
SMV.rw16801004 12 877 12 983 12 967 12 771 12 354 12 998 121032 121229 121574 12 res
SMV.rw16901126 121199 121336 121486 12 270 12 930 12 682 121221 121267 121254 12 res
SMV.rw17001106 121338 12 592 12 980 12 522 12 491 121223 12 648 12 976 121195 12 res
SMV.rw17101178 12 937 12 937 121154 12 754 12 961 12 740 12 939 121295 121226 12 res
SMV.rw17201307 121644 121243 12 827 121028 12 835 121565 12 756 121075 12 813 12 res
SMV.rw17301058 121350 12 633 121018 121398 12 509 121054 12 480 121464 121517 12 res
SMV.rw1740 761 121007 12 752 121161 12 917 12 664 121188 121194 12 279 121211 12 res

SMV.rw17501053 12 936 12 485 121134 121349 12 901 121285 121380 121145 121024 12 res
SMV.rw1760 802 121364 121106 12 978 121102 121075 12 835 12 977 12 737 12 686 12 res
SMV.rw1770 709 121100 12 537 12 966 121081 12 569 121043 131274 13 869 13 801 13 res
SMV.rw17801008 131097 131208 131364 131391 13 833 131111 131289 131608 13 560 13 res
SMV.rw17901625 131143 131383 131003 13 893 131305 13 841 13 909 13 749 131009 13 res
SMV.rw18001132 13 911 131194 131250 131066 13 985 13 711 131080 13 870 13 759 13 res
SMV.rw18101256 131322 131166 13 957 131407 131301 131317 13 990 13 538 13 726 13 res
SMV.rw1820 857 13 803 13 929 13 970 13 728 13 891 13 555 131454 131159 13 844 13 res
SMV.rw1830 660 131467 131044 131203 131003 13 988 13 638 131131 13 927 13 792 13 res
SMV.rw1840 646 13 806 13 512 13 934 13 851 13 817 13 948 13 838 13 852 13 888 13 res
SMV.rw18501109 13 399 131265 13 949 131137 13 955 13 872 13 816 131202 131161 13 res
SMV.rw18601177 13 968 131161 131327 131155 13 939 131441 13 966 13 404 131235 13 res
SMV.rw18701082 13 703 13 942 13 752 13 637 13 858 131057 131103 131239 13 581 13 res
SMV.rw1880 733 131002 131137 131093 131070 131393 13 867 131101 13 713 13 950 13 res
SMV.rw1890 576 131090 13 984 13 393 131000 131242 13 833 131149 131321 13 624 13 res
SMV.rw1900 696 13 726 13 548 131109 13 978 13 928 13 716 121558 121311 12 902 12 res
SMV.rw1910 640 121285 121304 121184 12 968 12 883 12 561 121140 12 931 121333 12 res
SMV.rw1920 813 121172 12 966 12 291 121104 121198 121242 121398 121159 12 926 12 res
SMV.rw1930 904 121108 121169 121258 12 536 121339 12 677 121142 121517 12 500 12 res
SMV.rw19401048 121484 12 925 12 994 121000 12 938 12 738 121175 121084 121086 12 res
SMV.rw1950 691 12 515 12 703 121074 12 773 12 991 12 627 121026 11 863 11 977 11 res
SMV.rw19601194 11 888 111078 111030 11 856 111317 111082 11 942 111002 111482 11 res
SMV.rw19701172 11 694 11 731 11 916 11 600 111448 11 958 111001 11 806 11 808 11 res
SMV.rw1980 547 111322 11 938 111238 111085 11 965 11 988 11 752 11 717 11 300 11 res
SMV.rw19901123 11 976 111019 111094 111358 111023 11 873 111098 111248 11 914 11 res
SMV.rw2000 547 11 761 11 245 11 912 11 834 111236 11 985 111323 11 724 6 726 6 res
SMV.rw20109990 09990 09990 09990 09990 09990 09990 09990 09990 09990 0 res
SMV.rwl -- no data title -- 1st itrdb line missing ars
SMV.rwl -- no data title -- 2nd itrdb line missing ars
SMV.rwl -- no data title -- 3rd itrdb line missing ars
SMV.rw-2689990 09990 01437 2 949 2 954 2 986 21065 2 910 2 284 2 570 2 ars
SMV.rw-260 726 2 517 2 820 21040 2 726 21568 21273 21503 21398 21683 2 ars
SMV.rw-250 737 21030 2 651 2 579 2 673 2 713 2 294 2 689 2 643 2 584 2 ars
SMV.rw-240 751 21100 21101 2 977 21044 21474 2 589 2 899 21223 21085 2 ars
SMV.rw-230 831 2 937 2 878 2 877 21293 21496 21174 21058 21093 21476 2 ars
SMV.rw-2201707 21342 21521 21527 21492 2 566 21271 21052 2 836 2 923 2 ars
SMV.rw-210 830 21155 21171 2 928 2 880 21100 21272 2 702 2 256 2 843 2 ars
SMV.rw-200 924 3 513 3 782 3 880 31100 31317 31068 3 962 3 802 3 674 3 ars
SMV.rw-190 796 3 870 3 876 31335 31139 31172 31509 31439 3 627 3 936 3 ars
SMV.rw-180 702 31613 31787 31358 31567 31339 31001 3 971 3 835 3 385 3 ars
SMV.rw-170 904 31051 31140 31533 31661 31037 31428 31457 32280 32035 3 ars
SMV.rw-160 975 3 615 31144 3 370 3 523 3 289 3 395 3 659 3 828 3 699 3 ars
SMV.rw-150 966 31357 31811 3 891 31293 31232 31467 31307 3 808 31126 3 ars
SMV.rw-1401322 31342 3 397 3 765 3 952 3 863 31312 31205 3 949 3 813 3 ars
SMV.rw-1301339 3 651 3 797 31255 3 906 31068 31639 31609 31188 31496 3 ars
SMV.rw-1201424 31195 31282 31262 31507 31226 31012 31354 31360 31198 3 ars
SMV.rw-1101447 31000 3 650 31457 31386 3 871 31811 31522 31115 31126 3 ars
SMV.rw-100 560 3 181 3 775 31041 3 697 3 851 31353 3 723 4 968 4 498 4 ars
SMV.rw -90 474 4 616 4 612 4 880 4 942 4 662 41243 4 991 41160 41044 4 ars
SMV.rw -80 592 41426 41106 41389 41018 5 586 5 634 51046 5 803 5 604 5 ars
SMV.rw -70 646 5 757 51058 5 735 51465 51388 51107 51047 51643 5 521 5 ars
SMV.rw -60 642 51450 51395 5 801 51186 5 830 5 934 51468 51188 5 850 5 ars
SMV.rw -501219 51060 51562 51574 51211 5 413 51266 51107 5 782 5 718 5 ars
SMV.rw -40 991 5 770 5 531 5 505 5 745 5 487 5 637 5 550 51143 51161 5 ars
SMV.rw -301693 5 932 5 670 51186 51419 51512 5 737 5 662 51077 5 555 5 ars
SMV.rw -201120 51454 51658 51553 51021 51413 51123 5 568 5 837 5 999 5 ars

SMV.rw -101367 51331 51723 5 979 51034 5 649 5 839 51729 5 530 51172 5 ars
SMV.rw   01402 5 983 5 360 5 876 5 397 5 165 5 571 51021 51430 5 683 5 ars
SMV.rw 10 473 5 366 5 517 5 448 5 608 5 675 5 432 5 627 5 605 51349 5 ars
SMV.rw 20 715 5 682 51444 51653 5 775 51198 51913 51656 51562 51726 5 ars
SMV.rw 301966 51312 51260 5 726 5 514 5 738 5 605 5 466 5 948 5 626 5 ars
SMV.rw 40 260 5 267 5 682 51155 5 870 51382 51003 51044 51376 51946 5 ars
SMV.rw 501172 51138 5 738 51274 51111 51578 5 779 5 508 5 237 5 488 5 ars
SMV.rw 60 324 51310 51661 5 784 51403 51702 5 719 5 999 5 656 5 576 5 ars
SMV.rw 70 524 51018 51131 51092 5 803 5 729 51333 51570 51493 51269 5 ars
SMV.rw 80 799 5 790 51100 51026 5 697 5 598 51088 5 513 51496 51121 5 ars
SMV.rw 901642 5 447 5 840 5 803 51015 5 520 5 825 5 905 5 722 5 808 5 ars
SMV.rw 100 669 6 434 6 563 7 552 7 928 7 966 71281 71064 71430 71435 7 ars
SMV.rw 1101461 71500 71122 71196 71367 7 952 7 438 7 501 7 543 7 587 7 ars
SMV.rw 1201477 71514 7 946 7 806 7 775 7 374 7 414 7 765 7 714 7 633 7 ars
SMV.rw 130 689 7 305 71060 7 564 7 649 7 813 7 809 7 285 7 619 7 911 7 ars
SMV.rw 140 742 7 366 7 574 7 956 7 698 7 918 7 801 7 726 7 595 7 906 7 ars
SMV.rw 150 331 7 519 7 551 7 975 7 274 71200 71288 7 791 7 456 7 402 7 ars
SMV.rw 160 515 7 199 7 493 7 772 7 235 7 272 7 619 7 986 7 365 71010 7 ars
SMV.rw 1701010 7 688 7 545 71602 71012 71207 71087 71240 7 734 7 432 7 ars
SMV.rw 1801095 7 881 71342 7 958 7 876 7 390 7 523 71105 71484 7 938 7 ars
SMV.rw 190 777 71020 7 908 7 558 7 821 7 530 71173 72111 71327 71249 7 ars
SMV.rw 200 925 7 610 71091 71305 71008 7 661 7 858 7 829 7 655 7 610 7 ars
SMV.rw 210 401 7 690 7 853 7 829 7 415 7 857 7 703 7 884 7 838 7 771 7 ars
SMV.rw 220 768 8 470 8 513 81096 81126 8 589 8 789 81471 8 864 81025 9 ars
SMV.rw 230 868 9 591 91402 91361 9 877 9 783 9 992 91151 9 654 91321 9 ars
SMV.rw 2401103 9 886 91056 91310 91259 9 556 9 740 91044 9 573 101243 10 ars
SMV.rw 2501273 101092 101184 10 666 101222 10 899 101011 10 754 10 622 10 970 10 ars
SMV.rw 260 984 10 663 10 469 101321 101108 10 751 10 875 101021 101234 10 883 10 ars
SMV.rw 270 413 10 898 10 549 10 759 10 502 10 481 101150 101071 10 629 10 563 10 ars
SMV.rw 2801366 101248 101540 101314 101306 101694 10 979 101025 101392 101118 10 ars
SMV.rw 290 977 10 466 101340 10 744 10 771 101315 101480 10 745 10 498 101248 10 ars
SMV.rw 3001532 101223 10 557 101125 101275 10 936 10 752 10 605 101058 10 465 10 ars
SMV.rw 3101166 101197 101266 10 535 101252 10 331 101189 101054 10 551 10 786 10 ars
SMV.rw 3201489 10 581 10 456 101030 10 831 10 736 10 702 10 786 10 576 101290 10 ars
SMV.rw 330 856 10 700 10 919 101208 101323 10 726 10 946 10 742 10 954 10 895 10 ars
SMV.rw 340 957 10 500 10 713 10 900 10 880 10 904 101077 10 907 10 630 101249 10 ars
SMV.rw 350 873 10 796 10 929 10 994 101055 10 902 10 974 10 569 10 927 10 373 10 ars
SMV.rw 3601094 101098 101083 10 819 10 823 101117 101063 101245 101047 11 595 11 ars
SMV.rw 370 543 111022 111206 11 610 11 847 111230 111050 10 812 10 976 10 744 10 ars
SMV.rw 380 793 101172 10 783 10 993 10 980 10 891 10 983 10 608 10 744 10 922 10 ars
SMV.rw 390 700 10 513 10 777 10 611 101069 101306 101020 101141 101322 10 994 10 ars
SMV.rw 400 978 101413 10 672 101018 101107 101168 101441 101335 101515 10 702 10 ars
SMV.rw 4101242 10 661 101166 101238 101368 101453 10 778 10 553 10 699 10 660 10 ars
SMV.rw 420 715 10 899 10 992 10 501 10 731 101306 101685 101101 101563 10 915 10 ars
SMV.rw 4301196 10 887 10 782 101164 10 834 10 757 101174 10 946 101246 101210 10 ars
SMV.rw 440 732 101187 10 970 101389 10 953 9 850 9 227 9 800 91235 91426 9 ars
SMV.rw 4501294 91210 91238 91280 9 948 9 766 9 792 91177 91097 9 884 9 ars
SMV.rw 460 255 9 801 91557 9 676 9 899 91142 9 786 9 994 91138 9 467 9 ars
SMV.rw 470 753 9 748 9 836 9 224 10 630 101166 101299 101053 10 819 10 968 10 ars
SMV.rw 4801229 10 792 10 863 101057 101002 101063 101036 101256 101111 101211 10 ars
SMV.rw 4901533 101280 101177 10 848 101507 101239 101288 101023 101180 10 934 10 ars
SMV.rw 500 912 10 753 101229 10 946 101168 101110 101006 10 747 10 734 10 511 10 ars
SMV.rw 510 628 10 787 10 579 10 953 111146 111186 11 979 111153 111398 11 559 11 ars
SMV.rw 5201060 11 881 111153 111554 111417 111173 11 728 111506 111137 111282 11 ars
SMV.rw 5301682 11 538 111008 111260 111176 11 714 11 746 11 997 11 874 11 630 11 ars
SMV.rw 540 810 11 820 11 593 11 665 11 998 11 911 111186 111012 111119 111457 11 ars

SMV.rw 5501336 111568 111536 111556 11 828 11 821 111075 111118 11 873 111212 11 ars
SMV.rw 560 944 11 768 111044 111446 11 678 11 765 111219 111510 11 860 111271 11 ars
SMV.rw 5701005 111588 111469 111390 111321 111911 11 985 11 823 11 617 111018 11 ars
SMV.rw 580 822 111377 111165 111005 11 793 111020 111219 111313 12 741 121487 12 ars
SMV.rw 5901277 12 769 121235 121207 12 955 12 602 121240 121309 121051 12 627 12 ars
SMV.rw 6001328 121511 121359 12 532 121086 121021 121152 121386 121412 121156 12 ars
SMV.rw 610 749 12 496 12 655 12 912 12 916 12 482 12 972 121028 121278 121025 12 ars
SMV.rw 620 622 121571 121325 121163 121384 12 833 12 664 12 931 121226 121413 12 ars
SMV.rw 630 416 12 819 12 497 121089 12 978 12 987 121451 121286 12 801 12 317 12 ars
SMV.rw 640 457 12 912 121011 12 707 13 692 13 356 13 944 13 383 13 809 13 965 13 ars
SMV.rw 6501019 13 619 131151 13 773 131012 131061 131033 13 991 13 734 13 862 13 ars
SMV.rw 660 456 131229 131729 13 845 131269 131376 131244 131329 131031 13 545 13 ars
SMV.rw 670 706 13 928 13 996 13 908 131325 13 899 13 837 13 591 13 549 13 937 13 ars
SMV.rw 680 875 13 683 131145 131288 131117 131356 13 672 13 824 131076 131152 13 ars
SMV.rw 690 618 13 680 13 738 13 770 13 936 13 587 131008 131093 13 653 131286 13 ars
SMV.rw 700 886 13 820 131485 131302 13 846 13 660 13 641 13 910 131172 131262 13 ars
SMV.rw 7101580 131559 131316 131387 131828 131280 131167 13 946 131086 131043 13 ars
SMV.rw 720 854 13 550 13 784 13 464 13 977 131135 131060 13 988 131559 131062 13 ars
SMV.rw 7301390 131210 131558 131658 131390 13 626 13 369 131109 13 675 13 525 13 ars
SMV.rw 7401574 131542 13 921 131253 131603 13 747 131412 13 853 131294 13 816 13 ars
SMV.rw 7501003 13 720 131296 13 853 131058 131109 131508 131447 131733 131188 13 ars
SMV.rw 7601062 13 811 131579 131291 131313 131459 131648 131038 131126 131219 13 ars
SMV.rw 770 311 13 533 131029 131347 13 665 131000 131093 13 768 131011 13 802 13 ars
SMV.rw 7801008 131160 13 728 13 743 131013 131378 13 655 131051 131138 131209 13 ars
SMV.rw 7901054 131031 131284 131207 131354 131465 131476 131207 13 924 13 929 13 ars
SMV.rw 8001591 131787 131498 131231 131201 131273 13 853 13 689 131050 13 216 13 ars
SMV.rw 810 944 13 933 13 777 131029 131139 131111 13 516 13 967 13 734 13 612 13 ars
SMV.rw 8201470 131622 131359 13 852 13 866 13 628 131095 131631 131819 131069 13 ars
SMV.rw 830 507 131072 131015 131068 131038 13 763 13 578 13 206 13 626 13 563 13 ars
SMV.rw 840 704 131115 131433 131617 131296 131212 13 622 13 796 131147 131540 13 ars
SMV.rw 8501515 13 803 131161 131053 131256 13 963 13 738 13 228 13 839 13 674 13 ars
SMV.rw 860 563 13 791 13 761 131009 13 912 13 790 13 851 13 876 13 729 13 991 13 ars
SMV.rw 8701353 131333 131102 131076 13 835 13 612 131263 131199 13 721 13 884 13 ars
SMV.rw 8801233 131025 13 698 13 918 13 662 13 713 131275 131054 131275 13 640 13 ars
SMV.rw 8901392 131142 13 868 131124 131389 131283 131316 13 649 13 809 13 939 13 ars
SMV.rw 900 717 13 659 13 616 13 518 131020 131052 13 650 13 579 131222 131362 13 ars
SMV.rw 9101131 131184 131299 13 524 13 804 13 605 13 988 131144 131184 141033 14 ars
SMV.rw 920 936 14 937 14 234 141091 14 705 15 777 151105 15 692 151061 15 870 15 ars
SMV.rw 9301069 151232 151058 151417 151021 151306 151530 151122 151347 151386 15 ars
SMV.rw 9401388 151491 151112 151367 15 901 151017 151209 15 853 15 860 15 913 15 ars
SMV.rw 9501131 151345 15 834 151170 15 860 15 920 151197 151017 15 681 151192 15 ars
SMV.rw 9601523 151069 151068 151279 151252 151354 151728 151723 151655 151103 14 ars
SMV.rw 9701243 14 984 14 568 141321 141325 14 523 14 698 141006 141071 141107 14 ars
SMV.rw 980 422 14 339 14 989 14 940 141031 141528 141400 141387 141162 141372 14 ars
SMV.rw 990 778 141252 14 991 141087 141106 141461 14 897 141281 14 408 14 286 14 ars
SMV.rw1000 933 13 553 13 785 13 617 13 941 13 295 131135 131585 131135 131259 13 ars
SMV.rw10101199 131089 131018 13 926 13 318 13 766 13 970 13 866 13 995 131277 13 ars
SMV.rw10201577 14 991 141115 14 711 141310 141321 141257 141415 141283 141416 13 ars
SMV.rw10301338 13 703 131153 131259 131017 14 762 14 570 14 510 14 419 14 811 14 ars
SMV.rw1040 815 14 839 14 874 14 888 14 613 14 799 14 966 141253 141305 14 965 14 ars
SMV.rw1050 930 141122 141409 141238 141072 141272 141266 14 770 14 900 141083 14 ars
SMV.rw10601357 141738 141193 14 899 14 878 131215 131173 13 610 13 862 13 815 13 ars
SMV.rw10701114 13 777 13 947 13 935 13 909 13 663 13 948 13 909 13 664 131163 13 ars
SMV.rw10801015 131131 131044 13 818 13 779 13 848 13 929 13 897 131322 131010 13 ars
SMV.rw1090 280 13 355 13 854 13 796 12 858 12 931 121030 12 411 12 640 12 578 12 ars
SMV.rw1100 694 121159 12 977 12 961 12 867 12 814 12 886 12 594 12 721 12 442 12 ars

SMV.rw1110 976 12 854 131238 13 892 131001 131075 131157 131362 131156 13 745 13 ars
SMV.rw1120 925 13 596 131141 13 788 13 842 131274 13 980 13 741 13 946 131168 13 ars
SMV.rw1130 702 13 485 13 505 13 807 13 921 131034 131071 131310 131181 13 955 13 ars
SMV.rw1140 305 131026 131210 13 575 13 598 131011 13 715 131096 12 643 12 780 12 ars
SMV.rw1150 288 121018 121641 121533 12 780 121106 12 908 121199 12 902 12 930 12 ars
SMV.rw1160 933 12 755 111452 111338 11 614 11 778 11 885 11 817 11 747 11 727 11 ars
SMV.rw1170 964 111418 111402 111459 11 708 11 639 11 942 11 284 111111 111058 11 ars
SMV.rw11801118 11 909 11 992 111706 111655 111205 11 548 11 961 11 654 11 814 11 ars
SMV.rw1190 912 111446 111037 11 897 11 994 10 942 10 674 10 836 10 800 10 629 10 ars
SMV.rw1200 700 101052 10 904 101021 9 650 9 619 9 463 9 612 9 769 9 567 9 ars
SMV.rw1210 716 91347 9 786 8 636 8 700 81075 8 807 8 520 8 807 8 582 8 ars
SMV.rw12201245 8 760 81204 81013 81014 81292 8 973 81072 81093 8 875 8 ars
SMV.rw1230 956 81225 8 734 8 630 8 432 8 955 8 888 8 887 81163 8 906 8 ars
SMV.rw1240 672 81196 81237 8 979 8 912 9 765 9 516 9 820 9 573 91047 9 ars
SMV.rw1250 659 9 409 9 670 91438 9 716 91171 9 955 91210 9 158 91014 9 ars
SMV.rw12601408 101092 10 724 101123 101128 10 682 10 719 101399 101152 101108 10 ars
SMV.rw1270 962 101270 101300 10 817 10 704 101567 101029 101329 101035 101008 9 ars
SMV.rw1280 671 9 765 91090 91015 91167 9 799 91132 91126 9 621 9 535 9 ars
SMV.rw1290 904 9 604 9 942 9 818 9 590 9 870 9 852 9 449 91073 91205 9 ars
SMV.rw1300 807 91287 91293 9 778 9 428 9 788 9 891 9 932 91319 91102 9 ars
SMV.rw13101319 91300 9 718 91149 91463 91183 9 477 9 857 9 661 9 916 9 ars
SMV.rw1320 986 10 941 101150 10 678 10 882 101404 101088 101031 101100 101532 10 ars
SMV.rw1330 976 101241 101010 10 895 10 934 10 772 10 734 10 843 10 354 10 545 11 ars
SMV.rw1340 893 11 662 11 780 111045 11 556 11 556 11 969 111010 11 926 11 647 11 ars
SMV.rw1350 946 111087 11 551 111018 11 858 11 552 101052 10 771 10 811 101253 10 ars
SMV.rw1360 618 10 914 101285 10 604 10 650 111216 111340 11 677 111069 12 823 12 ars
SMV.rw13701539 121676 121663 121443 121576 12 699 12 604 121435 121126 121565 12 ars
SMV.rw13802080 121632 121178 121371 121418 121950 122045 121096 121691 121518 12 ars
SMV.rw1390 832 121235 121563 12 691 12 828 121507 121388 12 982 12 972 12 260 12 ars
SMV.rw1400 499 12 634 12 912 12 857 121070 121236 121376 12 856 12 873 121491 12 ars
SMV.rw14101162 131121 13 947 13 812 13 761 13 578 13 754 13 788 13 936 13 815 13 ars
SMV.rw1420 771 13 768 13 863 13 326 13 772 131057 131602 131620 131879 131141 13 ars
SMV.rw14301657 131568 131292 131335 131756 121452 121400 12 686 12 506 12 910 12 ars
SMV.rw1440 992 121207 12 640 121012 12 908 12 309 121015 121293 121108 12 631 12 ars
SMV.rw14501076 121751 121165 12 974 121173 12 764 12 746 12 724 12 624 12 637 12 ars
SMV.rw14601048 12 855 12 840 121010 121150 12 960 12 813 12 843 12 807 12 577 12 ars
SMV.rw1470 930 12 603 121187 121372 121041 12 462 12 581 12 742 121188 121464 12 ars
SMV.rw1480 899 121324 12 944 12 723 12 990 121308 121299 12 973 12 788 121186 12 ars
SMV.rw14901728 121581 12 901 12 781 121141 12 345 12 607 121095 121202 12 825 12 ars
SMV.rw1500 532 121014 121686 121137 121470 121294 12 344 111588 111264 11 916 11 ars
SMV.rw1510 915 111042 111154 11 697 11 972 111072 11 613 11 919 11 934 111610 11 ars
SMV.rw15201162 111541 11 538 111198 11 492 111181 111158 11 945 11 504 111300 11 ars
SMV.rw15301472 111156 111489 11 966 11 767 111185 111413 111084 11 638 111206 11 ars
SMV.rw15401347 121208 121126 121083 121526 12 778 12 567 12 643 121042 121060 12 ars
SMV.rw15501239 12 853 12 850 121049 121224 121293 121368 12 996 12 375 12 746 12 ars
SMV.rw1560 557 12 805 12 860 121299 121446 121014 121161 12 749 121102 121375 12 ars
SMV.rw15701012 121050 12 993 12 490 12 458 12 872 12 916 12 929 12 835 12 683 12 ars
SMV.rw1580 742 12 419 121180 12 940 12 415 12 543 12 836 121011 121240 121298 12 ars
SMV.rw1590 963 12 894 121100 121054 121064 121591 121147 121416 12 993 121294 12 ars
SMV.rw16001254 12 781 12 951 121347 121343 121018 12 813 12 869 121335 12 836 12 ars
SMV.rw16101101 121236 12 625 121247 121155 12 835 12 775 12 998 12 857 121027 12 ars
SMV.rw1620 949 121270 12 830 12 604 12 704 12 651 12 942 121126 12 969 121280 12 ars
SMV.rw16301377 12 782 121115 12 970 121649 12 978 121329 121814 121544 121548 12 ars
SMV.rw16401599 12 930 121324 121273 12 848 12 305 12 953 121123 121081 12 698 12 ars
SMV.rw1650 777 121229 12 904 12 560 12 936 121589 121239 121258 12 622 12 873 12 ars
SMV.rw16601117 121625 121342 121494 121050 121268 12 455 12 788 12 713 12 856 12 ars

SMV.rw1670 991 121275 12 697 12 497 12 787 12 541 12 852 12 697 121092 12 748 12 ars
SMV.rw1680 883 12 827 12 911 12 914 12 724 12 239 12 710 12 904 121119 121549 12 ars
SMV.rw16901309 121322 121515 121745 12 599 12 852 12 730 121145 121288 121335 12 ars
SMV.rw17001230 121462 12 816 12 960 12 567 12 353 12 974 12 607 12 755 121066 12 ars
SMV.rw17101175 12 961 12 918 121149 12 825 12 893 12 713 12 835 121220 121284 12 ars
SMV.rw17201385 121799 121584 121099 121162 121003 121620 121012 121096 12 907 12 ars
SMV.rw17301073 121393 12 783 12 944 121421 12 680 12 923 12 489 121284 121601 12 ars
SMV.rw1740 942 12 980 12 819 121136 12 969 12 643 121061 121230 12 339 12 954 12 ars
SMV.rw17501066 12 928 12 416 12 926 121327 12 976 121237 121496 121355 121179 12 ars
SMV.rw1760 931 121407 121302 121102 121175 121198 12 944 12 984 12 765 12 615 12 ars
SMV.rw1770 567 12 926 12 469 12 715 12 947 12 507 12 808 131186 13 901 13 722 13 ars
SMV.rw1780 914 131077 131213 131423 131555 131067 131191 131440 131820 13 890 13 ars
SMV.rw17901639 131483 131613 131282 131086 131426 131070 13 967 13 783 13 970 13 ars
SMV.rw18001130 13 945 131163 131325 131197 131073 13 782 131043 13 912 13 720 13 ars
SMV.rw18101147 131379 131284 131062 131477 131533 131545 131241 13 709 13 705 13 ars
SMV.rw1820 811 13 732 13 792 13 864 13 650 13 733 13 438 131215 131200 13 860 13 ars
SMV.rw1830 594 131355 131184 131235 131098 131069 13 702 131051 13 965 13 765 13 ars
SMV.rw1840 550 13 647 13 367 13 654 13 670 13 626 13 745 13 700 13 695 13 735 13 ars
SMV.rw1850 976 13 352 13 989 13 932 131063 13 940 13 850 13 767 131121 131196 13 ars
SMV.rw18601227 131053 131211 131444 131345 131094 131533 131228 13 526 131115 13 ars
SMV.rw18701186 13 755 13 835 13 721 13 533 13 661 13 904 131017 131193 13 628 13 ars
SMV.rw1880 596 13 876 131080 131071 131065 131422 131041 131132 13 808 13 917 13 ars
SMV.rw1890 565 13 928 13 944 13 337 13 726 131138 13 833 131027 131330 13 748 13 ars
SMV.rw1900 600 13 613 13 413 13 848 13 870 13 812 13 601 121396 121440 121026 12 ars
SMV.rw1910 661 121229 121427 121323 121090 12 973 12 612 121032 12 954 121288 12 ars
SMV.rw1920 903 121141 121045 12 326 12 865 121168 121259 121444 121334 121089 12 ars
SMV.rw1930 997 121171 121269 121370 12 693 121265 12 831 121085 121556 12 717 12 ars
SMV.rw1940 945 121522 121139 121028 121056 121012 12 760 121099 121132 121122 12 ars
SMV.rw1950 735 12 441 12 522 12 890 12 675 12 801 12 518 12 821 11 765 11 844 11 ars
SMV.rw19601095 11 899 111018 111041 11 876 111272 111194 111012 111027 111532 11 ars
SMV.rw19701390 11 847 11 726 11 889 11 579 111266 111036 11 979 11 798 11 760 11 ars
SMV.rw1980 465 111112 11 954 111167 111126 111022 111013 11 785 11 654 11 181 11 ars
SMV.rw1990 810 11 870 11 887 11 988 111337 111136 11 921 111102 111326 111044 11 ars
SMV.rw2000 573 11 642 11 145 11 570 11 624 111009 11 902 111233 11 793 6 648 6 ars
SMV.rw20109990 09990 09990 09990 09990 09990 09990 09990 09990 09990 0 ars

APPENDIX B

1100 YEARS OF OCEANIC FINGERPRINTS ON WESTERN NORTH AMERICAN DROUGHTS AND PLUVIALS

B.1 Abstract

Western North American (WNA) drought has serious implications for water resources, yet long-term controls on WNA climate and drought remain poorly understood. Here we re-assess evidence linking ocean forcing to past WNA droughts and pluvials. We assess the strength of ocean-drought teleconnection patterns preserved in tree-ring reconstructed drought maps, and also explore anomalies in a global network of sea surface temperature reconstructions. Potential forcing mechanisms of climate during Medieval Climate Anomaly (MCA), and individual drought and pluvial events over the past 1100 years are tested. We also assess the potential causes of two multidecadal-length pluvials during the MCA. We find compelling links between the tropical Pacific, the North Atlantic, and some WNA droughts and pluvials, but have difficulty directly linking changes in WNA climate during the MCA to ocean forcing. We find that much of the evidence linking past WNA climate to SSTs is based on tenuous associations and extrapolations of modern observations to broad periods where causal mechanisms remain poorly defined. We suggest links between past SSTs and WNA climate may be more nuanced than often portrayed.

B.2 Introduction

Western North America (WNA) has experienced a wide range of hydroclimatic conditions over the past millennium. Two broad periods include the Medieval Climate Anomaly (MCA, ~900-1400 AD) and the post-MCA, often referred to as the Little Ice Age. Drought area increased during the MCA (Cook et al., 2004) and both drought and pluvial events lasted longer (e.g., Woodhouse and Overpeck 1998; Herweijer et al., 2007). The post-MCA had shorter drought and pluvial events and less area under drought on average. Most ominous over the past millennium was the occurrence of multidecadal-length "megadroughts", droughts more severe than any observed during the historical record (Woodhouse and Overpeck 1998). Megadroughts occurred primarily during the MCA, but are present throughout the past millennium (Cook et al. 2004, 2007, 2010; Meko et al. 2007; Woodhouse and Overpeck 1998), as are numerous multidecadal-length pluvials. Here, we re-visit links between these past changes in WNA climate and potential sea surface temperature (SST) forcing mechanisms.

During the observational period (up to ~100 years ago), SSTs have strongly influenced WNA climate. SSTs tend to have longer "memory" than the atmosphere alone, which is likely needed to force persistent multidecadal to centennial-length climate changes. WNA climate is most strongly related to the El Niño Southern Oscillation (ENSO). During La Niña events, cool conditions in the eastern equatorial Pacific tend to displace storm tracks northward, resulting in reduced cool season precipitation in southwestern North America (Southwest), and the opposite tends to be true for El Niño events (e.g. Cayan et al. 1999; Redmond and Koch 1991; Schubert et al. 2009). The Pacific Decadal Oscillation (PDO) reflects the dominant mode of SST in the North Pacific (Mantua et al. 1997). Although linked with tropical Pacific variability (Newman et al. 2003), the PDO varies on longer timescales (Mantua et al. 1997). The Indian Ocean works in concert with the Pacific whereby warming in the western Pacific and Indian oceans drives deep convection that influences the overlying atmosphere and subsequently the mean position of storm tracks and WNA cool season rainfall (Wang et al., 2008). ENSO, PDO, and Indian Oceans all tend to influence precipitation in southwestern and northwestern North America (Northwest) in opposite directions, whereby the Northwest is wet and the Southwest is dry and vice versa.

North Atlantic SSTs, characterized by the Atlantic Multidecadal Oscillation (AMO), may also influence WNA precipitation, although to a lesser degree than the Pacific (Schubert et al., 2009). Warm North Atlantic SSTs are associated with warmer WNA temperatures. Regional warming associated with a positive AMO was shown to decrease runoff efficiency and stream flow in the Upper Colorado River Basin (Nowak et al. 2012). The impact of the North Atlantic may not be limited, however, to regional temperature effects on the water cycle. Instrumental records and climate models suggest the largest precipitation anomalies in WNA tend to occur when Pacific and Atlantic SSTs are opposite in sign (McCabe et al. 2004; Feng et al. 2011; Schubert et al. 2009), reflecting a combined influence of ocean basins on global atmospheric circulation.

Much evidence supports the assumption that causes of past megadroughts were an extension or enhancement of the processes influencing WNA climate today. The primary candidate is the tropical Pacific whereby extended “La Niña-like” conditions forced medieval aridity and megadroughts (i.e. Conroy et al. 2009b; Graham et al. 2007; Herweijer et al. 2007; Seager et al. 2007; Stahle et al. 2000). Links also have been drawn between the AMO and past WNA drought as established by a tree-ring reconstruction of North Atlantic SST over the past 400 years (Conroy et al., 2009b; Gray et al., 2004; McCabe et al., 2008). North Atlantic SSTs are less well constrained before ~1500 AD, but some SST proxy records indicate tenuous multidecadal to centennial-scale relationships between North American climate and the North Atlantic (Conroy et al. 2009b; Feng et al. 2008, 2011; Oglesby et al. 2012). Various general circulation model studies support the proxy records regarding the causes of medieval megadroughts. A cool tropical Pacific has the strongest ability to simulate WNA megadroughts (Burgman et al. 2010; Graham et al. 2007; Seager et al. 2008), but some modeling results indicate a warm North Atlantic can force drought in the Southwest and Midwest (i.e. Feng et al. 2011; Oglesby et al. 2012).

To date, most analyses tend to focus on megadroughts, and do not adequately address wet periods and the different causes of both droughts and pluvials. Here we extend previous work, using a multifaceted approach to assess the evidence linking SSTs to persistent wet and dry periods in WNA over the past millennium. We use teleconnection patterns imbedded in gridded drought reconstructions, and a screened network of SST proxy records to address the following research questions:

1) What changes in ocean/atmosphere circulation are associated with WNA climate between the MCA and post-MCA?

2) What evidence links WNA megadroughts and pluvials to SST forcing?

3) If La Niña conditions persisted during the entire MCA and are responsible for widespread drought and aridity, what explains the existence of decadal-length pluvials within the MCA in the early 13^{th} and 14^{th} centuries?

We highlight key gaps in our current understanding of the causes of WNA climate variability. Although there are limitations to our approach, we find the storyline linking SSTs to WNA climate is complex and more nuanced than often portrayed.

B.3 Methods

PDSI

Western droughts and pluvials over the period 900-2006 AD were characterized by using the North American Drought Atlas (NADA, Cook et al. 2008). The NADA is a gridded network of tree-ring reconstructed PDSI. Western grid points (27.5ºN to 50º N, 97.5ºW to 125ºW, after Cook et al. 2004) were averaged and smoothed with a 50-year cubic smoothing spline in highlight multidecadal variability (Figure B.1). Pluvial and drought periods were identified as intervals during which the smoothed series exceeded 0.2 PDSI units above or below the series mean respectively (Table B.1).

Teleconnection Patterns

Teleconnection maps were used to investigate relationships between drought patterns and circulation indices. We assessed December-February averages of circulation indices including NINO3 (1856-2006; EXTENDED NINO3 index:

Kaplan et al. 1998; Reynolds et al. 2002), the PDO (1900-2006; Mantua et al. 1997) and the AMO (1880-2006; van Oldenborgh et al., 2009). Correlating the instrumental circulation indices with each grid-point in the NADA developed modern teleconnection pattern maps. Teleconnection pattern maps were then spatially correlated with NADA maps through time. To compute spatial correlations between maps, we reshaped the teleconnection map and tree-ring reconstructed PDSI map into columns, and then computed the r-value between the two columns. We assessed relationships between the modern teleconnection patterns and the NADA for every year in the 900–2006 AD analysis period, resulting in a time series of the teleconnection pattern strength in drought patterns. The modern teleconnection maps and past teleconnection strength (r-value) time series were developed using the entire NADA, not the subset used to define Western droughts and pluvials. We assessed the teleconnection time series during pluvials and droughts, and during the wettest years within pluvials and the driest years within droughts. The wettest and driest years were defined by unsmoothed PDSI deviations exceeding ±1 respectively.

Spectral Analysis

We performed spectral analysis on the tree-ring reconstructed PDSI and teleconnection time series to test if low frequency characteristics of the PDSI during the MCA (i.e. Herweijer et al., 2007) can be attributed to changes in a particular teleconnection pattern and associated ocean basin. We used the multi taper method (Thompson 1982). The series were normalized by their mean and variance and detrended prior to spectral analysis. The time series were split into MCA and post-

MCA segments. The 95% significance test for spectral peaks was developed using a Monti Carlo approach: spectra were computed on 5000 random series with the same AR1 autocorrelation and variance as the original series. The resulting spectral values were then sorted by power at each frequency to create a probability distribution of spectral estimates. The upper 95th percentile for each distribution was used as the confidence limit for the respective frequency.

PaleoSST Reconstruction Anomaly Maps

To further test links between WNA climate and SST forcing, we assessed proxy SST reconstructions. SST records where obtained from the Leduc database (Leduc et al. 2010), the NOAA paleoclimate data center (http://www.ncdc.noaa.gov/paleo/paleo.html), and personal communication with authors. Proxy SST records were screened by degree of resolution and age control (Table B.S1). Records were retained that have 30 or more data points in the analysis period, data points during the MCA and post-MCA periods, data points in drought and pluvial intervals, and 2 or more age control points in the analysis period. To assess potential relationships between SST's and past WNA climate, we evaluated proxy SST anomalies for MCA (900-1400AD) and post-MCA (1400-2000AD) periods, and for drought and pluvial intervals identified above. Proxy SST anomalies were computed with respect to the 900-2000 AD analysis period mean or series length mean if less than the analysis period. The sample and age resolution of the SST proxy records makes assessing SST anomalies during relatively short drought and pluvial intervals dubious at best. To alleviate this shortcoming, we combined all drought and pluvial intervals to average out some of the age uncertainty in the SST records, but results should still be viewed with caution.

B.4 Results

Smoothed WNA PDSI shows seven droughts and eight pluvials between 900 and 2000 AD (Figure B.1). Table B.1 shows the drought and pluvial intervals. Droughts occurred predominantly in the MCA whereas pluvials were more concentrated in the post-MCA period. Two extreme WNA pluvials, however, occurred in the MCA and two severe droughts occurred in the post-MCA. Western PDSI spans the Southwestern and Northwestern climate regions. As a result these widespread drought and pluvial events defined here span regions with somewhat different teleconnected remote forcing.

Our teleconnection pattern maps between instrumental circulation indices and North American PDSI are similar to those shown in Cook et al. (2013). The NINO3 and PDO teleconnection maps are characterized by a north-south dipole in Western climate whereby when the Southwest is dry, the Northwest is wet and vice versa (Figure B.2a-b). The NINO3 teleconnection pattern is stronger and more widespread in the Southwest whereas the PDO has a more widespread influence in the Northwest. However, the spatial patterns of the PDO and NINO3 are extremely similar. The modern relationship between the AMO and WNA climate is less pronounced. The AMO has a weakly negative but significant relationship with PDSI across much of North America during the instrumental period (Figure B.2c).

Correlating the teleconnection maps with the annual reconstructed NADA maps over the 900–2000 AD analysis period results in r-value “teleconnection” time series (Figure B.2d-f) that reflect the strength and direction of the associated teleconnection pattern in North American climate through time. The NINO3 teleconnection time series (Figure B.2d) ranges between $r = 0.81$ and $r = –0.80$ with a mean absolute teleconnection strength of $r = 0.32$. The PDO teleconnection time series (Figure B.2e) ranges between $r = 0.76$ and $r = –0.77$ with a mean absolute teleconnection strength of $r = 0.30$. Not surprisingly the PDO and NINO3 teleconnection time series are almost identical to each other ($r = 0.96$, $p < 0.0001$), as reflected by their teleconnection patterns. As a result, distinguishing between the NINO3 and PDO patterns is not feasible; so we will tend to refer to the NINO3 pattern or the combined “ENSO” pattern. Correlations between the AMO teleconnection pattern and Western PDSI (Figure B.2f) range between $r = \pm 0.61$ with a mean absolute teleconnection strength of $r = 0.18$. The NINO3 and AMO teleconnection series are negatively correlated with each other ($r = –0.57$, $p < 0.0001$).

Western pluvials and droughts are associated with distinct teleconnection patterns over much of the analysis period. NINO3 and PDO teleconnection time series (Figure B.2d-e) tend to have sequences of positive anomalies during pluvials and negative anomalies during droughts. Correlating the NINO3 teleconnection time series with WNA PDSI during drought and pluvial intervals suggests that the NINO3 pattern can explain between 41-64% of the variance in WNA droughts and pluvials (Table B.1), whereas the PDO explains between 12-46%. As we are characterizing them by averaging Western PDSI, Western droughts tend to be West-wide events. Thus the southward-displaced PDO dipole (Figure B.2b) would lower the correlation between the PDO pattern and West-wide droughts with respect to NINO3. Negative (La Niña) NINO3 teleconnection patterns are slightly more frequent during the MCA (59% of all years) than the post MCA (53% of all years). The average absolute strength of the NINO3 teleconnection pattern series does not change between the MCA ($r_{abs} = 0.32$) and post-MCA ($r_{abs} = 0.31$). Pluvials and droughts often are characterized by negative and positive AMO teleconnection patterns respectively (Figure B.2f). The AMO teleconnection time series explains between 1% and 35% of the variance in WNA droughts and pluvials (Table B.1). The frequency of positive/negative AMO teleconnection patterns changes slightly between the MCA and post MCA (54% of all years during the MCA are AMO+ and 45% of all years during the post MCA are AMO+) The average absolute AMO teleconnection pattern strength in the NADA increases in the MCA ($r_{abs} = 0.22$) with respect to the post-MCA ($r_{abs} = 0.14$).

Persistent drought and pluvial events tend to be composed of groups of anomalous years, which are not necessarily consecutive and are often separated by near average years. Figure B.3 shows histograms of teleconnection time series values during the driest drought years and the wettest pluvial years. The driest drought years have average correlations of: NINO3, $r = –0.39$; PDO, $r = –0.28$; and AMO, $r = 0.15$. Wettest pluvial years have a weaker relationship and wider distribution than dry drought years with average correlations of: NINO3, $r = 0.29$; PDO, $r = 0.21$; and the AMO, $r = –0.12$. The directions of the teleconnection pattern relationships are generally consistent, but distribution of correlations indicates that the most extreme years in the West do not always reflect the teleconnection patterns assessed.

Spectral analysis shows WNA PDSI has a significant spectral peak around 143 years during the MCA (Figure B.4a), which is not present after the MCA (Figure B.4b). Neither the NINO3 nor AMO teleconnection time series show an associated increase in low frequency variance during the MCA (Figure B.4c, e). Rather, both teleconnection patterns show an increase in variance at around 9.5 years during the MCA.

Turning from teleconnections to results from analyses that directly measure forcing; our proxy SST record analysis results are generally consistent with previous work. Overall SST anomalies in the Pacific during the MCA are La Niña-like (Figure B.5a). There are three records in the eastern Pacific indicating the presence of an enhanced cold tongue during the MCA, including diatom inferred SST from Galapagos island lake sediment (Conroy et al. 2008), fossil coral from Palmyra Island (Cobb et al. 2003), and foraminifera from Santa Barbara Basin sediments (Kennet and Kennet 2000). In the western Pacific there are four records that indicate a warmer Warm Pool during the MCA. In the North Atlantic the proxy records do not necessarily indicate overall MCA warming. Rather proxy records suggest that the MCA was characterized overall by cool or neutral conditions in the western North Atlantic and warm conditions in the northeastern Atlantic. In the post-MCA period, eastern tropical Pacific records have warm anomalies and western tropical Pacific records have cool anomalies indicating a transition toward a more El Niño-like background state (Figure B.5b). The post medieval North Atlantic is a mixture of warm and cold anomalies. Combined drought and combined pluvial groups have "La Niña-like" and "El Niño-like" proxy SST anomalies respectively (Figure B.5c-d). The drought SST anomaly pattern shows overall warming in the North Atlantic, contrasting the mix of warm and cold anomalies during the MCA. The pluvial SST anomaly pattern is weakly El Niño-like.

B.5 Discussion

Were changes in WNA climate between the MCA and post-MCA forced by ocean/atmosphere circulation patterns? As shown in Figure B.1, there are more long-lasting drought and pluvial events during the MCA. Spectral analysis of Western PDSI also shows this change, with more low frequency variance during the MCA (Figure B.4a). Much previous work has attributed the change in WNA MCA climate to the tropical Pacific (i.e. Conroy et al. 2009; Graham et al. 2007; Herweijer et al. 2007; Seager et al. 2007).

Our results regarding differences between the MCA and post MCA are somewhat nuanced. The NINO3 teleconnection pattern time series (Figure B.2d) suggests ENSO has been important in controlling WNA climate variability over the past millennium. Yet there is little change in the strength or direction of ENSO patterns during the MCA. There is little evidence in the teleconnection patterns suggesting stronger or more frequent La Niña events forced MCA megadroughts. Furthermore spectral analysis of the ENSO teleconnection series does not show an increase in low frequency variance coincident with greater persistence in PDSI (Figure B.4c). The AMO teleconnection series (Figure B.2f) has a weaker relationship with WNA climate than the NINO3 series, but the overall strength increases somewhat during the MCA. This could indicate the North Atlantic had a stronger influence on WNA climate during the MCA. In modern times the North Atlantic varies on long (60-80 year) time scales, which suggests a stronger North Atlantic teleconnection during the MCA could have driven the timing of medieval droughts and pluvials, and be responsible for increases in MCA low frequency climate variability. Spectral analysis of the AMO teleconnection series, however, does not strongly support this argument. Rather, both the NINO3 and the AMO teleconnection series have an increase in spectral power at around 9.5 years during the MCA (Figure B.4c, e).

Proxy SST records suggest a relatively straightforward change between the MCA and post MCA. As highlighted by previous work, SST records show “La Niña” like conditions in the Pacific (Figure B.5a) and a strong east-west SST gradient characterized the MCA (Figure 6a-b; Conroy et al 2010). Coincident increases in WNA MCA drought present a suggestive narrative. Yet, the teleconnection patterns are inconsistent with La Niña as a causal mechanism. If La Niña conditions were responsible for medieval WNA aridity, the teleconnection mechanism must have had a different spatial imprint.

Previous findings using Pacific precipitation proxy records further confound the “La Niña like” MCA story. Precipitation reconstructions show an increase in MCA eastern tropical Pacific rainfall (Figure B.6c; Conroy et al. 2008), and a decrease in western tropical Pacific rainfall (Figure B.6d; Tierney et al, 2010) accompanied by a decreases in western tropical Pacific sea surface salinity (Figure

B.6e, Oppo et al. 2009). On instrumental time scales rainfall in the tropical Pacific is closely linked with SST's (e.g. Conroy et al. 2008). Thus, precipitation records indicate the MCA was El Niño like and the post-MCA was La Niña like, neatly contradicting the SST reconstructions (e.g. Conroy et al. 2008; Oppo et al. 2009; Tierney et al, 2010; Yan et al., 2011). As a result, conditions in tropical Pacific during the MCA may have no modern analogue (Tierney et al, 2010). A possible explanation for this apparent enigma may be more frequent and or stronger El Niño events imposed on the La Niña like background state during the MCA (i.e. Conroy et al. 2009a; Routson et al. 2011).

Our second research question focuses on the causes of drought and pluvial events. Teleconnection patterns are informative here, showing that many severe droughts have sequences of years with La Niña-like precipitation patterns (Figure B.2d). The 16th century megadrought stands out, characterized by consecutive La Niña patterns between 1566 and 1578, and the period between 1566 and 1587 is interrupted by only two slightly positive teleconnection years (Figure B.2d). Many of the MCA droughts also have sequences of La Niña precipitation patterns, but they do not tend to persist through the entire droughts. Pluvials tend to have positive ENSO type teleconnection patterns, but these patterns are generally weaker than for droughts. Pluvials during the 17th and 18th centuries have sequences of El Niño-like patterns. Droughts tend to have a positive relationship with the AMO teleconnection pattern, especially during characteristically widespread MCA megadroughts, and the opposite tends to be true for pluvials (Figure B.2f). We also assessed the patterns during the most severe years within drought and pluvial events. The patterns are consistent, albeit more pronounced than the broader drought and pluvial intervals (Figure B.3), suggesting that climate forcing during extreme years has a stronger relationship with SSTs.

The resolution and age control of proxy SST reconstructions are poor, and caution is advised when interpreting these records on relatively short drought and pluvial length timescales. SST reconstructions suggest that droughts and pluvials tend to have La Niña-like and El Niño-like background conditions, respectively. Proxy SST anomalies in the North Atlantic are ubiquitously warm during WNA droughts (Figure B.5c). This somewhat contrasts the overall MCA, which has a mixture of warm and cold anomalies. Pluvials are associated with a cool North Atlantic, but the pattern is not as robust as warmth during droughts. Warm and cold North Atlantic SST anomalies during droughts and pluvials respectively, support the hypothesis that the AMO could be driving the timing of multidecadal length droughts and pluvials.

Our third research question revolves around the existence of the two pluvials that occur within the MCA between 1176-1215 and 1290-1350 respectively. How could MCA pluvials occur during a time where SST proxy records show persistent La Niña conditions in the Pacific? This could be partially due to the low temporal resolution of the SST proxy data, but they may also be a manifestation of the complexity presented by the various tropical Pacific proxy records for the MCA as discussed above. The two pluvials are pronounced in our west-wide PDSI average, and are wet in both Southwestern and Northwestern PDSI reconstruction composites (Cook et al. 2013). PDSI maps of the two pluvials show they have relatively different spatial patterns across North America (Figure B.7). The first pluvial is characterized by a strong east-west dipole, where WNA is wet and Eastern North America is dry. The smoothed NINO3 teleconnection series is neutral during this first pluvial and the smoothed AMO teleconnection series is slightly negative (Figure B.8). The east-west dipole pattern of the 1176-1215 pluvial (Figure B.7) is strikingly reminiscent of the second mode of North American drought variability identified by Woodhouse et al. (2009). They define two dominant modes of North American drought using principal components analysis. Their first principal component (PC1) reflects an ENSO type north-south dipole pattern, and their second principal component (PC2) reflects an east-west dipole they link to the jet stream or Northern Annular Mode. During the 1176-1215 pluvial PC2 has a positive anomaly (Figure B.8). The second pluvial has a widespread "Pan-American" pattern, with the largest anomalies centered directly in the middle of WNA (Figure B.7). The widespread pattern of the second MCA pluvial is reminiscent of the AMO teleconnection pattern. The unsmoothed AMO teleconnection time series has a sequence of negative years from 1296 AD, through 1305 AD. The smoothed series in Figure B.8 also shows the AMO is negative during the earlier portion of this pluvial, suggesting that the AMO may have played a role in causing the second MCA pluvial. The PC indexes (Woodhouse et al. 2009) are less clear during the second MCA pluvial, showing small anomalies in both the first and second modes. Together the evidence suggests medieval pluvials were forced by a combination of factors, but predominantly the Northern Annular Mode during the first pluvial and perhaps the North Atlantic during the second pluvial. Neither pluvial map has a characteristic ENSO dipole pattern when averaged across the entire pluvial duration (Figure B.7).

B.6 Conclusion

Evidence linking ocean forcing to past WNA climate is nuanced. PDSI has more low frequency variance during the MCA, but teleconnection patterns do not show pronounced changes between the MCA and post MCA. La Niña teleconnection patterns increase only slightly during the MCA, and the strength of the AMO teleconnection pattern also increases somewhat during the MCA. SST reconstructions show the MCA was La Niña like, whereas precipitation reconstructions from the tropical Pacific show more frequent or stronger El Niño events occurred during the MCA. Teleconnection patterns indicate that ENSO, PDO, and AMO likely influenced severe WNA droughts and pluvials over the past millennium. Iconic droughts like the 16^{th} century megadrought and some medieval droughts have sequences of La Niña teleconnection patterns implicating the tropical Pacific. SST reconstructions corroborate the teleconnection patterns and indicate that severe droughts are associated with a La Niña-like pattern in the Pacific and a warm North Atlantic. SST patterns are more mixed during past pluvials, but tend to have an El Niño-like pattern. The cause of the two MCA pluvials is enigmatic. One pluvial appears to have a spatial pattern associated with the Northern Annular mode characterized in previous work (Woodhouse et al. 2009), and the other could be linked to the North Atlantic, but a combination of factors likely contributed to these events. Together the evidence linking past WNA climate to SSTs is still based on tenuous associations and extrapolations of modern observations. We show that sequences of years with strong

SST teleconnections were important for forcing discrete drought and pluvial events, but the evidence does not indicate the same processes were responsible for multidecadal to centennial scale variance changes in WNA climate.

B.7 References

Burgman, R., R. Seager, A. Clement, and C. Herweijer, 2010: Role of tropical Pacific SSTs in global medieval hydroclimate: A modeling study. Geophysical Research Letters, 37 (6), doi:10.1029/2009GL042239.

Cayan, D. R., K. T. Redmond, and L. G. Riddle, 1999: ENSO and Hydrologic Extremes in the Western United States. Journal of Climate, 12 (9), 2881-2893. doi: http://dx.doi.org/10.1175/1520-0442(1999)012<2881:EAHEIT>2.0.CO;2

Cobb, K. M., C. D. Charles, H. Cheng, and R. L. Edwards, 2003: El Nin˜o/Southern Oscilla- tion and tropical Pacific climate during the last millennium. Nature, 424 (6946), 271–276, doi:doi:10.1038/nature01779.

Conroy, J. L., J. T. Overpeck, J. E. Cole, T. M. Shanahan, and M. Steinitz- Kannan, 2008: Holocene changes in eastern tropical Pacific climate inferred from a Galápagos lake sediment record, Quaternary Science Reviews, 27, 1166–1180, doi:10.1016/j.quascirev.2008.02.015.

Conroy, J. L., A. Restrepo, J. T. Overpeck, M. Steinitz-Kannan, J. E. Cole, M. B. Bush, and P. A. Colinvaux, 2009a; Unprecedented recent warming of surface temperatures in the eastern tropical Pacific Ocean. Nature Geoscience, 2, 46–50, doi:10.1038/ngeo390

Conroy, J. L., J. T. Overpeck, J. E. Cole, and M. Steinitz-Kannan, 2009b: Variable oceanic influences on western North American drought over the last 1200 years. Geophysical Research Letters, 36 (17), doi:10.1029/2009GL039558.

Conroy, J. L., J. T. Overpeck, and J. E. Cole, 2010: El Niño/Southern Oscillation and changes in the zonal gradient of tropical Pacific sea surface temperature over the last 1.2 ka. PAGES news, 18 (1), 32-34.

Cook, E. R., C. A. Woodhouse, C. M. Eakin, D. M. Meko, and D. W. Stahle, 2004: Long- Term Aridity Changes in the Western United States. Science, 306 (5698), 1015–1018, doi:10.1126/science.1102586.

Cook, E. R., R. Seager, M. A. Cane, and D. W. Stahle, 2007: North American drought: Reconstructions, causes, and consequences. Earth Science Reviews, 81 (1-2), 93–134, doi:http://dx.doi.org/10.1016/j.earscirev.2006.12.002.

Cook, E. R., R. Seager, R. R. Heim Jr, R. S. Vose, C. Herweijer, and C. Woodhouse, 2010: Megadroughts in North America: placing IPCC projections of hydroclimatic change in a long-term palaeoclimate context. Journal of Quaternary Science, 25 (1), 48–61, doi: 10.1002/jqs.1303.

Cook, E.R., et al. 2008: North American summer PDSI reconstructions, version 2a, IGBP PAGES World Data Cent. Paleoclimatology Data Contributions Service 2008-046, Paleoclimatology Program, NGDC, NOAA, Boulder, Colorado.

Cook, B. I., J. E. Smerdon, R. Seager, and E. R. Cook, 2013: Pan-continental droughts in North America over the last millennium. Journal of Climate, (2013).

Feng, S., R. J. Oglesby, C. M. Rowe, D. B. Loope, and Q. Hu, 2008: Atlantic and Pacific SST influences on Medieval drought in North America simulated by the Community Atmospheric Model. Journal of Geophysical Research: Atmospheres, 113 (D11), doi: 10.1029/2007JD009347.

Feng, S., Q. Hu, and R. J. Oglesby, 2011: Influence of Atlantic sea surface temperatures on persistent drought in North America. Climate dynamics, 37 (3-4), 569-586 doi:10.1007/s00382-010-0835-x

Forman, S. L., M. Spaeth, L. Marín, J. Pierson, J. Gómez, F. Bunch, and A. Valdez, 2006: Episodic Late Holocene dune movements on the sand-sheet area, Great Sand Dunes National Park and Preserve, San Luis Valley, Colorado, USA. Quaternary Research, 66 (1), 97-108.

Graham, N. E., et al., 2007: Tropical Pacific-mid-latitude teleconnections in medieval times, Climatic Change, 83, 241–285, doi:10.1007/s10584- 007-9239-2.

Graham, N. E., C. M. Ammann, D. Fleitmann, K. M. Cobb, and J. Luterbacher, 2011: Support for global climate reorganization during the “Medieval Climate Anomaly”. Climate Dynamics, 37, 1217–1245, doi:http://dx.doi.org/10.1007/s00382-010-0914-z.

Gray, S. T., L. J. Graumlich, J. L. Betancourt, and G. T. Pederson, 2004: A tree-ring based reconstruction of the Atlantic Multidecadal Oscillation since 1567 A.D. Geophysical Research Letters, 31 (12), doi:10.1029/2004GL019932.

Herweijer, C., R. Seager, E. R. Cook, and J. Emile-Geay, 2007: North American Droughts of the Last Millennium from a Gridded Network of Tree-Ring Data. Journal of Climate, 20 (7), 1353–1376, doi:http://dx.doi.org/10.1175/JCLI4042.1.

Hidalgo, H. G., 2004: Climate precursors of multidecadal drought variability in the western United States. Water Resources Research, 40 (12), W12504 doi:10.1029/2004WR003350

Kaplan, A., M. Cane, Y. Kushnir, A. Clement, M. Blumenthal, and B. Rajagopalan, 1998: Analyses of global sea surface temperature 1856-1991, Journal of Geophysical Research 103 (18) 567–589 doi:10.1029/97JC01736

Kennett, D. J., and J. P. Kennett, 2000: Competitive and cooperative responses to climatic instability in coastal southern California. American Antiquity, 379-395.

Mann, M. E., et al., 2009: Global signatures and dynamical origins of the Little Ice Age and Medieval Climate Anomaly. Science, 326 (5957), 1256–1260, doi:10.1126/science. 1177303.

Mantua, N. J., S. R. Hare, Y. Zhang, J. M. Wallace, and R. C. Francis, 1997: A Pacific Interdecadal Climate Oscillation with Impacts on Salmon Production. Bulletin of the American Meteorological Society, 78 (6), 1069–1079, doi:http://dx.doi.org/10.1175/ 1520-0477(1997)078⟨1069:APICOW⟩2.0.CO;2.

McCabe, G. J., M. A. Palecki, and J. L. Betancourt, 2004: Pacific and Atlantic Ocean influences on multidecadal drought frequency in the United States. Proceedings of the National Academy of Sciences, 101 (12), 4136–4141, doi:10.1073/pnas.0306738101.

Meko, D. M., C. A. Woodhouse, C. A. Baisan, T. Knight, J. J. Lukas, M. K. Hughes, and M. W. Salzer, 2007: Medieval drought in the upper Colorado River Basin. Geophysical Research Letters, 34 (10), 10 705–10 709, doi:10.1029/2007GL029988.

Newman, M., G. P. Compo, and M. A. Alexander, 2003: ENSO-Forced Variability of the Pacific Decadal Oscillation. Journal of Climate, 16 (23), 3853–3857, doi:10.1175/ 1520-0442(2003)016⟨3853:EVOTPD⟩2.0.CO;2.

Nowak, K., M. Hoerling, B. Rajagopalan, and E. Zagona, 2012: Colorado River Basin Hydroclimatic Variability. Journal of Climate 25 (12), 4389-4403 doi: http://dx.doi.org/10.1175/JCLI-D-11-00406.1

Oglesby, R., S. Feng, Q. Hu, and C. Rowe, 2012: The role of the Atlantic Multidecadal Oscillation on medieval drought in North America: Synthesizing results from proxy data and climate models. Global and Planetary Change, 84 - 85 (0), 56 – 65, doi:10.1016/j. gloplacha.2011.07.005.

Oppo, D. W., Y. Rosenthal, and B. K. Linsley, 2009: 2,000-year-long temperature and hydrology reconstructions from the Indo-Pacific warm pool, Nature, 460, 1113–1116, doi:10.1038/nature08233.

Redmond, K. T., and R. W. Koch, 1991: Surface climate and streamflow variability in the western United States and their relationship to large-scale circulation indices. Water Resources Research, 27 (9), 2381-2399.

Reynolds, R.W., N.A. Rayner, T.M. Smith, D.C. Stokes, and W. Wang, 2002: An improved in situ and satellite SST analysis for climate. Journal of Climate 15, 1609-1625, doi: http://dx.doi.org/10.1175/1520-0442(2002)015<1609:AIISAS>2.0.CO;2

Routson, C. C., C. A. Woodhouse, and J. T. Overpeck, 2011: Second century megadrought in the Rio Grande headwaters, Colorado: How unusual was medieval drought? Geophysical Research Letters, 38 (22), L22 703, doi:10.1029/2011GL050015.

Schubert, S., et al., 2009: A US CLIVAR Project to Assess and Compare the Responses of Global Climate Models to Drought-Related SST Forcing Patterns: Overview and Results. Journal of Climate, 22 (19), 5251–5272, doi:http://dx.doi.org/10.1175/2009JCLI3060.1.

Seager, R., R. Burgman, Y. Kushnir, A. Clement, E. Cook, N. Naik, and J. Miller, 2008: Tropical Pacific forcing of North American Medieval Megadroughts: Testing the Concept with an Atmosphere Model Forced by Coral-Reconstructed SSTs. Journal of Climate, 21 (23), 6175–6190, doi:http://dx.doi.org/10.1175/2008JCLI2170.1.

Seager, R., N. Graham, C. Herweijer, A. L. Gordon, Y. Kushnir, and E. Cook, 2007: Blueprints for Medieval hydroclimate. Quaternary Science Reviews, 26 (19-21), 2322– 2336, doi:http://dx.doi.org/10.1016/j.quascirev.2007.04.020.

Stine, S., 1994: Extreme and persistent drought in California and Patagonia during mediaeval time. Nature, 369 (6481), 546–549, URL http://dx.doi.org/10.1038/369546a0.

Tierney, J. E., D. W. Oppo, Y. Rosenthal, J. M. Russell, and B. K. Linsley, 2010: Coordinated hydrological regimes in the Indo-Pacific region during the past two millennia. Paleoceanography, 25(1), doi:10.1029/2009PA001871

Thomson, D. J., 1982: Spectrum Estimation and Harmonic-Analysis. Proceedings of the IEEE, 70 (9), 1055–1096.

van Oldenborgh, G. J., L. A. te Raa, H. A. Dijkstra, and S. Y. Philip, 2009: Frequency or amplitude-dependent effects of the Atlantic meridional overturning on the tropical Pacific Ocean, Ocean Science, 5, 293-301, doi:10.5194/os-5-293-2009.

Wang, H., and V. M. Mehta, 2008: Decadal variability of the Indo-Pacific warm pool and its association with atmospheric and oceanic variability in the NCEP-NCAR and SODA reanalyses. Journal of Climate, 21 (21), 5545-5565 doi:10.1175/2008JCLI2049.1

Weiss, J. L., C. L. Castro, and J. T. Overpeck, 2009: Distinguishing pronounced droughts in the southwestern United States: Seasonality and effects of warmer temperatures, Journal of Climate, 22, 5918–5932, doi:10.1175/ 2009JCLI2905.1.

Woodhouse, C. A. and J. T. Overpeck, 1998: 2000 Years of Drought Variability in the Central United States. Bulletin of the American Meteorological Society, 79 (12), 2693– 2714, doi:http://dx.doi.org/10.1175/1520-0477(1998)079⟨2693:YODVIT⟩2.0.CO;2.

Woodhouse, C. A., J. L. Russell, and E. R. Cook, 2009: Two modes of North American drought from instrumental and paleoclimatic data. Journal of Climate, 22 (16), 4336-4347, doi:10.1175/2009JCLI2705.1

Yan, H., L. Sun, Y. Wang, W. Huang, S. Qiu, and C. Yang, 2011: A record of the Southern Oscillation Index for the past 2,000 years from precipitation proxies. Nature Geoscience, 4(9), 611-614.

B.8 Figures

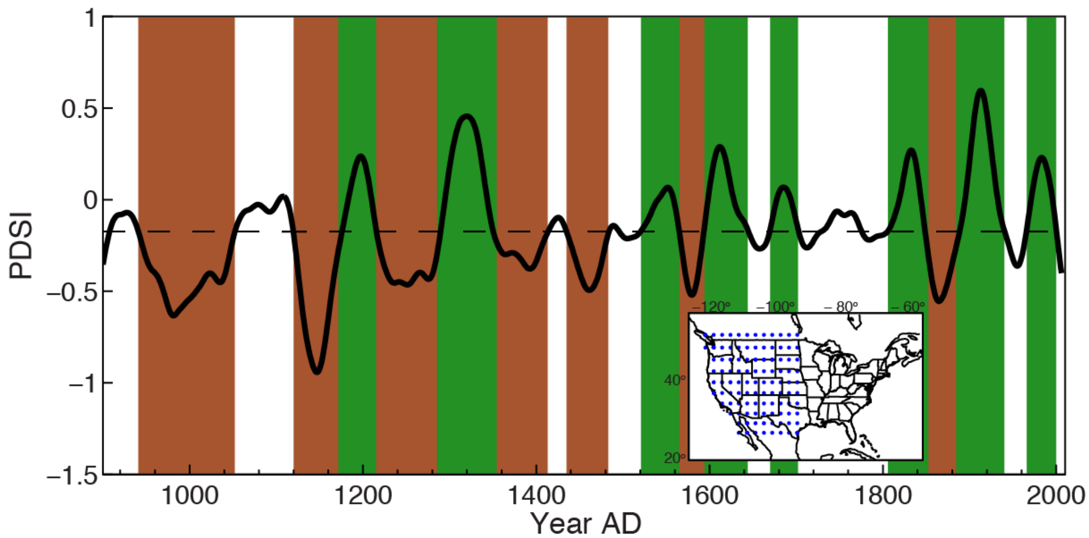

Figure B.1: Average of Western PDSI gridpoints (inset map), spanning 900-2006 AD, smoothed with a 50 yr cubic smoothing slpine. Droughts are defined as periods where the smoothed series exceeds -0.2 below the long-term mean. Pluvials are defined as periods where the smoothed series exceeds +0.2 above the long-term mean.

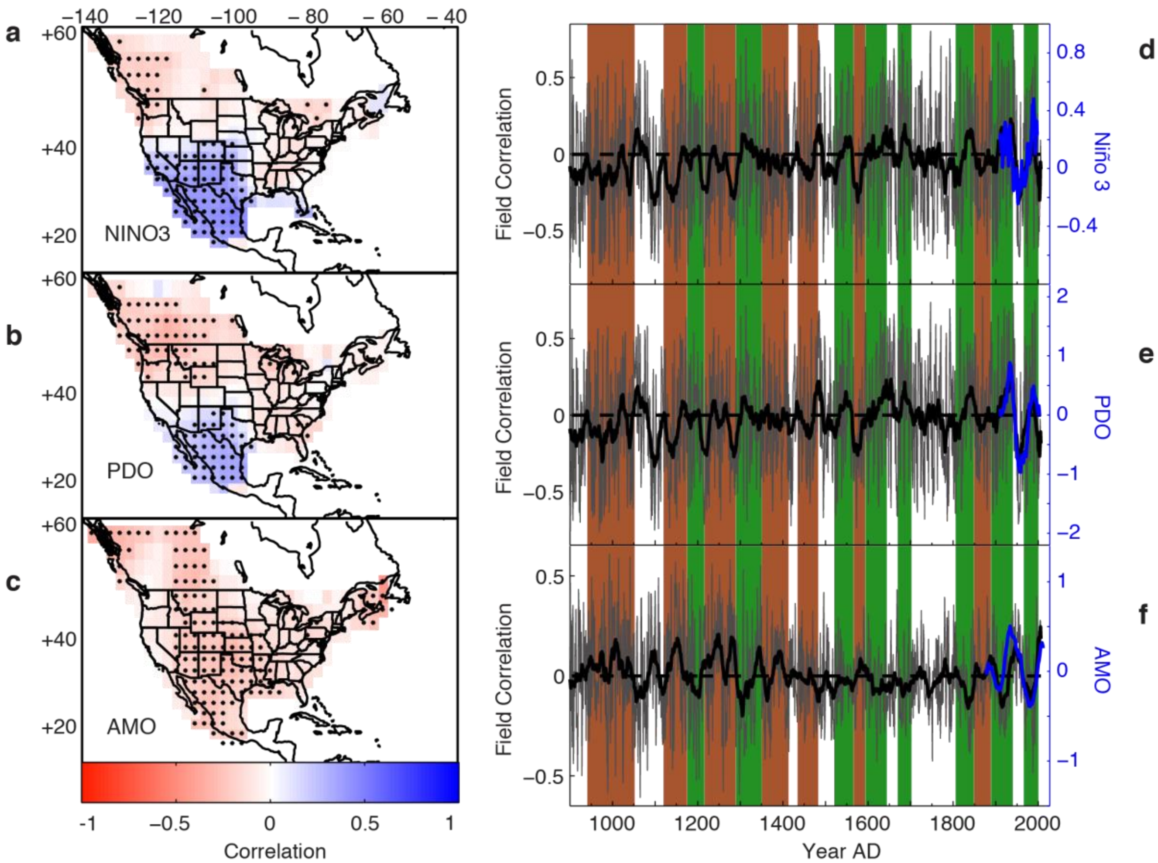

Figure B.2: Teleconnection pattern Analysis. Maps show the modern teleconnection relationship (correlation fields) between instrumental climate modes and the North American Drought Atlas. Black dots indicate significant local grid point correlations ($p \leq 0.1$). The time series show spatial correlations between the maps (left) and annual tree-ring reconstructed PDSI patterns in the NADA. The heavy black is smoothed with a 20 year moving average. The instrumental climate modes smoothed with a 20 year moving average are plotted against the teleconnection strength time series in blue.

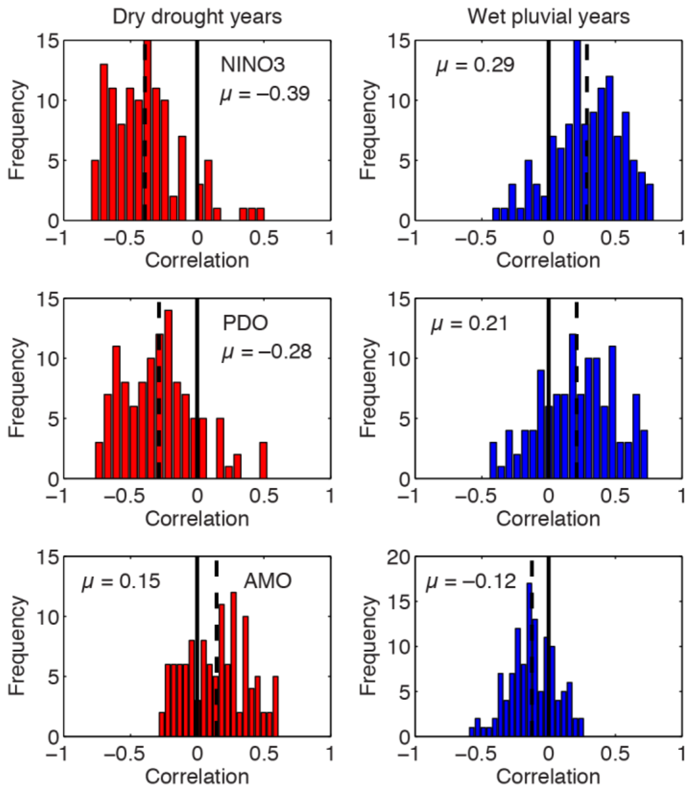

Figure B.3: Histograms showing the frequency of positive and negative teleconnection pattern correlations during all dry years during megadroughts and all wet years during pluvials. Negative ENSO correlations indicate a La Niña pattern and positive AMO correlations indicate a warm North Atlantic.

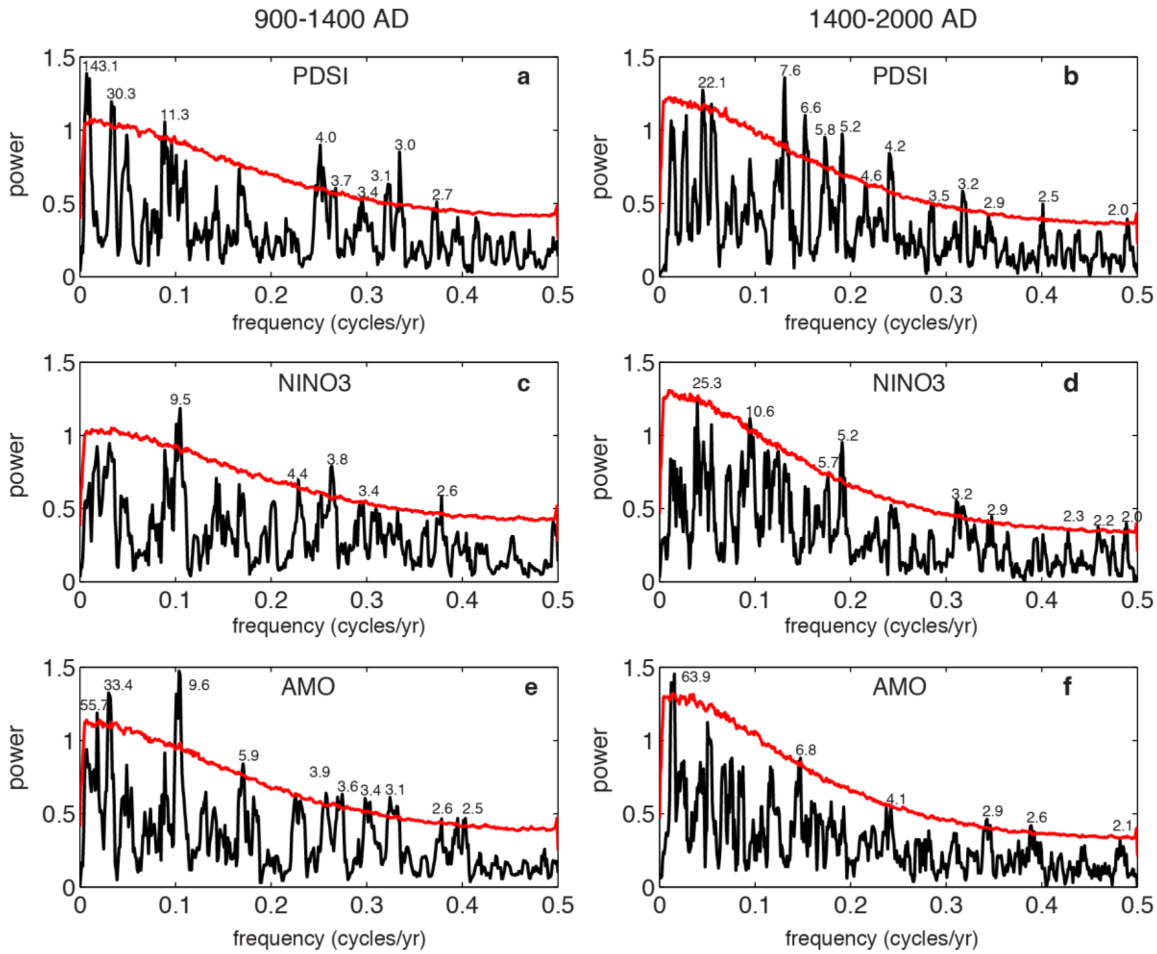

Figure B.4: Spectral analysis of the PDSI, NINO3 teleconnection series, and the AMO teleconnection series during the MCA (900-1400, left panels) and post-MCA (1400-2007, right panels) periods. Peaks significant above the 95% red noise confidence interval (red) are denoted in years.

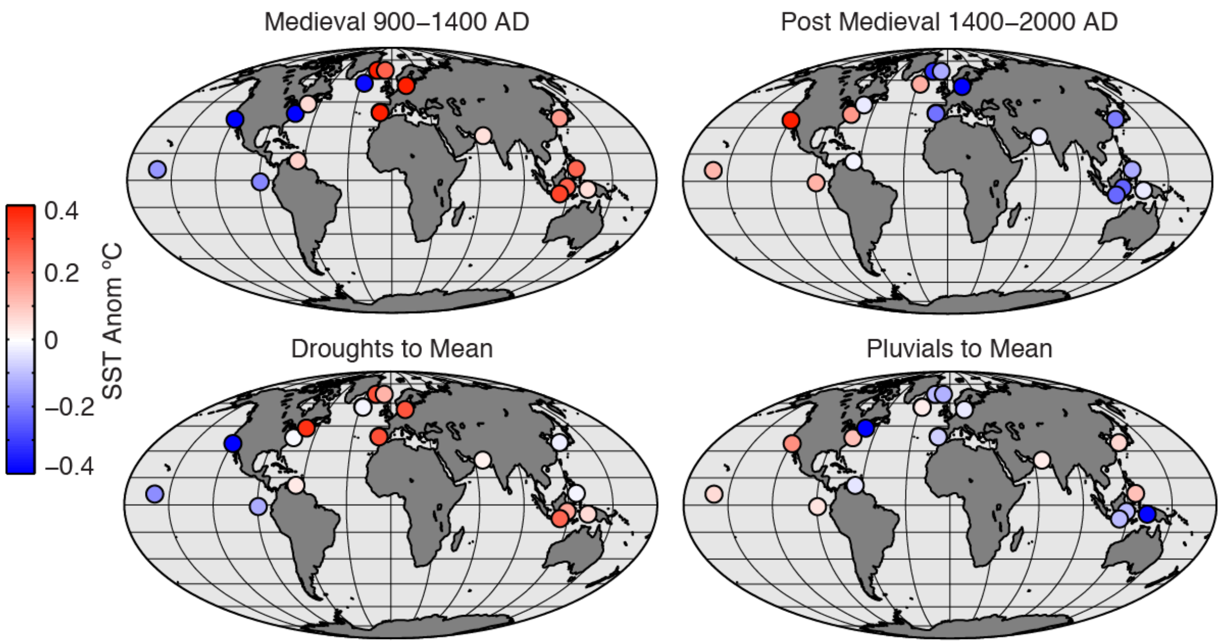

Figure B.5: SST anomalies during the medieval period, post medieval period, during all severe drought events, and all persistent pluvial events. Drought and pluvial events are defined by the smoothed series in Figure 1. Anomalies are computed with respect to the 900-2000 AD mean.

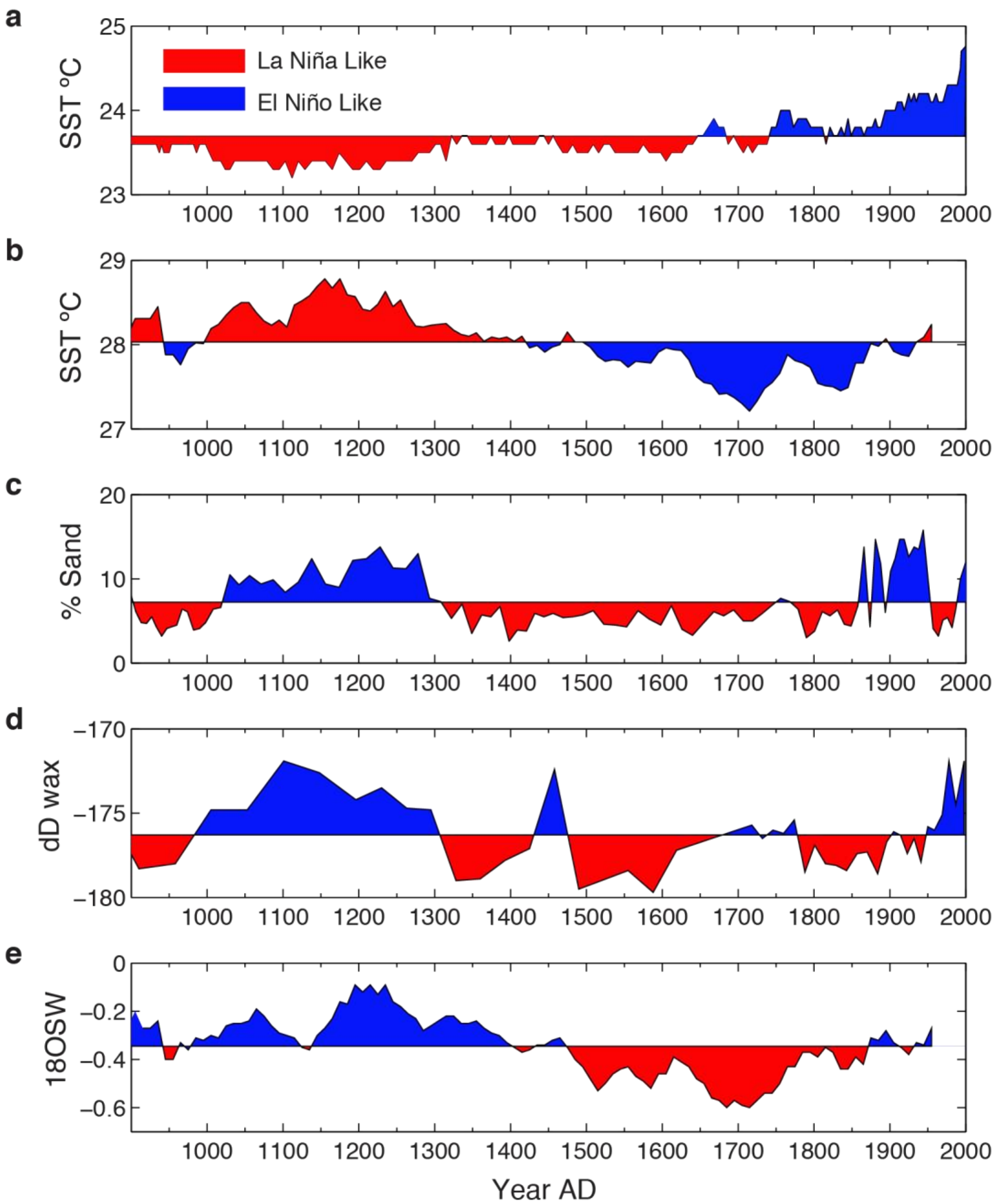

Figure B.6: Contradicting tropical Pacific SST and precipitation ENSO reconstructions. Records are from both sides of the tropical Pacific basin. Red coloring indicates La Niña like conditions and blue color indicates El Niño like conditions. a) Diatom inferred SST from the Lake El Junco in the Galapagos Islands (Conroy et al. 2009a), b) Mg/Ca inferred SST from the Indo Pacific Warm Pool (Oppo et al. 2009), c) grain size inferred precipitation intensity from Lake El Junco (Conroy et al. 2008), d) deuterium leaf wax isotope precipitation reconstruction from the Indo Pacific Warm Pool (Tierney et al. 2010), and e) $\delta^{18}O$ of sea water inferred salinity reconstruction from the Indo Pacific Warm Pool (Oppo et al. 2009).

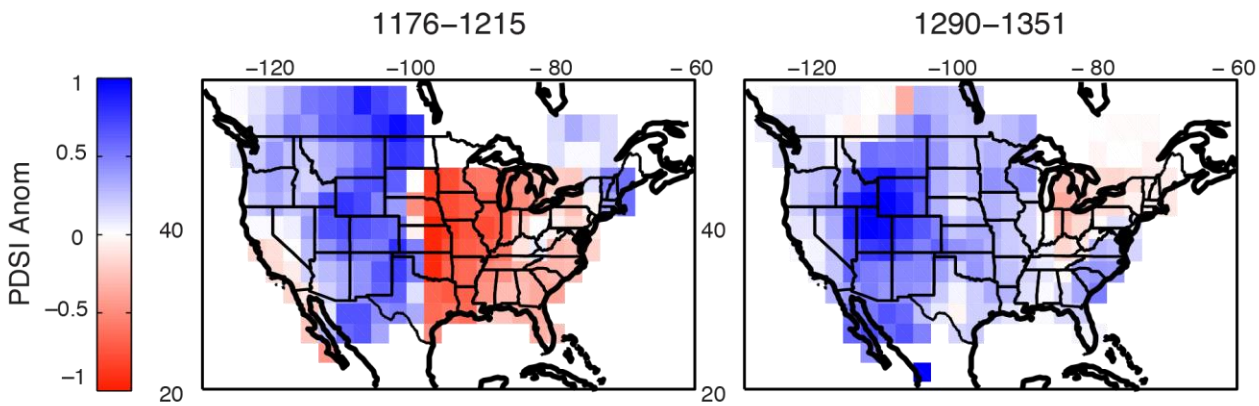

Figure B.7: Reconstructed PDSI maps for MCA pluvials including the 1176-1215 AD and 1290-1351 AD events. Anomalies are computed with respect to the 900-2007 AD mean.

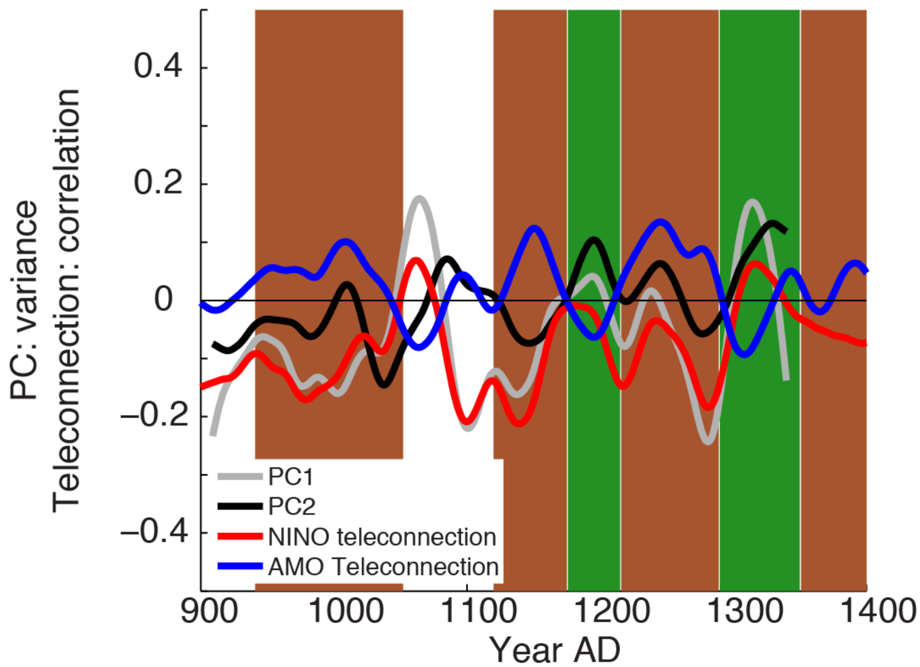

Figure B.8: Comparison of the leading principal components of WNA PDSI from Woodhouse et al. 2009 in grey (PC1) and black (PC2), with the NINO3 (red) and AMO (blue) teleconnection strength time series. All series are smoothed with a 50-year cubic smoothing spline. The units for the PCs are in variance and the units for the teleconnection time series are in r-value correlation.

Table B.1 Variance explained by teleconnection strength time series in Western droughts and pluvials.

Drought intervals (AD)	Teleconnection index correlation (R^2) with Western PDSI		
	ENSO	AMO	PDO
941-1052	0.49	0.29	0.37
1120-1175	0.56	0.27	0.42
1216-1289	0.55	0.34	0.41
1351-1413	0.64	0.1	0.52
1435-1483	0.56	0.05	0.35
1566-1593	0.41	0.19	0.12
1849-1888	0.44	0.01	0.24
Pluvial Intervals			
1176-1215	0.5	0.35	0.35
1290-1350	0.56	0.29	0.44
1521-1565	0.55	0.07	0.28
1594-1644	0.34	0.06	0.14
1670-1702	0.59	0.07	0.46
1806-1848	0.46	0.22	0.24
1889-1940	0.39	0.2	0.21
1966-2000	0.41	0.01	0.16
Series length			
900-2000	0.49	0.18	0.3

B.9 Supplemental Figures

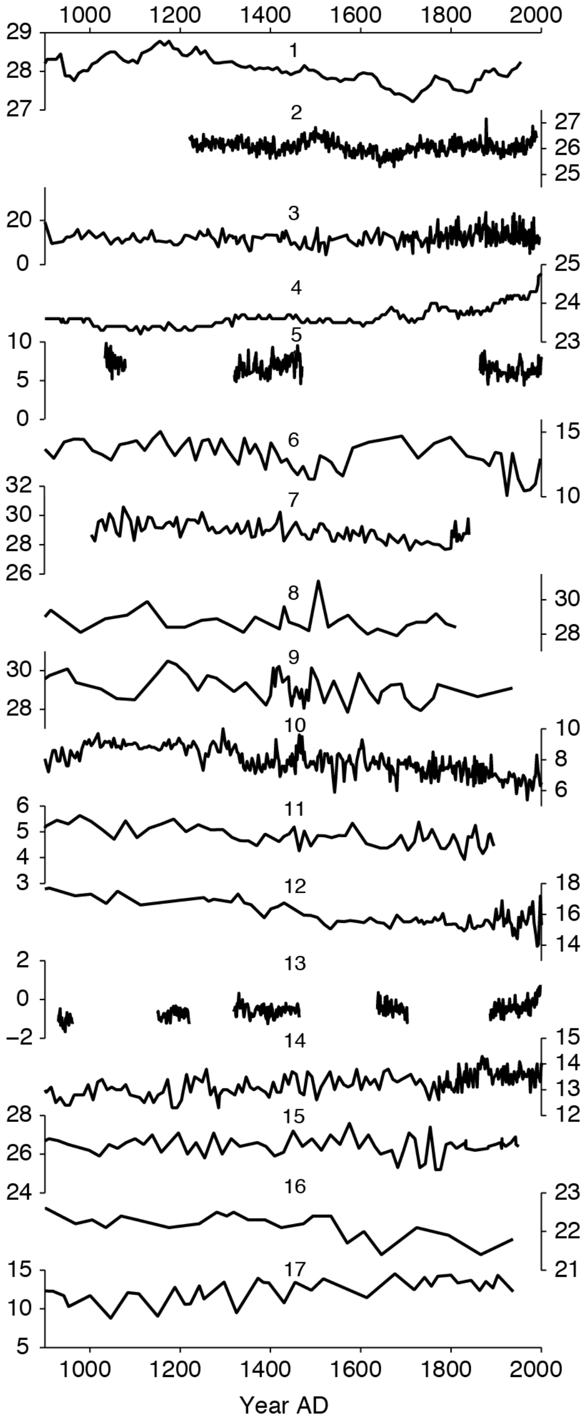

Figure B.S1: SST proxy records used in analysis. References for records by number are shown in table S1, and a map of locations in figure S2.

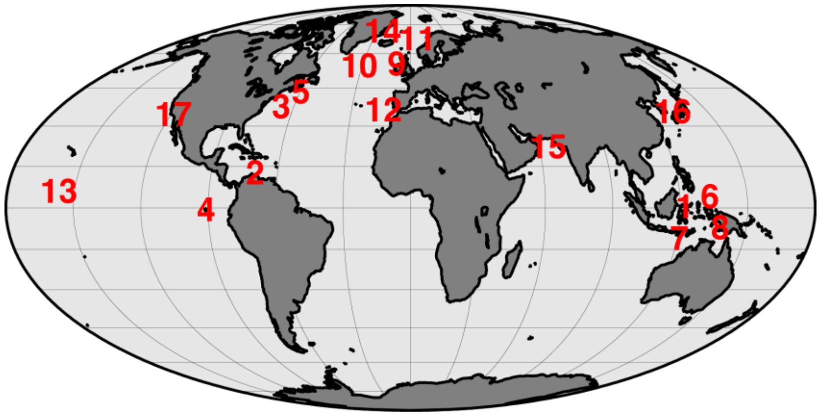

Figure B.S2: SST record locations. Records are shown in figure B.S1

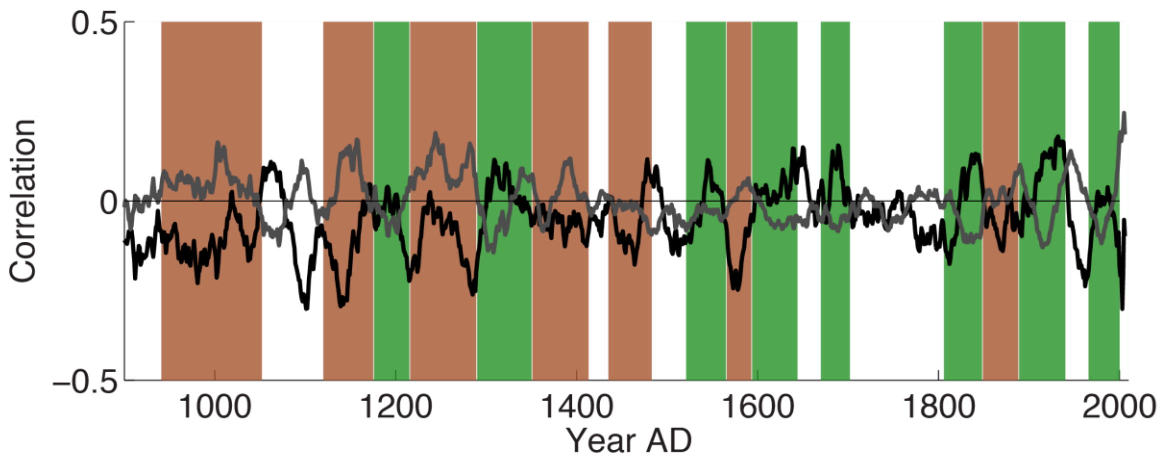

Figure B.S3: NINO3 teleconnection time series in black and the AMO teleconnection time series plotted in grey with drought and pluvial intervals.

B.10 Supplemental Circulation Reconstruction Analysis

We assessed a suite of published climate mode reconstructions in hopes that they would reflect the teleconnection patterns preserved in the gridded drought maps. We used two AMO reconstructions (Gray et al. 2004; Mann et al. 2009), four PDO reconstructions (D'Arrigo et al. 2006; MacDonald et al. 2005; Mann et al. 2009; Shen et al. 2006), and four ENSO reconstructions (Braganza et al. 2009; Emil-Geay et al. 2013; Li et al. 2013; Mann et al. 2009). All were obtained from the National Oceanic and Atmospheric Administration (NOAA) paleoclimate data center (http://www.ncdc.noaa.gov/paleo/paleo.html). We only included climate mode reconstructions that spanned two or more drought and pluvial intervals. Anomalies in the mode reconstructions were assessed during drought and pluvial intervals and are shown Tables B.S2 and B.S3 respectively.

Climate mode reconstructions (Figure B.S4) were not especially informative regarding the causes of past WNA megadroughts pluvials. Mode reconstructions were inconsistent within and between records during droughts and pluvials. Mode reconstruction anomalies during droughts and pluvials are shown in tables B.S2 and B.S3 respectively. ENSO reconstructions are negative 57.9% of the time during droughts and positive 55.2% of the time during pluvials. AMO reconstructions are positive 66.7% of the time during droughts and negative 61.5% of the time during pluvials. PDO reconstructions are negative 42.6% of the time during droughts, and positive 50% of the time during pluvials.

B.11 Supplemental Circulation References:

D'Arrigo, R., R. Villalba, and G. Wiles, 2001: Tree-ring estimates of Pacific decadal climate variability. Climate Dynamics, 18 (3-4), 219–224, doi:dx.doi.org/10.1007/s003820100177.

Emile-Geay, J., K. M. Cobb, M. E. Mann, and A. T. Wittenberg, 2013a: Estimating Central Equatorial Pacific SST variability over the Past Millennium. Part 1: Method- ology and Validation. Journal of Climate, 26, 2302–2328, doi:http://dx.doi.org/10.1175/ JCLI-D-11-00510.1.

Emile-Geay, J., K. M. Cobb, M. E. Mann, and A. T. Wittenberg, 2013b: Estimating Cen- tral Equatorial Pacific SST variability over the Past Millennium. Part 2: Reconstructions and Implications. Journal of Climate, 26, 2329–2352, doi:http://dx.doi.org/10.1175/ JCLI-D-11-00510.1.

Li, J., et al., 2013: El Nino modulations over the past seven centuries. Nature Climate Change, 3 (9), 822-826.

MacDonald, G. M., and R. A. Case, 2005: Variations in the Pacific Decadal Oscillation over the past millennium. Geophysical Research Letters, 32 (8).

Mann, M. E., et al., 2009: Global signatures and dynamical origins of the Little Ice Age and Medieval Climate Anomaly. Science, 326 (5957), 1256–1260, doi:10.1126/science. 1177303.

Shen, C., W. C. Wang, W. Gong, and Z. Hao, 2006: A Pacific Decadal Oscillation record since 1470 AD reconstructed from proxy data of summer rainfall over eastern China. Geophysical Research Letters, 33(3).

B.12 Supplemental Circulation Figure

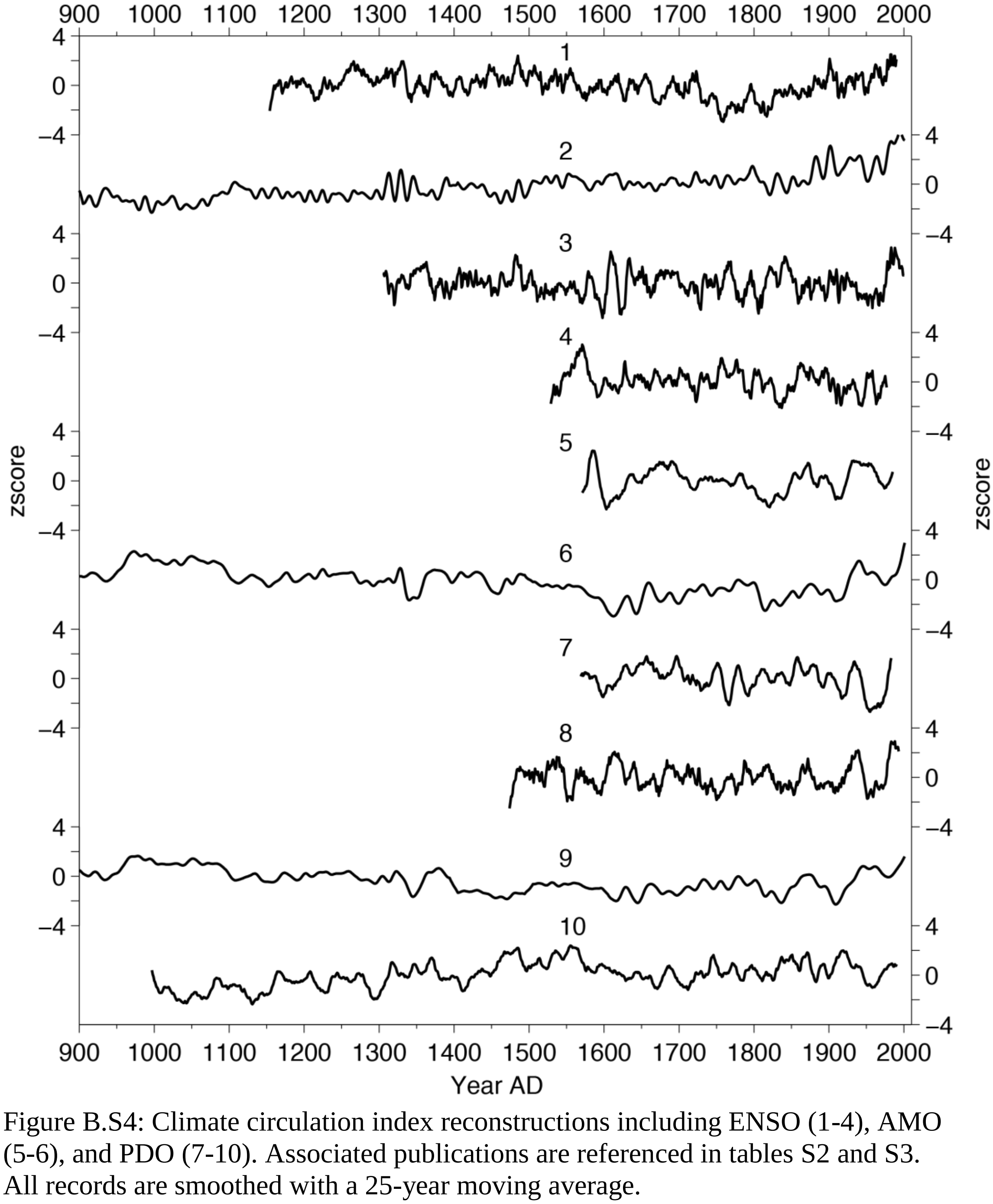

Figure B.S4: Climate circulation index reconstructions including ENSO (1-4), AMO (5-6), and PDO (7-10). Associated publications are referenced in tables S2 and S3. All records are smoothed with a 25-year moving average.

B.13 Supplemental Tables

Table B.S1: SST reconstruction information

#	Site or Core	Citation	Lat	Lon	Resolution: mean (min max) yr/smpl	Proxy	Dating Method	# of 14C	# of 210PB	Total Tie points
1	BJ-03-32GGC	Oppo et al 2009	-3.53	119.27	10 (10-10)	Mg/Ca	210Pb, AMS 14C, Tephra	5	13	19
2	PL07-73	Black et al 2007	10.75	-64.77	1.3 (.49-2.6)	Mg/Ca	Varve, 210Pb, AMS 14C	12	30	42+varves
3	MD99-2209	Cronin et al 2003	37.82	-76.12	3.2 (0.1-34.7)	MgCa	137Cs, 210Pb, AMS 14C	9	Mltpl.	
4	El Junco	Conroy et al 2009	-0.9	-89.48	5.5 (1-9)	Diatom	137Cs, 210Pb, AMS 14C	4	9	14
5	Gulf of Maine Shells	Wanamaker et al 2008	43.65	-69.8	1 (1-1)	Bivalves	Varves AMS 14C	3		3+varves
6	M200309/ENAM9606	Richter et al 2009	55.65	13.99	17.4 (11-37)	Mg/Ca	226Ra, 137Cs, 210Pb, AMS 14C	4	13	17
7	MD98-2160	Newton et al 2006	-5.2	117.48	7.5 (1-20)	Mg/Ca	AMS 14C, Tephra	3		4
8	MD98-2176	Stott et al 2004	-5	133.44	27.2 (10-66)	Mg/Ca	AMS 14C	2		2
9	MD98-2181	Stott et al 2004	6.3	125.82	19.7 (2-88)	Mg/Ca	AMS 14C	5		5
10	MD99-2275	Sicre et al 2008/2011	66.56	-17.7	3.2 (1-6)	Alkenone	Tephra Chronology, 210pb		23	28
11	MD99-2275	Eriksson et al 2006	66.55	17.7	15.3 (3.2-27.2)	Diatom	AMS 14C, Tephra Chronology	7		11
12	PO287-26	Rodrigues et al 2009	38.55	9.35	11.6 (3-85)	Alkenone	210Pb, AMS 14C	6	12	18
13	Palmyra	Cobb et al 2003	6	-160	1 (1-1)	Coral	U/Th			25
14	Rapid21-COM	Miettinen et al 2012	57.27	-27.54	5.6 (1-21)	Diatom	210Pb, AMS 14C	9	5	14
15	SO9039KG	Doose-Rolinski et al 2001	24.83	65.92	15.5 (1-46)	Alkenone	Varve, AMS 14C	5		5+varves
16	SSDP102	Kim et al 2004	34.95	128.88	45 (15-78)	Alkenone	AMS 14C	3		3
17	ODP893A	Kennet and Kennet 2000	34.29	-120.04	28.8 (10.1-96.1)	Foram	AMS 14C	11		11

Table B.S2: Circulation reconstruction anomalies during drought periods. Time series can be seen in figure S4.

Mode	Reconstruction	Anomaly by Drought Period						
		941-1052	1120-1175	1216-1289	1351-1413	1435-1483	1566-1593	1849-1888
ENSO	1. Emile Geay et al. 2013	NaN	**-0.183**	0.118	0.023	0.174	**-0.157**	**-0.102**
	2. Mann et al. 2009	**-0.277**	**-0.118**	**-0.165**	**-0.058**	**-0.138**	0.022	0.194
	3. Li et al. 2013	NaN	NaN	NaN	0.061	**-0.015**	**-0.192**	**-0.071**
	4. Braganza et al. 2009	NaN	NaN	NaN	NaN	NaN	0.603	0.205
AMO	5. Mann et al. 2009	**0.275**	**0.028**	**0.078**	**0.064**	-0.040	-0.160	-0.111
	6. Gray et al. 2004	NaN	NaN	NaN	NaN	NaN	**0.518**	**0.337**
PDO	7. D'Aarrigo et al. 2006	NaN	NaN	NaN	NaN	NaN	0.201	0.461
	8. MacDonald et al. 2005	**-0.865**	**-0.787**	**-0.368**	0.018	0.665	0.438	0.511
	9. Mann et al. 2009	0.296	0.049	0.101	0.023	**-0.254**	**-0.112**	0.009
	10. Shen et al. 2006	NaN	NaN	NaN	NaN	**-0.489**	**-0.136**	**-0.074**

57.9% of the time reconstructions are ENSO– during drought
66.7% of the time reconstructions are AMO+ during drought
42.6% of the time reconstructions are PDO– during drought

Table B.S3: Circulation index reconstruction anomalies during pluvial periods.

Mode	Reconstruction	Anomaly by Pluvial Period							
		1176-1215	1290-1350	1521-1565	1594-1644	1670-1702	1806-1848	1889-1940	1966-2000
ENSO	1. Emile Geay et al. 2013	**0.024**	**0.135**	**0.098**	-0.018	-0.179	-0.336	**0.090**	**0.448**
	2. Mann et al. 2009	-0.134	-0.013	**0.136**	**0.094**	**0.077**	**0.004**	**0.368**	**0.621**
	3. Li et al. 2013	NaN	**0.067**	-0.125	-0.052	**0.251**	**0.093**	-0.050	**0.230**
	4. Braganza et al. 2009	NaN	NaN	-0.089	-0.067	**0.043**	-0.392	-0.113	-0.302
AMO	5. Mann et al. 2009	0.059	**-0.034**	**-0.057**	**-0.336**	**-0.233**	**-0.290**	**-0.077**	0.091
	6. Gray et al. 2004	NaN	NaN	NaN	**-0.665**	0.884	**-1.136**	0.031	0.062
PDO	7. D'Aarrigo et al. 2006	NaN	NaN	-0.608	-0.103	**0.399**	**0.062**	-0.087	-0.115
	8. MacDonald et al. 2005	-0.236	-0.153	**1.044**	**0.133**	-0.068	**0.212**	**0.646**	**0.375**
	9. Mann et al. 2009	**0.067**	-0.022	-0.060	-0.237	-0.210	-0.241	-0.157	**0.154**
	10. Shen et al. 2006	NaN	NaN	**0.030**	**0.237**	**0.032**	-0.027	**0.019**	**0.421**

55.2% of the time reconstructions are ENSO+ during pluvials
61.5% of the time reconstructions are AMO+ during pluvials
50% of the time reconstructions are PDO+ during pluvials

APPENDIX C

THREE MILLENNIA OF SOUTHWEST NORTH AMERICAN DUSTINESS AND FUTURE IMPLICATIONS

Cody C. Routson [1, 2, *], Jonathan T. Overpeck [1, 3, 4], Connie A. Woodhouse [1, 2, 5], and William F. Kenney [6]

1 Department of Geosciences, University of Arizona, Tucson, Arizona, USA.

2 Laboratory of Tree-Ring Research, University of Arizona, Tucson, Arizona, USA.

3 Institute of the Environment, University of Arizona, Tucson, Arizona, USA.

4 Department of Atmospheric Sciences, University of Arizona, Tucson, Arizona, USA.

5 School of Geography and Development, University of Arizona, Tucson, Arizona, USA.

6 Land Use and Environmental Change Institute, University of Florida, Gainesville, Florida, USA.

*e-mail: routson@email.arizona.edu

Manuscript submitted to Nature Geoscience

C.1 Abstract

We generated a 2940-year-long, sub-decadal resolution dust deposition record from Fish Lake, in the southern San Juan Mountains, Colorado documenting relationships between southwest United Sates (Southwest) drought and atmospheric dustiness. We used µXray-fluorescence to analyze the geochemical composition of sediment cores,

local bedrock, and dust deposited on local snowpack to constrain dust-input end-members. We employed an end-member mixing method to calculate the fraction of wind-deposited dust in the lake sediment through time. Independent high-resolution grain-size records were combined with the geochemical results to create a composite dust record. The new record confirms anomalous dustiness in the 19th and 20th centuries, associated with recent land disturbance, drought, and livestock grazing [1-3]. Before anthropogenic influences, drought and aridity also generated higher than average atmospheric dust loading. Medieval times were associated with high levels of dustiness, consistent with widespread medieval aridity. The period between 800 and 300 BC was also unusually dusty, approaching peak mid-20th century levels. High levels of pre-industrial dustiness indicate the Southwest is naturally prone to desertification. As global and regional temperatures rise and the Southwest shifts toward a more arid landscape [4] the Southwest will likely become dustier, driving negative impacts on snowpack and water availability [5], as well as human health [6].

C.2 Introduction

Dust entrained by spring winds and southwesterly storm systems is deposited on mountain snowpack where it increases solar radiation absorption [5, 7, 8, 9]. Recent dust on snow events in the Rocky Mountains, which are the headwaters to major river systems that support over 60 million people [10], have accelerated melt, decreased runoff, and reduced snow-cover duration by up to 51 days [5, 7, 8, 9]. Southwestern dustiness increased substantially with historical and modern land use [2], but recent drought has also enhanced windblown dust off undisturbed landscapes [11]. Across the Southwest, increases in airborne dust prompted extensive research on the fate and transport of dust and implications for regional water resources [5, 7, 8, 9, 11, 12]. However, these studies are focused on a relatively short period of record. It is unclear whether dustiness in the Southwest is predominantly a modern phenomenon associated with widespread settlement and disturbance [1-3], or if intermittent dusty conditions have occurred over longer timescales as suggested by regional eolian sediment features [13].

Dune and loess deposits indicate that some locations in the West experienced extremely arid and dusty intervals during the Holocene [14, 15]. At the same time Southwest tree ring records provide strong evidence for multi-decadal-length droughts during Roman [16, 17] (1-400 AD) and medieval times [16, 17, 18] (900-1400 AD), but were these droughts severe enough to mobilize dust? Some dune deposits in the Southwest may have activated in response to these droughts [13]. However, existing dust records with low temporal resolution in the San Juan Mountains show no change in dust accumulation rates before the mid 1800's AD [1, 2], suggesting biologic crusts may have stabilized soils during severe droughts [19]. Higher resolution dust records are needed to characterize the natural variability of dustiness to more thoroughly understand the relationship between dust and drought in the Southwest.

C.3 Reconstructing Dustiness

To assess links between dustiness and Southwestern aridity, we developed a 2940-year-long sub-decadal resolution dust record. We used lake sediments from Fish Lake (37.25ºN, 106.68ºW) in the south San Juan Mountains, a relatively narrow mountain chain that defines the northeastern boundary of the high desert Colorado Plateau (Figure C.1). Alpine Fish Lake is lake located above the treeline (3718 meters elevation), where prevailing southwesterly winds and storm systems deposit dust eroded from the Colorado Plateau desert. Dust is deposited in the San Juan Mountains at a rate of 5-10 g $m^{-2}yr^{-1}$ [20], and Google Earth imagery taken in spring 2011 clearly shows dust on the melting snow surface around Fish Lake (Figure C.1). Fish Lake is located in the San Juan Volcanic Field, which has geochemistry distinct from the weathered sedimentary desert soils of the Colorado Plateau. Sediment cores and samples of local bedrock material were collected in the summers of 2009 and 2011. Windblown dust was collected off the melting snow surface near Wolf Creek Pass in April 2012.

Sediment cores were analyzed for age control, grain size, and geochemistry. We established age-depth chronologies with radiocarbon dating of terrestrial plant macrofossils and ^{210}Pb dating of the upper surface sediments (Figure C.S1 and Figure C.S2). Sediments were sampled at 0.5 cm intervals for grain size. Dust obtained from local snowpack is predominantly composed of fine silt and clay grain sizes (Figure C.2a). Over the record length, Fish Lake sediment is composed of an average of 83.7% dust grain sizes. Fish Lake sediment also has a coarser grain fraction derived from weathering and decomposition of local bedrock, indicating a small portion of the dust grain size fraction is probably locally derived.

Micro scanning X-ray fluorescence (µXRF) was used to characterize the geochemistry of sediment, dust, and local bedrock. Windblown dust and local bedrock have similar titanium counts; dust is slightly enriched in potassium, whereas calcium and strontium are higher in the local bedrock (Figure C.S3). Strontium concentrations however, were too low to measure in the sediment reliably. Calcium shows the greatest difference between local rock and windblown dust. Calcium is present in moderate to high concentrations in windblown dust collected from southwestern landscapes [20, 21] (Figure C.S3); however, µXRF analysis shows that calcium abundance in south San Juan Volcanic Field bedrock around Fish Lake is over 4 times higher than in dust deposited on local snow (Figure C.S3). To calculate the fraction of dust (fd) in the sediment we applied a geochemical end-member mixing model (Equation 1) using potassium and calcium ratios in dust, local bedrock, and sediment.

$$fd = \frac{\frac{K}{Ca} sed - \frac{K}{Ca} rock}{\frac{K}{Ca} dust - \frac{K}{Ca} rock} \tag{1}$$

The sediment is a mixture of two end members, dust and local bedrock (Figure C.2b). The mixing model indicates Fish Lake sediment is composed of an average of 54% dust: far less than the grain size estimation (84%). Nonetheless, the relative constancy of sediment accumulation rates in Fish Lake (Figure C.S1 and Figure C.S2) indicate that our dust record is relatively free of sediment dilution bias. We standardized the grain size and µXRF dust records from short and long cores to account for variable sediment accumulation between cores (Figure C.S4), and we combined these data using the median into one composite dust record, utilizing the common variability between cores and between methods to produce a more realistic representation of past dustiness.

The resulting 2940-year-long Fish Lake dust record (Figure C.3a) provides a new perspective on Southwestern climate and aridity. Low dust intervals occur notably during the post-Roman (500-700AD) and post-medieval (1400-1700AD) periods. Tree-ring records including nearby Summitville [16] (21 km away; Figure C.3b) and reconstructed Southwestern gridded Palmer Drought Severity Index [22] (PDSI; Figure C.3c; 20 grid points averaged, 32ºN to 40ºN and 105ºW to 115ºW) help characterize local and regional moisture balance conditions. Low dust periods tend to correspond with wetter, or at least non-arid intervals. The Fish Lake record also shows persistent dusty periods. A downward trend in dustiness over the first half of the record may reflect a long-term change in Southwestern aridity. High dust levels occur between 900 BC and 200 BC. Dust levels in the earliest portion of our record (i.e. before 800 BC) are comparable to those of peak dustiness during the 20th century. The Roman Period, characterized by extreme drought in some areas of the Southwest [16, 17, 22], is only moderately dusty. A medieval period of relatively high dustiness occurred between 700 AD and 1400 AD. Dust levels first increase in the mid 700's coincident with drought events in the western US [17], but before the onset of the most severe Southwestern medieval droughts (Figure C.3). High medieval dust levels are consistent with widespread increases in drought area [23]. Based on our age model, the highest dust peak in the record occurs between 1540 and 1555. This peak is present in both short and long µXRF records, but is not well represented in the lower resolution grain size record (Figure C.S5). This high dust interval is within radiocarbon age error of the multidecadal 16th century Southwestern megadrought [24], and could reflect associated dustiness.

The Fish Lake dust record also confirms anomalous dustiness likely related to 19th century mass livestock introductions and human land use changes [2]. Livestock were initially introduced in low numbers into the Southwest as early as the mid 1500's with the first Spanish explorers [25]. Completion of the railroad in the late 1800's enabled an exponential increase in livestock populations, with numbers of sheep and cattle in hundreds of thousands. Fragile desert ecosystems were quickly denuded of grasses and vegetation, resulting in widespread arroyo cutting, soil destabilization, and landscape changes across the Southwest [26]. By the 1920's livestock numbers had stabilized and begun to decline [25, 26]. Livestock declines however, came shortly before the 1930's dust bowl drought, followed by the 1950's drought. The Fish Lake record shows dust levels began to increase in the mid to late 1800's, rising until the 1950's, when dust deposition stabilized and then declined. Declines are probably related to a relative decrease in livestock abundance coupled with land management practices. The Fish Lake record suggests that dust levels increased somewhat since the mid 1980's perhaps associated with recent droughts in the Southwest. The Fish Lake record shows that recent human-induced dustiness is anomalous, but it does not represent a 500% increase over preindustrial dustiness [2] (Figure C.S6).

The chronology of dune and loess activity dates from around the western and central US indicate some dusty periods in the Fish Lake record were associated with widespread dune migration and loess deposition (Figure C.3d). The Great Sand Dunes National Park located 115 km northeast of Fish Lake experienced medieval and recent dune activity consistent with our record [13]. The Great Plains also record some recent dune and loess activity in the last 150 years [14, 15]. Dune mobilization and loess deposition also occurred in the Great Plains during medieval times and before 300 BC [15]. Dust deposited at Fish Lake during these intervals likely reflects the widespread impact of drought.

C.4 Conclusion

In conclusion, dust has been an important component of Southwestern climate over the past several millennia, implying that Southwest landscapes undisturbed by humans and their animals can become significant dust sources during prolonged arid periods. Recent dust levels may be anomalous, but they are not necessarily unprecedented. Persistently dusty periods occurred numerous times over the past three millennia. Southwestern tree-ring records indicate that low dust periods are associated with regionally wetter conditions and high dust periods are associated with periods of persistent or frequent drought. Dune and loess deposits in the Southwest and the Great Plains confirm that some dusty periods at Fish Lake are related to widespread aridity. Recent research has documented impacts of dust on snow causing reductions in runoff and streamflow (e.g., in the Colorado River) [5, 8, 9]. Furthermore, mineral dust aerosols have also been implicated in past precipitation suppression [27]. It is not clear if preindustrial dust levels at Fish Lake were sufficient to suppress precipitation, but evidence suggests that atmospheric dust loading amplifies the impacts of drought [27]. As the earth warms, the Southwest is projected to see a decrease in mean precipitation, and an increase in consecutive dry days [4]. These changes will lead to an increased risk of prolonged drought [28], worsened by warming and increased atmospheric moisture demand [29]. Resulting aridity- and human-driven atmospheric mineral dust loading will amplify severe climate change impacts on water resources [5] and human health [6], exacerbating the regional impacts of anthropogenic climate change.

C.5 Methods

Core Sampling

In summers of 2009 and 2011 a 170 cm long core and a 30 cm long core were taken respectively from Fish Lake using Alpacka rafts and a universal gravity corer. The sediment water interface was preserved on the short core by siphoning off water above the sediment surface, carefully packing with a sponge to absorb water and prevent slumping, cutting off the remaining core tube above the sponge, and capping for transport. See supplemental material for discussion of age control on the sediment cores.

Grain Size Analysis

Grain size samples were pretreated using a modification of the methods described by Dr. Donald Rodbell of Union College (http://www1.union.edu/rodbelld/grainsizeprep.htm). In a sequence of treatments 10% HCL was used to remove potential carbonates, 30% H_2O_2 was used to remove organics, and 1 M NaOH was used to remove biogenic silica. Sediment samples were rinsed, centrifuged, and decanted three times between each step, following the methods used in ref. 30. We also added $(NaPO_3)_6$ to the samples before analysis as a dispersant to inhibit aggregation of clay-sized particles. Grain size distributions were analyzed using a laser-diffraction Malvern Mastersizer, 2000 particle size analyzer. The average of five measurements was used for each sample. Dust samples were pretreated and analyzed using the same grain size protocol. Using the overlapping portions of dust and sediment grain size distributions (Figure C.3), dust in sediment was characterized as grain sizes less than or equal to 45.7µm.

Geochemical µXRF Analysis

Sediments were sampled by carefully removing wet slabs 4.5 x 2.0 x 0.5 cm in size. Acetone exchanges were used to remove water, and the slabs were imbedded in an epoxy resin. Imbedded sediment slabs were split using a diamond saw and surfaced on 600 grit sanding paper. Half of each slab was used to make glass microscope thin-sections. The other half was analyzed using an EDAX Eagle III tabletop scanning µXRF analyzer at the University of Arizona Department of Geosciences. Line scans down each slab were run using 40kv, 300µa, at 25 micron resolution, and 16 seconds of spot measurement time. For µXRF analysis of dust and local bedrock, samples were pulverized using a mortar and pestle, compressed into pellets, and run using the same µXRF instrument settings as on the sediment.

A mean count adjustment was applied to the sediments to conceptualize the mixing model (Figure C.2b). When analyzing the sediment, X-rays travel through epoxy imbedding resin and organic sediment in addition to the mineral component of the sediment. The epoxy resin and organic matter reduce the µXRF signal and respective element abundances relative to the dust and bedrock samples (Figure

C.S7). Different elements are influenced slightly differently. A constant value of 40 was added to the potassium and calcium mean counts, and the value 20 was added to titanium mean counts (Figure C.S7). The adjustment has no influence on the final record because potassium and calcium ratios were used, but is useful for understanding the theoretical framework using the ratio/ratio scatter plot (Figure C.2b)

Turbidites and shrinkage

Thirty turbidites (distinct packages of sediment deposited instantaneously by underwater landslides) were removed from the Fish Lake grain size and geochemical records. Turbidite depths were visually characterized from the core and digitized thin section photographs in GIS. Thin sections were digitized using a digital SLR camera through an Olympus microscope. The thin-section photographs were imported into GIS and scaled to depth using µXRF line-scans on the sediment slabs. Turbidite depths were measured in GIS and verified with measurements on the wet sediment core.

There were also some cases of sediment shrinkage when imbedding the sediment pucks. Shrinkage was accounted for by using the depth differences of 36 marker layers between the thin-sections and the wet core. Shrinkage was adjusted linearly between the marker layers. Both turbidites and shrinkage were also visible in the grain size and µXRF records. Turbidites were coarse intervals in the grain size record and spikes of calcium counts in the µXRF record, which were used to check that the various records were all on the same depth-scale after adjusting for the shrinkage (Figure C.S8).

Composite Record

A method similar to tree-ring techniques was applied to reduce method and core dependent variability. Grain-size and the µXRF methods were applied to the short and long cores. The four resulting records were normalized by their mean and variance. Grain-size dust records were then interpolated to 5-year sample resolution and the µXRF dust records were binned to 5-year sample resolution, and all records were combined using the median.

Age Control (for supplemental material)

Age control was developed using ^{210}Pb and ^{14}C dating. Sediments of the upper most portion of the surface core were sampled at 0.5 cm intervals and radiometric measurements (^{210}Pb and ^{226}Ra) were made using low-background gamma counting with well-type intrinsic germanium detectors (Appleby et al., 1987; Schelske et al., 1994). Sediment ages were calculated using the constant rate of supply model (Figure C.S2; Appleby and Oldfield 1983). Age errors were propagated using first-order approximations and calculated according to Binford (1990). Radiocarbon dating on terrestrial macrofossils was used to constrain ages beyond the ^{210}Pb chronology. Radiocarbon samples were combusted and analyzed at the University of Arizona's Accelerator Mass Spectrometer facility. Marker layers were used to correlate age depths between the short and long cores. Radiocarbon ages were calibrated and age depth models were developed using the R program for Classic Age-Depth Modeling (Clam; Blaauw 2010). Radiocarbon dates were calibrated using the IntCal09.14C calibration curve (Reimer et al., 2009). Clam creates probability distributions of ages for each ^{14}C date then iteratively fits age-depth models (here a smoothing spline) and bases its final age-depth model (Figure C.S1) off the best fit of 1000 iterations (Blaauw 2010).

Acknowledgements

We thank K. Routson, R. Yetman, and C. Stielstra for extensive help in the field. We thank N. Mckay, J. Betancourt, A. Cohen, E. Brown, D. Meko, J. Conroy, and R. Reynolds for comments and insights. The National Oceanic and Atmospheric Administration (NOAA), the National Science Foundation, the Science Foundation Arizona, the NOAA funded Climate Assessment for the Southwest, the Colorado Scientific Society, and the University of Arizona Department of Geoscience contributed funding and support for this research.

Author Contributions

J.T.O. and C.A.W. conceived the project idea. C.C.R identified the lake, collected the sediment cores, developed the geochemical and grain-size records, performed the data analysis, and wrote the paper. W.F.K. developed the ^{210}Pb chronology. All authors commented on the manuscript.

Additional Information

The authors declare no competing financial interests. Correspondence and requests for materials should be directed to C.C.R.

C.6 References

1. Ballantyne, A. P., Brahney, J., Fernandez, D., Lawrence, C. L., Saros, J., Neff, J. C., & Naqvi, S. W. A. Biogeochemical response of alpine lakes to a recent increase in dust deposition in the Southwestern, US. *Biogeosciences*, **8,** 2689–2706 (2011).

2. Neff, J. C., Ballantyne, A. P., Farmer, G. L., Mahowald, N. M., Conroy, J. L., Landry, C. C., ... & Reynolds, R. L. Increasing eolian dust deposition in the western United States linked to human activity. *Nature Geosci.* **1,** 189–195 (2008).

3. Reynolds, R. L., Mordecai, J. S., Rosenbaum, J. G., Ketterer, M. E., Walsh, M. K., & Moser, K. A. Compositional changes in sediments of subalpine lakes, Uinta Mountains (Utah): evidence for the effects of human activity on atmospheric dust inputs. *J. Paleolim.* **44,** 161–175 (2010).

4. Collins, M., R. et al., Long-term Climate Change: Projections, Commitments and Irreversibility. In: *Climate Change 2013: The Physical Science Basis. Contribution of Working Group I to the Fifth Assessment Report of the Intergovernmental Panel on Climate Change*, Cambridge University Press, Cambridge, United Kingdom and New York, NY, USA (2013).

5. Painter, T. H., Deems, J. S., Belnap, J., Hamlet, A. F., Landry, C. C., & Udall, B. Response of Colorado River runoff to dust radiative forcing in snow. *Proc. of the Nat. Acad. of Sci.* **107,** 17125–17130 (2010).

6. Morman, S. A., & Plumlee, G. S. The role of airborne mineral dusts in human disease. *Aeolian Res.* **9,** 203–212 (2013).

7. Painter, T. H., Barrett, A. P., Landry, C. C., Neff, J. C., Cassidy, M. P., Lawrence, C. R., ... & Farmer, G. L. Impact of disturbed desert soils on duration of mountain snow cover. *Geophys. Res. Lett.* **34,** L12502 (2007).

8. Painter, T. H., Skiles, S. M., Deems, J. S., Bryant, A. C., & Landry, C. C. Dust radiative forcing in snow of the Upper Colorado River Basin: 1. A 6 year record of energy balance, radiation, and dust concentrations. *Water Resources Res.* **48,** W07521 (2012).

9. Skiles, S. M., Painter, T. H., Deems, J. S., Bryant, A. C., & Landry, C. C. Dust radiative forcing in snow of the Upper Colorado River Basin: 2. Interannual variability in radiative forcing and snowmelt rates. *Water Resources. Res.* **48,** W07522 (2012).

10. Bales, R. C., Molotch, N. P., Painter, T. H., Dettinger, M. D., Rice, R., &

Dozier, J. Mountain hydrology of the western United States. *Water Resources. Res.* **42,** W08432 (2006).

11. Munson, S. M., Belnap, J., & Okin, G. S. Responses of wind erosion to climate-induced vegetation changes on the Colorado Plateau. *Proceedings of the National Academy of Sciences* **108,** 3854–3859 (2011).

12. Neff, J. C., Reynolds, R. L., Munson, S. M., Fernandez, D., & Belnap, J. The role of dust storms in total atmospheric particle concentrations at two sites in the western US. *J. Geophys. Res. Atmos.* **118,** 201–212 (2013).

13. Forman, S. L., Spaeth, M., Marín, L., Pierson, J., Gómez, J., Bunch, F., & Valdez, A. Episodic Late Holocene dune movements on the sand-sheet area, Great Sand Dunes National Park and Preserve, San Luis Valley, Colorado, USA. *Quat. Res.* **66,** 97–108 (2006).

14. Halfen, A. F., & Johnson, W. C. A review of Great Plains dune field chronologies. *Aeolian Res.* **10,** 135–160 (2013).

15. Miao, X., Mason, J. A., Swinehart, J. B., Loope, D. B., Hanson, P. R., Goble, R. J., & Liu, X. A 10,000 year record of dune activity, dust storms, and severe drought in the central Great Plains. *Geology* **35,** 119–122 (2007).

16. Routson, C. C., Woodhouse, C. A., & Overpeck, J. T. Second century megadrought in the Rio Grande headwaters, Colorado: How unusual was medieval drought? *Geophys. Res. Lett.* **38,** L22703 (2011).

17. Woodhouse, C. A., & Overpeck, J. T. 2000 years of drought variability in the central United States. *Bull. Amer. Meteor. Soc.* **79,** 2693–2714 (1998).

18. Cook, E. R., Seager, R., Heim, R. R., Vose, R. S., Herweijer, C., & Woodhouse, C. Megadroughts in North America: Placing IPCC projections of hydroclimatic change in a long term palaeoclimate context. *J. Quat. Sci.* **25,** 48–61 (2010).

19. Belnap, J., & Gillette, D. A. Disturbance of biological soil crusts: impacts on potential wind erodibility of sandy desert soils in southeastern Utah. *Land Deg. & Devel.*, **8,** 355–362 (1997).

20. Lawrence, C. R., Painter, T. H., Landry, C. C., & Neff, J. C. Contemporary geochemical composition and flux of aeolian dust to the San Juan Mountains, Colorado, United States. *J. Geophys. Res.* **115,** 2005–2012 (2010).

21. Brahney, J., Ballantyne, A. P., Sievers, C., & Neff, J. C. Increasing Ca^{2+} deposition in the western US: The role of mineral aerosols. *Aeolian Res.* **10,** 77–87 (2013).

22. Cook, E. R., et al. North American summer PDSI reconstructions, version 2a, IGBP PAGES World Data Cent. Paleoclimatol. Data Contrib. Ser. 2008- 046, Paleoclimatol. Program, NCDC, NOAA, Boulder, Colo (2008).

23. Cook, E. R., Woodhouse, C. A., Eakin, C. M., Meko, D. M., & Stahle, D. W. Long-term aridity changes in the western United States. *Science* **306,** 1015–1018 (2004).

24. Stahle, D. W., et al. Tree-ring data document 16th century megadrought over North America. *EOS, Trans. Amer. Geophys. Union* **81,** 121–125 (2000).

25. Sayre, N. The cattle boom in southern Arizona: towards a critical political ecology. *J. Southwest* **41,** 239–271 (1999).

26. Abruzzi, W. S. The social and ecological consequences of early cattle ranching in the Little Colorado River Basin. *Human Ecol.* **23**, 75–98 (1995).

27. Cook, B. I., Seager, R., Miller, R. L., & Mason, J. A. Intensification of North American megadroughts through surface and dust aerosol forcing. *J. Clim.* **26,** 7635–7649 (2013).

28. Ault, T.R. J. E. Cole, J. T. Overpeck, G. T. Pederson and D. M. Meko. Assessing the risk of persistent drought using climate model simulations and paleoclimate data. *J. Clim.* (2014).

29. Williams, A. P., Allen, C. D., Macalady, A. K., Griffin, D., Woodhouse, C. A., Meko, D. M., ... & McDowell, N. G. Temperature as a potent driver of regional forest drought stress and tree mortality. *Nature Clim. Change* **3,** 292–297 (2012).

30. Conroy, J. L., Overpeck, J. T., Cole, J. E., Shanahan, T. M., & Steinitz-Kannan, M. Holocene changes in eastern tropical Pacific climate inferred from a Galápagos lake sediment record. *Quat. Sci. Rev.* **27,** 1166–1180 (2008).

Supplemental References:

Appleby, P. G., Oldield F. The assessment of ^{210}Pb data from sites with varying sediment accumulation rates. *Hydrobiologia* **103,** 29–35 (1983).

Appleby P. G., Nolan P. J., Gifford D. W., Godfrey M. J., Oldfield F., Anderson N. J., Battarbee R. W. ^{210}Pb dating by low background gamma counting. *Hydrobiologia* **143,** 21–27 (1986).

Binford, M. W. Calculation and uncertainty analysis of ^{210}Pb dates for PIRLA project lake sediment cores. *J. of Paleolim.* **3,** 253–267 (1990).

Blaauw, M. Methods and code for ‘classical’ age-modeling of radiocarbon sequences. *Quat. Geochron.* **5,** 512–518 (2010).

Reimer, P. J., Baillie, M. G., Bard, E., Bayliss, A., Beck, J. W., Blackwell, P. G., ... & Weyhenmeyer, C. E. IntCal09 and Marine09 radiocarbon age calibration curves, 0-50,000 years cal BP. *Radiocarbon* **51,** 1111–1150 (2009).

Schelske, C. L., Peplow, A., Brenner, M., & Spencer, C. N. Low-background gamma counting: applications for ^{210}Pb dating of sediments. *Journal of Paleolimnology* **10,** 115–128 (1994).

C.7 Figures

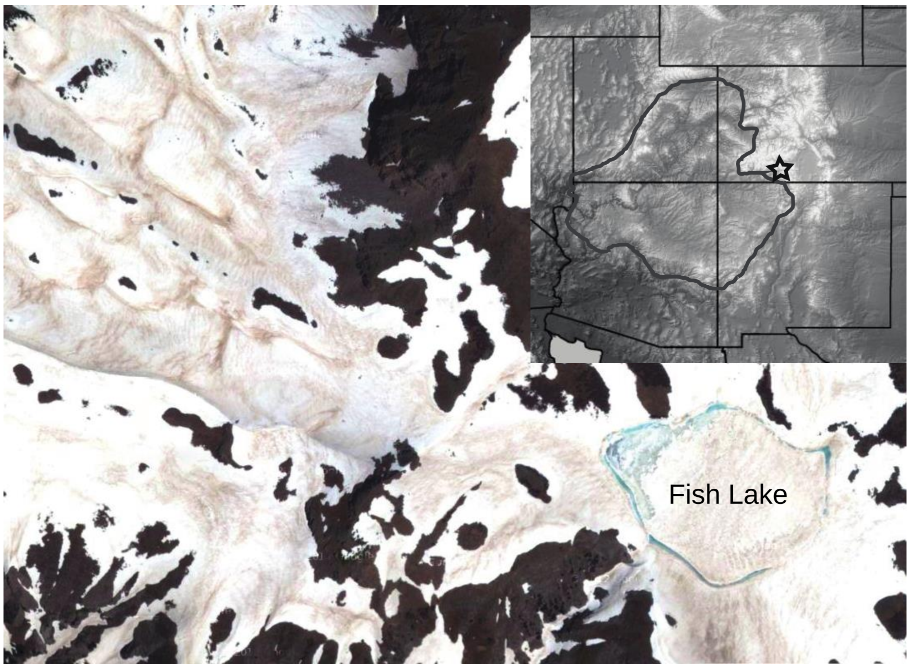

Figure C.1: **Study Site.** Google earth imagery from Spring 2011 shows dust accumulating on the snow surface on and around Fish Lake (37.25ºN, 106.68ºW). Inset map shows Fish Lake in the south San Juan Mountains (star), and the Colorado Plateau outlined in grey.

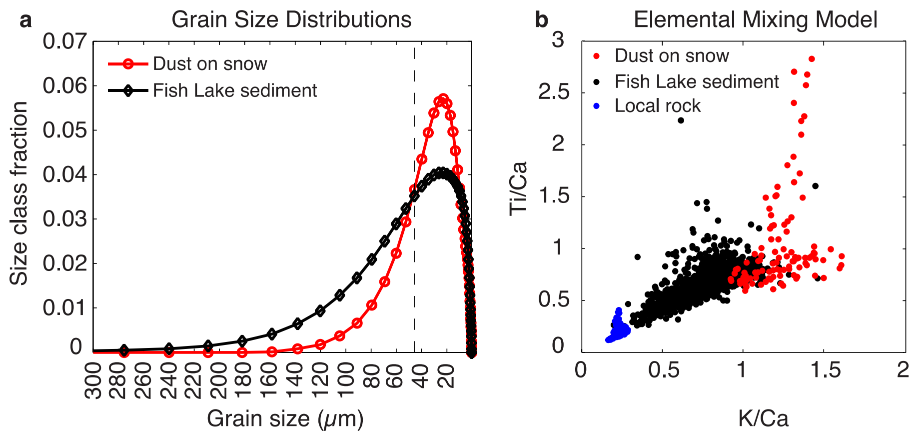

Figure C.2: **Reconstruction Methods. a** Grain size distributions of dust of snow (red) and Fish Lake sediment (black). Sediments diverge from dust toward coarser grain sizes representing locally derived material. The dashed vertical line denotes 45.7µm where the sediment begins to diverge from wind deposited dust. **b** The elemental ratio/ratio end-member mixing model using µXRF abundance counts of titanium, potassium, and calcium, showing sediment (black) distributed between bedrock (blue) and windblown dust (red) end-members.

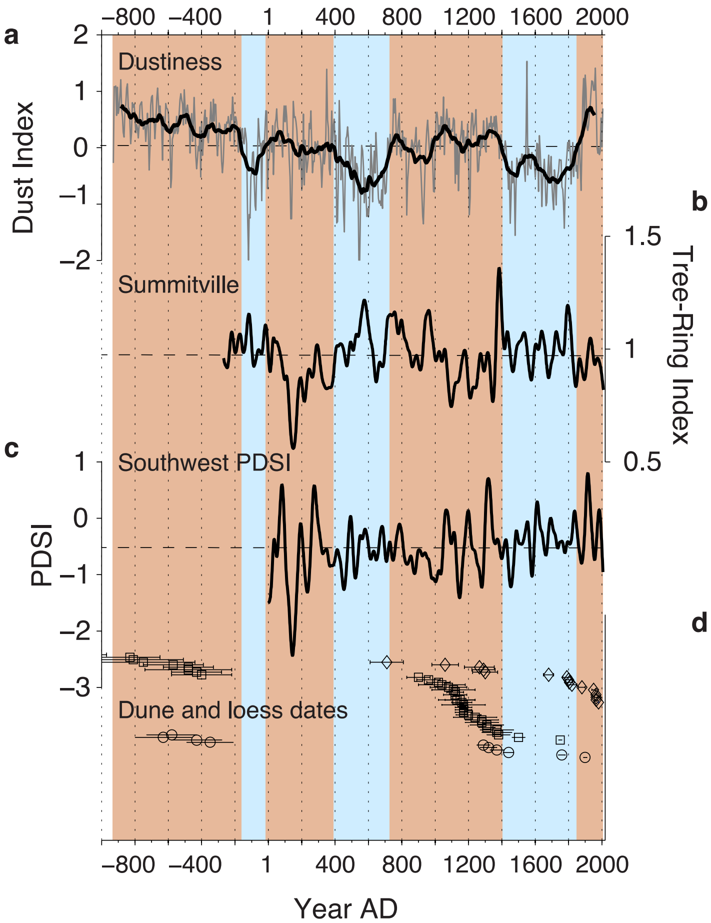

Figure C.3: **Comparison of Fish Lake dust index with regional drought indicatiors. a** Fish Lake dust reconstruction compared with **b** a tree-ring record of local Summitville spring time moisture balance[16], and **c** Southwestern PDSI[22]. Both moisture records are smoothed with a 70-year cubic smoothing spline to highlight long-term variabilty in aridity. **d** Dune activity dates from the Great Sand Dunes National Park[13] (diamonds), and dune (squares) and loess (circles) activity dates from the Great Plains[15].

C.8 Supplemental Figures

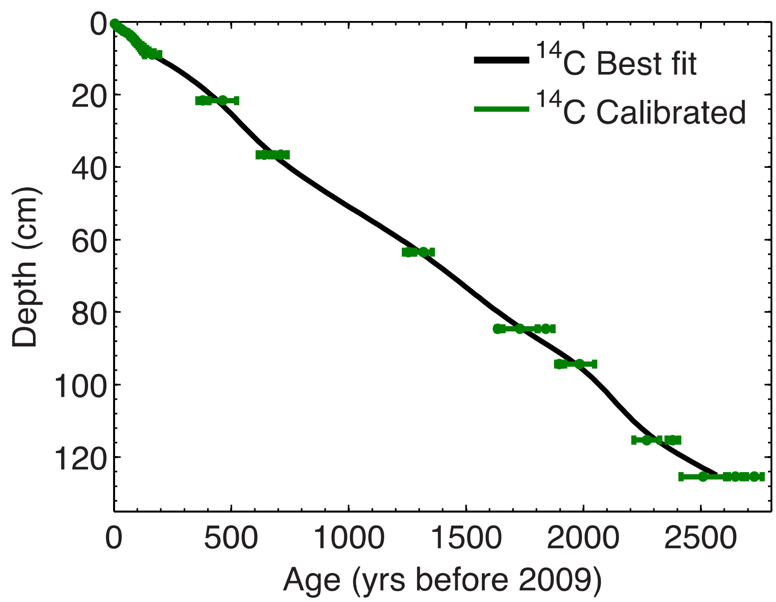

Figure C.S1**Fish Lake age model.** Calibrated ^{210}Pb and ^{14}C dates in green with the best fit of 1000 smoothing spline age models in black.

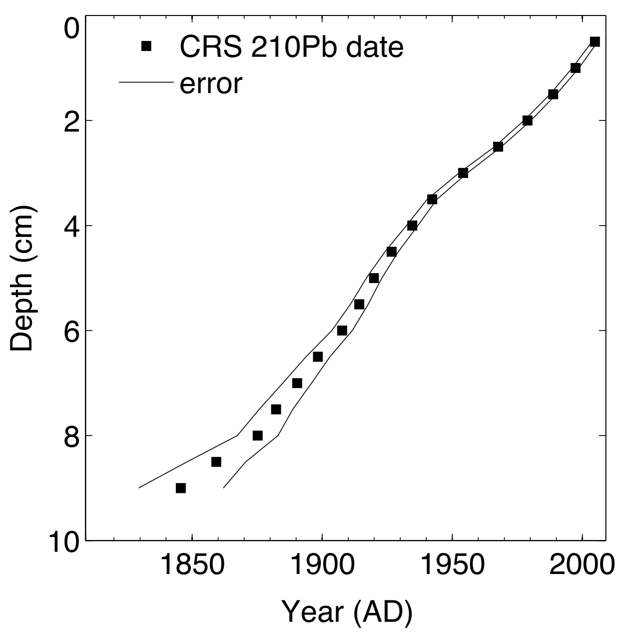

Figure C.S2: **Fish Lake ^{210}Pb age model.** Dates shown in the filled squares plotted with associated error based on a constant rate of supply model (Appleby and Oldfield 1983).

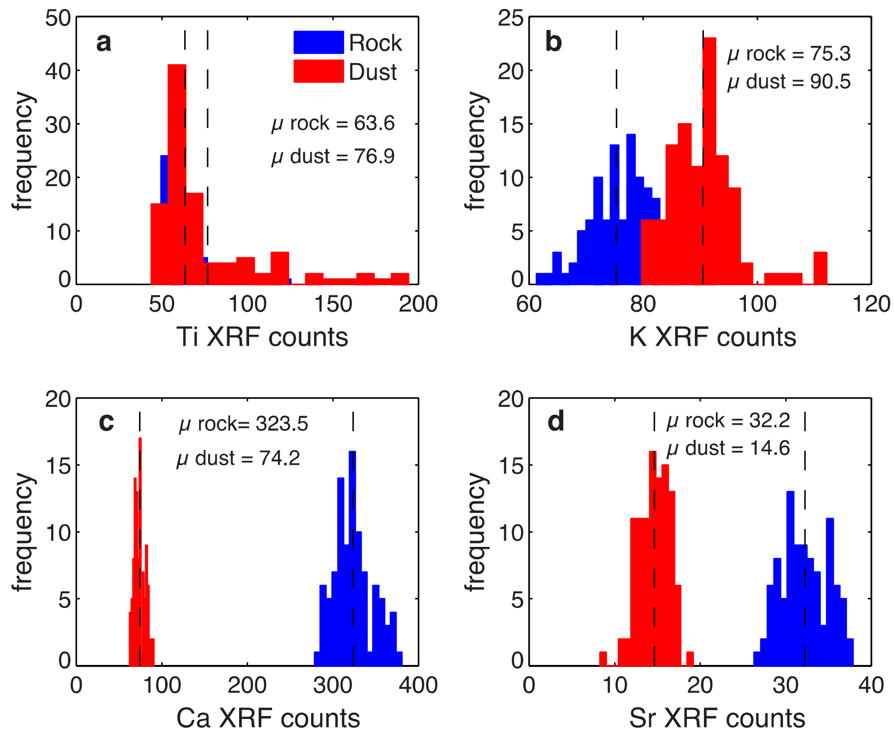

Figure C.S3: **Dust versus bedrock geochemistry.** Histograms showing the frequency of elemental abundances characterized using µXRF counts. Counts increase to the right on the x-axis. X-axis scale differs between plots. Titanium has similar abundances in local bedrock and in windblown dust. Potassium has slightly higher abundance in windblown dust. Calcium has moderate to high abundance in windblown dust and much higher abundance in local bedrock. Strontium has slightly higher abundance in local bedrock than windblown dust, but counts were too low to measure in the sediment reliably.

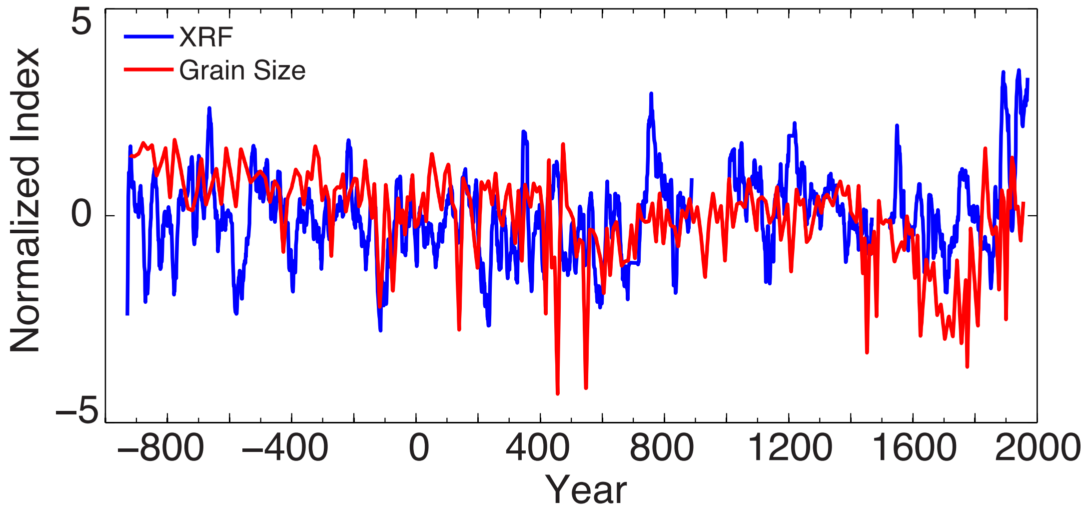

Figure C.S4: **Grain size and geochemical records.** Comparing grain size dust record (red) with µXRF dust record (blue). The records have been normalized by their mean and variance, and the short and long cores were combined using the mean. The µXRF record has been smoothed with a 25-point running mean for comparison purposes.

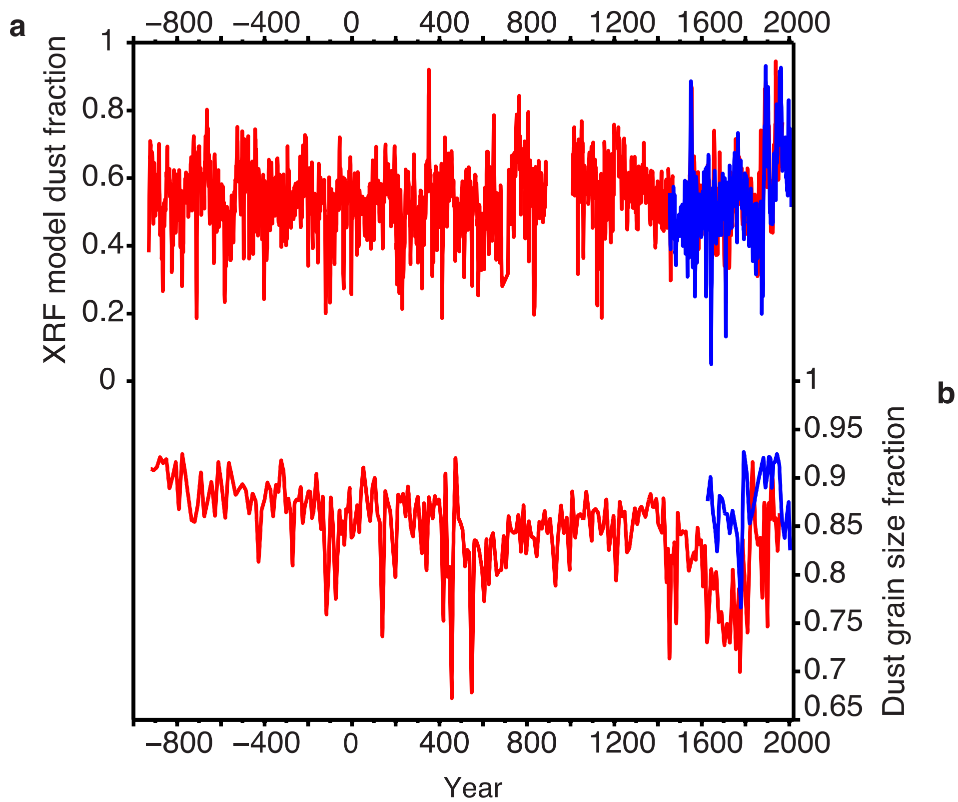

Figure C.S5: **Grain size and geochemical records on short and long cores.** Dust µXRF record (top) and dust grain size record (bottom) and from short (blue) and long (red) cores. The gaps in the µXRF record are sections of sediment that did not imbed properly.

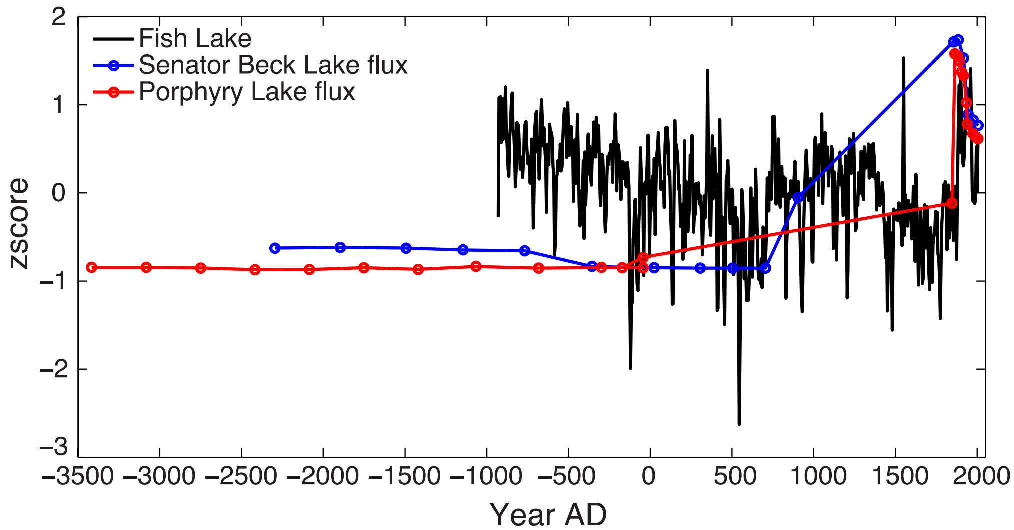

Figure C.S6: **Fish Lake versus Senator Beck and Porphery Lakes.** Senator Beck and Porphery Lakes dust records developed by ref. 2 are from the central San Juan Mountains. The Fish Lake record closely matches the last 100 years where all records have the best age control, but Fish Lake differs earlier in time where flux rate estimations from Senator Beck and Porphery Lakes are limited by age control points.

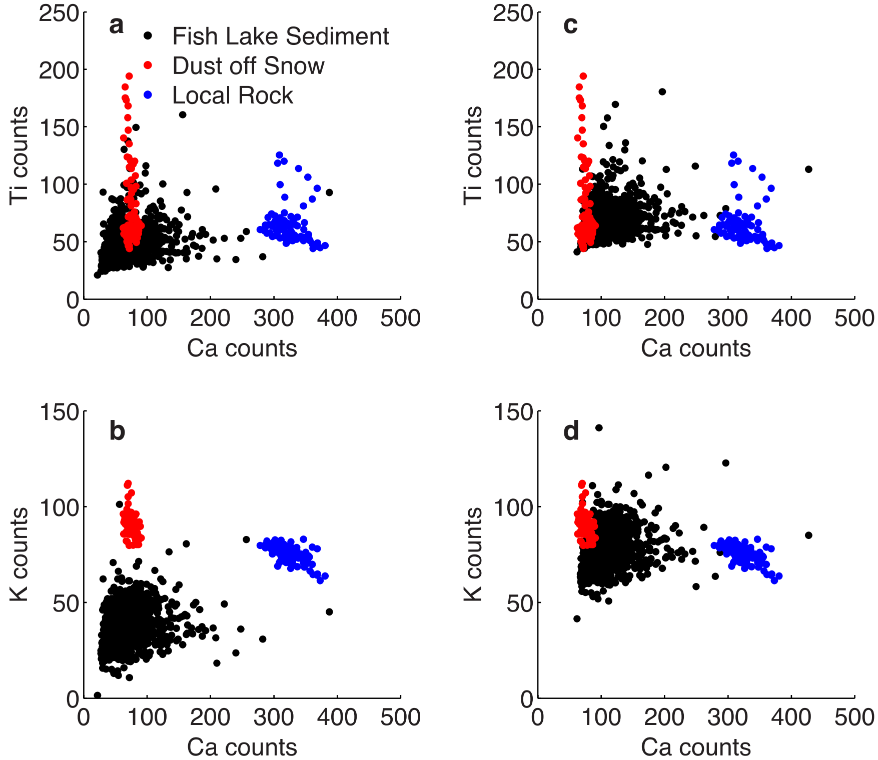

Figure C.S7: **Epoxy elemental abundance adjustment.** Elemental ratio scatter plots of µXRF counts of dust off snow (red), bedrock from around Fish Lake (blue), and Fish Lake sediment (black). Panels a–b are raw µXRF counts of Ti/Ca and K/Ca. Counts are diluted in the sediment with respect to the dust and bedrock due to epoxy resin and organic matter. Panels c–d show the adjusted fish lake sediment with respect to dust and local bedrock (Shifting sediment elemental counts higher to account for µXRF count reductions), illustrating how the sediment is a mixture of the two sources.

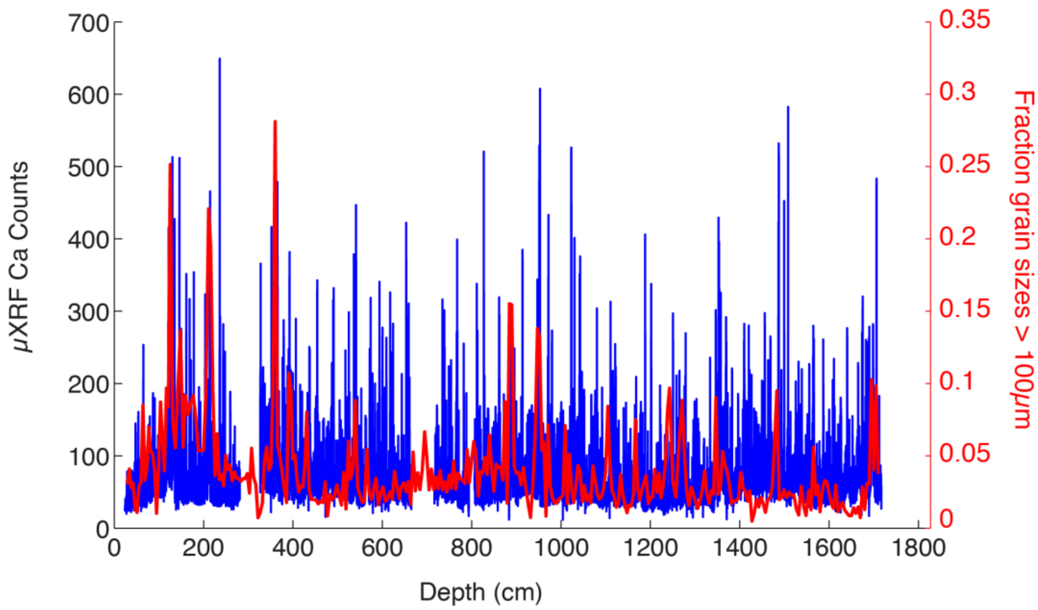

Figure C.S8: **Coarse grain sizes versus calcium abundance.** Coarse grain size fraction (>100μm, red), plotted with μXRF estimated calcium abundance (blue) before turbidites were removed. Plot shows coarse grain sizes correspond with high calcium concentrations.

C.9 Supplemental Tables

Table C.S1: Fish Lake radiocarbon measurements and dates

Sample Name	Depth (cm)	Lab Number	$\delta^{13}C$	FMC	^{14}C (year bp)	Error
Bulk Sed.	0	AA89058	-29.9	1.0071 ± 0.0042	pst bomb	NA
Aqtc. grass	21.67	AA90931	-26.1	0.9628 ± 0.004	305	33
Wood	36.64	AA99397	-26.3	0.9201 ± 0.0044	699	38
Pine cone	63.44	AA90932	-22.6	0.8485 ± 0.0036	1320	34
Wood	84.62	AA90935	-26.5	0.8026 ± 0.0035	1767	35
Wood	94.34	AA90933	-26.8	0.7837 ± 0.0034	1958	35
Wood	115.31	AA90937	-27.2	0.7546 ± 0.0033	2262	36
Wood	125.41	AA90941	-25.2	0.7375 ± 0.0033	2446	36

Table C.S2: Fish Lake 210Pb dates on the upper surface sediments. Dates are calculated based on the constant rate of supply model.

	Constant Rate of Supply (year AD)		
Depth (cm)	Lower	Mean	Upper
1	1996.1	1997.4	1998.7
1.5	1987.6	1988.8	1990
2	1977.6	1978.9	1980.2
2.5	1966.3	1967.6	1968.9
3	1952.6	1954.2	1955.8
3.5	1940.4	1942.3	1944.1
4	1932.4	1934.6	1936.8
4.5	1924.1	1926.7	1929.3
5	1917	1919.9	1922.9
5.5	1910.9	1914.3	1917.7
6	1903.7	1907.7	1911.6
6.5	1893.8	1898.4	1903
7	1884.9	1890.4	1895.9
7.5	1875.8	1882.3	1888.7
8	1867.4	1875.2	1883
8.5	1848	1859.3	1870.6
9	1829.4	1845.7	1862
9.5	1775.9	1815.5	1855.1
10	1573.7	1763.2	1952.6

APPENDIX D

THE MEGADROUGHT ENVIRONMENT

D.1 Abstract:

We suggest warm temperatures exacerbated megadroughts in the southwestern United States over the past 2000 years. We present a new temperature reconstruction from the south San Juan Mountains in southern Colorado in conjunction with recently developed dust and moisture balance records that span the last 2000 years. The reconstruction indicates the San Juan Mountains may have been warmer in the past than present, and elevated temperatures coincided with periods of anomalous aridity. Warm temperatures and dustiness during megadroughts imply that temperature and dust may have acted as important drought feedback mechanisms over the past 2000 years in the Southwest. As headwaters of the Rio Grande and San Juan Rivers, the San Juan Mountains are a critical contributor to Southwest water resources, and their current rate of warming is outpacing many regions in the West. Past temperature extremes in our record indicate that the San Juan Mountains are highly sensitive to temperature change, which will impact surface water supplies in a future of rapid warming.

D.2 Body

Megadroughts (multidecadal in length) have occurred several times in the Southwestern United States (Southwest) over the past 2000 years (Routson et al.

2011; Woodhouse and Overpeck 1998). Documented in tree-rings and other natural climate archives, megadroughts are associated with substantial decreases in Colorado River flow (Meko et al. 2007) and the collapse of the ancient pueblo culture (Douglas et al. 1929). The timing and duration of Southwestern megadroughts have been well characterized (Cook et al., 2007; 2010; Meko et al., 2007; Routson et al., 2011; Woodhouse and Overpeck 1998), but uncertainty still surrounds other local environmental conditions.

Recent warming in the Southwest has been implicated in widespread drought and has strongly impacted regional water resources. At high elevations, warming has driven declines in snowfall, faster snowpack ablation, and shortened snow-covered season, resulting in decreased runoff available for downstream users (Barnett et al., 2008; Bales et al., 2006; Harpold et al., 2012; Nowak et al., 2012). Furthermore, warming combined with drought stress has driven widespread forest mortality via fire, moisture deficit, and insect attacks (Breshears et al., 2008; Westerling et al., 2006; Van Mantgem et al., 2009), which can also result in less available water (Harpold et al., 2013; Biederman et al., 2012). Warmer air temperatures increase atmospheric moisture demand, and intensify the effects of precipitation deficits (Breshears et al., 2005; Weiss et al., 2009; Williams et al., 2012). On the Colorado Plateau, vegetation mortality and dustiness have increased with temperature (Munson et al., 2011). Windblown dust deposited on Rocky Mountain snowpack then works in concert with warmer air temperatures, causing faster ablation and decreased runoff efficiency (Painter et al., 2007, 2010, 2012). Given current feedbacks between temperature, dustiness, and moisture deficit, to what degree did anomalous temperature influence megadroughts in the Southwest?

To date, the temperature history of the Southwest during megadroughts is poorly constrained. The most notable megadroughts occurred during the Roman Period (~1-400 AD) and the Medieval Climate Anomaly (MCA, ~900-1400 AD; Cook et al., 2010; Meko et al., 2007; Routson et al., 2011), which are thought to have been warmer than average in the Northern Hemisphere (Christiansen and Ljungqvist 2012, Ljungqvist 2010; Mann et al., 2008, 2009; Moberg et al., 2005). Limited evidence suggests the Southwest may have been warmer at times during the MCA (i.e. Mann et al., 2009; Salzer and Kipfmueller 2005), and that some megadroughts may have coincided with warm temperatures (Meko et al., 2007; Woodhouse et al., 2010).

To better constrain the paleoenvironmental temperatures of megadroughts, we tested a new biomarker proxy known as gycerol dialkyl glycerol tetraethers (GDGTs). GDGTs are series of membrane lipids closely linked with mean annual air temperature (Loomis et al., 2012; Tierney et al., 2010). We used a lake sediment core from south San Juan Mountains to reconstruct 2000 years of temperature variability. The San Juan Mountains are located in southern Colorado, the epicenter of Southwestern megadroughts (Cook et al., 2013b), and an important headwaters region to the San Juan and Rio Grande Rivers. Sediment cores were obtained from Blue Lake at 3500 meters elevation (Figure D.1). We established age control using ^{210}Pb of the upper most surface sediments, and ^{14}C dating of terrestrial macrofossils (Figure D.2). GDGTs were extracted from sediment samples and analyzed on a mass spectrometer (i.e. Tierney et al. 2010; see methods section). GDGT compound relative abundance was calibrated to mean annual air temperature using the Loomis et al. (2012) calibration (henceforth the Loomis calibration).

The association between GDGTs and temperature was characterized using high elevation snow telemetry (SNOTEL) stations (Table D.S1, NRCS 2013) and National Weather Service (NWS) stations (Table D.S2, WRCC 2013). The sediment core was sampled at 3-5 year resolution over the past ~100 years to compare with instrumental station data. The GDGT record has a good match with regional high elevation (> 3000 m) SNOTEL stations (Figure D.3a-b), however the SNOTEL stations have only been in place since the mid 1980's. The GDGTs have no significant relationship with NWS stations. Most NWS stations however, are located at low elevations and tend to have variable relationships between each other and with the high elevation SNOTEL stations (See supplemental material), indicating there is spatial heterogeneity in temperature and that the NWS stations may not be the most reliable for estimating temperatures at Blue Lake. The close relationship between the Blue Lake record and the SNOTEL stations, implies the GDGTs are at least representative of local high elevation temperatures.

The new Blue Lake temperature reconstruction spans the last 2300 years and indicates the south San Juan Mountains were warmer in the past than they are today (Figure D.4a). The record has an overall downward trend, where long-term cooling continued into the mid 1980's when the GDGTs and instrumental records show the San Juan Mountains began rapidly warming (Ragwala and Miller 2010). The GDGT record shows the Roman and Medieval periods were unusually warm. The average temperature during the Roman Period (1-400 AD) was 2.7ºC warmer than the last 100 years and average temperature during the medieval period (900-1400 AD) was 1.8ºC warmer than the last 100 years. The Blue Lake record shows a maximum temperature during the Roman Period was 4.2ºC above the 1950-2009 mean at 338 AD, compared with most recent maximum of 2.3ºC at the end of the record in 2009. To put past warm periods in the context of future warming, downscaled regional CMIP5 multi-model ensemble climate projections suggest the San Juan area could warm as much as 6ºC over the next century, and SNOTEL stations and our record already show warming at a faster rate than predicted (Figure D.4a).

Considerable error is associated with the absolute temperature estimates presented here. The Loomis calibration is based off 111 east African lakes, and has root mean square error of prediction of 2.1 ºC with a maximum bias of 1 ºC. Although the Loomis calibration is based off tropical lakes, mean GDGT temperatures at Blue Lake (1.8 ºC for 1950-2009) do fall within the Loomis calibration range. Furthermore, recent work shows the Loomis calibration applies to GDGTs in Arctic lakes for some seasons (Shanahan et al., 2013). Nonetheless, GDGT's have not been well tested in temperate environments, and a local calibration set is needed. There is also error associated with measurements on the mass-spectrometer and in integrating the compound concentration curves. The GDGT temperatures could be biased warm. Comparing mean annual air temperatures between the GDGT record and the closest SNOTEL station Lily Pond between 1985 and 2009, the GDGT record has a mean temperature of 2.1ºC whereas Lily Pond has a mean temperature of 1.5ºC. Blue Lake is slightly higher in elevation than Lily Pond, but without an understanding of local cold air drainage patterns (i.e. Lundquist et al 2007) it is hard to assess the nature of potential microsite climate bias.

It is not clear from the GDGT record if the timing and magnitude of Roman Period and MCA warming at Blue Lake was confined to the higher elevations of the south San Juan Mountains or was more regional in scale. At the hemispheric scale, the MCA was warmer than average (Christansan and Ljungqvist 2012; Ljungqvist 2010; Mann et al., 2008, 2009; Moberg et al., 2005), but not consistently across all regions (Hughes and Diaz 1994; Mann et al., 2009). Although fewer reconstructions are available, two out of three Northern Hemisphere temperature reconstructions indicate the Roman Period was also warmer than average (Figure D.S1a; Christansan and Ljungqvist 2012; Ljungqvist 2010; Moberg et al., 2005). Moving toward finer scales, North American temperatures constrained by pollen suggest the MCA was up to 0.1 ºC warmer than the 1904-1980 average, which is a much smaller degree of change that we see in our record (Figure D.S2b, Trouet et al. 2013). The Mann et al. (2009) gridded temperature reconstruction suggests Western MCA temperatures were up to 0.3 ºC warmer than their 1961 to 1990 reference period mean (Figure D.S2c).

While few regional temperature records of this length exist, two multimillennial-length bristlecone pine temperature reconstructions from Northern Arizona and the Great Basin compare poorly with the Blue Lake Temperature record. In Northern Arizona 500 km southwest of Blue Lake, temperatures reconstructed on the San Francisco Peaks show warming coincident with some megadroughts, but no overall warming during the Roman Period or the MCA (Figure D.S2d, Salzer and Kipfmueller 2005). Temperatures constrained by bristlecone ring width and changes in the position of treeline in the Great Basin (700 km or more from Blue Lake) indicate there were long-term changes, but not coincident with periods of anomalous warming in the GDGT record (Figure D.S2e, Salzer et al., 2013). The seasonality of the temperature signal and spatial variability in past temperatures may account for these discrepancies. The Blue Lake record is calibrated to mean annual temperature whereas the bristlecone records are calibrated to July maximum temperature for the San Francisco Peaks and July-September temperature in the Great Basin.

Comparing the Blue Lake temperature reconstruction with local drought and dust records (Routson et al., 2011; Routson et al., in prep) shows relationships between drought, dustiness and warm temperatures, suggesting that megadroughts and periods of persistent aridity in the Southwest may have been forced in part by unusually warm temperatures (Figure D.4). A moisture-sensitive bristlecone pine drought record from Summitville (21 km from Blue Lake) shows extreme drought within the Roman and medieval periods (Figure D.4b, Routson et al., 2011). GDGT's indicate that anomalously warm temperatures accompanied these dry intervals in the south San Juan Mountains. Instrumental analyses show the Summitville bristlecone growth has an independent negative relationship with temperature (Routson et al., 2011). High temperatures increase evapotranspiration rates, amplifying the effect of moisture deficit on already moisture-limited trees and exacerbating drought conditions. Dust deposition in Fish Lake (5 km from Blue Lake) indicates these periods of anomalous temperature and drought in the south San Juan Mountains were associated with elevated dustiness (Figure D.4c, Routson et al., in prep). Dust deposited in the San Juan Mountains integrates regional drought conditions, especially across the desert landscapes to the Southwest (Painter et al., 2007). High dust deposition suggests regional scale aridity, perhaps also exacerbated by unusual warming. The GDGT's and bristlecone moisture records indicate the Roman Period was warmer and drier in the south San Juan Mountains than the medieval period; however, dust deposition was higher and longer lasting during the medieval period. Higher medieval dust deposition may indicate that arid conditions during the medieval period were regional in scale while the 2nd century drought was locally acute, although tree-ring reconstructed PDSI in addition to tree-ring records from New Mexico and Utah corroborate the regional severity of the 2nd century drought (Cook et al., 2008; Grissino-Mayor 1998; Knight et al., 2010; Routson et al., 2011).

The new GDGT reconstruction suggests the San Juan Mountains may be highly sensitive to temperature change. SNOTEL stations indicate that high elevation environments in Colorado are warming over twice as fast as the Colorado state average (Clow 2010), and the San Juan Mountains are currently warming at one of the fastest rates in North America (Rangwala and Miller 2010). The poor relationship with lower elevation NWS stations limits our ability to extrapolate beyond local conditions in the San Juan Mountains. However, given the critical role of this sensitive, high elevation system as headwaters of the Rio Grande and the San Juan River, a major tributary of the Colorado River, local conditions in the San Juan Mountains have regional implications for water resources.

In conclusion, a new temperature reconstruction from the south San Juan Mountains suggests that temperatures warmer than today occurred during the Roman and Medieval periods. Records of dustiness and drought stress reveal coincident timing of warm temperatures, severe drought, and high dustiness. These observations lead us to speculate that dust and temperature may have worked in concert as a drought enhancing feedback, whereby high temperatures caused increased drought stress and vegetation mortality, higher atmospheric dust loading, more frequent dust on snow events, and subsequent decreases in runoff. To further support the fidelity of our results we need a local GDGT calibration set and corroboration with other high-resolution regional temperature reconstructions that capture low frequency temperature variability. Nonetheless, our results suggest that past temperatures the San Juan Mountains were highly variable. Given the projected rate of future warming, sensitive mountain environments like the San Juan and greater Rock Mountain region are a key vulnerability for future Southwestern water resources.

D.3 Methods

We collected short (20cm) and long (180cm) sediment cores using packable rafts and a universal gravity corer. Age control was established using ^{210}Pb on the upper sediment of an undisturbed short core. The upper 8 cm was sampled at 0.5 cm resolution and ^{210}Pb and ^{226}Ra measurements were made using low-background gamma counting with well-type intrinsic germanium detectors (Appleby et al., 1987; Schelske et al., 1994). A constant rate of supply (CRS) model was used to calculate ^{210}Pb ages (Appleby and Oldfield 1983), and error was calculated using first-order approximations (e.g. Binford 1990). Radiocarbon (^{14}C) dating of terrestrial macrofossils on two longer cores was used to constrain ages before the ^{210}Pb chronology. Radio carbon samples were pretreated and combusted at the University of Arizona Accelerator Mass Spectrometer (AMS) facility. Cores were crosscorrelated using marker layers to get dates from different cores on the same depth-scale. One ^{14}C age was excluded due to an age reversal. The date was on wood fragment that likely grew well before washing into the lake, and is thus not an accurate date of sedimentation. Age modeling was conducted using the Classic Age Depth Modeling program (clam; Blaauw 2010). We used clam to calibrate ^{14}C dates with the IntCal09.14C calibration curve (Reimer et al 2009). Clam develops an age model based on the best of 1000 age models iteratively fit to probability distributions radiometric ages (Blaauw 2010).

We sampled a single core with undisturbed surface sediment that spanned the last 2000 years for the reconstruction. The upper 9 cm were sampled at 2.5mm (average 4.5 year) resolution for comparison with instrumental temperature data. Between 9 cm and 131 cm the core was sampled at 1cm (average 20.5 year) resolution. Samples were freeze-dried and homogenized. Organic lipid compounds were extracted in a 9:1 v/v mixture of dichloromethane and alcohol in an accelerated solvent extraction system. The lipid extracts were separated by polarity using Al_2O_3 column chromatography. The polar compounds were then dried under N_2 gas, dissolved in 9:1 hexane/isopropanol and analyzed on a high performance liquid chromatography/atmospheric pressure chemical ionization-mass spectrometer (HPLC/APCIMS) following methods described in Tierney et al. (2010) and others (Schouten et al., 2007, 2009). Data were analyzed using the Agilent Chemstation program to assess ions including m/z 1292 (IV), m/z 1050 (III), m/z 1048 (IIIb), m/z 1046 (IIIc), m/z 1036 (II), m/z 1034 (IIb), m/z 1032 (IIc), m/z 1022 (I), m/z 1020 (Ib), m/z 1018 (Ic). Compound concentration peaks were integrated visually using the methods described in Weijers et al. (2007). Relative compound abundance was calibrated to mean annual air temperature (MAAT) using the Loomis et al. (2012) calibration, a stepwise forward selection regression model derived from 111 east African lakes:

$$MAAT = 22.77 - 33.58 \times f(\boldsymbol{III}) - 12.88 \times f(\boldsymbol{II}) - 418.53 \times (\boldsymbol{IIc}) + 86.43 \times (\boldsymbol{Ib})$$

For the instrumental period we compared our new proxy record against regional Snow Telemetry (SNOTEL) stations, NWS stations, and an average of the nearest 4 PRISM pixels (Daly et al 2002). SNOTEL data were accessed through the Natural Resource Conservation Service website: http://www.wcc.nrcs.usda.gov/snow/. SNOTEL station data were screened for daily outliers that exceed ±2 standard deviations from the daily mean (e.g. Harpold et al. 2012). The closest SNOTEL station is at Lily Pond, located 17 km from Blue Lake at 3339 meters elevation. Ten SNOTEL stations located above 3000 m elevation in the San Juan Mountains were used to characterize recent high elevation temperature change (Table S1). The data were converted to anomalies by subtracting the series length mean prior to 1995, and then the stations were combined using the arithmetic mean. To compute correlations with the Blue Lake record, the SNOTEL data were binned to the same resolution as the GDGT record using an arithmetic mean. NWS coop station data were obtained through the Western Regional Climate Center website: http://www.wrcc.dri.edu. Downscaled CMIP5 RCP 8.5 climate projection ensembles over period 1950 through 2099 for the local Blue Lake grid cell (latitude: 37.125, 37.25 ºN; Longitude: –105.75, –106.25 ºW) were obtained from: http://gdodcp.ucllnl.org/downscaled_cmip_projections/ (Maurer et al., 2007).

D.4 References

Appleby, P. G., Nolan, P. J., Gifford, D. W., Godfrey, M. J., Oldfield, F. J. A. N., Anderson, N. J., & Battarbee, R. W. 210Pb dating by low background gamma counting. In *Paleolimnology IV* (pp. 21-27). Springer Netherlands (1987).

Ault, T. R., Cole, J. E., Overpeck, J. T., Pederson, G. T., George, S. S., Otto-Bliesner, B., ... & Deser, C. (2013). The continuum of hydroclimate variability in western North America during the last millennium. *Journal of Climate*, (2013).

Bales, R. C., Molotch, N. P., Painter, T. H., Dettinger, M. D., Rice, R., & Dozier, J. (2006). Mountain hydrology of the western United States. *Water Resources Research*, *42*(8).

Barnett, T. P., Pierce, D. W., Hidalgo, H. G., Bonfils, C., Santer, B. D., Das, T., ... & Dettinger, M. D. (2008). Human-induced changes in the hydrology of the western United States. *science*, *319*(5866), 1080-1083.

Biederman, J. A., Brooks, P. D., Harpold, A. A., Gochis, D. J., Gutmann, E., Reed, D. E., ... & Ewers, B. E. (2012). Multiscale observations of snow accumulation and peak snowpack following widespread, insect-induced lodgepole pine mortality. *Ecohydrology*.

Binford, M. W. Calculation and uncertainty analysis of 210Pb dates for PIRLA project lake sediment cores. *Journal of Paleolimnology*, *3*(3), 253-267 (1990).

Blaauw, M. Methods and code for 'classical'age-modelling of radiocarbon sequences. *Quaternary Geochronology*, *5*(5), 512-518 (2010).

Breshears, D. D., et al. (2005), Regional vegetation die- off in response to global-change- type drought, Proc. Natl. Acad. Sci. U. S. A., 102(42), 15,144–15,148, doi:10.1073/pnas.0505734102.

Breshears, D. D., Myers, O. B., Meyer, C. W., Barnes, F. J., Zou, C. B., Allen, C. D., ... & Pockman, W. T. (2008). Tree die-off in response to global change-type drought: mortality insights from a decade of plant water potential measurements. *Frontiers in Ecology and the Environment*, *7*(4), 185-189.

Clow DW (2010) Changes in the timing of snowmelt and streamflow in Colorado: a response to recent warming. J Clim 23(9), 2293–2306

Cook, E. R., K. R. Briffa, D. M. Meko, D. A. Graybill, and G. Funkhouser (1995), The "segment length curse" in long tree- ring chronology development for palaeolclimatic studies, Holocene, 5(2), 229–237, doi:10.1177/ 095968369500500211.

Cook, B. I., Seager, R., Miller, R. L., & Mason, J. A. Intensification of North American megadroughts through surface and dust aerosol forcing. *Journal of Climate*, (2013a).

Cook, B. I., J. E. Smerdon, R. Seager, and E. R. Cook, 2013: Pan-continental droughts in North America over the last millennium. Journal of Climate, (2013b).

Cook, E. R., Seager, R., Heim, R. R., Vose, R. S., Herweijer, C., & Woodhouse, C. Megadroughts in North America: Placing IPCC projections of hydroclimatic change in a long term palaeoclimate context. *Journal of Quaternary Science*, *25*(1), 48-61 (2010).

Cook, E.R., et al. 2008: North American summer PDSI reconstructions, version 2a, IGBP PAGES World Data Cent. Paleoclimatology Data Contributions Service 2008-046, Paleoclimatology Program, NGDC, NOAA, Boulder, Colorado.

Daly, C., W. P. Gibson, G. H. Taylor, G. L. Johnson, and P. Pasteris (2002), A knowledge- based approach to the statistical mapping of climate, Clim. Res., 22, 99–113, doi:10.3354/cr022099.

Douglass, A. E. (1929), The Secret of the Southwest Solved With Talkative Tree Rings, pp. 736–770, Judd and Detweiler, Washington, D. C.

Grissino- Mayor, H. (1996), A 2129- year reconstruction of precipitation for northwestern New Mexico, USA, in Tree Rings, Environment, and Humanity, edited by J. S. Dean, D. M. Meko, and T. W. Swetnam, pp. 191–204, Radiocarbon, Tucson, Ariz.

Harpold, A., Brooks, P., Rajagopal, S., Heidbuchel, I., Jardine, A., & Stielstra, C. (2012a). Changes in snowpack accumulation and ablation in the intermountain west. *Water Resources Research*, *48*(11).

Harpold, A. A., Biederman, J. A., Condon, K., Merino, M., Korgaonkar, Y., Nan, T., ... & Brooks, P. D. (2013). Changes in snow accumulation and ablation following the Las Conchas Forest Fire, New Mexico, USA. *Ecohydrology*.

Hughes, M. K., & Diaz, H. F. (1994). Was there a 'Medieval Warm Period', and if so, where and when?. *Climatic Change*, *26*(2-3), 109-142.

Knight, T. A., D. M. Meko, and C. H. Baisan (2010), A bimillennial- length tree- ring reconstruction of precipitation for the Tavaputs Plateau, north-eastern Utah, Quat. Res., 73, 107–117, doi:10.1016/j.yqres.2009.08.002.

Ljungqvist, F. C. (2010), A new reconstruction of temperature variability in the extra- tropical Northern Hemisphere during the last two millennia, Geogr. Ann., 92, 339–351, doi:10.1111/j.1468-0459.2010.00399.x.

Loomis, S. E., Russell, J. M., Ladd, B., Street-Perrott, F. A., & Sinninghe Damsté, J. S. (2012). Calibration and application of the branched GDGT temperature proxy on East African lake sediments. *Earth and Planetary Science Letters*, *357*, 277-288.

Mann, M. E., et al., 2009: Global signatures and dynamical origins of the Little Ice Age and Medieval Climate Anomaly. Science, 326 (5957), 1256–1260, doi:10.1126/science. 1177303.

Maurer, E. P., L. Brekke, T. Pruitt, and P. B. Duffy (2007), 'Fine-resolution climate projections enhance regional climate change impact studies', Eos Trans. AGU, 88(47), 504.

Meko, D. M., C. A. Woodhouse, C. A. Baisan, T. Knight, J. J. Lukas, M. K. Hughes, and M. W. Salzer, 2007: Medieval drought in the upper Colorado River Basin. Geophysical Research Letters, 34 (10), 10 705–10 709, doi:10.1029/2007GL029988.

Moberg, A., Sonechkin, D. M., Holmgren, K., Datsenko, N. M., & Karlén, W. (2005). Highly variable Northern Hemisphere temperatures reconstructed from low- and high-resolution proxy data. *Nature*, *433*(7026), 613-617.

Munson, S. M., Belnap, J., & Okin, G. S. Responses of wind erosion to climate-induced vegetation changes on the Colorado Plateau. *Proceedings of the National Academy of Sciences*, *108*(10), 3854-3859 (2011).

Nowak, K., M. Hoerling, B. Rajagopalan, and E. Zagona, 2012: Colorado River Basin Hydroclimatic Variability. Journal of Climate 25 (12), 4389-4403 doi: http://dx.doi.org/10.1175/JCLI-D-11-00406.1

NRCS 2013: SNOTEL data and products. Available online: http://www.wcc.nrcs.usda.gov/snow/

Painter, T. H., Barrett, A. P., Landry, C. C., Neff, J. C., Cassidy, M. P., Lawrence, C. R., ... & Farmer, G. L. Impact of disturbed desert soils on duration of mountain snow cover. *Geophysical Research Letters*, *34*(12), L12502 (2007).

Painter, T. H., Deems, J. S., Belnap, J., Hamlet, A. F., Landry, C. C., & Udall, B. Response of Colorado River runoff to dust radiative forcing in snow. *Proceedings of the National Academy of Sciences*, *107*(40), 17125-17130 (2010).

Painter, T. H., Skiles, S. M., Deems, J. S., Bryant, A. C., & Landry, C. C. Dust radiative forcing in snow of the Upper Colorado River Basin: 1. A 6-year record of energy balance, radiation, and dust concentrations. *Water Resources Research*, *48*(7) (2012).

Reimer, P. J., Baillie, M. G., Bard, E., Bayliss, A., Beck, J. W., Blackwell, P. G., ... & Weyhenmeyer, C. E. IntCal09 and Marine09 radiocarbon age calibration curves, 0-50,000 years cal BP (2009).

Routson, C. C., C. A. Woodhouse, and J. T. Overpeck, 2011: Second century megadrought in the Rio Grande headwaters, Colorado: How unusual was medieval drought? Geophysical Research Letters, 38 (22), L22 703, doi:10.1029/2011GL050015.

Salzer, M. W., and K. F. Kipfmueller (2005), Reconstructed temperature and precipitation on a millennial timescale from tree- rings in the southern Colorado Plateau, Clim. Change, 70, 465–487, doi:10.1007/s10584-005-5922-3.

Salzer, M. W., Bunn, A. G., Graham, N. E., & Hughes, M. K. (2013). Five millennia of paleotemperature from tree-rings in the Great Basin, USA. *Climate Dynamics*, 1-10.

Schelske, C. L., Peplow, A., Brenner, M., & Spencer, C. N. Low-background gamma counting: applications for 210Pb dating of sediments. *Journal of Paleolimnology*, *10*(2), 115-128 (1994).

Schouten, S., et al. 2009. An interlaboratory study of TEX_{86} and BIT analysis using high-performance liquid chromatography-mass spectrometry. Geochemistry, Geophysics, Geosystems 10, Q03012.

Schouten, S., Huguet, C., Hopmans, E.C., Kienhuis, M.V.M., Sinninghe Damsté, J.S., 2007. Analytical methodology for TEX_{86} paleothermometry by high-performance liquid chromatography/atmospheric pressure chemical ionization-mass spectrometry. Analytical Chemistry 79, 2940-2944.

Tierney, J. E., Russell, J. M., Eggermont, H., Hopmans, E. C., Verschuren, D., & Sinninghe Damsté, J. S. (2010). Environmental controls on branched tetraether lipid distributions in tropical East African lake sediments.

Geochimica et Cosmochimica Acta, *74*(17), 4902-4918.

Van Mantgem, P. J., Stephenson, N. L., Byrne, J. C., Daniels, L. D., Franklin, J. F., Fulé, P. Z., ... & Veblen, T. T. (2009). Widespread increase of tree mortality rates in the western United States. *Science*, *323*(5913), 521-524.

Weiss, J. L., C. L. Castro, and J. T. Overpeck, 2009: Distinguishing pronounced droughts in the southwestern United States: Seasonality and effects of warmer temperatures, Journal of Climate, 22, 5918–5932, doi:10.1175/ 2009JCLI2905.1.

Westerling, A. L., Hidalgo, H. G., Cayan, D. R., & Swetnam, T. W. (2006). Warming and earlier spring increase western US forest wildfire activity. *Science*, *313*(5789), 940-943.

Williams, A. P., Allen, C. D., Macalady, A. K., Griffin, D., Woodhouse, C. A., Meko, D. M., ... & McDowell, N. G. Temperature as a potent driver of regional forest drought stress and tree mortality. *Nature Climate Change* (2012).

Woodhouse, C. A. and J. T. Overpeck, 1998: 2000 Years of Drought Variability in the Central United States. Bulletin of the American Meteorological Society, 79 (12), 2693– 2714, doi:http://dx.doi.org/10.1175/1520-0477(1998)079〈2693:YODVIT〉2.0.CO;2.

WRCC 2013: Western Regional Climate Center, Cooperative Climatological Data Summaries. Available Online: http://www.wrcc.dri.edu/climatedata/climsum/

D.5 Figures

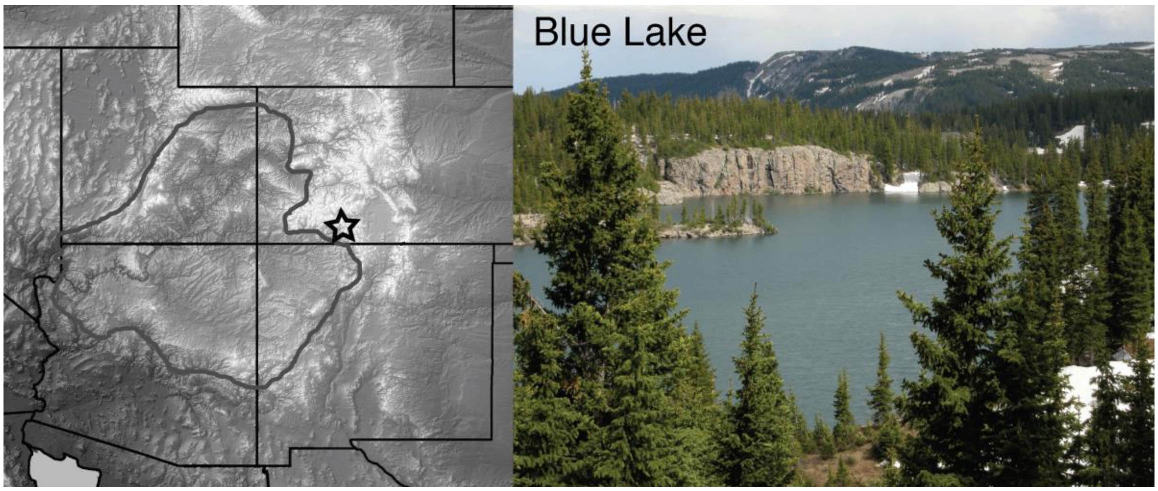

Figure D.1: Blue Lake, located under the star in the south San Juan Mountains in southern Colorado. The heavy grey line delineates the Colorado Plateau.

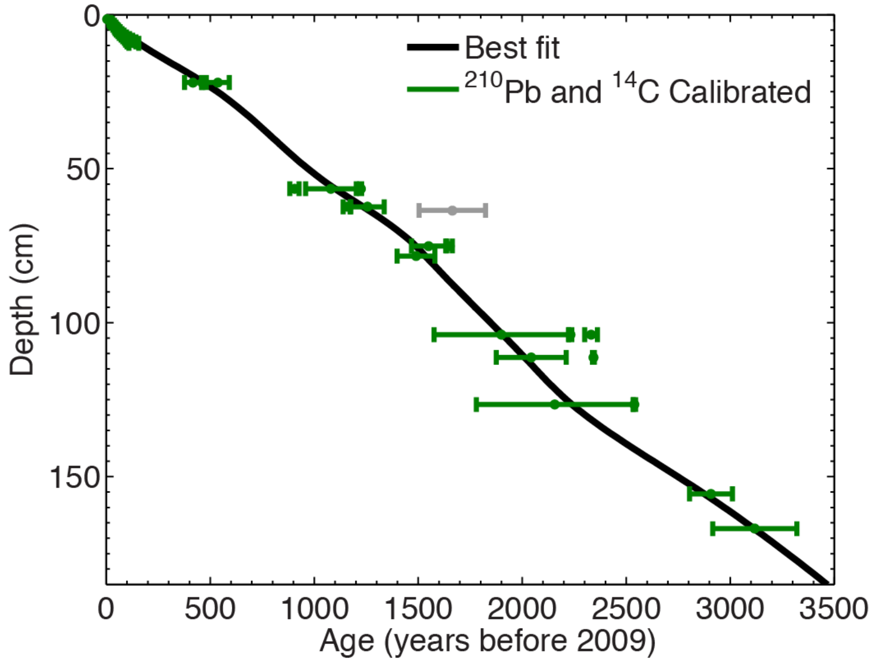

Figure D.2: Blue lake age model showing ^{210}Pb, ^{14}C dates in green and the best-fit age model curve in black. The grey date is an excluded radiocarbon date with an age reversal. The date was on a piece of wood, that likely grew well before being washed into the lake and thus is not accurate date of sediment deposition.

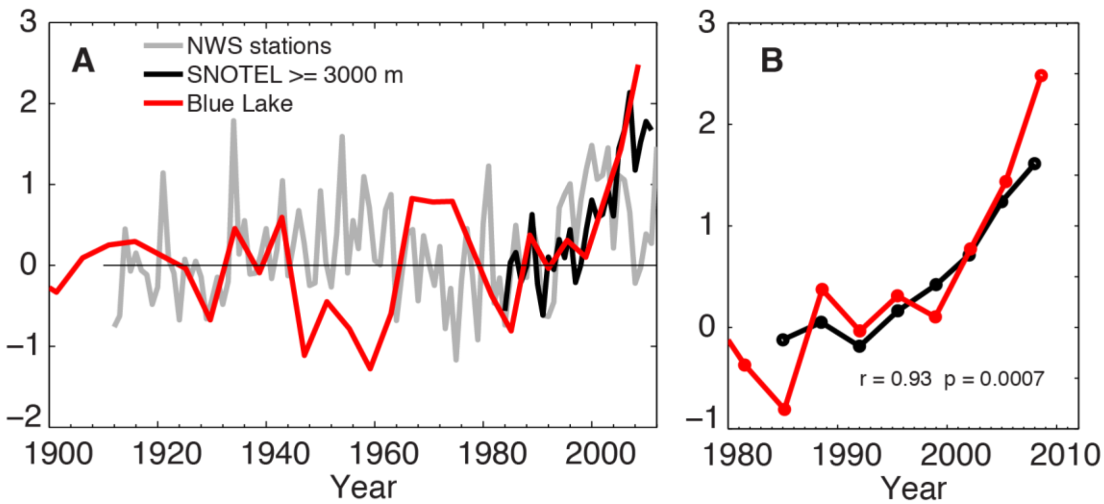

Figure D.3: **A)** Blue Lake (red) versus 21 National Weather Service stations (grey) and 9 SNOTEL stations located above 3000 meters elevation (black). All SNOTEL stations are within the San Juan Mountains, and NWS stations in the San Juan Mountain region. Anomalies are computed on the individual stations to avoid elevation bias with changes in sample depth. Anomalies are with respect to the 1960-1995 mean for the NWS stations and for the series length mean before 1995 for the SNOTEL stations. **B)** SNOTEL stations versus Blue Lake. SNOTEL data are binned to the same resolution as Blue Lake for computing correlations.

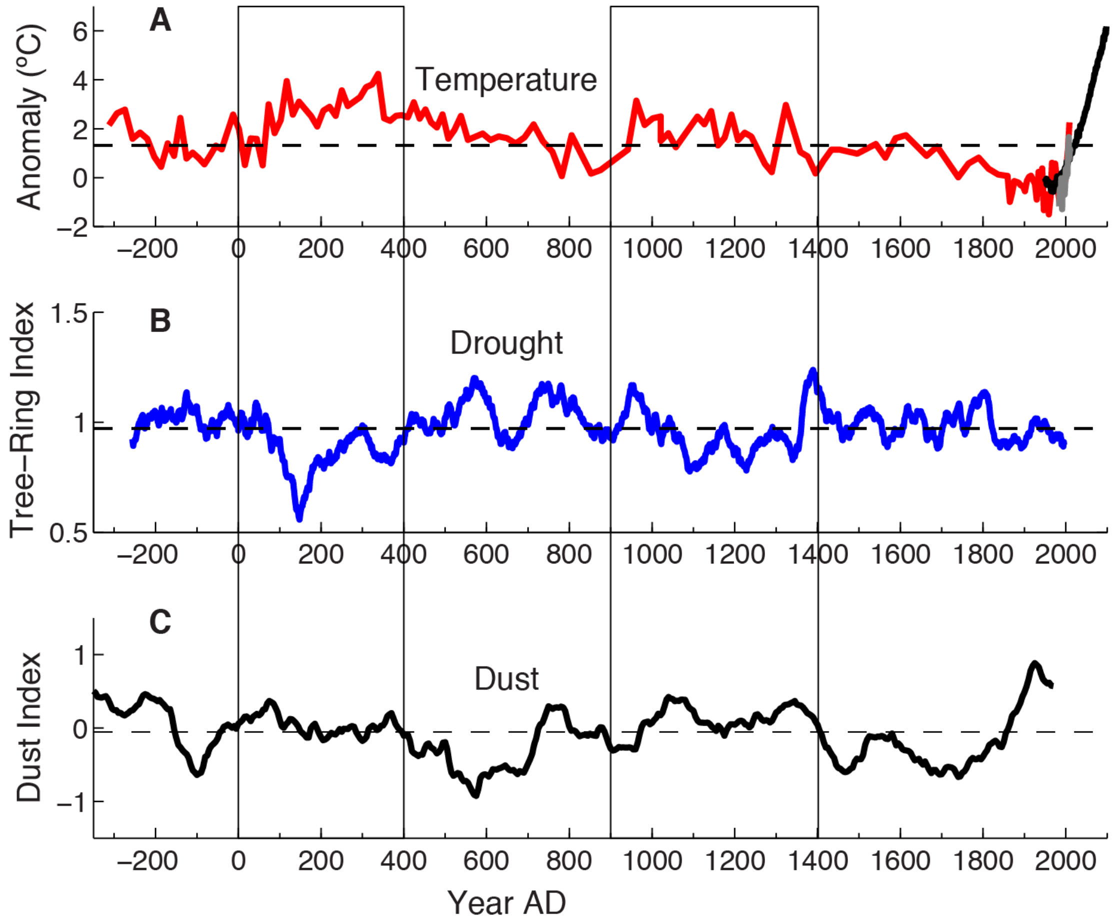

Figure D.4: **A)** Blue Lake temperature (this study). The mean of 10 SNOTEL stations is plotted in grey, and the average of the CMIP5 RCP8.5 temperature projections is plotted in black. Anomalies are computed with respect to the 1960-2000 mean for the reconstruction and projections, and with respect to the series length mean for the SNOTEL record. **B)** Summitville Bristlecone Pine moisture (Routson et al., 2011), smoothed with a 50-year moving average. **C)** San Juan Mountain dust deposition (Routson et al., in prep) smoothed with a 15 year moving average. Vertical boxes show the Roman (0-400 AD) and Medieval (900-1400 AD) warm periods in the Blue Lake record. Warm temperatures during the Medieval and Roman periods are coincident with severe droughts, and elevated dustiness. The warmest period in the last 2000 years occurs associated with the 2nd century megadrought.

D.6 Supplemental Text

Instrumental Record Comparisons

To test the fidelity of the calibration, the upper 9 cm of sediment core was sampled at 0.25 cm (~4.5yr) resolution to compare with instrumental temperature records. The reconstruction matches poorly with the average of four local gridded PRISM temperature data points (Daly et al., 2002). To further explore instrumental record relationships we compared our record with a subset of 10 high elevation (>3000 m) snow telemetry (SNOTEL) station data from the San Juan Mountains (Figure D.3a). Binned to the same resolution as the biomarker record, the SNOTEL station temperatures are highly and significantly correlated with our record despite the limited degrees of freedom (Figure D.3b, $r = 0.93$, $p = 0.001$). There is no significant relationship between our record and average temperature anomalies of 20 regional National Weather Service (NWS) stations (Figure D.3a). The NWS, however, do not all agree with one another. Correlations between NWS stations range between $r = –0.44$ and $r = 0.90$, with a mean station correlation of $r = 0.51$. Only four national NWS stations are located above 2700 m elevation, and they are not strongly correlated with each other either (Figure D.S1). Correlations between the four high elevation NWS stations range between $r = 0.16$ and $r = 0.53$ with a mean correlation of $r = 0.34$. To test if high elevation temperatures in the San Juan Mountains respond differently than temperature at lower elevations, we compared the 10 (>3000m) SNOTEL stations with a subset of 15 regional lower elevation (< 2400m) NWS stations (Figure D.S3). The comparison shows the high elevation SNOTEL stations diverge somewhat from the NWS stations, especially since 2005. We also correlated each SNOTEL station with each NWS station (Table D.S3). The table is ordered by elevation, but does not show clear elevation related patterns. Rather individual stations (e.g., Del Norte and Montevista) have poor and or negative relationships to the SNOTEL stations. The discrepancies between the SNOTEL stations and the low elevation NWS stations and between individual stations might result in part from regional variability in temperature patterns across a range of elevations and terrain.

Analysis of Abrupt Change

The Blue Lake record shows periods of abrupt temperature change in the San Juan Mountains, especially transitioning into the Roman and Medieval Periods. We employed a simple assessment of rates of change using 100-year moving window linear-regressions (Figure D.S4). Low sample resolution resulted in some windows having limited numbers of sample points to constrain the regressions. The transition into the Roman Period between 30-130 AD warmed at a rate of 2.4 ºC per century. Similarly, the transition into the medieval period from 876-976 AD also occurred rapidly, warming at a rate of 2.8 ºC per century. Cooling at the end of the medieval period occurred at a rate of 2.8 ºC per century. Over the last 100 years the average rate of warming has been 0.6ºC per century based the 100-year window regression or our record. Within the last 20 years alone however, the San Juan Mountains have warmed by almost 1ºC (Rangwala and Miller 2010). The relatively short duration of recent warming and low-resolution sampling prior to instrumental records prohibits us from assessing recent change in the context of the last two millennia.

D.7 Supplemental Figures

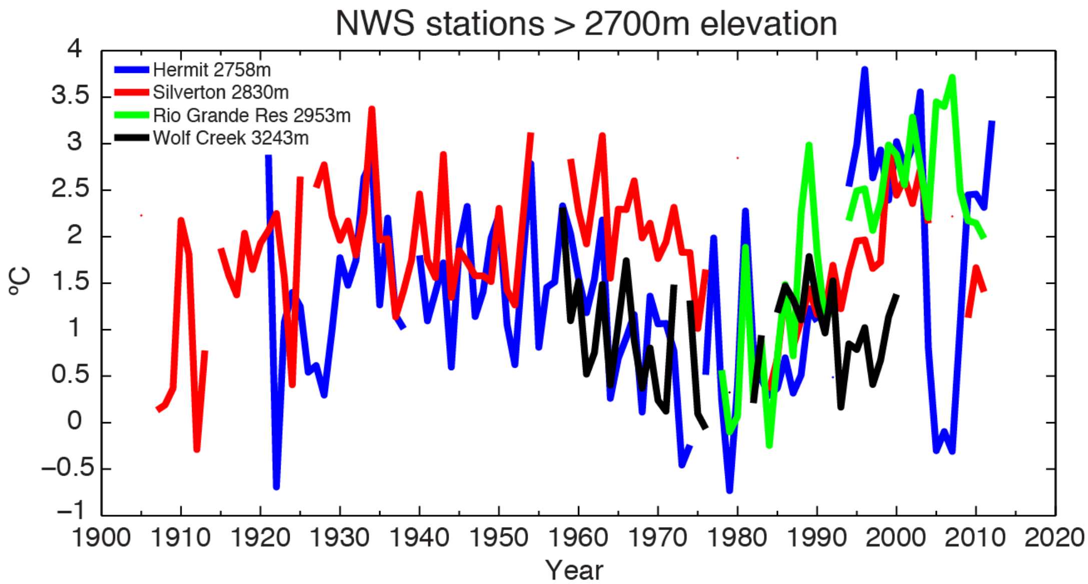

Figure D.S1: San Juan Mountain National Weather Service stations above 2700 meters elevation.

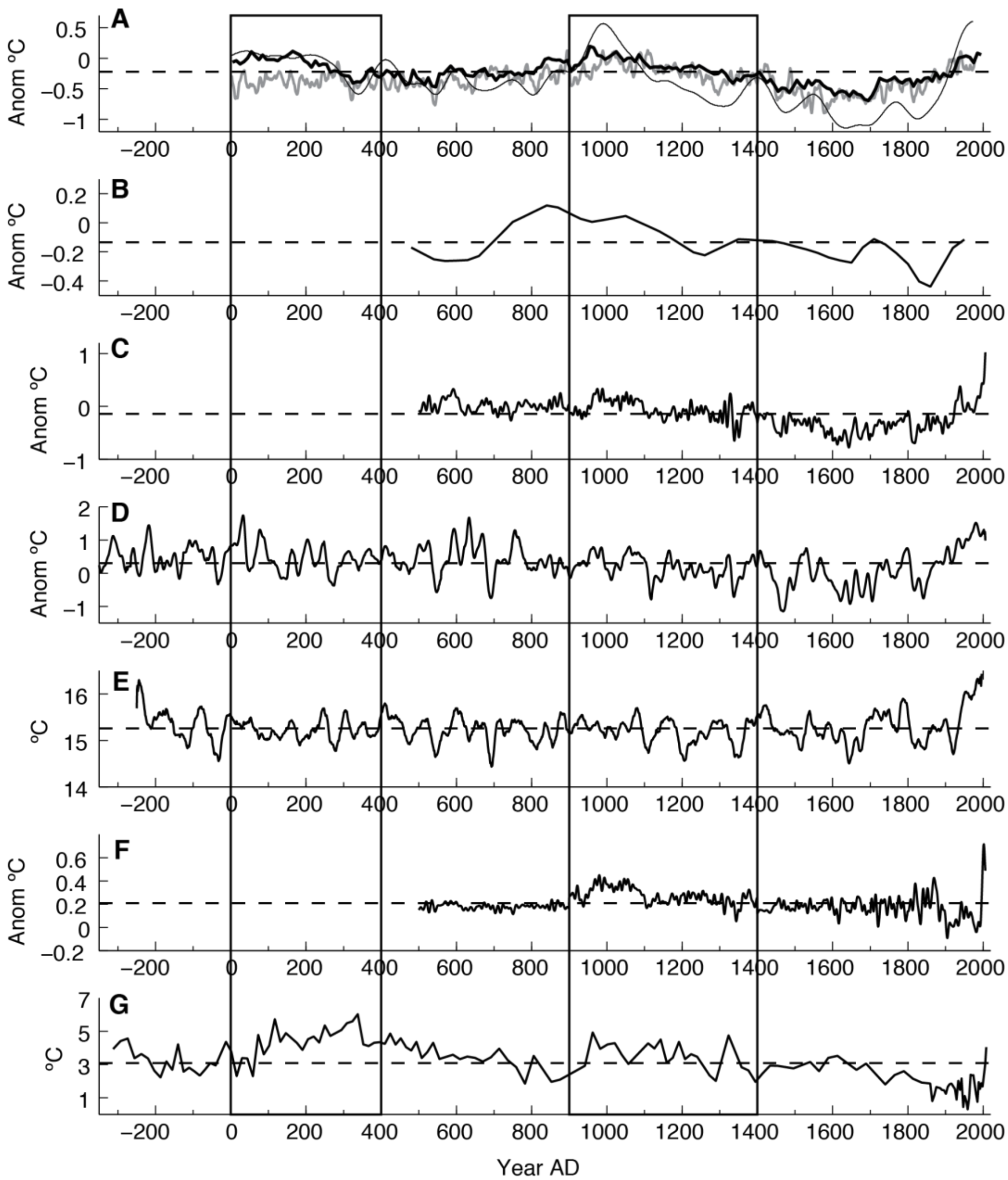

Figure D.S2: Temperature reconstruction comparisons. **A**) Three Northern Hemisphere 2000-year temperature reconstructions. Moberg et al., 2005 is shown in the grey line, Ljungvist 2010 in the heavy weight black line, and the smoothed version of Christiansen and Ljungvist (2012) is shown in the lightweight black line. **B**) North American pollen based temperature reconstruction (Trouet et al 2013). **C**) Average of Western temperature grid points from Mann et al. (2009) (27.5 to 47.5, and –97.5 to –122.5). **D**) Great Basin bristlecone pine ring width and treeline based temperature reconstruction (Salzer et al., 2013). **E)** San Francisco Peaks bristlecone pine mean summer maximum temperature reconstruction smoothed with a 21 year moving average (Salzer and Kipfmueller 2005). **F**) The closest pixel to Blue Lake (37.5, –107.5) from Mann et al. (2009). **G**) Blue Lake GDGT temperature. Boxes show the Roman (0-400 AD) and Medieval (900-1400 AD) period intervals.

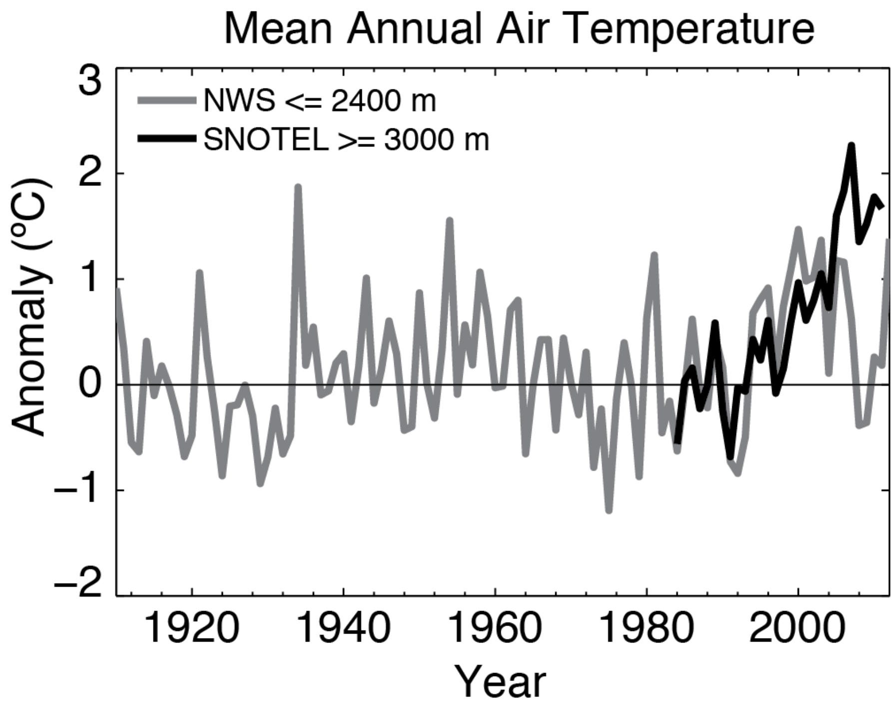

Figure D.S3: Comparison of 15 National Weather Service stations below 2400 meters in the San Juan Mountain region with 9 San Juan Mountain SNOTEL stations above 3000 meters elevation. Anomalies are computed on the individual stations to avoid elevation bias with changes in sample depth. Anomalies are with respect to the 1960-1995 mean for the NWS stations and for the series length mean before 1995 for the SNOTEL stations.

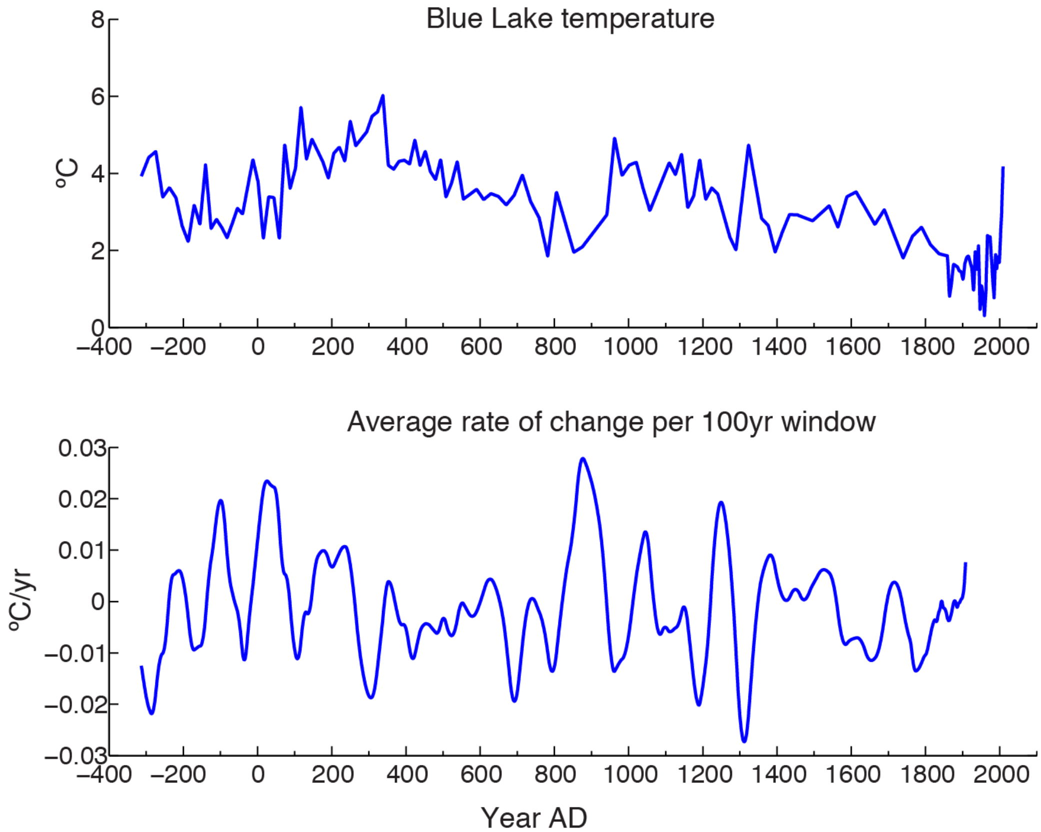

Figure D.S4: Assessing average rates of temperature change in the Blue Lake record (top) using linear regressions on 100-year moving windows. The window was advanced by one year for each regression. The slope of each regression line is plotted in the second panel at the first year of the 100-year window. The highest rates of change are between 2 and 3 degrees per century transitioning into the Roman and medieval periods. Sample resolution is around 20-years for most of the record, so an average of 5 points controlling the slope of each regression.

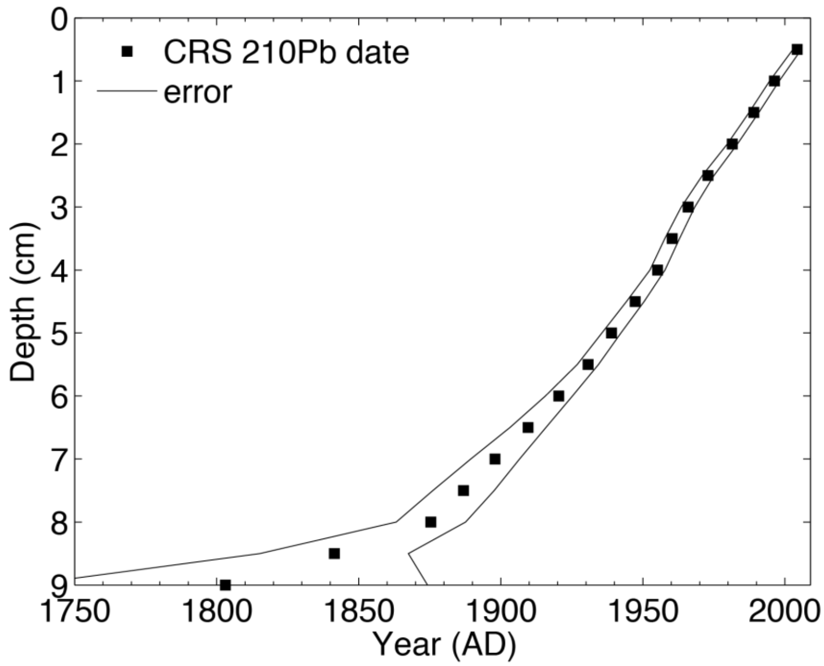

Figure D.S5: Blue Lake ^{210}Pb age model (filled squares) with error plotted in black lines. Ages based on a constant rate of supply model (Appleby and Oldfield 1983).

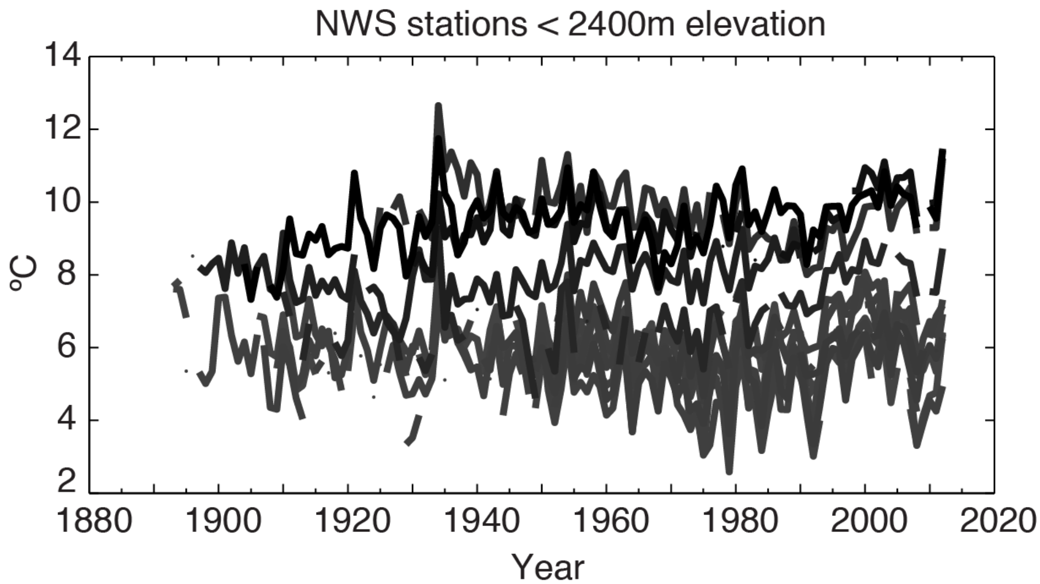

Figure D.S6: Fifteen NWS stations below 2400 meters elevation in the San Juan Mountain Region.

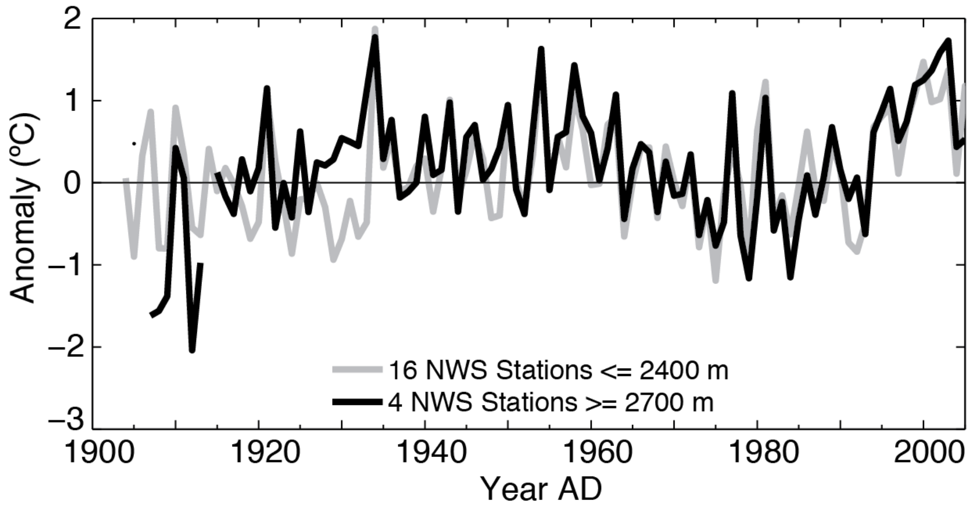

Figure D.S7: High elevation versus low elevation NWS stations. Only four NWS stations exist above 2700 m elevation.

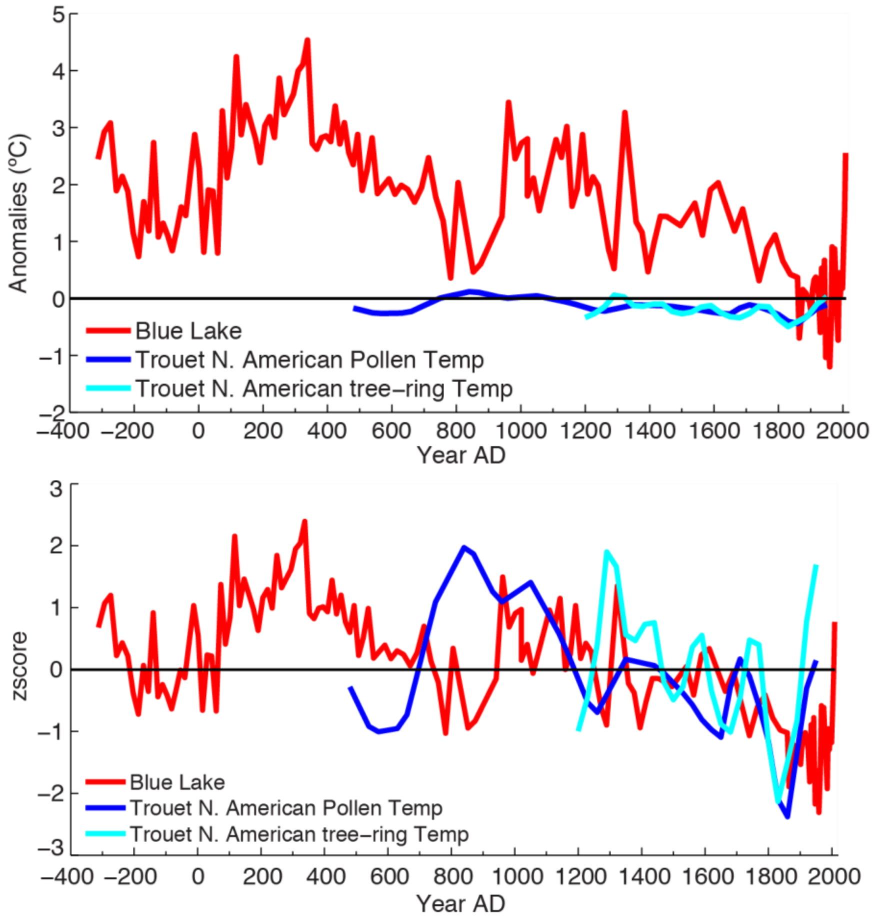

Figure D.S8: Blue Lake versus tree-ring and pollen based North American temperature reconstructions (Trouet et al., 2013).

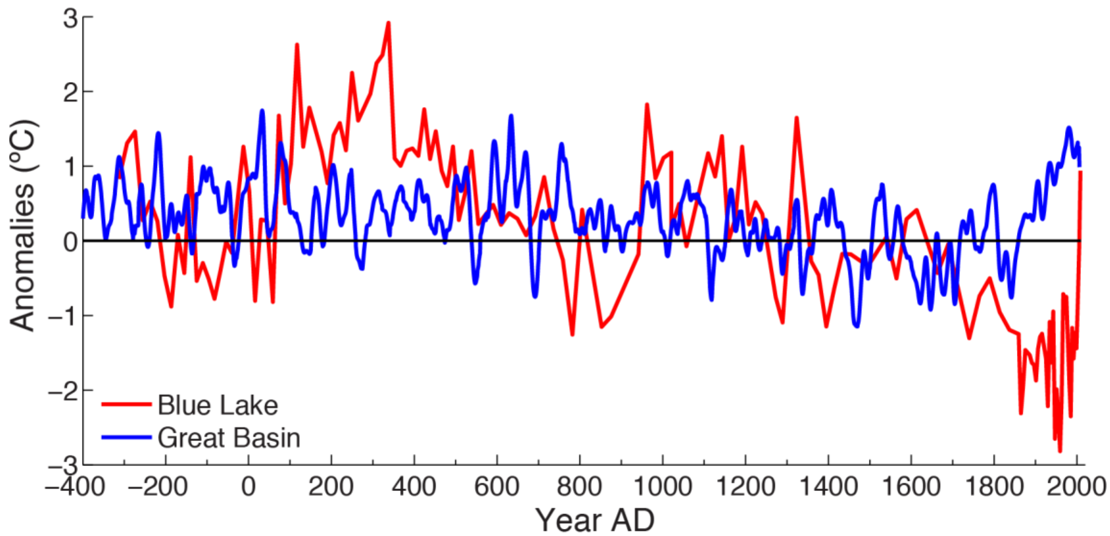

Figure D.S9: Great basin temperature in blue (Salzer et al. 2013) compared with Blue Lake in red. Anomalies are computed with respect to the series length mean.

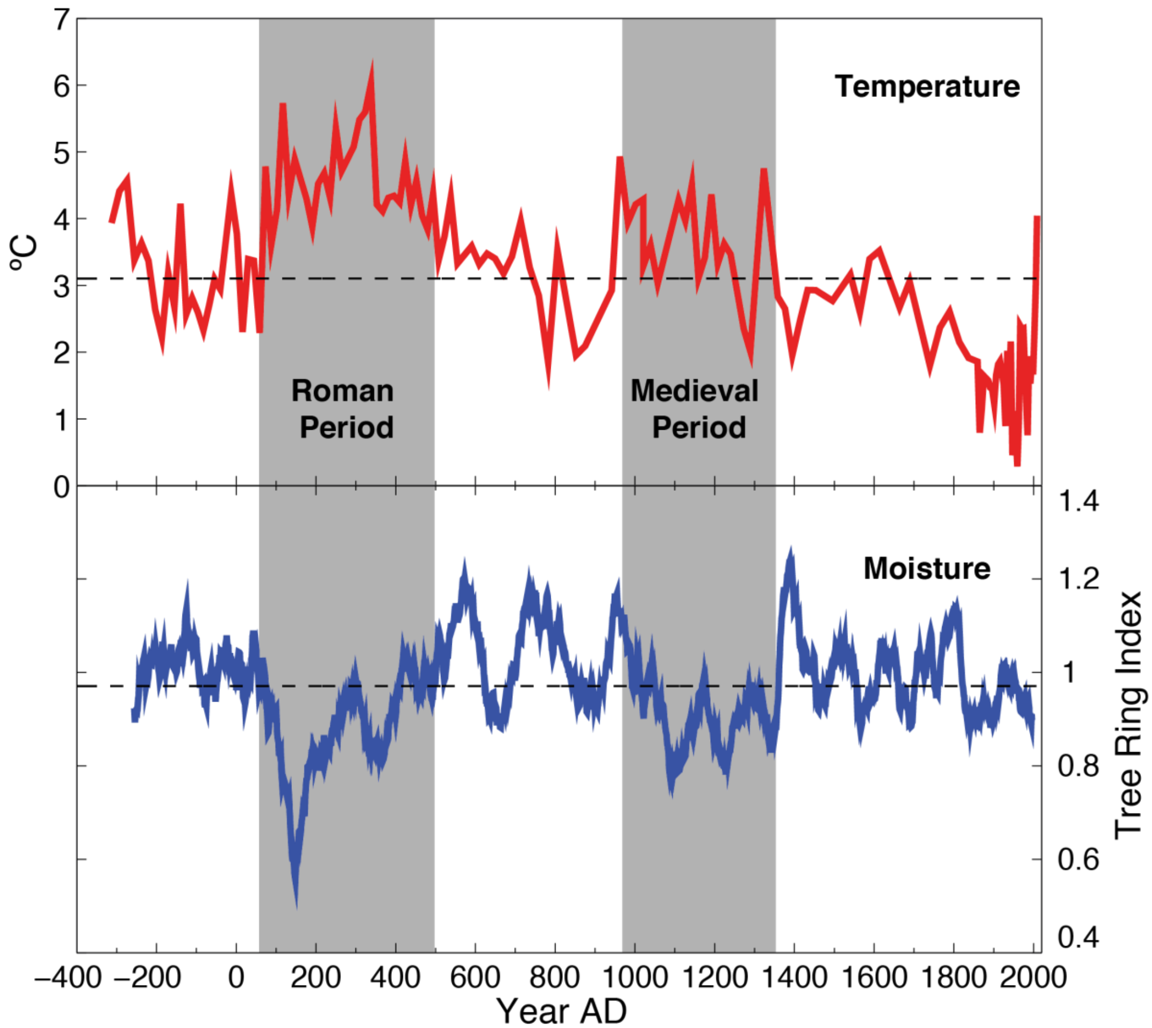

Figure D.S10: Another perspective on the relationship between south San Juan Mountain temperature (top) and droughts (bottom). The temperature record is the Blue Lake biomarker reconstruction (this study) and the drought record is from Summitville bristlecone pine (Routson et al., 2011).

D.8 Supplemental Tables

Table D.S1: SNOTEL stations

Station	Number	Lat	Lon	Elevation
Cumbres Trestle	431	37.02	-106.45	3060
El Diente Peak	465	37.78	-108.02	3048
Lily Pond	580	37.38	-106.55	3353
Lizard Head Pass	586	37.8	-107.92	3109
Mineral Creek	629	37.85	-107.73	3060
Slumgullion	762	37.98	-107.2	3487
Upper San Juan	840	37.48	-106.83	3109
Vallecito	843	37.48	-107.5	3316
Wolf Creek Summit	874	37.48	-106.8	3353
Stump Lakes	797	37.48	-107.63	3414

Table D.S2: National Weather Service Stations

Station	ID	Lat	Lon	Elevation (m)
MONTROSE #2	55722	38.49	-107.88	1764
CORTEZ	51886	37.34	-108.59	1880
DURANGO	52432	37.28	-107.88	2012
DULCE	292608	36.94	-107.00	2071
MESA VERDE NP	55531	37.20	-108.49	2160
TIERRA AMARILLA 4 N	298845	36.77	-106.55	2275
ALAMOSA	50125	37.47	-105.88	2297
FT LEWIS	53016	37.23	-108.05	2329
CENTER 4 SSW	51458	37.71	-106.14	2339
MANASSA	55322	37.17	-105.94	2344
MONTE VISTA 2W	55706	37.58	-106.19	2345
SAGUACHE	57337	38.09	-106.14	2347
CHAMA	291664	36.92	-106.58	2393
DEL NORTE 2E	52184	37.67	-106.32	2397
TELLURIDE 4 WNW	58204	37.95	-107.87	2636
LAKE CITY	54734	38.02	-107.31	2642
HERMIT 7 ESE	53951	37.77	-107.11	2758
SILVERTON	57656	37.81	-107.66	2830
RIO GRANDE RSVR	57050	37.73	-107.27	2953
WOLF CREEK PASS 1 E	59181	37.47	-106.79	3243

Table D.S3: A correlation matrix between the NWS and SNOTEL stations. The stations are ordered by low to high elevations from left to right for the SNOTEL and from top to bottom for the NWS stations. See tables D.S1 and D.S2 for elevations. All the SNOTEL stations used are located above 3000 m, but the NWS stations don not show an elevation trend toward stronger relationships with the high elevation SNOTEL stations. Rather, individual stations such as Del Norte (NWS), or Stump Lakes (SNOTEL) have poor and or negative relationships with the other stations.

	Diente Peak	Cumbres Trestle	Mineral Creek	Lizard Head	Upper San Juan	Vallecito	Lily Pond	Wolf Creek Summit	Slumgullion	Stump Lakes
Montrose	0.38	0.71	0.58	0.61	0.38	0.46	0.37	0.73	0.21	-0.02
Cortez	0.4	0.68	0.66	0.72	0.5	0.63	0.27	0.77	0.31	0.28
Dulce	0.51	0.61	0.47	0.54	0.27	0.45	0.2	0.68	0.23	-0.07
Mesa Verde	0.56	0.88	0.79	0.72	0.66	0.74	0.52	0.89	0.44	0.21
T. Amarilla	0.29	0.57	0.37	0.4	0.19	0.26	0.19	0.6	-0.04	-0.11
Alamosa	0.43	0.55	0.58	0.5	0.4	0.43	0.32	0.68	0.27	-0.05
Fort Lewis	0.56	0.42	0.24	0.32	0.08	-0.02	0.1	0.36	0.15	-0.48
Center 4	0.25	0.45	0.49	0.45	0.31	0.39	0.15	0.66	0.12	-0.16
Manassa	0.36	0.54	0.45	0.48	0.25	0.29	0.18	0.6	0.23	-0.19
Monte Vista	-0.06	0.2	-0.12	0.02	-0.37	-0.23	-0.2	0.32	-0.11	-0.3
Saguache	0.39	0.48	0.46	0.52	0.34	0.35	0.21	0.57	0.23	-0.28
Chama	0.59	0.67	0.55	0.57	0.35	0.48	0.27	0.81	0.24	0.08
Del Norte	-0.11	-0.23	-0.42	-0.34	-0.55	-0.54	-0.54	-0.16	-0.48	-0.61
Telluride	0	-0.21	-0.25	-0.55	-0.23	-0.38	-0.17	-0.25	-0.34	0.06
Lake City	0.48	0.56	0.59	0.45	0.39	0.42	0.31	0.74	0.33	0.08
Hermit	0.06	-0.47	-0.23	-0.01	-0.21	-0.22	-0.22	-0.36	0.07	-0.46
Silverton	0.18	0.69	0.37	0.44	0.21	0.37	0.09	0.73	0.19	0.06
Rio Grande	0.5	0.92	0.7	0.64	0.53	0.5	0.51	0.83	0.48	0.04
Wolf Creek	0.42	0.52	0.43	-0.04	0.58	0.49	0.34	0.54	-0.29	0.55

Table D.S4: Radiocarbon measurements and ages from Blue Lake

Core	Sample Name	Depth (cm)	Lab Number	13C	FMC	14C (yr bp)	Error (yr)
NA	Bulk Sed	0	AA89049	-29.9	1.1157 ± 0.0052	pst bomb	NA
2	Pine Needle	22	AA99391	-27.3	0.9496 ± 0.0063	415	53
1	Pine Needle	56.5	AA99388	-25.8	0.8761 ± 0.007	1063	64
2	Bark	62.4	AA99392	-22.9	0.8555 ± 0.0041	1254	38
1	Wood,(excld)	63.5	AA89050	-25.6	0.816 ± 0.015	1640	150
2	Pine Cone	75.1	AA99393	-23.8	0.8174 ± 0.004	1619	39
1	Pine Needle	78.4	AA99389	-22.7	0.8174 ± 0.004	1525	39
1	Conifer Bract	103.9	AA89052	-22.1	0.79 ± 0.015	1900	150
1	Grass	111.3	AA99390	-24.8	0.7786 ± 0.007	2010	72
1	Pine Needle	126.6	AA89054	-23.8	0.767 ± 0.014	2130	150
2	Pine needle	155.6	AA99394	-24.5	0.7132 ± 0.0055	2715	62
2	Pine Needle	166.9	AA99395	-25.4	0.6967 ± 0.0061	2903	71
2	Pine Needle	240.2	AA99396	-25.2	0.614 ± 0.0035	3918	46

Table D.S5: Blue Lake ^{210}Pb dates, depth, and upper and lower boundaries. Dates are based on the constant rate of supply model.

	Constant Rate of Supply (year AD)		
Depth (cm)	Lower	Mean	Upper
0.5	2002.8	2004.3	2005.8
1	1994.6	1996.3	1998
1.5	1987.4	1989.1	1990.8
2	1979.7	1981.5	1983.3
2.5	1970.9	1972.9	1975
3	1963.5	1965.9	1968.3
3.5	1957.7	1960.3	1962.9
4	1952.5	1955.2	1957.8
4.5	1944.2	1947.3	1950.4
5	1935.6	1939	1942.3
5.5	1926.9	1930.7	1934.4
6	1915.7	1920.4	1925.2
6.5	1903.2	1909.6	1915.9
7	1889.4	1898	1906.6
7.5	1876.1	1886.9	1897.7
8	1863.2	1875.4	1887.6
8.5	1815.2	1841.4	1867.5

Table D.S6
Fractional GDGT compound abundance

Depth cm	Year AD	GDGT III	GDGT III b	GDGT III c	GDGT II	GDGT II b	GDGT II c	GDGT I	GDGT I b	GDGT I c	Loomis ºC
0.25	2008.6	0.361	0.009	0.001	0.449	0.029	0.004	0.135	0.009	0.003	4.045
0.5	2005.4	0.407	0.010	0.001	0.418	0.030	0.003	0.114	0.008	0.008	3.001
0.75	2002.1	0.450	0.014	0.002	0.358	0.044	0.004	0.112	0.013	0.003	2.338
1	1998.9	0.487	0.014	0.002	0.310	0.056	0.005	0.105	0.017	0.003	1.667
1.25	1995.5	0.469	0.016	0.002	0.325	0.055	0.005	0.108	0.015	0.004	1.876
1.5	1992.0	0.488	0.016	0.003	0.279	0.065	0.007	0.121	0.019	0.004	1.529
1.75	1988.6	0.465	0.020	0.003	0.293	0.064	0.008	0.120	0.022	0.005	1.939
2	1985.1	0.514	0.016	0.003	0.284	0.046	0.006	0.111	0.016	0.002	0.757
2.25	1981.5	0.520	0.015	0.003	0.292	0.040	0.004	0.111	0.013	0.003	1.195
2.75	1974.3	0.461	0.015	0.003	0.319	0.045	0.005	0.136	0.015	0.002	2.357
3	1970.7	0.452	0.019	0.003	0.317	0.051	0.006	0.134	0.015	0.002	2.349
3.25	1966.8	0.457	0.022	0.004	0.310	0.054	0.006	0.128	0.016	0.004	2.393
3.5	1963.0	0.473	0.030	0.004	0.292	0.063	0.009	0.109	0.016	0.005	0.969
3.75	1959.2	0.502	0.033	0.004	0.274	0.064	0.008	0.095	0.016	0.003	0.289
4	1955.3	0.483	0.033	0.004	0.279	0.065	0.009	0.102	0.017	0.007	0.783
4.25	1951.2	0.476	0.033	0.004	0.286	0.069	0.008	0.102	0.016	0.007	1.117
4.5	1947.0	0.518	0.031	0.003	0.268	0.065	0.006	0.093	0.013	0.003	0.454
4.75	1942.9	0.483	0.024	0.003	0.288	0.070	0.005	0.112	0.014	0.002	2.159
5	1938.8	0.489	0.027	0.003	0.280	0.072	0.006	0.106	0.014	0.003	1.475
5.25	1934.2	0.485	0.022	0.003	0.285	0.066	0.005	0.115	0.015	0.004	2.020
5.5	1929.7	0.508	0.020	0.003	0.276	0.063	0.006	0.108	0.014	0.002	0.892
5.75	1925.2	0.491	0.021	0.003	0.285	0.063	0.006	0.113	0.016	0.003	1.528
6.25	1915.8	0.475	0.021	0.003	0.293	0.066	0.006	0.115	0.016	0.004	1.861
6.5	1911.0	0.486	0.021	0.003	0.290	0.063	0.006	0.112	0.016	0.004	1.817
6.75	1906.2	0.487	0.020	0.003	0.295	0.060	0.006	0.112	0.016	0.002	1.659
7	1901.3	0.504	0.021	0.003	0.285	0.059	0.005	0.109	0.013	0.002	1.234
7.25	1896.2	0.491	0.020	0.003	0.289	0.064	0.006	0.110	0.014	0.002	1.447
7.5	1891.1	0.493	0.021	0.003	0.290	0.062	0.005	0.109	0.014	0.002	1.470
7.75	1886.0	0.485	0.023	0.003	0.284	0.066	0.006	0.108	0.015	0.010	1.576
8.25	1875.5	0.484	0.024	0.003	0.295	0.069	0.005	0.106	0.013	0.001	1.643
8.5	1870.1	0.503	0.022	0.003	0.281	0.061	0.006	0.108	0.014	0.002	1.145
8.75	1864.7	0.512	0.021	0.003	0.273	0.064	0.006	0.105	0.014	0.002	0.795
9	1859.3	0.480	0.022	0.003	0.286	0.069	0.006	0.112	0.017	0.004	1.858
10	1836.8	0.482	0.022	0.003	0.291	0.068	0.005	0.112	0.016	0.002	1.913
11	1813.5	0.483	0.020	0.003	0.290	0.065	0.005	0.115	0.017	0.003	2.150
12	1789.5	0.473	0.019	0.002	0.290	0.063	0.005	0.123	0.020	0.004	2.605
13	1764.9	0.466	0.019	0.002	0.293	0.064	0.007	0.123	0.021	0.004	2.368

Cont'd. Depth cm	Year AD	GDGT III	GDGT III b	GDGT III c	GDGT II	GDGT II b	GDGT II c	GDGT I	GDGT I b	GDGT I c	Loomis ºC
14	1739.9	0.477	0.018	0.003	0.286	0.065	0.007	0.121	0.019	0.004	1.802
16	1689.1	0.436	0.020	0.003	0.296	0.073	0.008	0.130	0.026	0.006	3.058
17	1663.6	0.466	0.020	0.003	0.284	0.071	0.006	0.122	0.022	0.005	2.675
19	1613.2	0.445	0.020	0.003	0.295	0.073	0.006	0.130	0.023	0.004	3.520
20	1588.4	0.451	0.019	0.002	0.298	0.072	0.006	0.126	0.023	0.004	3.395
21	1564.2	0.465	0.019	0.003	0.293	0.065	0.006	0.123	0.021	0.005	2.602
22	1540.6	0.457	0.020	0.002	0.294	0.073	0.006	0.122	0.022	0.003	3.162
24	1495.7	0.458	0.017	0.002	0.298	0.067	0.006	0.125	0.021	0.004	2.769
26	1453.6	0.426	0.017	0.003	0.293	0.074	0.011	0.139	0.031	0.007	2.927
27	1433.5	0.433	0.017	0.003	0.292	0.077	0.010	0.132	0.029	0.007	2.931
28	1414.0	0.443	0.017	0.003	0.288	0.076	0.010	0.129	0.028	0.006	2.470
29	1395.0	0.449	0.016	0.003	0.286	0.070	0.011	0.131	0.028	0.006	1.959
30	1376.4	0.442	0.017	0.003	0.291	0.072	0.010	0.130	0.029	0.007	2.648
31	1358.3	0.439	0.017	0.003	0.296	0.073	0.010	0.128	0.030	0.005	2.832
33	1323.2	0.395	0.017	0.003	0.291	0.083	0.011	0.150	0.040	0.011	4.754
35	1289.4	0.444	0.015	0.003	0.290	0.070	0.011	0.129	0.030	0.008	2.012
36	1272.8	0.437	0.015	0.003	0.279	0.073	0.012	0.137	0.034	0.010	2.347
38	1240.1	0.441	0.016	0.003	0.280	0.071	0.009	0.138	0.033	0.009	3.467
39	1223.9	0.425	0.017	0.003	0.287	0.085	0.010	0.140	0.034	0.000	3.622
40	1207.8	0.449	0.017	0.003	0.283	0.075	0.008	0.132	0.030	0.004	3.325
41	1191.7	0.423	0.017	0.003	0.288	0.080	0.009	0.137	0.036	0.008	4.366
42	1175.5	0.443	0.016	0.003	0.279	0.077	0.009	0.136	0.032	0.006	3.415
43	1159.2	0.435	0.018	0.003	0.284	0.081	0.010	0.131	0.032	0.006	3.108
44	1142.8	0.418	0.019	0.003	0.280	0.091	0.009	0.132	0.039	0.008	4.507
45	1126.3	0.444	0.021	0.003	0.265	0.090	0.009	0.124	0.038	0.006	3.967
46	1109.5	0.441	0.022	0.003	0.269	0.088	0.008	0.127	0.037	0.005	4.278
49	1057.4	0.423	0.020	0.003	0.267	0.093	0.013	0.132	0.038	0.010	3.033
50	1039.3	0.443	0.020	0.003	0.269	0.088	0.010	0.123	0.038	0.006	3.601
51	1020.8	0.416	0.019	0.003	0.290	0.079	0.009	0.144	0.034	0.006	4.290
52	1001.8	0.413	0.019	0.003	0.289	0.082	0.010	0.142	0.036	0.006	4.214
53	982.3	0.426	0.021	0.003	0.273	0.088	0.010	0.134	0.037	0.007	3.944
54	962.2	0.409	0.020	0.003	0.291	0.084	0.009	0.140	0.038	0.007	4.931
55	941.5	0.435	0.021	0.003	0.283	0.078	0.010	0.135	0.030	0.005	2.927
58	875.5	0.413	0.020	0.003	0.294	0.085	0.013	0.136	0.029	0.007	2.093
59	852.4	0.429	0.020	0.003	0.288	0.082	0.012	0.132	0.028	0.006	1.953
61	805.5	0.395	0.021	0.004	0.293	0.092	0.012	0.145	0.033	0.006	3.523
62	782.1	0.427	0.020	0.003	0.285	0.085	0.013	0.131	0.029	0.007	1.850
63	758.9	0.409	0.020	0.003	0.297	0.083	0.012	0.139	0.031	0.007	2.847
64	736.1	0.417	0.019	0.003	0.284	0.085	0.012	0.136	0.036	0.008	3.267
65	713.7	0.406	0.019	0.003	0.306	0.081	0.009	0.138	0.031	0.006	3.959
66	691.8	0.407	0.019	0.003	0.297	0.080	0.011	0.141	0.033	0.008	3.434

Cont'd. Depth cm	Year AD	GDGT III	GDGT III b	GDGT III c	GDGT II	GDGT II b	GDGT II c	GDGT I	GDGT I b	GDGT I c	Loomis ºC
67	670.3	0.421	0.020	0.003	0.287	0.079	0.011	0.140	0.033	0.006	3.181
68	649.4	0.423	0.018	0.003	0.278	0.079	0.012	0.140	0.038	0.008	3.401
69	629.1	0.412	0.018	0.003	0.299	0.072	0.011	0.146	0.033	0.006	3.475
70	609.5	0.418	0.017	0.003	0.297	0.069	0.011	0.146	0.033	0.007	3.320
71	590.5	0.411	0.018	0.003	0.295	0.074	0.011	0.143	0.036	0.008	3.587
73	554.8	0.414	0.018	0.003	0.304	0.067	0.010	0.149	0.029	0.006	3.331
74	538.3	0.415	0.017	0.003	0.305	0.067	0.008	0.147	0.032	0.005	4.308
75	522.6	0.413	0.016	0.003	0.311	0.065	0.009	0.147	0.030	0.006	3.739
76	507.8	0.409	0.018	0.003	0.312	0.067	0.010	0.144	0.030	0.007	3.385
77	493.6	0.406	0.017	0.003	0.304	0.070	0.009	0.149	0.034	0.008	4.367
78	479.8	0.411	0.017	0.003	0.314	0.070	0.009	0.141	0.031	0.005	3.840
79	466.0	0.413	0.016	0.003	0.304	0.070	0.009	0.145	0.032	0.007	4.046
80	452.1	0.415	0.019	0.003	0.296	0.074	0.008	0.147	0.034	0.005	4.573
81	438.2	0.417	0.021	0.003	0.293	0.078	0.008	0.144	0.030	0.005	4.202
82	424.1	0.394	0.019	0.003	0.295	0.079	0.010	0.154	0.037	0.008	4.865
83	409.9	0.406	0.019	0.003	0.303	0.074	0.009	0.145	0.034	0.007	4.244
84	395.7	0.398	0.018	0.003	0.305	0.076	0.010	0.148	0.035	0.009	4.342
85	381.4	0.414	0.017	0.004	0.296	0.072	0.009	0.143	0.037	0.008	4.313
86	367.0	0.408	0.017	0.003	0.304	0.069	0.010	0.147	0.035	0.007	4.109
87	352.5	0.402	0.018	0.003	0.291	0.077	0.011	0.148	0.039	0.010	4.210
88	338.0	0.375	0.016	0.003	0.301	0.077	0.010	0.160	0.048	0.010	6.025
89	323.4	0.380	0.017	0.004	0.302	0.078	0.011	0.154	0.045	0.010	5.596
90	308.8	0.380	0.017	0.003	0.320	0.071	0.009	0.153	0.040	0.006	5.484
91	294.2	0.389	0.018	0.004	0.303	0.075	0.010	0.155	0.039	0.007	5.076
93	264.7	0.395	0.018	0.003	0.304	0.075	0.010	0.150	0.037	0.007	4.718
94	250.0	0.389	0.021	0.004	0.301	0.078	0.009	0.151	0.040	0.007	5.354
95	235.2	0.402	0.018	0.003	0.309	0.072	0.009	0.150	0.031	0.008	4.317
96	220.5	0.398	0.018	0.003	0.311	0.070	0.008	0.153	0.032	0.006	4.682
97	205.7	0.416	0.021	0.003	0.296	0.074	0.008	0.143	0.033	0.006	4.523
98	190.9	0.418	0.019	0.003	0.305	0.072	0.008	0.142	0.029	0.005	3.877
99	176.1	0.394	0.017	0.003	0.310	0.076	0.010	0.147	0.033	0.009	4.299
101	146.6	0.390	0.016	0.003	0.304	0.073	0.010	0.155	0.040	0.009	4.889
102	131.9	0.403	0.016	0.003	0.303	0.071	0.010	0.152	0.036	0.007	4.365
103	117.2	0.393	0.015	0.003	0.293	0.077	0.009	0.155	0.044	0.010	5.733
104	102.5	0.398	0.015	0.003	0.299	0.072	0.011	0.155	0.038	0.009	4.140
105	87.9	0.400	0.015	0.003	0.313	0.068	0.011	0.149	0.033	0.009	3.607
106	73.3	0.388	0.017	0.003	0.308	0.078	0.010	0.152	0.036	0.009	4.783
107	58.8	0.445	0.017	0.004	0.287	0.064	0.010	0.145	0.026	0.002	2.287
108	44.4	0.413	0.018	0.003	0.296	0.073	0.011	0.144	0.033	0.009	3.372
109	30.0	0.426	0.020	0.003	0.288	0.074	0.009	0.142	0.030	0.007	3.393
110	15.8	0.463	0.018	0.005	0.280	0.068	0.009	0.121	0.029	0.007	2.303

Cont'd. Depth cm	Year AD	GDGT III	GDGT III b	GDGT III c	GDGT II	GDGT II b	GDGT II c	GDGT I	GDGT I b	GDGT I c	Loomis ºC
111	1.6	0.419	0.017	0.003	0.292	0.070	0.010	0.147	0.036	0.007	3.774
112	-12.4	0.405	0.017	0.003	0.294	0.079	0.010	0.152	0.034	0.006	4.366
114	-40.2	0.438	0.023	0.003	0.305	0.011	0.011	0.157	0.041	0.010	2.946
115	-54.1	0.430	0.020	0.003	0.293	0.072	0.009	0.139	0.028	0.006	3.094
116	-68.0	0.422	0.020	0.004	0.299	0.067	0.010	0.144	0.026	0.008	2.700
117	-82.0	0.434	0.020	0.003	0.295	0.065	0.010	0.144	0.024	0.005	2.330
118	-96.2	0.422	0.014	0.003	0.306	0.060	0.010	0.151	0.027	0.007	2.596
119	-110.5	0.429	0.015	0.003	0.310	0.060	0.008	0.147	0.022	0.005	2.809
120	-125.1	0.444	0.015	0.003	0.288	0.059	0.009	0.153	0.023	0.006	2.569
121	-140.0	0.415	0.020	0.004	0.289	0.074	0.009	0.148	0.035	0.006	4.224
122	-155.1	0.428	0.016	0.003	0.295	0.060	0.010	0.156	0.026	0.006	2.675
123	-170.7	0.423	0.016	0.004	0.289	0.067	0.010	0.156	0.027	0.007	3.186
124	-186.6	0.449	0.017	0.003	0.290	0.061	0.009	0.144	0.022	0.005	2.226
125	-203.0	0.438	0.016	0.003	0.288	0.062	0.009	0.150	0.026	0.008	2.635
126	-219.9	0.423	0.019	0.003	0.287	0.070	0.010	0.150	0.030	0.008	3.370
127	-237.4	0.420	0.019	0.003	0.297	0.070	0.009	0.147	0.029	0.005	3.631
128	-255.5	0.415	0.019	0.003	0.298	0.069	0.010	0.151	0.029	0.005	3.381
129	-274.0	0.405	0.020	0.003	0.294	0.072	0.009	0.156	0.034	0.007	4.568
130	-293.1	0.403	0.018	0.003	0.299	0.072	0.009	0.155	0.033	0.007	4.413
131	-312.7	0.412	0.018	0.003	0.303	0.070	0.009	0.150	0.031	0.005	3.935

D.9 Supplemental Comparison of Calibrations

The Tierney et al. (2010) calibration is based on redundancy analysis on a subset of 36 non-saline lakes out of 46 east African lakes across a 3730 m elevation gradient. Their final equation is based on a three-component regression consisting of three major branched GDGTs. The Loomis et al. (2012) calibration is based on an expanded dataset totaling 111 east African lakes including the original lakes. Loomis et al use a stepwise forward selection model that employs four combined GDGT variables that explain the most variance in their calibration set. Loomis et al (2012) compare their calibration with other published calibrations. Their reconstruction does a better job of characterizing cooler temperatures and removing the influence of Lake pH. They also test the performance of their calibration by applying the calibration to a 48-kyr-temperature reconstruction and comparing it with other calibrations and published regional temperature reconstructions.

Tierney et al. (2010)

$$MAAT = 50.47 - 74.18 \times f(\boldsymbol{III}) - 31.60 \times f(\boldsymbol{II}) - 34.69 \times f(\boldsymbol{I})$$

Loomis et al. (2012)

$$MAAT = 22.77 - 33.58 \times f(\boldsymbol{III}) - 12.88 \times f(\boldsymbol{II}) - 418.53 \times (\boldsymbol{IIc}) + 86.43 \times (\boldsymbol{Ib})$$

The Loomis calibration produces the lowest error and explains the most variance of their lakes of the proposed calibrations ($R^2 = 0.94$, RMSE = 1.9ºC). Recent work has also shown the Loomis calibration applies to GDGT distributions in artic lakes (Shanahan 2013). Shanahan et al show that GDGTs calibrated with the Loomis method are representative of summer or growing season temperatures in 59 lakes across Baffin Island. The GDGTs are most representative of summer temperatures, during which time there is light and the lakes are somewhat ice free.

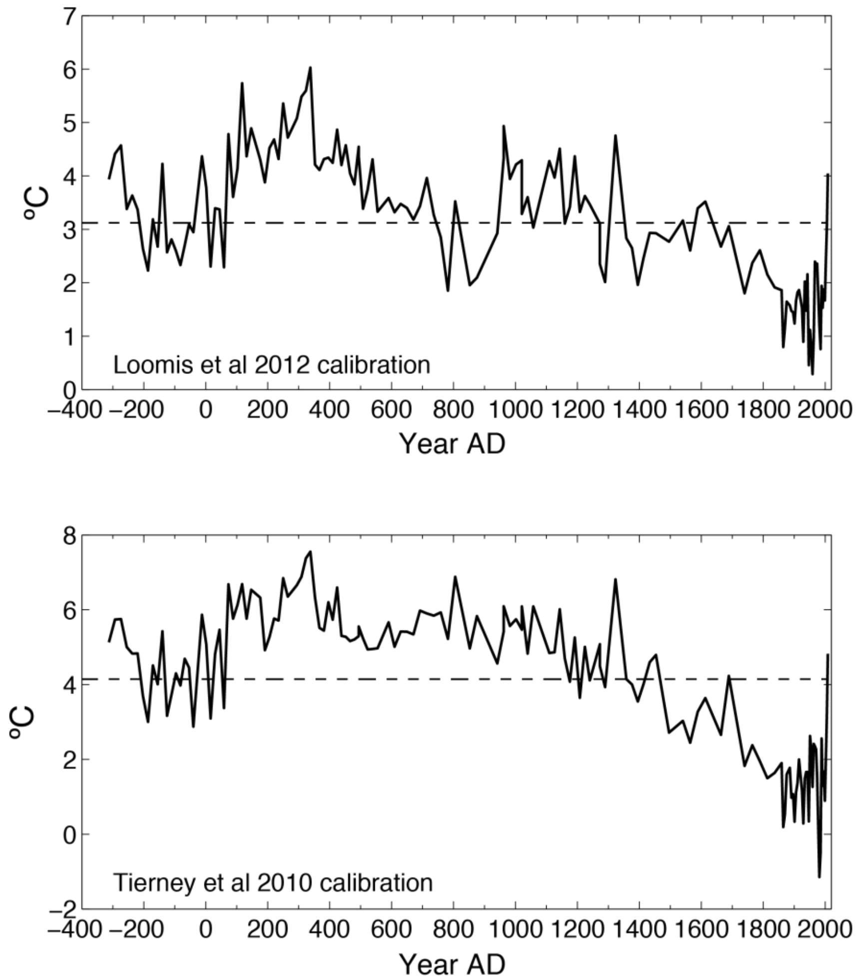

Figure D.S11: Comparison of the Loomis et al. (2012) GDGT temperature calibration versus the Tierney et al. (2010) calibration.

APPENDIX E: PERMISSIONS

APPENDIX A: SECOND CENTURY MEGADROUGHT IN THE RIO GRANDE HEADWATERS, COLORADO: HOW UNUSUAL WAS MEDIEVAL DROUGHT? Reprinted with permission from John Wiley and Sons.

Routson, C. C., C. A. Woodhouse, and J. T. Overpeck, 2011: Second century megadrought in the Rio Grande headwaters, Colorado: How unusual was medieval drought? Geophysical Research Letters, 38 (22), L22 703, doi:10.1029/2011GL050015.

Rightslink Printable License 10/31/13 3:32 PM

JOHN WILEY AND SONS LICENSE TERMS AND CONDITIONS

Oct 31, 2013

This is a License Agreement between Cody C Routson ("You") and John Wiley and Sons ("John Wiley and Sons") provided by Copyright Clearance Center ("CCC"). The license consists of your order details, the terms and conditions provided by John Wiley and Sons, and the payment terms and conditions.

All payments must be made in full to CCC. For payment instructions, please see information listed at the bottom of this form.

License Number	3259580500434
License date	Oct 31, 2013
Order Content Publisher	John Wiley and Sons
Order Content Publication	Geophysical Research Letters
Order Content Title	Second century megadrought in the Rio Grande headwaters, Colorado: How unusual was medieval drought?
Licensed copyright line	Copyright 2011 by the American Geophysical Union.
Order Content Author	Cody C. Routson, Connie A. Woodhouse, Jonathan T. Overpeck
Order Content Date	Nov 19, 2011
Start page	n/a
End page	n/a
Type of use	Dissertation/Thesis
Requestor type	Author of this Wiley article
Format	Print and electronic
Portion	Full article
Will you be translating?	No
Total	**0.00 USD**

TERMS AND CONDITIONS

This copyrighted material is owned by or exclusively licensed to John Wiley & Sons, Inc. or one of its group companies (each a "Wiley Company") or a society for whom a Wiley Company has exclusive publishing rights in relation to a particular journal (collectively "WILEY"). By clicking "accept" in connection with completing this licensing transaction, you agree that the following terms and conditions apply to this transaction (along with the billing and payment terms and conditions established by the Copyright Clearance Center Inc., ("CCC's Billing and Payment terms and conditions"), at the time that you opened your RightsLink account (these are available at any time at http://myaccount.copyright.com).

Terms and Conditions

1. The materials you have requested permission to reproduce (the "Materials") are protected by copyright.

2.You are hereby granted a personal, non-exclusive, non-sublicensable, non-transferable, worldwide, limited license to reproduce the Materials for the purpose specified in the licensing process. This license is for a one-time use only with a maximum distribution equal to the number that you identified in the licensing process. Any form of republication granted by this license must be completed within two years of the date of the grant of this license (although copies prepared before may be distributed thereafter). The Materials shall not be used in any other manner or for any other purpose. Permission is granted subject to an appropriate acknowledgement given to the author, title of the material/book/journal and the publisher. You shall also duplicate the copyright notice that appears in the Wiley publication in your use of the Material. Permission is also granted on the understanding that nowhere in the text is a previously published source acknowledged for all or part of this Material. Any third party material is expressly excluded from this permission.

3. With respect to the Materials, all rights are reserved. Except as expressly granted by the terms of the license, no part of the Materials may be copied, modified, adapted (except for minor reformatting required by the new Publication), translated, reproduced, transferred or distributed, in any form or by any means, and no derivative works may be made based on the Materials without the prior permission of the respective copyright owner. You may not alter, remove or suppress in any manner any copyright, trademark or other notices displayed by the Materials. You may not license, rent, sell, loan, lease, pledge, offer as security, transfer or assign the Materials, or any of the rights granted to you hereunder to any other person.

4. The Materials and all of the intellectual property rights therein shall at all times remain the exclusive property of John Wiley & Sons Inc or one of its related companies (WILEY) or their respective licensors, and your interest therein is only that of having possession of and the right to reproduce the Materials pursuant to Section 2 herein during the continuance of this Agreement. You agree that you own no right, title or interest in or to the Materials or any of the intellectual property rights

therein. You shall have no rights hereunder other than the license as provided for above in Section 2. No right, license or interest to any trademark, trade name, service mark or other branding ("Marks") of WILEY or its licensors is granted hereunder, and you agree that you shall not assert any such right, license or interest with respect thereto.

5. NEITHER WILEY NOR ITS LICENSORS MAKES ANY WARRANTY OR REPRESENTATION OF ANY KIND TO YOU OR ANY THIRD PARTY, EXPRESS, IMPLIED OR STATUTORY, WITH RESPECT TO THE MATERIALS OR THE ACCURACY OF ANY INFORMATION CONTAINED IN THE MATERIALS, INCLUDING, WITHOUT LIMITATION, ANY IMPLIED WARRANTY OF MERCHANTABILITY, ACCURACY, SATISFACTORY QUALITY, FITNESS FOR A PARTICULAR PURPOSE, USABILITY, INTEGRATION OR NON-INFRINGEMENT AND ALL SUCH WARRANTIES ARE HEREBY EXCLUDED BY WILEY AND ITS LICENSORS AND WAIVED BY YOU.

6. WILEY shall have the right to terminate this Agreement immediately upon breach of this Agreement by you.

7. You shall indemnify, defend and hold harmless WILEY, its Licensors and their respective directors, officers, agents and employees, from and against any actual or threatened claims, demands, causes of action or proceedings arising from any breach of this Agreement by you.

8. IN NO EVENT SHALL WILEY OR ITS LICENSORS BE LIABLE TO YOU OR ANY OTHER PARTY OR ANY OTHER PERSON OR ENTITY FOR ANY SPECIAL, CONSEQUENTIAL, INCIDENTAL, INDIRECT, EXEMPLARY OR PUNITIVE DAMAGES, HOWEVER CAUSED, ARISING OUT OF OR IN CONNECTION WITH THE DOWNLOADING, PROVISIONING, VIEWING OR USE OF THE MATERIALS REGARDLESS OF THE FORM OF ACTION, WHETHER FOR BREACH OF CONTRACT, BREACH OF WARRANTY, TORT, NEGLIGENCE, INFRINGEMENT OR OTHERWISE (INCLUDING, WITHOUT LIMITATION, DAMAGES BASED ON LOSS OF PROFITS, DATA, FILES, USE, BUSINESS OPPORTUNITY OR CLAIMS OF THIRD PARTIES), AND WHETHER OR NOT THE PARTY HAS BEEN ADVISED OF THE POSSIBILITY OF SUCH DAMAGES. THIS LIMITATION SHALL APPLY NOTWITHSTANDING ANY FAILURE OF ESSENTIAL PURPOSE OF ANY LIMITED REMEDY PROVIDED HEREIN.

9. Should any provision of this Agreement be held by a court of competent jurisdiction to be illegal, invalid, or unenforceable, that provision shall be deemed amended to achieve as nearly as possible the same economic effect as the original provision, and the legality, validity and enforceability of the remaining provisions of this Agreement shall not be affected or impaired thereby.

10. The failure of either party to enforce any term or condition of this Agreement

shall not constitute a waiver of either party's right to enforce each and every term and condition of this Agreement. No breach under this agreement shall be deemed waived or excused by either party unless such waiver or consent is in writing signed by the party granting such waiver or consent. The waiver by or consent of a party to a breach of any provision of this Agreement shall not operate or be construed as a waiver of or consent to any other or subsequent breach by such other party.

11. This Agreement may not be assigned (including by operation of law or otherwise) by you without WILEY's prior written consent.

12. Any fee required for this permission shall be non-refundable after thirty (30) days from receipt

13. These terms and conditions together with CCC's Billing and Payment terms and conditions (which are incorporated herein) form the entire agreement between you and WILEY concerning this licensing transaction and (in the absence of fraud) supersedes all prior agreements and representations of the parties, oral or written. This Agreement may not be amended except in writing signed by both parties. This Agreement shall be binding upon and inure to the benefit of the parties' successors, legal representatives, and authorized assigns.

14. In the event of any conflict between your obligations established by these terms and conditions and those established by CCC's Billing and Payment terms and conditions, these terms and conditions shall prevail.

15. WILEY expressly reserves all rights not specifically granted in the combination of (i) the license details provided by you and accepted in the course of this licensing transaction, (ii) these terms and conditions and (iii) CCC's Billing and Payment terms and conditions.

16. This Agreement will be void if the Type of Use, Format, Circulation, or Requestor Type was misrepresented during the licensing process.

17. This Agreement shall be governed by and construed in accordance with the laws of the State of New York, USA, without regards to such state's conflict of law rules. Any legal action, suit or proceeding arising out of or relating to these Terms and Conditions or the breach thereof shall be instituted in a court of competent jurisdiction in New York County in the State of New York in the United States of America and each party hereby consents and submits to the personal jurisdiction of such court, waives any objection to venue in such court and consents to service of process by registered or certified mail, return receipt requested, at the last known address of such party.

Wiley Open Access Terms and Conditions

Wiley publishes Open Access articles in both its Wiley Open Access Journals program [http://www.wileyopenaccess.com/view/index.html] and as Online Open articles in its subscription journals. The majority of Wiley Open Access Journals have

adopted the Creative Commons Attribution License (CC BY) which permits the unrestricted use, distribution, reproduction, adaptation and commercial exploitation of the article in any medium. No permission is required to use the article in this way provided that the article is properly cited and other license terms are observed. A small number of Wiley Open Access journals have retained the Creative Commons Attribution Non Commercial License (CC BY-NC), which permits use, distribution and reproduction in any medium, provided the original work is properly cited and is not used for commercial purposes.

Online Open articles - Authors selecting Online Open are, unless particular exceptions apply, offered a choice of Creative Commons licenses. They may therefore select from the CC BY, the CC BY-NC and the Attribution-NoDerivatives (CC BY-NC-ND). The CC BY- NC-ND is more restrictive than the CC BY-NC as it does not permit adaptations or modifications without rights holder consent.

Wiley Open Access articles are protected by copyright and are posted to repositories and websites in accordance with the terms of the applicable Creative Commons license referenced on the article. At the time of deposit, Wiley Open Access articles include all changes made during peer review, copyediting, and publishing. Repositories and websites that host the article are responsible for incorporating any publisher-supplied amendments or retractions issued subsequently. Wiley Open Access articles are also available without charge on Wiley's publishing platform, **Wiley Online Library** or any successor sites.

Conditions applicable to all Wiley Open Access articles:

The authors' moral rights must not be compromised. These rights include the right of "paternity" (also known as "attribution" - the right for the author to be identified as such) and "integrity" (the right for the author not to have the work altered in such a way that the author's reputation or integrity may be damaged).

Where content in the article is identified as belonging to a third party, it is the obligation of the user to ensure that any reuse complies with the copyright policies of the owner of that content.

If article content is copied, downloaded or otherwise reused for research and other purposes as permitted, a link to the appropriate bibliographic citation (authors, journal, article title, volume, issue, page numbers, DOI and the link to the definitive published version on Wiley Online Library) should be maintained. Copyright notices and disclaimers must not be deleted.

Creative Commons licenses are copyright licenses and do not confer any other rights, including but not limited to trademark or patent rights.

Any translations, for which a prior translation agreement with Wiley has not been agreed, must prominently display the statement: "This is an unofficial translation of an article that appeared in a Wiley publication. The publisher has not endorsed this translation."

Conditions applicable to non-commercial licenses (CC BY-NC and CC BY-NC-ND)

For non-commercial and non-promotional purposes individual non-commercial users may access, download, copy, display and redistribute to colleagues Wiley Open Access articles. In addition, articles adopting the CC BY-NC may be adapted, translated, and text- and data-mined subject to the conditions above.

Use by commercial "for-profit" organizations

Use of non-commercial Wiley Open Access articles for commercial, promotional, or marketing purposes requires further explicit permission from Wiley and will be subject to a fee. Commercial purposes include:

Copying or downloading of articles, or linking to such articles for further redistribution, sale or licensing;

Copying, downloading or posting by a site or service that incorporates advertising with such content;

The inclusion or incorporation of article content in other works or services (other than normal quotations with an appropriate citation) that is then available for sale or licensing, for a fee (for example, a compilation produced for marketing purposes, inclusion in a sales pack)

Use of article content (other than normal quotations with appropriate citation) by for-profit organizations for promotional purposes

Linking to article content in e-mails redistributed for promotional, marketing or educational purposes;

Use for the purposes of monetary reward by means of sale, resale, license, loan, transfer or other form of commercial exploitation such as marketing products

Print reprints of Wiley Open Access articles can be purchased from:

corporatesales@wiley.com

The modification or adaptation for any purpose of an article referencing the CC BY-NC-ND License requires consent which can be requested from RightsLink@wiley.com .

Other Terms and Conditions:

BY CLICKING ON THE "I AGREE..." BOX, YOU ACKNOWLEDGE THAT YOU HAVE READ AND FULLY UNDERSTAND EACH OF THE SECTIONS OF AND PROVISIONS SET FORTH IN THIS AGREEMENT AND THAT YOU ARE IN AGREEMENT WITH AND ARE WILLING TO ACCEPT ALL OF YOUR

OBLIGATIONS AS SET FORTH IN THIS AGREEMENT.

v1.8

If you would like to pay for this license now, please remit this license along with your payment made payable to "COPYRIGHT CLEARANCE CENTER" otherwise you will be invoiced within 48 hours of the license date. Payment should be in the form of a check or money order referencing your account number and this invoice number RLNK501148955.

Once you receive your invoice for this order, you may pay your invoice by credit card. Please follow instructions provided at that time.

Make Payment To: Copyright Clearance Center Dept 001 P.O. Box 843006 Boston, MA 02284-3006

For suggestions or comments regarding this order, contact RightsLink Customer Support: customercare@copyright.com or +1-877-622-5543 (toll free in the US) or +1- 978-646-2777.

Gratis licenses (referencing $0 in the Total field) are free. Please retain this printable license for your reference. No payment is required.